



## COMPLEMENTARY SYNTHESIS OF ORGANOBORANES TO POPULATE THE CHEMICAL FUNCTIONALITY TO A GIVEN AREA OF BIOMEDICAL INTEREST

Jordi Royes Buisan

**ADVERTIMENT.** L'accés als continguts d'aquesta tesi doctoral i la seva utilització ha de respectar els drets de la persona autora. Pot ser utilitzada per a consulta o estudi personal, així com en activitats o materials d'investigació i docència en els termes establerts a l'art. 32 del Text Refós de la Llei de Propietat Intel·lectual (RDL 1/1996). Per altres utilitzacions es requereix l'autorització prèvia i expressa de la persona autora. En qualsevol cas, en la utilització dels seus continguts caldrà indicar de forma clara el nom i cognoms de la persona autora i el títol de la tesi doctoral. No s'autoritza la seva reproducció o altres formes d'explotació efectuades amb finalitats de lucre ni la seva comunicació pública des d'un lloc aliè al servei TDX. Tampoc s'autoritza la presentació del seu contingut en una finestra o marc aliè a TDX (framing). Aquesta reserva de drets afecta tant als continguts de la tesi com als seus resums i índexs.

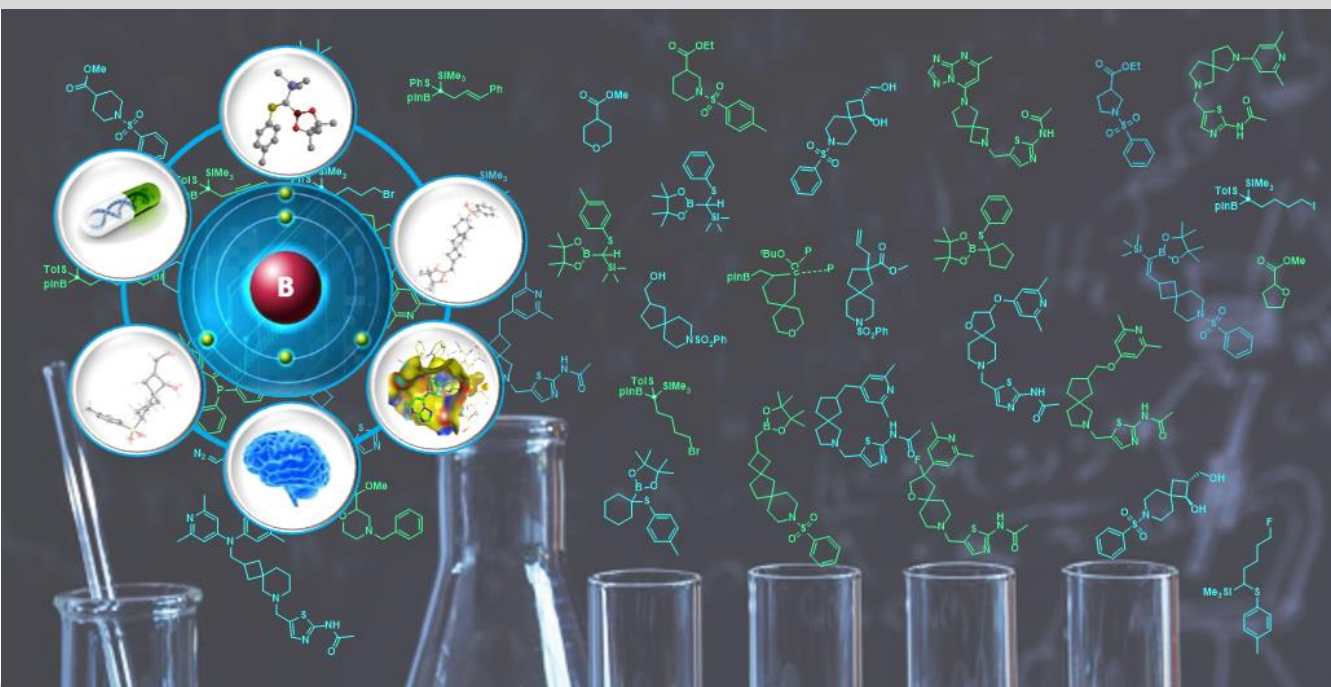
**ADVERTENCIA.** El acceso a los contenidos de esta tesis doctoral y su utilización debe respetar los derechos de la persona autora. Puede ser utilizada para consulta o estudio personal, así como en actividades o materiales de investigación y docencia en los términos establecidos en el art. 32 del Texto Refundido de la Ley de Propiedad Intelectual (RDL 1/1996). Para otros usos se requiere la autorización previa y expresa de la persona autora. En cualquier caso, en la utilización de sus contenidos se deberá indicar de forma clara el nombre y apellidos de la persona autora y el título de la tesis doctoral. No se autoriza su reproducción u otras formas de explotación efectuadas con fines lucrativos ni su comunicación pública desde un sitio ajeno al servicio TDR. Tampoco se autoriza la presentación de su contenido en una ventana o marco ajeno a TDR (framing). Esta reserva de derechos afecta tanto al contenido de la tesis como a sus resúmenes e índices.

**WARNING.** Access to the contents of this doctoral thesis and its use must respect the rights of the author. It can be used for reference or private study, as well as research and learning activities or materials in the terms established by the 32nd article of the Spanish Consolidated Copyright Act (RDL 1/1996). Express and previous authorization of the author is required for any other uses. In any case, when using its content, full name of the author and title of the thesis must be clearly indicated. Reproduction or other forms of for profit use or public communication from outside TDX service is not allowed. Presentation of its content in a window or frame external to TDX (framing) is not authorized either. These rights affect both the content of the thesis and its abstracts and indexes.



# Complementary synthesis of organoboranes to populate the chemical functionality to a given area of biomedical interest

Jordi Royes Buisan



DOCTORAL THESIS  
2019

UNIVERSITAT ROVIRA I VIRGILI  
COMPLEMENTARY SYNTHESIS OF ORGANOBORANES TO POPULATE THE CHEMICAL  
FUNCTIONALITY TO A GIVEN AREA OF BIOMEDICAL INTEREST  
Jordi Royes Buisan

UNIVERSITAT ROVIRA I VIRGILI  
COMPLEMENTARY SYNTHESIS OF ORGANOBORANES TO POPULATE THE CHEMICAL  
FUNCTIONALITY TO A GIVEN AREA OF BIOMEDICAL INTEREST  
Jordi Royes Buisan



UNIVERSITAT ROVIRA I VIRGILI  
COMPLEMENTARY SYNTHESIS OF ORGANOBORANES TO POPULATE THE CHEMICAL  
FUNCTIONALITY TO A GIVEN AREA OF BIOMEDICAL INTEREST  
Jordi Royes Buisan

Jordi Royes Buisan

Complementary synthesis of organoboranes  
to populate the chemical functionality to a  
given area of biomedical interest

Doctoral Thesis

Supervised by:

Prof. María Elena Fernández Gutiérrez

Dr. Ana Belén Cuenca González

Dr. Andrés Avelino Trabanco Suárez

Departament de Química Física i Inorgànica (URV)

Centro Investigación Janssen Cilag



Tarragona, December 2019

UNIVERSITAT ROVIRA I VIRGILI  
COMPLEMENTARY SYNTHESIS OF ORGANOBORANES TO POPULATE THE CHEMICAL  
FUNCTIONALITY TO A GIVEN AREA OF BIOMEDICAL INTEREST  
Jordi Royes Buisan



Prof. María Elena Fernández Gutiérrez, profesora titular del Departamento de Química Física e Inorgánica de la Universitat Rovira i Virgili, Dra. Ana Belén Cuenca González, profesora asociada al Departamento de Química Orgánica y Farmacéutica, Dr. Andrés Avelino Trabanco Suárez, director científico de química médica en la compañía farmacéutica Janssen Cilag de Johnson & Johnson,

HACEMOS CONSTAR que el presente trabajo, titulado:

“Complementary synthesis of organoboranes to populate the chemical functionality to a given area of biomedical interest”,

que presenta Jordi Royes Buisan para la obtención del título de Doctor y que cumple los requerimientos para poder optar a la Mención de Doctorado Industrial, ha sido realizado bajo nuestra dirección en el Departamento de Química Física e Inorgánica de la Universidad Rovira i Virgili y en el centro de investigación de la empresa Janssen Cilag con sede en Toledo.

Tarragona, 28 de Octubre de 2019

La directora de la tesis

Prof. María Elena  
Fernández Gutiérrez

La codirectora de la tesis

Dra. Ana Belén Cuenca  
González

El codirector de la tesis

Dr. Andrés Avelino  
Trabanco Suárez

UNIVERSITAT ROVIRA I VIRGILI  
COMPLEMENTARY SYNTHESIS OF ORGANOBORANES TO POPULATE THE CHEMICAL  
FUNCTIONALITY TO A GIVEN AREA OF BIOMEDICAL INTEREST  
Jordi Royes Buisan

El presente trabajo se ha desarrollado mediante una beca FI (2019 FI\_B1 00163) y una beca CITIUS (P/2017/26817). El contenido descrito en la presente tesis ha sido financiado por:

- El Ministerio de Economía, Industria y Competitividad de España (MINECO) mediante los proyectos CTQ2013-43395-P y CTQ2016-80328-P.
- La Generalitat de Catalunya mediante el proyecto 2014SGR670 de ayudas a los grupos reconocidos y consolidados.
- La Universitat Rovira i Virgili mediante los proyectos 2015PFR-URV-B2-21 i 2016PFR-URV-B2-22 del Programa de Foment a l'Activitat de la Recerca (PFR).



UNIVERSITAT ROVIRA I VIRGILI  
COMPLEMENTARY SYNTHESIS OF ORGANOBORANES TO POPULATE THE CHEMICAL  
FUNCTIONALITY TO A GIVEN AREA OF BIOMEDICAL INTEREST  
Jordi Royes Buisan

## Agradecimientos

Primero de todo me gustaría agradecer a los tres directores de tesis que me han guiado durante este camino. Elena, gracias por confiar en mí desde el primer momento. Nada más al volver del Erasmus, empezamos un camino científico juntos con el master y finalmente con el doctorado, haciéndome partícipe del grupo del Boro. Gracias por brindarme toda tu ayuda y conocimientos durante las reuniones diarias en el despacho, en el campo de la ciencia pero sobre todo en la química del boro, una química tan versátil y bonita.

A ti Ana Belén, una gran guía desde mi primer día en el laboratorio, dejando tus prioridades de lado para enseñarme todos tus conocimientos teóricos y técnicas experimentales, sin duda una codirectora con quien siempre he podido contar para consultar mis dudas e inquietudes. De ti aprendí a trabajar con rigor, sobre todo a no asegurar nada hasta que todas las técnicas disponibles certificaran lo mismo. Como te gustaba que analizáramos los GC-MS, cualquier impureza era susceptible de ser revisitada e incluso intentar purificarla para saber que estaba sucediendo en nuestra reacción y con ello poder progresar día a día en el proyecto. Eres una gran química pero sin duda a la vez una gran persona con la que siempre puedo contar.

Andrés, la verdad es que empezar dentro de una empresa de gran nivel como es Janssen para mí fue todo un reto. Desde que surgió la oportunidad de colaboración mi impaciencia e inquietudes fueron *in crescendo*. Con tu forma de ser hiciste que, des del inicio, esta etapa fuera muy fácil, siempre transmitiéndome tranquilidad, haciéndome sentir uno más del grupo de *HIT generation* e involucrándome íntegramente en el proyecto de OGA. Además, siempre recordaré la igualdad y cercanía que mostrabas siendo un Team Leader, poniendo reacciones aun teniendo gran cantidad de trabajo de ordenador, viniendo a la vitrina a preguntarme cosas de química e incluso pidiendo algún consejo para utilizar los reactores que había utilizado o algún consejo con los equipos purificadores. Sin ninguna duda eres más que un codirector de una tesis, muchísimas gracias Andrés por formar parte de ella.

Als Omichis/Inncat, una gran familia encara que petita al mateix temps ... amb els comiats d'aquells que han finalitzat el seu màster o tesis, i les noves incorporacions amb el seu projecte acadèmic de futur. No tinc cap dubte que tots vosaltres heu fet que cada dia fos un bona jornada de laboratori, amb esmorzars rutinaris buscant sempre qualsevol excusa per fer portar a un o altre pastetes i entrepans.



El grup del Bor, el post-doc Thierry gran treballador però sobre tot un gran tio amb qui he compartit laboratori. Amb el teu humor gironí i sempre dient que, el bon català era de Girona, poc a poc vas anar aprenent que els bons pilots de karts no sempre són de Girona.....jeje, ens queda una revenja pendent. Enrico que momentos tan divertidos de conversaciones, bailes de bachata y papa pa paaaaaaa.....que nos dabas por el laboratorio. Marc, company de projecte de les insercions durant el primer any...quines columnes més llargues que vam suar juntament amb l'Ana, va valer la pena!! A tu Núria, que vas ser la primera en posarme un o dos mots....recordes lo de iogu o pollito? Segurament que si, sense dubtar-ho vas obrir-me des d'un primer moment les portes del grup del Bor donant-me sempre ajuda en allò que en un nou vingut podia necessitar. Vaig poder veure que dintre d'aquella personalitat de dona treballadora, lluitadora i amb coratge, hi havia algú molt més especial que una companya de laboratori, amb qui poc a poc vam compartir més i més moments fora d'ell. Al DJ del grup, l'Albert un tio caracteritzat pel seu positivisme i insistència en allò que vol, sobre tot en el camp del amor. Els dies amb la teva música i les tardes al gimnàs feien que les setmanes passessin volant, gràcies per fer el teu màster en el grup del Bor i ja saps que ens queda pendent la visita al Zermatt, Suïssa. Al malagueño del grupo Ricardo, que productos tan buenos tienen por allí, sobre todo el vinito de Jerez que ayudan a ver la química más clara....muchu suerte con lo que queda de tesis. To Eliot, the British and very friendly boy. Al Ricardo G. italiano y el Oriol, el dúo de la LTMP y de las columnas conjuntas, parecíais dos hermanos inmersos en un mismo proyecto, mucha gracias Ricardo por tus consejos, i a tu Oriol, molta sort en aquesta nova etapa de PhD que tot just acaba de començar. A la única noia present actualment en el grup del Bor, la Jana. Sabia des d'un bon moment que entraries trepitjant fort i així ho has fet. Gràcies pels moments compartits dintre del laboratori, així com fora d'ell obrint-me la porta al apassionant món de l'escalada i donant-me els teus petits consells.....vinga "bouaaaa" que el PhD ja es teu també!!!

A tots aquells amb qui hem compartit el Lab 216, les estones d'espera en el rotavapor, el fregadero i el forn....tots sabem que hem ficat de la nostra part per ser el més ordenats possibles. Alberto, al Valencià amb el seu humor característic de dibuixos que no sempre era compartit per tots, tenim pendent una sortida amb bici. Nanette, always very polite and answering when your help was needed!! El Fran, el tio de Reus, del Mini, del sushi, fem un Ogura?...quins dies pel laboratori, quants bons moments sumats i quines magnífiques cinètiques amb el teu super casio, m'emporto un gran amic Reusenc!! Per altra banda, el Toni un gran amic Tarragoní,

parlar amb tu de química era divertit, però esquiar ho superava....o no recordes aquella baixada per Boi Taüll? Jo si i a més recordo la mítica frase....”Si no arribo baix, recordeu-me com un heroi” Sincerament crec que no les tenies totes amb tu mateix!! Myriam, la chica francesa con una gran capacidad de entendimiento del castellano y catalán, sin duda hemos realizado esta etapa sinérgicamente y así la terminamos, te deseo lo mejor en tu futuro y gracias por esos dulces de Francia que siempre traes en tus visitas a tu ciudad. Al Roger, el químic de poble....no hi havia dia que no et sentís dir pel laboratori, quina merda això de les columnes...jeje, espero que en aquest nou projecte en el CTQC t’hagis alliberat d’elles, sort en el doctorat. Lola, la chica del sur, aunque hemos compartido poco tiempo veo que en ti hay una gran persona y con un carácter muy afable, te deseo lo mejor en esta etapa y en tu vida. Al Javi, los pocos días que hemos compartido he visto que esto de la química te gusta...sigue y lucha por tus objetivos, ánimo!!

Als amics del Lab 217, separats físicament per una porta però que segurament estimen molt el Lab 216 ja que sempre els teníem de visita amb la excusa del rotavapor. Al Marc Magre, el fan numero 1 dels “burilles” com tu deies....segur que tard o d’hora incorporaràs aquest àtom en els teus projectes, gràcies i sort en els teues metes!! A la Zahra, la chica de *Privalia* y de horarios de tarde-noche. A la Carlota, aquella noia amb un caràcter sempre educatiu, sempre buscant la cara positiva de les coses i donant segones oportunitats a molts assumptes. Quina alegria haver-te conegut en aquesta etapa i poder compartir moments junts amb el *Petit comitè*, però sens dubte em va sorprendre molt la teu passió per les motos...quan tornem a Montmeló? A la Maria, un gran exemple com a química, mai sabíem si eres la computacional o la experimental del grup...sincerament eren llargues les hores que hi dedicaves als dos àmbits a més de lo artista que estàs feta amb aquells dibuixos que utilitzàvem pels regals de tesi. Efrem, el mastercito que va entrar amb l’Albert, menudo dueto formàveu, sempre buscàveu la excusa per anar de festa els dijous...espero que aviat coincidim i així et sento tocar en el teu grup!! El Joan, compañero desde que empezamos la carrera, mucha suerte en lo que te queda de doctorado y.....pórtate bien con el resto del grupo!! A la Jèssica, la cuinetes del grup, quins tupperes més saludables i apetitosos que portes sempre 😊!! Polete, segueix amb el teu caràcter, em mola molt el teu rotllo i els “bon dia” traduïts al que paxaaaaa?? Al Jordi, l’última incorporació al grup, segueix amb la teva il·lusió en la química però sobre tot no t’agobies que encara et queda molt.

Als del pis de dalt, els orgànics Adrià, David Collado aviam si ens retrobem i fem un karting. A Jordi, Irene i Macarena...siempre apunto para buscar un CAS y dejarnos un reactivo que no teníamos, muchas gracias por prestar vuestra mano y ayudarnos a completar aquellas reacciones puestas a última hora.

A todos los técnicos, pero sobre todo a ti Raquel, alguien con quien siempre se puede contar, solucionando cualquier inconveniente y dejando tu trabajo para ayudarnos en aquello en lo que se nos escapa, sin duda una técnico de 10!! Sin ti el laboratorio no sería posible!! Al Josep, gràcies per prestar-nos reactius, material i estar sempre al cas del solvents que s'anaven acabant. I per suposat, als tècnics del Servei. Irene, Sonia i Carme a masses, sempre ajudant amb el GC-MS i barallant-nos per buscar la massa d'aquells compostos que ho posaven més difícil. Al Ramón, el tècnic de RMN sempre apunt per sintonitzar el boro....*su btune* i *pinayu pinyau*!!

Me gustaría también agradecer a todos aquellos que formaron parte de la colaboración realizada en la empresa Janssen en Toledo. A Jose Manuel Bartolomé, líder del proyecto, sin duda tú primera reunión explicándonos las bases del proyecto me hizo ver del nivel tan alto de investigación que se realizaba en el centro. Gracias por aportar tus conocimientos y tu cercanía... los quesos de Castilla la Mancha están buenísimos!! Sobre todo en este punto me gustaría agradecer al Mondejano de la empresa, Juan Antonio Vega, un gran hombre y gran mentor a la vez. No había cosa más importante para él que la química y su pueblo, Mondéjar. De ti aprendí una gran cantidad de cosas, tanto a nivel experimental como la forma de trabajar en la empresa, como también de tus grandes conocimientos en el campo de la química orgánica y médica. Tu ayuda fue fundamental para coger el ritmo de trabajo en Janssen y pensar siempre en ideas nuevas para los espiro ciclos. Gracias sinceramente por confiar en mí en todo momento y volcarte íntegramente en la colaboración. Me gustaría agradecer también a todos los técnicos, con ellos era mucho más fácil identificar los productos, Alberto Fontana siempre sacando tiempo de donde no lo había y Jose Manuel Alonso identificando la configuración relativa de los compuestos finales, muchas gracias. A todos los investigadores presentes en los laboratorios de Síntesis I, II, III y IV, cada uno de vosotros siempre me habéis prestado algún conocimiento o consejo de vuestra buena y larga experiencia en el mundo científico, gracias por hacer la química un poco más fácil.

Al grupo de estudiantes CITIUS, los "Hanssens", sin duda muchos buenos ratos de cafés, desayunos, tardes de gym y cervezas en el Alquimia o Trebol. Fran, el chico

del pueblo *perdio* de la mano de *Dioh*, siempre tan simpático y contento....benditos columnadores automáticos, esperemos que los del futuro también coloquen los tubos por si surge un descuido. Gloria, la de Colmenar Viejo, compartir laboratorio fue divertido, con tus extracciones asquerosas que se formaban emulsiones inseparables, tengo que confesarte que rezaba por no utilizar tus reactivos y tu química, suerte por Cambridge. Cristina, la malagueña de Janssen, siempre simpática y agobiada a la vez. “No vea eh” innumerables veces pude escuchar esto de ti, siempre tan carismática y dispuesta a acogernos en tu casa...¿nos vemos en la feria de Málaga? Ana la “madrileña-maña”, menudo caos tenías siempre montado con tubos de columna en esa vitrina, no sé cómo te aclarabas!! No pierdas tu simpatía y tus risas, sigue siempre así de feliz. Nacho sevillano, siempre buscándole la mejora y la explicación a cada reacción....los mecanismos de reacción es sin duda tu pasión. Inma compartimos muy poquito en Janssen y por ICIQ tampoco te he visto mucho, pero desde el primer momento mostraste tu ayuda y tu preocupación por el...no se hablar catalán, ¿qué hare en ICIQ? Nicola, el italiano de flow chemistry siempre corriendo por los pasillos de Janssen, se nota que el flow no lo llevabas solamente en la química sino por tu cuerpo.

Finalment m’agradaria agrair aquesta tesis a tots aquells més propers, aquells que fa 4 anys em vau encoratjar a realitzar el doctorat, a donar-me una empenta cap endavant en els moments més difícils, i per suposat compartir aquells moments més fructífers i satisfactoris. Núria, ets el millor a nivell personal que m’ha donat aquesta etapa, saps perfectament com estic d’agraït per totes les petites empentes cap endavant i per la comprensió que has tingut amb mi en els últims mesos i l’ajuda en tot el procés pretesis, ets sens dubte la millor companya de viatge de futur!♥ A tota la família avis, tiets i cosins per les seues preguntes de curiositat i ànims donats. Per suposat a vosaltres tres: papa, mama i Carlos, vau ser els que em vau fer decidir finalment per aquest camí que aquí culmina, clarament ha sigut un encert! 🤔 Gràcies per tota la ajuda durant aquest període, per les visites, per les trucades a la distancia, pels abraços i petons de cap de setmana, per les preguntes diàries de, que, com van les reaccions? Avancem? No et preocupis lo que un dia és negre al següent és blanc. M’agradava com mostràveu interès en mi, com escoltàveu atentament la química que feia, que segurament no enteníeu molt be, i acabàveu dient semblen colmenes de abelles...Per això i per molt més, gràcies per aquest suport incondicional!!!😊😊😊

UNIVERSITAT ROVIRA I VIRGILI  
COMPLEMENTARY SYNTHESIS OF ORGANOBORANES TO POPULATE THE CHEMICAL  
FUNCTIONALITY TO A GIVEN AREA OF BIOMEDICAL INTEREST  
Jordi Royes Buisan

UNIVERSITAT ROVIRA I VIRGILI  
COMPLEMENTARY SYNTHESIS OF ORGANOBORANES TO POPULATE THE CHEMICAL  
FUNCTIONALITY TO A GIVEN AREA OF BIOMEDICAL INTEREST  
Jordi Royes Buisan

*“Lo que sabemos es una  
gota de agua, lo que  
ignoramos es el océano”*

UNIVERSITAT ROVIRA I VIRGILI  
COMPLEMENTARY SYNTHESIS OF ORGANOBORANES TO POPULATE THE CHEMICAL  
FUNCTIONALITY TO A GIVEN AREA OF BIOMEDICAL INTEREST  
Jordi Royes Buisan

## Contents

1.	Introduction	1
1.1	Context of the thesis	3
1.2	Organoborane reagents	3
1.3	Intramolecular borylative cyclization involving bis(pinacolato)diboron	4
1.3.1	Borylative cyclization of alkynes	4
1.3.2	Borylative cyclization of allenes	6
1.3.3	Borylative cyclization of allenynes	7
1.3.4	Borylative cyclization of enallenes	8
1.3.5	Borylative cyclization of enynes	9
1.4	Intramolecular borylative cyclization of alkenes	10
1.4.1	Borylative ring-closing of alkenes bearing good leaving groups	10
1.4.2	Borylative ring-closing of alkenes bearing carbonyl electrophiles	18
1.4.3	Borylative ring-closing of alkenes bearing isocyanides	21
1.4.4	Borylative ring-closing of alkenes bearing imines	23
1.5	References Chapter 1	25
2.	Objectives	29
2.1	Specific Objectives of the thesis	31
3.	Inter and intramolecular selective alkylations of CH(Bpin)(SiMe <sub>3</sub> )(SR) with alkyl halides	33
3.1	State of the art	35
3.1.1	Selective deborylative alkylation of <i>germinal</i> -diboron compounds	36
3.1.2	Desilylative alkylation	39
3.1.3	Selective deprotonative alkylation sequence $\alpha$ to a boryl moiety	40
3.1.4	Synthesis of <i>germinal</i> diboryl alkanes by insertion of diazo compounds into boron containing reagents	42
3.2	Aim of the Chapter	45
3.3	Results and discussion	46

---



## Contents

---

3.4	Conclusions	56
3.5	References Chapter 3	58
4.	Intramolecular borylative ring-closing C-C coupling toward spiro- and dispiro-heterocycles	61
4.1	State of the art	63
4.1.1	Intramolecular carboboration	63
4.1.2	The interest of spiro-bicyclic motifs	64
4.2	Aim of the Chapter	66
4.3	Results and discussion	67
4.4	Conclusions	79
4.5	References Chapter 4	80
5.	Synthesis and application of novel spiro-boronate compounds for the treatment of Alzheimer's disease	83
5.1	State of the art	85
5.1.1	Alzheimer's disease	85
5.1.2	Epidemiology	86
5.1.3	Pathophysiology	87
5.1.4	Tau hypothesis	89
5.1.5	Spiro-bicyclic scaffolds as source of OGA inhibitors: rationale	92
5.2	Aim of the Chapter	95
5.3	Results and discussion	96
5.3.1	Synthesis of spiro-bicyclic central scaffolds	96
5.3.2	Synthesis of target molecules by derivatization of the spiro-bicyclic central scaffolds	100
5.3.3	SAR analysis from the final target spiro-compounds	116
5.4	Conclusions	125
5.5	References Chapter 5	126
6.	Intramolecular diastereoselective borylative spiro-cyclization through alkenyl aldehydes	131
6.1	State of the art	133
6.1.1	1,2-Carboboration of alkenyl aldehydes	133

---

6.1.2	1,2-Borylation of aldehydes catalyzed by copper complexes	136
6.2	Aim of the chapter	138
6.3	Results and discussion	139
6.4	Conclusions	144
6.5	References Chapter 6	145
7.	Concluding remarks	147
8.	Experimental part	151
8.1	General considerations	153
8.2	Experimental procedures and spectral data of Chapter 3	154
8.3	Experimental procedures and spectral data of Chapter 4	165
8.4	Experimental procedures and spectral data of Chapter 5	183
8.5	Experimental procedures and spectral data of Chapter 6	223
8.6	References Chapter 8	231
9.	Summary	235
9.1	Summary of the thesis	237
9.2	References Chapter 9	242
10.	List of publications, conferences and research collaboration	243

---

UNIVERSITAT ROVIRA I VIRGILI  
COMPLEMENTARY SYNTHESIS OF ORGANOBORANES TO POPULATE THE CHEMICAL  
FUNCTIONALITY TO A GIVEN AREA OF BIOMEDICAL INTEREST  
Jordi Royes Buisan

# Chapter 1

## Introduction

---

UNIVERSITAT ROVIRA I VIRGILI  
COMPLEMENTARY SYNTHESIS OF ORGANOBORANES TO POPULATE THE CHEMICAL  
FUNCTIONALITY TO A GIVEN AREA OF BIOMEDICAL INTEREST  
Jordi Royes Buisan

## 1.1. Context of the thesis

In the last two decades, the organoborane chemistry has evolved from proof of concept to several advanced applications. The practical use of new synthetic methods requires to be inexpensive, atom-economical and environmentally friendly. Related to that, borylative cyclization reactions with the concomitant incorporation of a reactive functional group such a boronate moiety, fulfill all the requirements previously mentioned. The presence of a boron unit guarantees further functionalizations and derivatizations such as, oxidation and cross-coupling reactions among others. For that reason, organoborane compounds have been considered powerful synthetic tools for many different applications. Moreover, compounds containing boryl groups have special benefits due to their low toxicity and high functional group tolerance.<sup>[1]</sup>

Currently, organoboron reagents offer prominent transformations in both metal catalyzed<sup>[1c]</sup> and transition metal-free<sup>[2]</sup> methodologies for the synthesis of selective C-B bonds.

In this context, the present thesis is focused in the formation of cyclic systems, through C-C and C-B bonds formation, considered to be very interesting building blocks for many applications. Taking advantage of the Lewis acidity of the boron unit, these cyclic systems have been derivatized into a series of *O*-GlcNAcase inhibitors with potential application in the treatment of Alzheimer's disease. For the synthesis of those molecules, different diboron reagents as well as *gem*-diborylalkane substituted and non-substituted reagents have been used.

## 1.2. Organoborane reagents

Organodiboron reagents can be divided principally in two groups: diboron and *gem*-diborylalkane reagents. Among the most interesting diboron reagents containing a B-B  $\sigma$ -bond are the boronic esters bis(pinacolato)diboron [B<sub>2</sub>pin<sub>2</sub>] (**1**), bis(neopentylglycolato)diboron [B<sub>2</sub>neop<sub>2</sub>] (**2**) and bis(hexylenglycolato)diboron [B<sub>2</sub>hex<sub>2</sub>] (**3**). Among them, B<sub>2</sub>pin<sub>2</sub> (**1**) is the most frequently used since it is commercially available, easy to handle and to store. Alternatively, *gem*-diborylalkanes represent a new and diverse class of boron compounds with similar properties than the diboron species. These *gem*-diborylalkanes are deemed as attractive reagents for constructing new complex molecules and expand the chemical library.<sup>[3]</sup> The most widely used *gem*-diborylalkane is the commercially available 1,1-diborylmethane [CH<sub>2</sub>(Bpin)<sub>2</sub>] (**4**). The landmark transformation of *gem*-diborylalkane reagents is the one-pot carbon-homologation through a CH<sub>2</sub>Bpin fragment. Substituted *gem*-diborylalkanes can contain other versatile functional group such as trimethylsilyl group as substituent in (bis(4,4,5,5-tetramethyl-1,3,2-

## Introduction

---

dioxaborolan-2-yl)methyl)trimethylsilane [CH(Bpin)<sub>2</sub>(SiMe<sub>3</sub>)] (**5**). Interelement boron reagents of formula pinB-SR (R= Ph, Tol) (**6**) have been prepared in the group of Prof. Westcott<sup>[4]</sup> to be used in this thesis towards the preparation of multifunctional systems CH(Bpin)(SiMe<sub>3</sub>)(SR) (Figure 1.1).

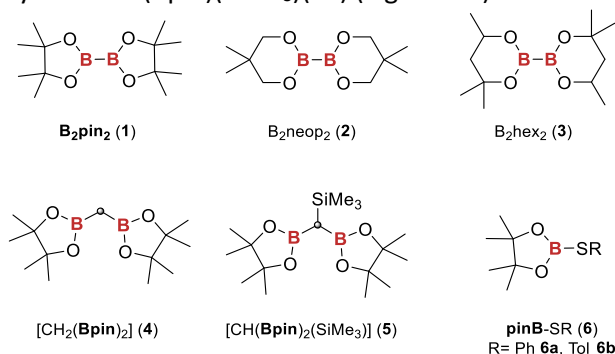


**Figure 1.1** Commercially and non-commercially available diboron and boron interelement reagents used in this thesis.

### 1.3. Intramolecular borylative cyclization involving bis(pinacolato)diboron

One of the greatest challenge of modern chemistry is the increasing need for developing sustainable synthetic methods. Among these, borylative ring-closing reactions with *in situ* incorporation of a boryl unit along with the formation of a cyclic compound, provide efficient routes while satisfying these requirements. The following sections of this introduction describe the transition metal catalyzed borylative ring-closing reactions using B<sub>2</sub>pin<sub>2</sub> as the boron source developed over the last decades.

#### 1.3.1 Borylative cyclization of alkynes

Copper (I) is the most widely used transition metal for the activation of diboron reagents and addition to alkynes in order to promote an intramolecular cyclization (Scheme 1.1).<sup>[5]</sup> The principal reason for this is the high compatibility of copper (I) with many functional groups as well as its low price. Ito and co-workers<sup>[6]</sup> reported the formation of cyclic products (Scheme 1.1a) by initial borylcupration of silylated alkynes.

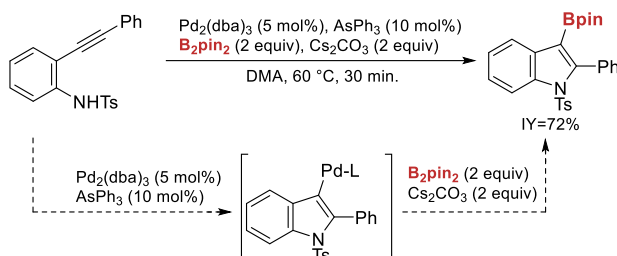
Later, the same group<sup>[7]</sup> combined the previous methodology with the introduction of different heteroatoms in the substrates, leading to the formation of borylated cyclic systems including ether or amine groups (Scheme 1.1b).





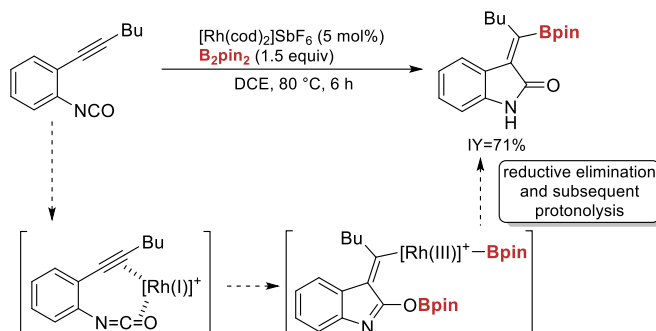
## Introduction

Apart from copper catalysis, palladium complexes are also suitable catalysts towards borylative cyclization.<sup>[10]</sup> Harrity and co-workers<sup>[11]</sup> developed the aminative ring-closing borylation reaction of *ortho*-alkynylanilines catalyzed by Pd<sub>2</sub>(dba)<sub>3</sub> in the presence of AsPh<sub>3</sub> as ligand (Scheme 1.3). It is well known the ability of palladium (II) complexes to promote the indole forming cyclization and then subsequent addition of the Bpin unit.



**Scheme 1.3** Palladium catalyzed borylative cyclization of *ortho*-alkynylanilines.

Murakami and co-workers<sup>[12]</sup> have reported the synthesis of interesting building blocks such as oxindoles by the combination of rhodium catalyst and *ortho*-alkynylphenyl isocyanates (Scheme 1.4).



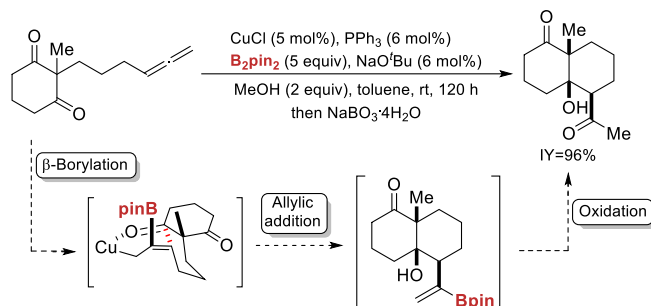
**Scheme 1.4** Rhodium catalyzed borylative cyclization of *ortho*-alkynylphenyl isocyanates.

### 1.3.2 Borylative cyclization of allenes

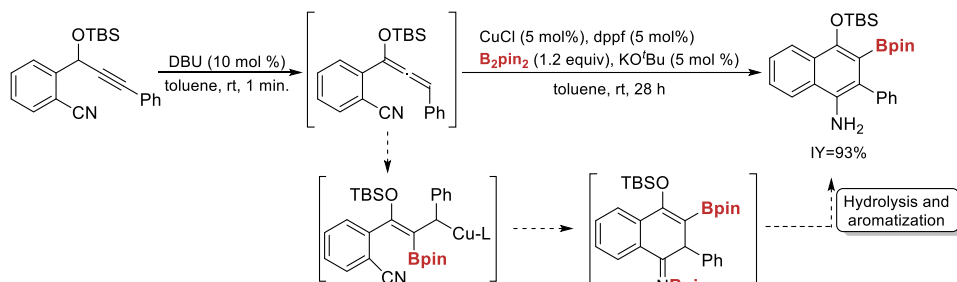
The use of allenes as substrates, has also been reported in the borylative cyclization context. Lin and co-workers,<sup>[13]</sup> reported the borylcupration of allenes with the concomitant intramolecular 1,3-addition process, generating *cis*-decalinol derivatives (Scheme 1.5a). The cyclization required high amounts of B<sub>2</sub>pin<sub>2</sub> (**1**) and the borylated products showed low stability under purification in silica gel chromatography. For this reason, the borylated intermediates were oxidized *in situ* after consumption of the substrate. In addition, Liu's group<sup>[14]</sup> also reported a similar

strategy with *in situ* generation of the allene, followed by borylcupration and subsequent intramolecular addition to a cyano group leading to the formation of cyclic imine intermediates, which underwent hydrolysis and aromatization to deliver highly substituted 3-boryl-naphthylamines (Scheme 1.5b).

a) Borylative ring-closing of allenes towards the formation of *cis*-decalin derivatives



b) Borylative ring-closing of *in situ* generated allenes towards the formation of substituted 3-boryl-naphthylamines



Scheme 1.5 Borylative cyclization of allenes catalyzed by Cu (I) complexes.

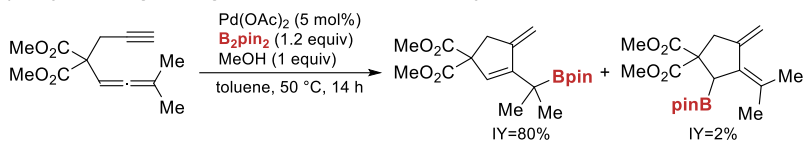
### 1.3.3 Borylative cyclization of allenynes

In contrast to the above mentioned Cu (I) catalyzed borylative cyclization protocols, the use of palladium catalysis in combination with allenynes substrates, is key in the efficient generation of the corresponding cyclic products containing the boron function.

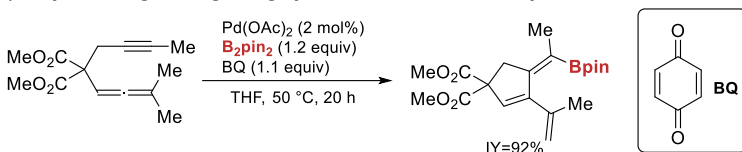
Cárdenas and co-workers<sup>[15]</sup> have contributed to the palladium-catalyzed cyclization of substituted allenynes towards cyclopentene derivatives in a highly selective manner (Scheme 1.6a). Following with this idea, Bäckvall and co-workers<sup>[16]</sup> made use of highly substituted allenynes, now containing an internal alkyne, accessing different alkenylboron cyclic products to the ones described by Cardenas under oxidative conditions (BQ) and also with excellent selectivities (Scheme 1.6b).

## Introduction

### a) Borylative ring-closing of substituted terminal allenynes



### b) Borylative ring-closing of highly substituted internal allenynes

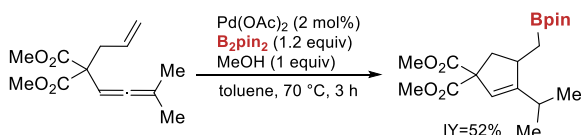


Scheme 1.6 Palladium catalyzed borylative cyclization of allenynes.

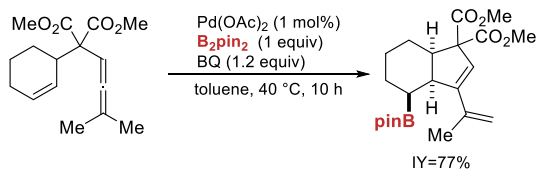
## 1.3.4 Borylative cyclization of enallenes

Palladium complexes are the catalyst of choice for the borylative cyclization of enallenes. Cárdenas and co-workers<sup>[15]</sup> described the borylative cyclization of enallenes in the presence of a catalytic amount of Pd(OAc)<sub>2</sub> under non-oxidative conditions (Scheme 1.7a). Subsequently, Bäckvall's group<sup>[17]</sup> developed the borylative ring-closing of enallenes under oxidative conditions, leading to unsaturated cyclic products (Scheme 1.7b). The same group reported on the enantioselective version of enallenes extending Cárdena's methodology with the use of a chiral phosphoric acid.<sup>[18]</sup> This asymmetric version allows access to the formation of chiral cyclic carbocycles with a pendant boronate unit with excellent enantioselectivities (Scheme 1.7c).

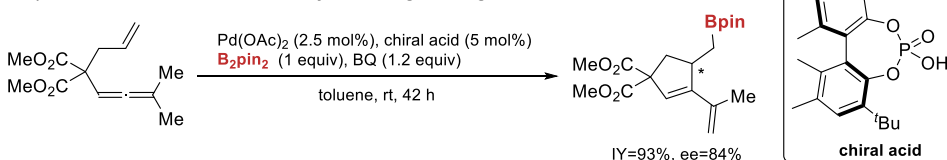
### a) Non-oxidative borylative ring-closing of enallenes



### b) Oxidative borylative ring-closing of enallenes



### c) Enantioselective oxidative borylative ring-closing of enallenes

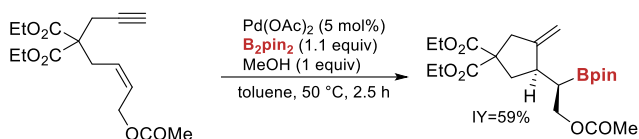


Scheme 1.7 Palladium catalyzed borylative cyclization of enallenes.

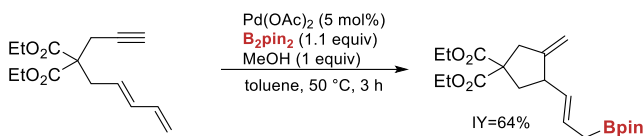
### 1.3.5 Borylative cyclization of enynes

Enynes has shown high reactivity in borylative cyclization reactions towards the formation of carbocyclic and heterocyclic structures. Cárdenas and co-workers have extensively studied these transformations (Scheme 1.8). The first example reported by this group involved a variety of 1,6-enynes as substrates which lead to the formation of 5-membered rings containing homoallylic boronates. This reaction was also extended to 1,7-enynes (Scheme 1.8a).<sup>[19]</sup> The same group reported as well the ring-closing of enynes containing an internal alkyne.<sup>[20]</sup> Encouraged by the rich reactivity showed by enynes, Cárdenas and co-workers<sup>[21]</sup> also demonstrated that dienyynes are suitable substrates in the palladium-catalyzed borylative ring-closing reaction (Scheme 1.8b). Moreover, non-conjugated systems containing polyunsaturated multiple C-C bonds also participate of this transformation leading to double cyclization products in a one-pot reaction (Scheme 1.8c).<sup>[22]</sup>

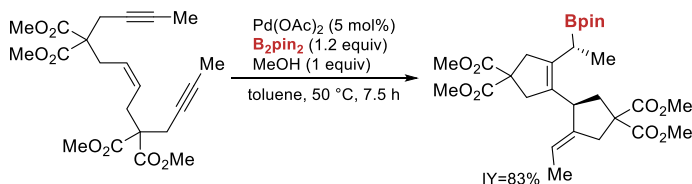
#### a) Borylative ring-closing of enynes



#### b) Borylative ring-closing of dienyynes



#### c) Borylative ring-closing of polyunsaturated compounds containing nonconjugated multiple C-C bonds

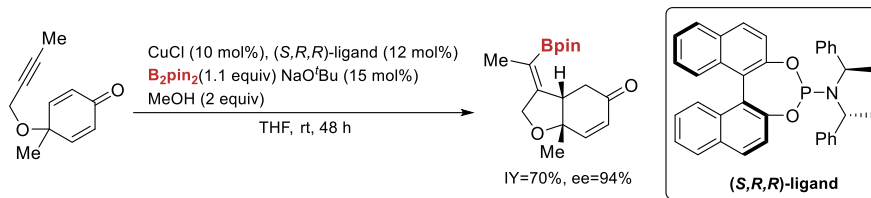


**Scheme 1.8** Borylative ring-closing of enynes, dienyynes or polyunsaturated substrates catalyzed by palladium.

The use of copper for the enantioselective borylative cyclization of enynes was also demonstrated by Lin and co-workers.<sup>[23]</sup> This reaction proceeds with the use of CuCl and a chiral phosphoramidite ligand, which facilitate the  $\beta$ -borylation of the internal alkyne by subsequent conjugated addition to the Michael acceptor. Hence, provided the formation of the targeted products with good yields and high levels of enantioselectivity (Scheme 1.9).

## Introduction

---



**Scheme 1.9** Copper-catalyzed enantioselective borylative cyclization of cyclic 1,6-enynes.

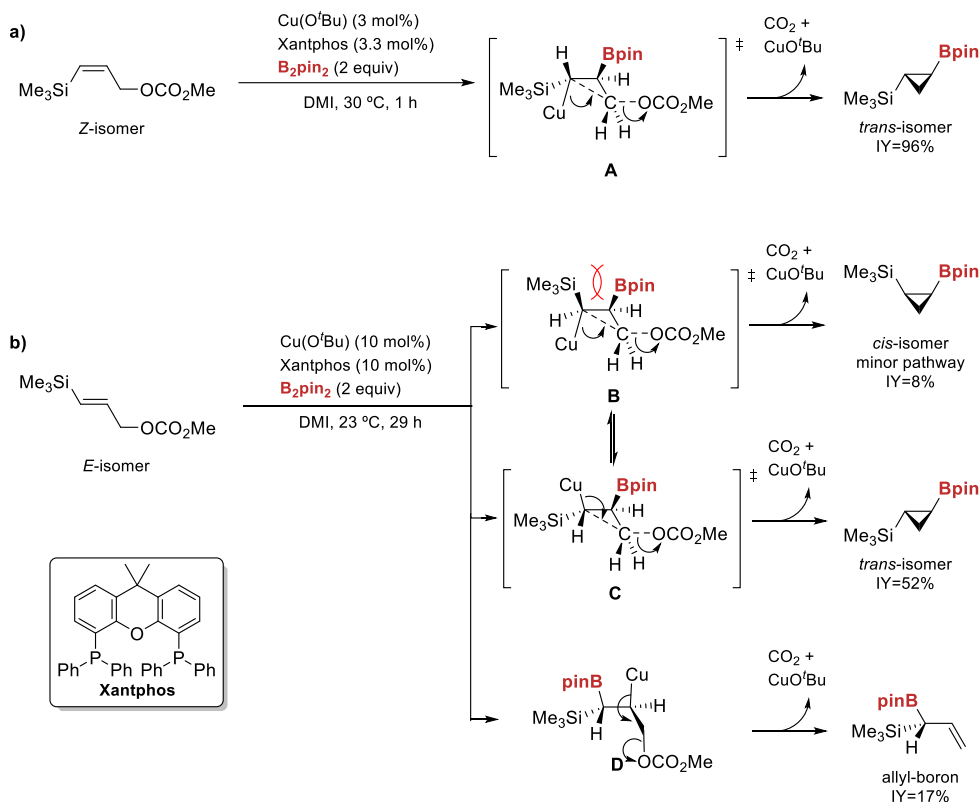
## 1.4. Intramolecular borylative cyclization of alkenes

The transition metal catalyzed addition of diboron reagents to double bonds can generate hydroborated products<sup>[24]</sup> or lead to intramolecular cyclization products via 1,2-carboboration process when electrophilic sites are present in the same molecule. A variety of alkenes bearing different leaving groups, carbonyl groups, isocyanides or imines can be employed for the carboboration reaction. The preferred catalysts for all these transformations are copper (I) complexes modified with basic ligands, such as phosphines or *N*-heterocyclic carbene ligands.

### 1.4.1 Borylative ring-closing of alkenes bearing good leaving groups

The copper (I) catalyzed ring-closing reaction of alkenes, in substrates containing good leaving groups, commonly proceeds via regioselective addition of the boryl copper (I) species, forming the *endo*- or *exo*-cyclic product under substrate control, followed by subsequent intramolecular nucleophilic substitution to the C-LG (LG= leaving group), with the concomitant formation of the cyclic borylated product.

Ito and Sawamura's group<sup>[25]</sup> reported the first copper catalyzed intramolecular carboboration process with the use of silylated allylic carbonates and B<sub>2</sub>pin<sub>2</sub> as diboron reagent. The process leads to boryl cyclopropane derivatives with high efficiency. The stereochemistry of the alkene (*Z/E*) was found to have large influence on the reaction rate and chemoselectivity (Scheme 1.10). Notably, when the *Z*-isomer was used, a faster formation of the *trans*-cyclopropane isomer was observed, with high chemoselectivity and diastereoselectivity, without competition for the formation of the corresponding allyl boron compound. These results have been attributed to the activating effect from the corresponding silyl group (Scheme 1.10a). However, the reaction with the *E*-isomer required higher catalyst loading and longer reaction times compared to the *Z*-isomer and displayed lower reactivity, chemoselectivity and *trans/cis*-diastereoselectivity (Scheme 1.10b). Once the *E*-isomer is submitted to borylative conditions, the intermediate **B** might be formed with retention of the configuration leading to the formation of the *cis*-isomer. However intermediate **B** is disfavored due to the steric hindrance between the silyl group and the boron unit, being this a minor reaction pathway (Scheme 1.10b).



**Scheme 1.10** Study of substrate effect (*Z/E*-isomer) on the copper (I) catalyzed borylative cyclization.

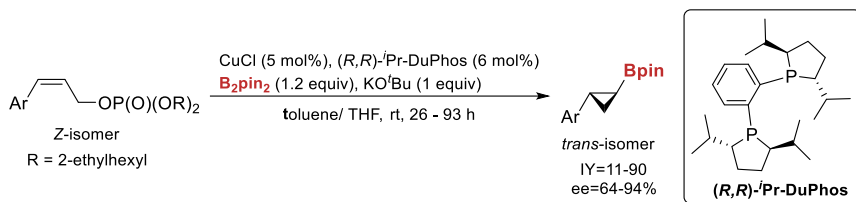
For that reason, intermediate **B** might undergo interconversion to intermediate **C**, which demands an inversion of the Cu-C bond configuration and a pseudo linear Cu-C-C-O arrangement. Intermediate **C** would then be the major reaction pathway to provide the *trans*-isomer. Due to the slow formation of the cyclopropane ring with the *E*-isomer, it seems reasonable that the formation of the allyl boron compound competes.

Additionally, the enantioselective version of this reaction was developed for the *Z*-isomer as substrate and the use of (*R,R*)-QuinoxP\* as chiral ligand. The reaction took place with high enantioselectivity, affording exclusively the formation of the (1*S*,2*S*)-(trimethylsilyl)cyclopropan-2-ylboronate.

The same group reported a new asymmetric synthesis of aryl and heteroaryl substituted cyclopropanes from the corresponding *Z*-allylic phosphate and (*R,R*)-*i*-Pr-DuPhos as chiral ligand. Under these conditions a variety of *trans*-cyclopropane products substituted with different aryl and heteroaryl groups could be obtained

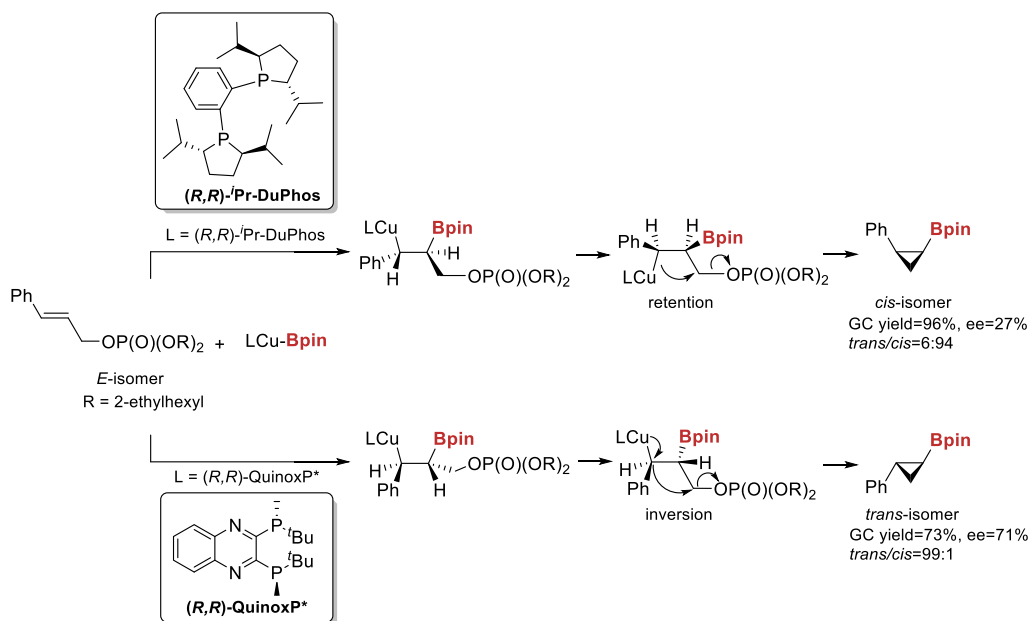
## Introduction

(Scheme 1.11).<sup>[26]</sup> The best enantioselectivities were observed when electron-donating substituents were placed in the benzene ring. Different functional groups such as chloro, ether, ester, BocNR<sub>2</sub>, and acetal are tolerated in this transformation.



**Scheme 1.11** Borylative ring-closing of aryl substituted alkenes with phosphate as leaving group.

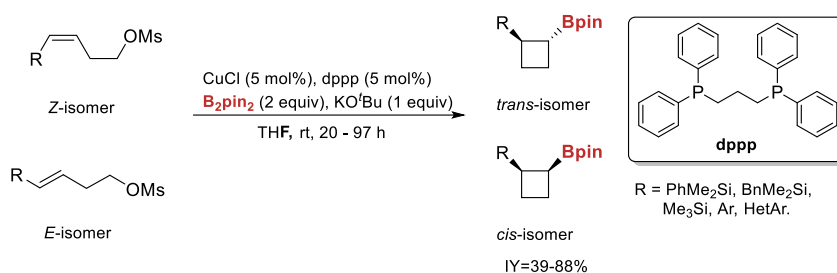
Furthermore, when the corresponding *E*-allylic phosphates were submitted to the borylative conditions, a ligand dependence was observed. Switching from the (R,R)-iPr-DuPhos to the (R,R)-QuinoxP\*, *cis*-cyclopropane or the *trans*-cyclopropane were formed respectively in excellent yield (Scheme 1.12).



**Scheme 1.12** Ligand dependence on the formation of the *cis/trans*-cyclopropane isomer.

As depicted in Scheme 1.12, when the *E*-isomer was submitted to borylative conditions with  $(R,R)$ -*i*-Pr-DuPhos, the intermediate formed underwent intramolecular substitution with retention of the stereochemistry towards the formation of the *cis*-isomer. In contrast, when the ligand of choice was  $(R,R)$ -QuinoxP\*, it was suggested that an inversion of the stereochemistry should take place during the cyclization process, hence leading to the formation of the *trans*-isomer.

Similar reactivity was observed by Ito and Sawamura<sup>[27]</sup> in the borylative cyclization of the corresponding *E*- and *Z*-homoallylic substituted sulfonates. This reaction generated the corresponding 1,2-disubstituted cyclobutanes in a stereospecific *cis*- or *trans*-manner (Scheme 1.13).

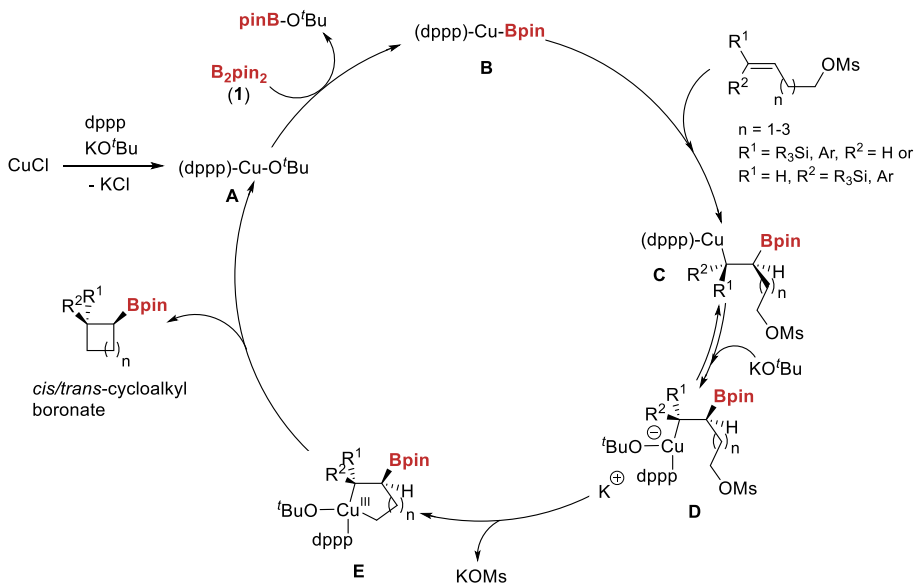


This reactivity is in contrast to the observed reactivity in previous studies with *E*- or *Z*-allylic carbonates,<sup>[25]</sup> where only the *trans*-cyclopropane isomer was obtained as the predominant product independently of the configuration of the starting alkene. Interestingly, the transformation was extended the formation of the five and six cyclic membered ring. However, in the second case only traces were observed.

In this work, a mechanistic proposal for the borylative cyclization of alkenes wearing good leaving groups was reported for the first time (Scheme 1.14).<sup>[27]</sup>



## Introduction

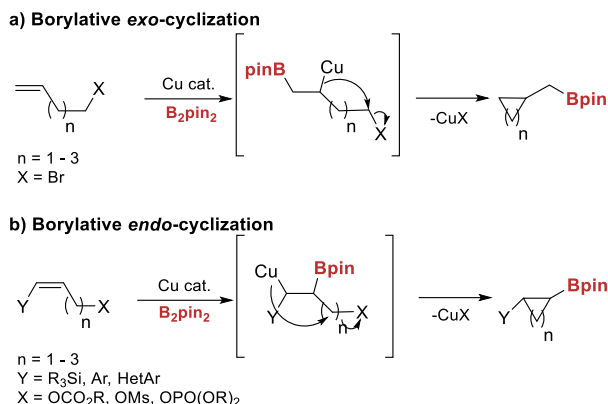


**Scheme 1.14** Suggested mechanism for the borylative ring-closing catalyzed by copper.<sup>[27]</sup>

The catalytic cycle starts with the generation of the specie **A**, formed from the reaction of CuCl, KO<sup>t</sup>Bu and dppp. Then, upon addition of **1** through  $\sigma$ -bond metathesis the reactive specie **B** is formed. At that point, the insertion of the Cu-B specie **B** into the double bond of the substrate leading to **C** occurs regioselectively and it is stabilized by the electronic effect of the adjacent silyl or aryl group (R<sup>1</sup> or R<sup>2</sup>). Then, coordination of KO<sup>t</sup>Bu (**D**) favors the intramolecular oxidative addition towards intermediate **E**. Finally, reductive elimination in **E** generated the cycloalkyl boronate product and recovers the active specie **A** (Scheme 1.14).

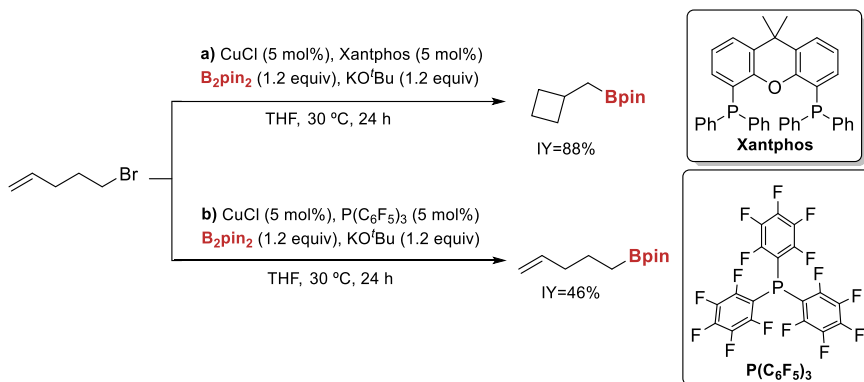
The fact that the ring-closing step proceeds through the Cu (III) metallacycle intermediate **E** is in agreement with the traces of product observed for the formation of the six-membered ring. The formation of the four- and five-membered rings occurs with good yields, as it would go through a five- and six-metallacycle intermediate. However, the formation of the six-membered ring involves an unfavored seven-metallacycle Cu (III) intermediate, hence the low efficiency of the cyclization.

Ito and co-workers,<sup>[28]</sup> also reported on the cyclization of the more challenging non-activated alkenes. Interestingly, the reaction takes place with opposite regioselectivity providing the *exo*-cyclic product (Scheme 1.15a), meanwhile in the previous works dealing with activated alkenes the *endo*-cyclized products were obtained (Scheme 1.15b).<sup>[27]</sup>



**Scheme 1.15** Possible borylative cyclization pathways catalyzed by copper (I) salts.

The first copper (I) catalyzed *exo*-cyclic carboboration process was developed using alkenyl bromine as substrates and Xantphos as ligand (Scheme 1.16a). However, strikingly, when an electron deficient monodentate phosphine ligand was used instead, the major compound observed was the non-cyclic borylated product with only traces of the desired cyclized compound (Scheme 1.16b).<sup>[29]</sup>



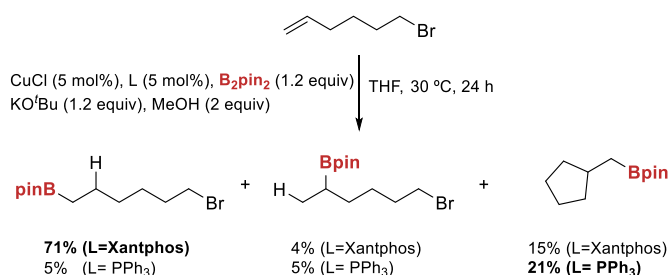
**Scheme 1.16** Effect of the phosphine in the borylative cyclization of 5-bromopentene.

Under the optimal conditions a wide range of substrates led to the formation of the corresponding three-, four- and five-membered boryl substituted cyclic products. The preparation of boryl six-membered ring products proved challenging and was unsuccessful.

Marder and co-workers<sup>[29b]</sup> suggested that the use of  $\text{PPh}_3$  as ligand could lead to the formation of the five-membered ring borylated compound. In order to understand this transformation, Ito and co-workers performed some experiments

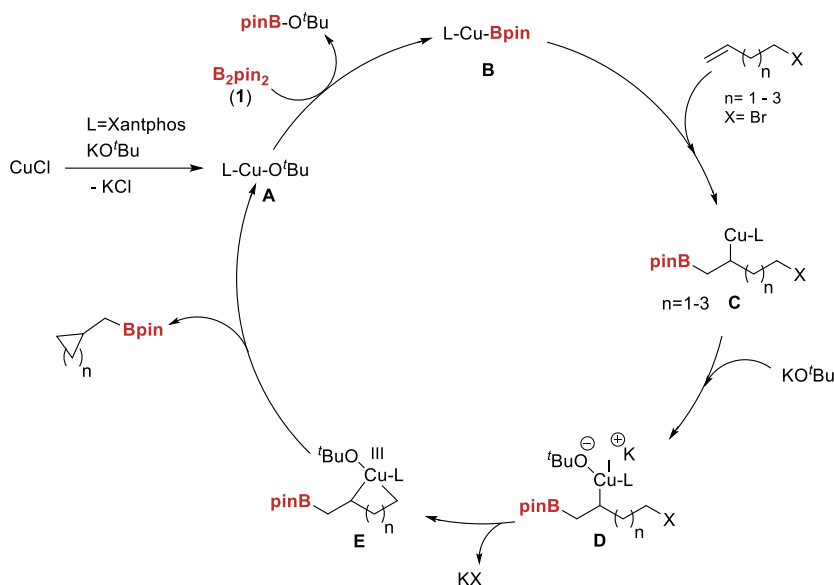
## Introduction

to study whether the borylative cyclization goes through a radical pathway or not (Scheme 1.17). The difference on the mechanism was evidenced through protonation experiments. Hence, adding 2 equiv of MeOH as the proton source, when Xantphos was used as ligand, the hydroborated compounds were now isolated as major products. This suggest that the cyclization proceeds through the borylcupration of the alkene, then the MeOH protonates the C-Cu bond to render the hydroborated product. In contrast, when PPh<sub>3</sub> was used, the cyclized product was formed predominantly even in the presence of MeOH. From these experiments, it was concluded that using PPh<sub>3</sub> the reaction would proceed through a radical mediated pathway, since no effect was detected by addition of MeOH as proton source.



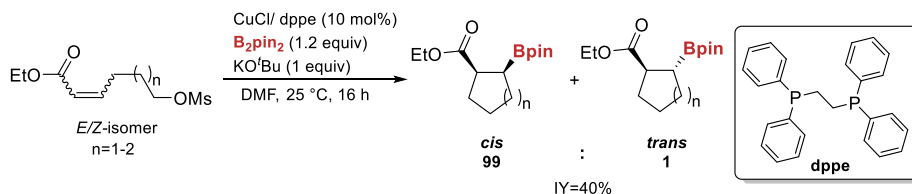
**Scheme 1.17** Influence of the proton source in the reaction outcome.

A mechanistic proposal has been suggested from this work (Scheme 1.18). Once the copper (I) alkoxide (**A**) is formed via reaction of CuCl, ligand and KO<sup>t</sup>Bu, it reacts with the diboron reagent **1**, which via  $\sigma$ -bond metathesis might form the borylcopper (I) reactive specie **B**. When Xantphos was used, due to the higher HOMO energy of copper complex formed, intermediate **B** has the ability to undergo the insertion into the non-activated alkene to form the alkyl copper species **C** with concomitant formation of an ionic complex **D** by coordination of the alkoxide. Subsequent intramolecular oxidative addition and elimination of bromide with inversion of the stereochemistry provides the copper (III) metallacycle intermediate **E**. Finally, reductive elimination of the copper species to produce the borylated cyclized product, and the regeneration of the catalyst to form **A** closes the catalytic cycle. The proposed mechanism explains why formation of the six-membered ring would not proceed, since reductive elimination would occur on a disfavored seven-membered metallacycle (**E**).



**Scheme 1.18** Proposed mechanism for the exo-borylative cyclization of non-activated alkenes.

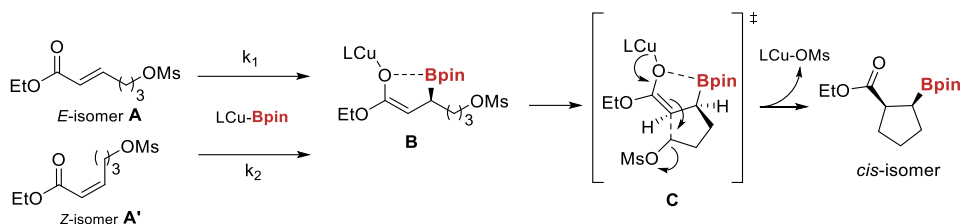
More recently, Zhong and co-workers<sup>[30]</sup> reported for the first time the stereoconvergent copper catalyzed borylative cyclization of  $\alpha,\beta$ -unsaturated esters and ketones bearing a *O*-mesylate as leaving group (Scheme 1.19).



**Scheme 1.19** Stereoconvergent formation of cycloalkyl boronates.

With the use of 10 mol% dppe, the exclusive formation of the *cis*-product was observed either starting from the *E*- or *Z*- $\omega$ -mesylate-functionalized  $\alpha,\beta$ -unsaturated ester. This methodology allows the formation of the five- and six-membered cycloalkyl boronate esters in good yields. The authors proposed the reactions mechanism shown in Scheme 1.20 to explain the formation of the *cis*-product from both the *E*- and *Z*-isomer.

## Introduction



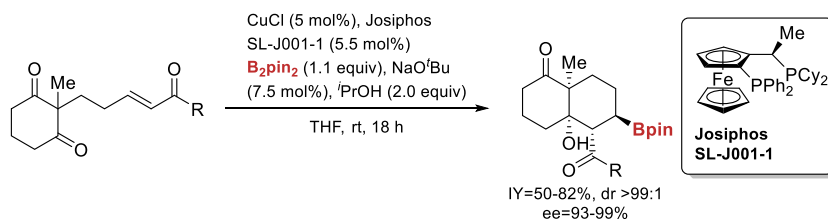
**Scheme 1.20** Plausible mechanism for the stereoconvergent formation of the *cis*-product.

The addition of the boryl copper species to **A** or **A'** involves a fast enolization process to form species **B**. From this moment, a coordination between the oxygen and the boryl moiety might occur, facilitating the formation of the five membered ring enolate. Subsequent intramolecular nucleophilic substitution reaction via transition state **C**, where the boryl moiety and the ester group are at the same side, leads to the *cis*-product.

### 1.4.2 Borylative ring-closing of alkenes bearing carbonyl electrophiles

Complementary to a nucleophilic substitution, the addition to carbonyl electrophiles also provides a variety of cyclic borylated products while generating an extra alcohol functional group. Commonly these reactions proceed through the regioselective addition of the boryl copper (I) species to the double bond, followed by intramolecular addition to the carbonyl group.

The group of Lam<sup>[31]</sup> reported for the first time the enantioselective copper catalyzed tandem conjugated borylation/aldol ring-closing reaction of  $\alpha,\beta$ -unsaturated ketones providing a variety of bicyclic boronates of five- and six-membered rings. During the formation of the bicyclic systems, a desymmetrization process took place with the generation of the C-B bond and the new C-C bond along with four contiguous stereocenters with high diastereoselectivity and enantioselectivity (Scheme 1.21).



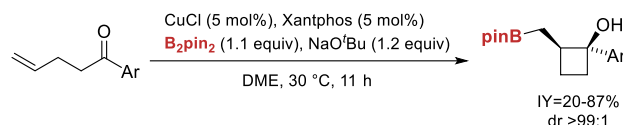
**Scheme 1.21** Borylative aldol cyclizations of enone diones to form decalines.

The selectivity of this reaction can be explained by a Zimmerman-Traxler-type model, that propose that some aldol reactions have six-membered transition states having a chair conformation, with the observed diastereoisomer being formed through the corresponding aldol cyclization in the *Z*-enolate transition state (Scheme 1.22).



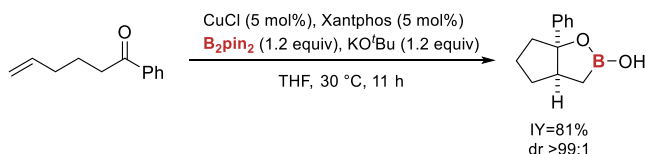
**Scheme 1.22** Explanation through the Zimmerman-Traxler-type model.

Ito and co-workers<sup>[32]</sup> reported the copper (I) catalyzed diastereoselective borylative ring-closing reaction of  $\gamma$ -alkenyl aryl ketones, providing a variety of *syn*-1-aryl-2-(borylmethyl)cyclobutanol derivatives in moderate to high yields and with excellent diastereoselectivity (Scheme 1.23).



**Scheme 1.23** Borylative ring-closing of alkenyl aryl ketones catalyzed by copper (I) salts.

In this transformation, the boryl copper (I) species reacts with the terminal alkene in a regioselective manner, followed by an intramolecular 1,2-addition of the ketone carbonyl group to afford the borylated cyclobutanol derivative. A longer carbon-chain in the substrate led to the bicyclic structure containing a 1,2-oxaborolane, with high yield and excellent diastereoselectivity (Scheme 1.24).

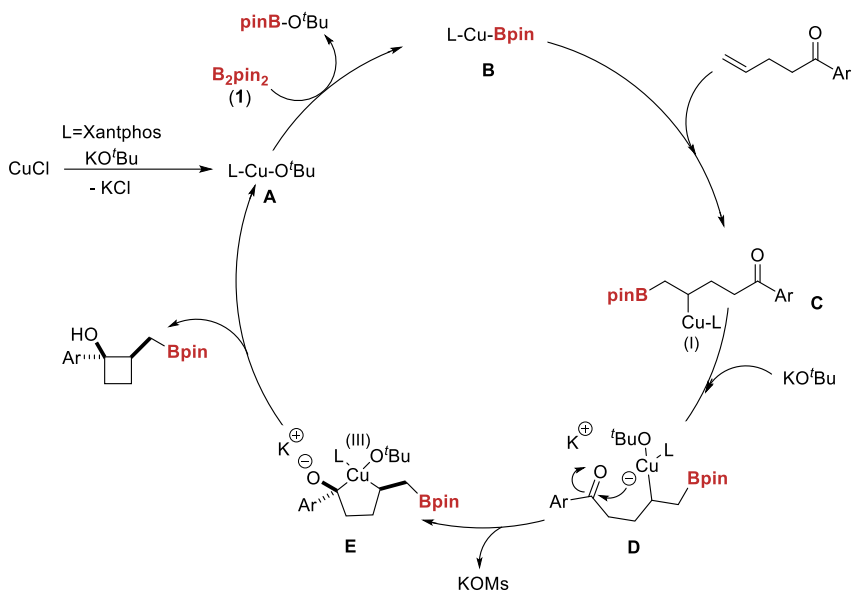


**Scheme 1.24** Oxaborolane formation through  $\delta$ -alkenyl phenyl ketone catalyzed by copper (I) salt.

The mechanistic proposal for the borylative cyclization with intramolecular addition to carbonyl groups is shown in Scheme 1.25. The suggested catalytic cycle starts

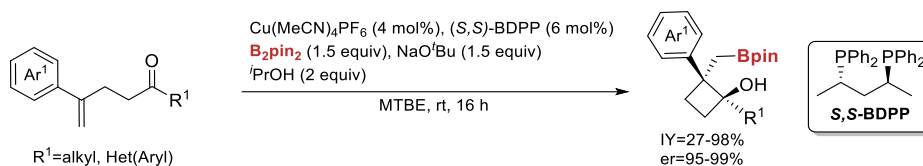
## Introduction

with the formation of the  $\text{LCu}^{\text{I}}\text{O}^t\text{Bu}$  complex **A**, which upon reaction with **1** via  $\sigma$ -bond metathesis provides the active boryl copper (I) species **B**. The L-Cu-Bpin complex has the ability to insert into the alkene to form the alkyl copper (I) species **C**. Subsequent coordination of the alkoxy group facilitates the formation of the more nucleophilic cuprate **D**. Further intramolecular nucleophilic attack of the copper (I) to the carbonyl carbon may occur to form the dialkylcopper (III) **E**, which follows a reductive elimination leading to the formation of the organoborane cyclized product and recovery of the active species **A**. The *syn*-selectivity observed in the resulting products could be attributed to the favored transition state through the less sterically hindered pathway (Scheme 1.25).



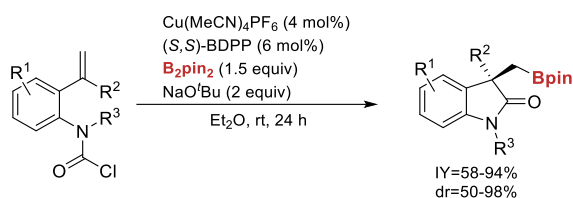
**Scheme 1.25** Proposed mechanism of the borylative cyclization with intramolecular addition to the carbonyl.

More recently, Lautens and co-workers<sup>[33]</sup> reported the enantioselective version of alkenes containing aryl ketones. This transformation involved the use of alkenes which have tethered different aryl groups and the use of (*S,S*)-BDPP as chiral ligand, providing a wide scope of products in moderate to excellent yields and excellent enantiomeric ratios (Scheme 1.26).



**Scheme 1.26** Enantioselective borylative ring-closing through substituted diarylpentenones.

The same group developed the enantioselective copper catalyzed intramolecular borylacylation of carbamoyl chlorides giving access to chiral borylated 3,3-disubstituted oxindoles (Scheme 1.27).<sup>[34]</sup>



**Scheme 1.27** Enantioselective intramolecular copper-catalyzed borylacylation.

The position and nature of the substituents ( $\text{R}^1$ ) in the aromatic ring played a role in the reaction outcome. Thus, electron-withdrawing substituents led to lower reaction yields and enantioselectivities. Substituents at *ortho*-position to the alkene tend to diminish the enantioselectivities. Substituents in *para*-position were in general detrimental and a large decrease in the enantioselectivities, as well as longer reaction times, were observed.

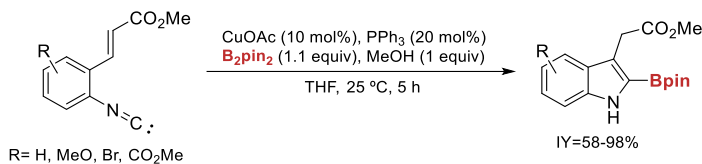
The influence of the alkene substituent ( $\text{R}^2$ ) was also examined. Slightly changes in this substituent affect directly to the reaction outcome in terms of yield and enantioselectivity. A good diversity of substituents in nitrogen atom ( $\text{R}^3$ ) was tolerated leading to the formation of the cyclized products with very good yields and enantioselectivities.

### 1.4.3 Borylative ring-closing of alkenes bearing isocyanides

Chatani and co-workers<sup>[35]</sup> have reported the only example of borylative cyclization reaction with alkenes bearing isocyanides. This transformation gives access to a variety of different 2-borylindoles (Scheme 1.28).

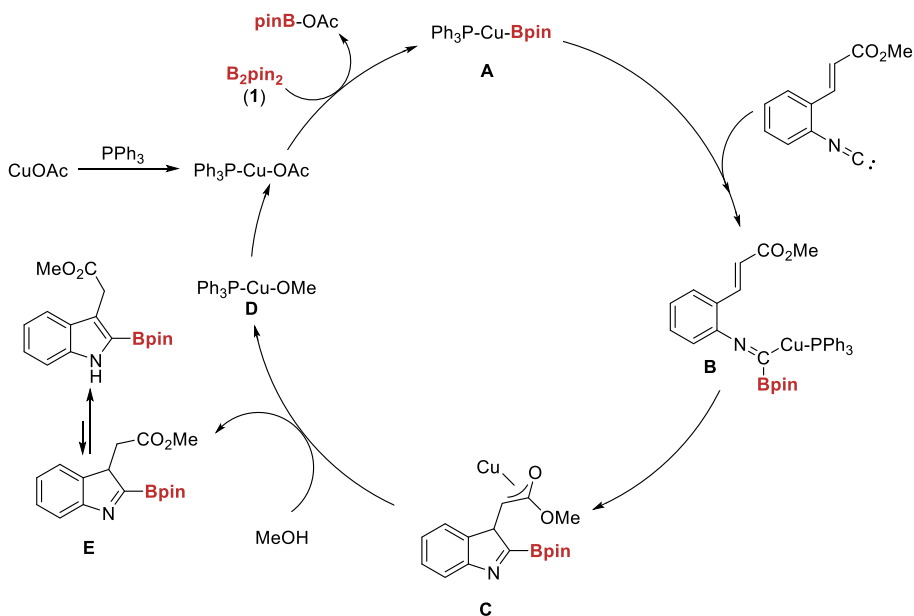


## Introduction



**Scheme 1.28** Copper catalyzed borylative cyclization of 2-alkenylaryl isocyanides.

Inverse reactivity has been observed since the boryl copper (I) species reacts first with the isocyanide group (Scheme 1.29), which is in contrast to the previous reactivity observed with alkenes bearing good leaving groups or containing carbonyl electrophiles where the boryl copper (I) species reacts first with the alkene. The proposed catalytic cycle is shown in (Scheme 1.29). The catalytic borylation starts with the addition of the reactive boryl copper (I) species to the isocyanide group of the substrate to form **B**. Subsequent intramolecular 1,4-addition of imido-copper **B** leads to the formation of the copper enolate **C**. Then MeOH is required to generate the borylated indole product **E** and the Cu-OMe (**D**) to end up with the transmetalation that regenerate the species **A**.

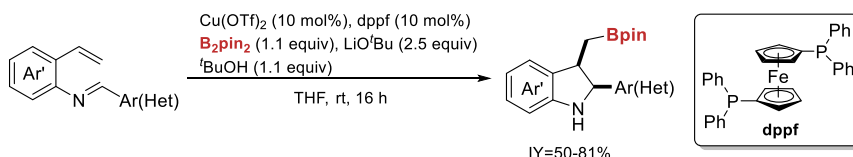


**Scheme 1.29** Plausible mechanism for the borylative cyclization of alkenes bearing isocyanides.

### 1.4.4 Borylative ring-closing of alkenes bearing imines

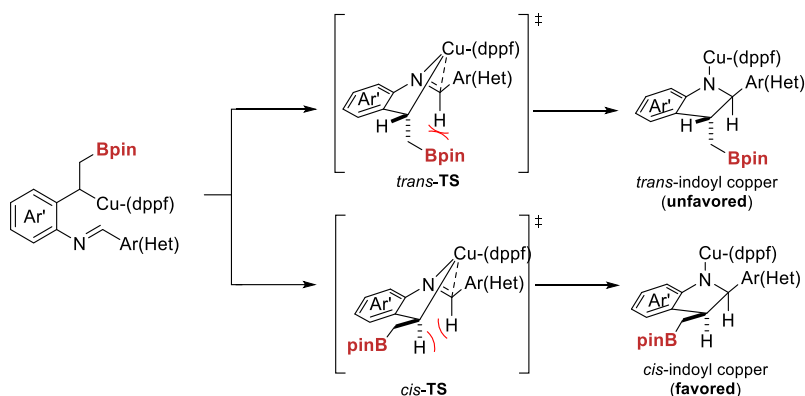
Due to the pharmaceutical interest of 2,3-disubstituted indoles two examples of synthesis have been reported through borylative ring-closing of alkenes bearing imines.

Xu and co-workers<sup>[36]</sup> developed the first borylative ring-closing reaction bearing imines with different functional groups providing a wide range of 2,3-disubstituted indolines (Scheme 1.30).



**Scheme 1.30** Borylative cyclization of substituted N-(2-vinylaryl)benzaldimines catalyzed by copper.

The proposed reaction mechanism involves the insertion of L-Cu-Bpin species in the alkene and subsequent addition to the electrophilic position of the imine, providing the 2,3-disubstituted indoline derivatives with high diastereoselectivities, with the exclusive formation of the *cis*-product (Scheme 1.31).



**Scheme 1.31** Suggested explanation for the diastereoselectivity

It has been suggested that the diastereoselectivity might be controlled in the step coming from the favored *cis*-transition state established after the Cu-Bpin insertion into the C=C bond. Observing the two transition states formed, the *trans*-TS suffers from steric hindrance between the CH<sub>2</sub>Bpin moiety and the hydrogen from the imine. Contrarily, the *cis*-TS has the CH<sub>2</sub>Bpin moiety pointing out and the two

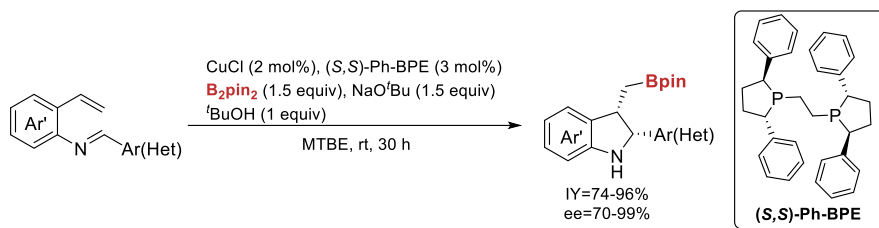
## Introduction

---

hydrogens in the same direction being more favored than the analogous mentioned *trans*-**TS**.

Following this reactivity the group of Zhang<sup>[37]</sup> developed the enantioselective version of the reaction.

Some modifications in the catalytic system as well as, the use of a chiral ligand as (*S,S*)-Ph-BPE and the use of an ethereal solvent allowed the preparation of boryl indolines with high chemoselectivity, diastereoselectivity and enantioselectivity (Scheme 1.32). A wide scope of different products was prepared containing aryl and heteroaryl systems, with substituents placed in *ortho*-, *meta*- and *para*-position. However, the efficiency of the reaction is directly affected to modifications around the substrate.



**Scheme 1.32** Enantioselective synthesis of 2,3-disubstituted boryl indoles.

## 1.5. References Chapter 1

- [1] a) E. Fernández, A. Whiting, *Synthesis and Application of Organoboron Compounds*, Vol. 49, Springer, Berlin, **2015**; b) D. G. Hall, *Boronic Acids: Preparation and Applications in Organic Synthesis, Medicine and Materials*, 2nd ed., Wiley-VCH, Weinheim, **2011**; c) E. C. Neeve, S. J. Geier, I. A. I. Mkhalid, S. A. Westcott, T. B. Marder, *Chem. Rev.* **2016**, *116*, 9091-9161.
- [2] A. B. Cuenca, R. Shishido, H. Ito, E. Fernández, *Chem. Soc. Rev.* **2017**, *46*, 415-430.
- [3] a) N. Miralles, R. J. Maza, E. Fernández, *Adv. Synth. Catal.* **2018**, *360*, 1306-1327; b) R. Nallagonda, K. Padala, A. Masarwa, *Org. Biomol. Chem.* **2018**, *16*, 1050-1064; c) C. Wu, J. Wang, *Tetrahedron Lett.* **2018**, *59*, 2128-2140.
- [4] S. A. Westcott, J. D. Webb, D. I. Mclsaac, C. M. Vogels, **2006/089402 A1 Patent**.
- [5] K. Kubota, H. Iwamoto, H. Ito, *Org. Biomol. Chem.* **2017**, *15*, 285-300.
- [6] K. Kubota, H. Iwamoto, E. Yamamoto, H. Ito, *Org. Lett.* **2015**, *17*, 620-623.
- [7] H. Iwamoto, Y. Ozawa, K. Kubota, H. Ito, *J. Org. Chem.* **2017**, *82*, 10563-10573.
- [8] M. Xiong, H. Hu, X. Hu, Y. Liu, *Org. Lett.* **2018**, *20*, 3661-3665.
- [9] S. H. Kim, I. Alonso, P. Mauleón, R. G. Arrayás, J. C. Carretero, *ACS Catal.* **2018**, *8*, 8993-9005.
- [10] E. Buñuel, D. J. Cárdenas, *Eur. J. Org. Chem.* **2016**, *2016*, 5446-5464.
- [11] J. Huang, S. J. F. Macdonald, J. P. A. Harrity, *Chem. Commun.* **2010**, *46*, 8770-8772.
- [12] T. Miura, Y. Takahashi, M. Murakami, *Org. Lett.* **2008**, *10*, 1743-1745.
- [13] Y. S. Zhao, X. Q. Tang, J. C. Tao, P. Tian, G. Q. Lin, *Org. Biomol. Chem.* **2016**, *14*, 4400-4404.
- [14] M. Xiong, X. Xie, Y. Liu, *Org. Lett.* **2017**, *19*, 3398-3401.
- [15] V. Pardo, J. M. Martínez, E. Buñuel, D. J. Cárdenas, *Org. Lett.* **2009**, *11*, 4548-4551.
- [16] a) Y. Deng, T. Bartholomeyzik, J.-E. Bäckvall, *Angew. Chem. Int. Ed.* **2013**, *52*, 6283-6287; b) Y. Deng, T. Bartholomeyzik, A. K. Å. Persson, J. Sun, J.-E. Bäckvall, *Angew. Chem. Int. Ed.* **2012**, *51*, 2703-2707.
- [17] A. K. Å. Persson, T. Jiang, M. T. Johnson, J. E. Bäckvall, *Angew. Chem. Int. Ed.* **2011**, *50*, 6155-6159.

## Introduction

---

- [18] T. Jiang, T. Bartholomeyzik, J. Mazuela, J. Willersinn, J.-E. Bäckvall, *Angew. Chem. Int. Ed.* **2015**, *54*, 6024-6027.
- [19] a) V. Pardo, E. Buñuel, D. Collado, D. J. Cárdenas, *Chem. Commun.* **2012**, *48*, 10517-10519; b) J. M. Martínez, V. López, E. Buñuel, R. Simancas, D. J. Cárdenas, *J. Am. Chem. Soc.* **2007**, *129*, 1874-1875.
- [20] A. Martos, R. López, E. Buñuel, D. J. Cárdenas, *Chem. Commun.* **2014**, *50*, 10094-10097.
- [21] R. López, A. Martos, E. Buñuel, V. Pardo, D. J. Cárdenas, *Chem. Commun.* **2013**, *49*, 10691-10693.
- [22] J. M. Martínez, E. Buñuel, R. Muñoz, D. J. Cárdenas, *Org. Lett.* **2008**, *10*, 3619-3621.
- [23] P. Liu, Y. Fukui, P. Tian, Z. T. He, C. Y. Sun, N. Y. Wu, G. Q. Lin, *J. Am. Chem. Soc.* **2013**, *135*, 11700-11703.
- [24] Cathleen M. Crudden, D. Edwards, *Eur. J. Org. Chem.* **2003**, *2003*, 4695-4712.
- [25] H. Ito, Y. Kosaka, K. Nonoyama, Y. Sasaki, M. Sawamura, *Angew. Chem. Int. Ed.* **2008**, *47*, 7424-7427.
- [26] C. Zhong, S. Kunii, Y. Kosaka, M. Sawamura, H. Ito, *J. Am. Chem. Soc.* **2010**, *132*, 11440-11442.
- [27] H. Ito, T. Toyoda, M. Sawamura, *J. Am. Chem. Soc.* **2010**, *132*, 5990-5992.
- [28] K. Kubota, E. Yamamoto, H. Ito, *J. Am. Chem. Soc.* **2013**, *135*, 2635-2640.
- [29] a) H. Ito, K. Kubota, *Org. Lett.* **2012**, *14*, 890-893; b) C. T. Yang, Z. Q. Zhang, H. Tajuddin, C. C. Wu, J. Liang, J. H. Liu, Y. Fu, M. Czyzewska, P. G. Steel, T. B. Marder, L. Liu, *Angew. Chem. Int. Ed.* **2012**, *51*, 528-532.
- [30] Y. J. Zuo, X. T. Chang, Z. M. Hao, C. M. Zhong, *Org. Biomol. Chem.* **2017**, *15*, 6323-6327.
- [31] A. R. Burns, J. Solana González, H. W. Lam, *Angew. Chem. Int. Ed.* **2012**, *51*, 10827-10831.
- [32] E. Yamamoto, R. Kojima, K. Kubota, H. Ito, *Synlett* **2016**, *27*, 272-276.
- [33] A. Whyte, B. Mirabi, A. Torelli, L. Prieto, J. Bajohr, M. Lautens, *ACS Catal.* **2019**, *9*, 9253-9258.

- [34] A. Whyte, K. I. Burton, J. Zhang, M. Lautens, *Angew. Chem. Int. Ed.* **2018**, *57*, 13927-13930.
- [35] M. Tobisu, H. Fujihara, K. Koh, N. Chatani, *J. Org. Chem.* **2010**, *75*, 4841-4847.
- [36] H. M. Wang, H. Zhou, Q. S. Xu, T. S. Liu, C. L. Zhuang, M. H. Shen, H. D. Xu, *Org. Lett.* **2018**, *20*, 1777-1780.
- [37] G. Zhang, A. Cang, Y. Wang, Y. Li, G. Xu, Q. Zhang, T. Xiong, Q. Zhang, *Org. Lett.* **2018**, *20*, 1798-1801.

UNIVERSITAT ROVIRA I VIRGILI  
COMPLEMENTARY SYNTHESIS OF ORGANOBORANES TO POPULATE THE CHEMICAL  
FUNCTIONALITY TO A GIVEN AREA OF BIOMEDICAL INTEREST  
Jordi Royes Buisan

# Chapter 2

## Objectives

---



UNIVERSITAT ROVIRA I VIRGILI  
COMPLEMENTARY SYNTHESIS OF ORGANOBORANES TO POPULATE THE CHEMICAL  
FUNCTIONALITY TO A GIVEN AREA OF BIOMEDICAL INTEREST  
Jordi Royes Buisan

## 2.1. Specific objectives of the thesis

The **specific objectives** of the thesis are:

- The generation of a method for the insertion of the diazo compound  $\text{CH}(\text{N}_2)(\text{SiMe}_3)$  into B-S  $\sigma$ -bonds of pinB-SR reagents to promote a direct synthesis of multisubstituted  $\text{sp}^3$  carbons in  $\text{CH}(\text{Bpin})(\text{SiMe}_3)(\text{SR})$ . The objective also involves the selective derivatization of  $\text{CH}(\text{Bpin})(\text{SiMe}_3)(\text{SR})$  via base-mediated alkylation including intramolecular cyclizative reactions.
  
- The study of the borylative cyclization of alkenes containing good leaving groups to form spiro-bicyclic compounds. This objective is based on the copper (I) catalyzed reaction, searching for optimized reaction conditions and general scope.
  
- The application of borylative cyclization methodologies to the preparation of spiro-cyclic scaffolds and their derivatization towards a series of *O*-GlcNAcase inhibitors with potential interest for the treatment of Alzheimer's disease.
  
- The development of a synthetic methodology towards the borylative cyclization of alkenes containing an aldehyde group via copper (I) complexes, with a special emphasis on the diastereoselectivity of the process.

UNIVERSITAT ROVIRA I VIRGILI  
COMPLEMENTARY SYNTHESIS OF ORGANOBORANES TO POPULATE THE CHEMICAL  
FUNCTIONALITY TO A GIVEN AREA OF BIOMEDICAL INTEREST  
Jordi Royes Buisan

# Chapter 3

## Inter and intramolecular selective alkylations of $\text{CH}(\text{Bpin})(\text{SiMe}_3)(\text{SR})$ with alkyl halides

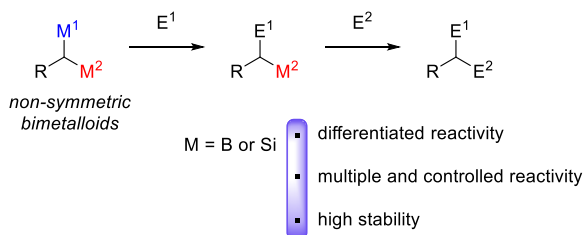
---

UNIVERSITAT ROVIRA I VIRGILI  
COMPLEMENTARY SYNTHESIS OF ORGANOBORANES TO POPULATE THE CHEMICAL  
FUNCTIONALITY TO A GIVEN AREA OF BIOMEDICAL INTEREST  
Jordi Royes Buisan

### 3.1. State of the art

The discovery of new and efficient processes that assure the access to complex molecular entities involving low number of chemical stages keeps constituting one of the main challenges of organic synthesis. Researchers have intensively focused on methodologies based on distinguishing reactivity patterns thus providing the convenient route in a stereocontrolled manner. Hence, it is necessary to synthesize substrates endowed with various substituents capable to undergo chemoselective reactivity, as the *geminal* organodimetallic compounds, for instance. Such kind of species presents two reactive and versatile nucleophiles which allow the straightforward preparation of diverse and useful building blocks for biomedical and material science needs.

For decades, the symmetrical or non-symmetrical *geminal* dimetallic reagents have been prepared using metals as lithium, magnesium, aluminum, copper, zinc or zirconium, among others. Despite all the possible combinations, and according to the experimental studies later described, we became interested in the use of metalloid species, such as boron and silicon, which provide a higher stability in terms of handling and storing, when compare with the rest of purely metallic species. They also provide multiple controlled reactivity, offering a great opportunity for their application in different selective demetallative alkylation sequences and/or in transition metal catalysis (Scheme 3.1).



**Scheme 3.1** Interest of bismetalloid compounds in a *geminal* arrangement.

In this context, along the next sections we will review some of the possible selective transformations that can be applied to *gem*-bismetalloid species. More precisely some selective alkylation reactions that are closely related to this work are going to be highlighted.

For instance, the type of *gem*-silyl boryl bismetalloid showed in Figure 3.1, could be selectively functionalized following three different strategies: a) deborylative-alkylation sequence in the presence of an oxygenated base, b) in the case of *Y* = silicon, and making use of the appropriate base, a selective desilylation-alkylation

## Inter and Intramolecular selective alkylations of CH(Bpin)(SiMe<sub>3</sub>)(SR) with alkyl halides

could be envisaged, and c) thanks to the acidity of the C-H bond located adjacent to the metalloid fragments, a classic deprotonation-alkylation approach could be as well imagined, thus giving access to interesting building blocks.<sup>[1]</sup>

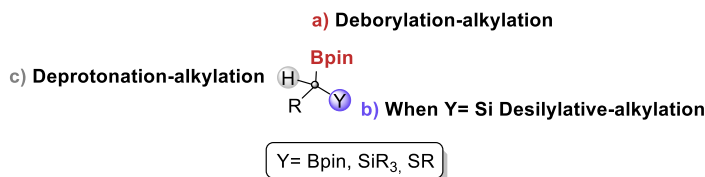


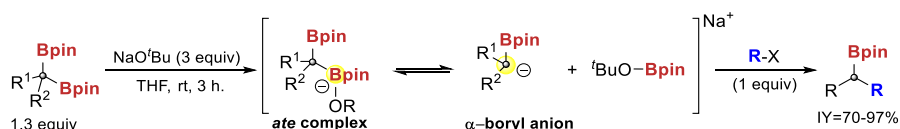
Figure 3.1 Selective functionalization of polymetalloids.

### 3.1.1 Selective deborylative alkylation of *geminal* diboron compounds

*Geminal* bis(boronate) compounds have demonstrated the ability to behave as nucleophilic partners in cross-coupling reactions. The outcome of this type of reactions is consistent with a mechanism involving the formation of an *ate* complex and its subsequent transmetalation. The possibility to generate in situ the corresponding *ate* complex of a *geminal* bis(boronate) that reacts with and electrophilic Pd complex, opens the door to the reaction of this type of species with other electrophiles like alkyl halides as we illustrate along the next sections.

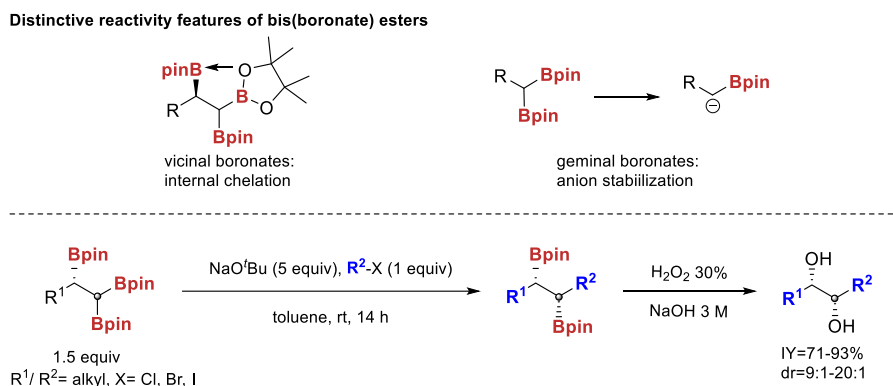
#### a) Intermolecular deborylative alkylation

Morken and co-workers<sup>[2]</sup> have taken advantage of the use of stable *geminal* bis(boronate) esters and reported the alkoxide assisted monodeborylative alkylation of these species with alkyl halides as electrophiles (Scheme 3.2). Experimental evidences demonstrate that these alkylations proceed through alkoxide induced deborylation and subsequent generation of the  $\alpha$ -boryl stabilized carbanion that it is in equilibrium with the formed *ate* complex, which, in turn, could be trapped with an alkyl halide electrophile (Scheme 3.2). To validate the versatility of the reaction, the transformation was applied to primary and secondary alkyl halides. The use of di-, mono- and non-substituted *gem*-diboron reagents was well tolerated.



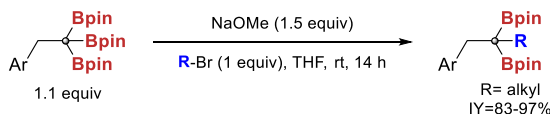
Scheme 3.2 Formation of  $\alpha$ -boryl carbanion by alkoxy assisted deborylation.

Interestingly, the same group was able to apply this deborylative functionalization to a series of 1,1,2-tris(boronates), compounds that also present two boronate fragments in a *geminal* disposition.<sup>[3]</sup> While using these substrates, it has been observed that their reactivity is partially governed by the relationship between the neighboring boronate units. Hence, the internal chelation by the adjacent boron units is proposed to enhance their Lewis acidity of one of the geminal boryl units, therefore facilitating the cross-coupling reaction in a highly efficient manner. On the other hand, the ability of three-coordinate boron to stabilize adjacent carbanions appears to facilitate deborylation of *geminal* bis(boronate) esters providing reactive  $\alpha$ -boryl carbanions. Since the carbanion formed is stable enough, it can be alkylated by addition of an electrophile. Moreover, these products were finally oxidized to produce the corresponding diols with enhanced diastereoselectivity (Scheme 3.3).



**Scheme 3.3** Stereoselective deborylative alkylation of 1,1,2-tris(boronate) derivatives.

Complementary, Huang and co-workers<sup>[4]</sup> reported the access to  $\alpha$ -boryl carbanions by the base-assisted deborylation of 1,1,1-tris(boronates) substrates. Noticeable, the 1,1,1-tris(boronate) esters seem to be more reactive than the corresponding 1,1,2-tris(boronate) compounds (Scheme 3.3) or 1,1-bis(boronate) compounds (Scheme 3.2), since lesser excess of the base is required to the formation of the *ate* complex; the necessary species for the successive alkylation to happen in an efficient manner (Scheme 3.4).



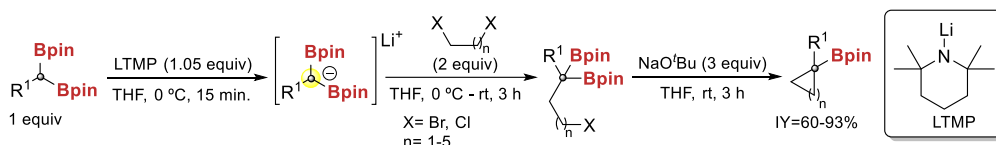
**Scheme 3.4** Selective deborylative alkylation of 1,1,1-tris(boronate) derivatives.



## Inter and Intramolecular selective alkylations of CH(Bpin)(SiMe<sub>3</sub>)(SR) with alkyl halides

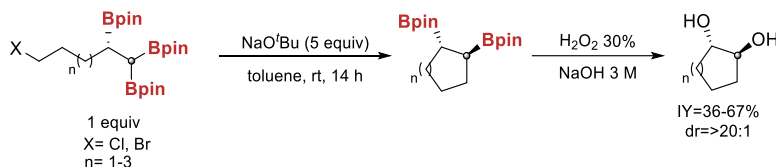
### b) Intramolecular deborylative alkylation

The rich reactivity demonstrated by the monodeborylative alkylation of *gem*-bis(boronates) could be even used in an intramolecular manner. Hence, if 1,*n*-dihalides are used in the first alkylation reaction, the product obtained can undergo subsequent ring forming reaction through intramolecular deborylative alkylation as reported by Morken and co-workers (Scheme 3.5).<sup>[2]</sup>



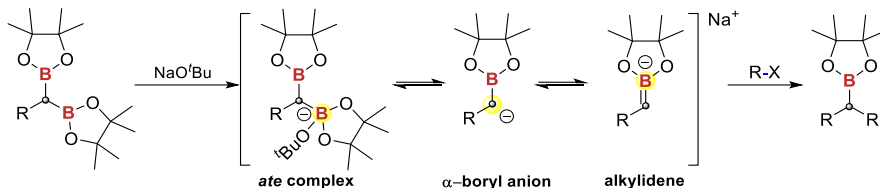
**Scheme 3.5** Intramolecular stereoselective deborylative alkylation of *gem*-bis(boronate) compounds.

The same group<sup>[3]</sup> demonstrated the feasibility of the intramolecular deborylative alkylation using 1,1,2-tris(boronate) compounds that presented an alkyl halide in their structure as substrates. One of the most reactive Bpin fragments among the three boryl moieties present in the molecule can be, in fact, alkylated in an intramolecular fashion by means of the use of an excess of NaO<sup>t</sup>Bu. In this way, a series of cyclic 1,2-bis(boronates) can be accessed. After the corresponding oxidative treatment, this transformation enables the formation of a range of cyclic diols in *anti*-disposition of different ring sizes (Scheme 3.6).



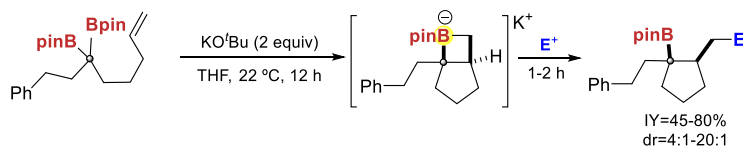
**Scheme 3.6** Intramolecular stereoselective deborylative alkylation of 1,1,2-tris(boronate) esters to construct cyclic diols.

The investigation of the real nature of these  $\alpha$ -boryl carbanions was object of a recent and very elegant study carried out by the group of Morken.<sup>[5]</sup> On the bases of some spectroscopic techniques the authors suggested that the boron stabilized carbanion might display significant  $\pi$ -bonding between the carbanionic carbon atom and the three coordinate boron center, thus indicating that the anion can be alternatively represented as boron alkylidene (Scheme 3.7).



**Scheme 3.7** Boron-alkylidene formation in the deborylative alkylation processes.

In principle, the proposed boron-alkylidene species should be able to participate in cycloaddition processes. To probe this hypothesis, a *gem*-diborylalkane bearing a tethered alkene was designed. In the presence of an alkoxide base, a deborylative cyclization was observed after 14 hours. Since the cycloadduct species is itself an *ate* complex, if an electrophile is added at this point, such bora-bicyclic intermediate could be efficiently trapped (Scheme 3.8). Overall the cyclization is conceived as a [2+2] cycloaddition between an unactivated alkene and the boron alkylidene.

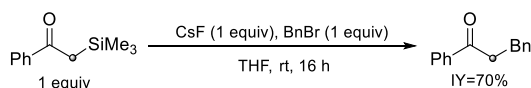


**Scheme 3.8** Deborylative [2+2] cyclization via boron-alkylidene formation.

### 3.1.2 Desilylative alkylation

Silyl groups are often used as protecting groups due to their straightforward removal with fluorinated bases. Fluoride induced desilylation is particularly efficient because the formation of the strong Si-F bond is a highly selective procedure.<sup>[6]</sup> On the basis of this premise, a series of selected desilylative alkylation processes reported in the literature are going to be listed in this section. This particular synthetic approach is directly related to some of the functionalizations that will be described in the results and discussion section of this memory.

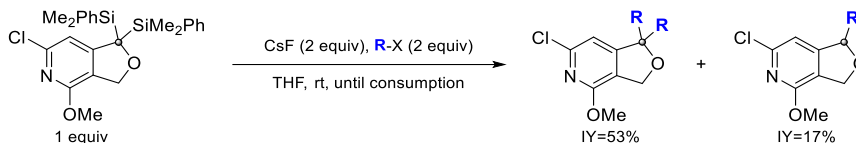
The first synthetic desilylative alkylation approach reported, involved  $\beta$ -ketosilanes as substrates.<sup>[7]</sup> These highly reactive species underwent efficient intermolecular desilylative alkylation with benzyl bromide. The reaction used cesium fluoride as base and the corresponding  $\alpha$ -benzyl ketones were nicely obtained (Scheme 3.9).



**Scheme 3.9** Desilylative-alkylation of  $\beta$ -ketosilanes.

## Inter and Intramolecular selective alkylations of CH(Bpin)(SiMe<sub>3</sub>)(SR) with alkyl halides

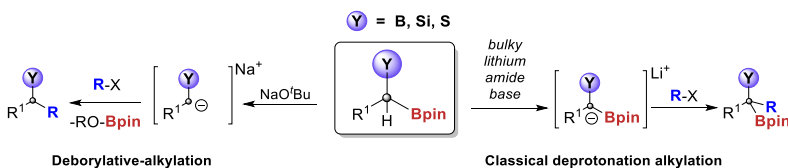
On the other hand, Sarkar and co-workers<sup>[8]</sup> reported an interesting intermolecular desilylative alkylation of azaphthalans. In this case, cesium fluoride was, once more, the fluorinated base responsible to promote the sequential introduction of two alkyl groups, thus enabling a double desilylation-alkylation strategy of the *gem*-(bis)silyl azaphthalane (Scheme 3.10). However, besides the formation of the double desilylated product, the mono-alkylated compound was observed as byproduct of the reaction (Scheme 3.10).



**Scheme 3.10** Mono- and di-alkylation of azaphthalanes through intermolecular desilylative fluorination.

### 3.1.3 Selective deprotonative alkylation sequence $\alpha$ to a boryl moiety

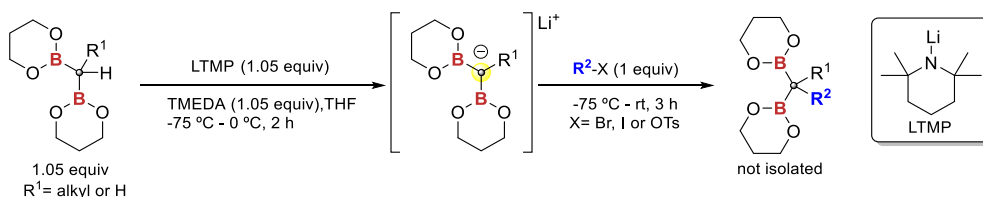
The examples gathered in section 3.1.1 have involved a series of deborylative alkylations assisted by an alkoxide base. These type of oxygenated bases, owing the high boron-oxygen affinity, are able to coordinate to the boryl fragment thus generating a nucleophilic *ate* complex in equilibria with the corresponding  $\alpha$ -boron stabilized carbanion that undergoes alkylation (Scheme 3.11, left). However, with the switch to a bulky lithium amide, a less borophilic base in comparison with an alkoxide, the outcome of the reaction can be totally altered. In this case, a simple deprotonation of any proton located  $\alpha$  to the metalloid fragments could be achieved. In this way, an  $\alpha$ -boryl carbanion susceptible of being alkylated by regular electrophiles can be generated (Scheme 3.11, right). Some examples of this type of reactivity, related to the behavior of the bimetalloid species included in this chapter, are described in this section.



**Scheme 3.11** Selective functionalization of *gem*-silyl boryl polymetalloids as a function of the base employed: deborylative alkylation versus  $\alpha$ -boryl deprotonation.

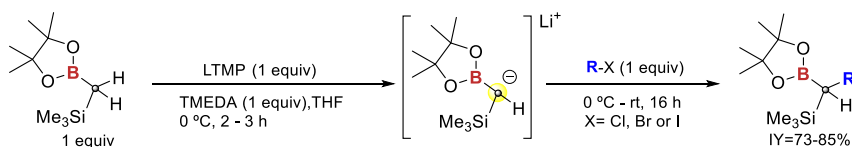
Matteson and co-workers reported the first deprotonation of *gem*-diboronic esters with the use of a bulky nitrogenated base as lithium tetramethylpiperidide (LTMP).<sup>[9]</sup> The deprotonation turned out to be quite efficient and the resulting

diborylcarbanion generated underwent straightforward alkylation with alkyl halides (Scheme 3.12). When using a bis(boronate)methane derivative ( $R^1 = H$  in Scheme 3.12), the resulting monoalkylated product could be in turn deprotonated and alkylated twice.<sup>[9]</sup> The alkylation reaction takes place with different types of boronates and the use of primary alkyl iodides, bromides and tosylates affording the desired alkylated *gem*-diboronate products. Instead, the reaction proved to be more sluggish with secondary halides, therefore, these reactions yielded little or no alkylated product.<sup>[10]</sup>



**Scheme 3.12** First deprotonation-alkylation of bis(boronate) esters reported using LTMP.

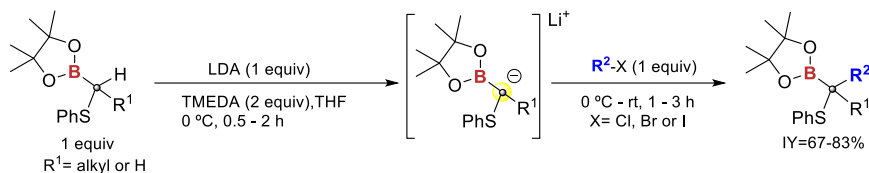
Additionally, the use of (bis)heterometalloid species containing two different metalloid fragments, such as silicon and boron, in combination with LTMP resulted in the generation of the doubly stabilized  $\alpha$ -boryl /  $\alpha$ -silyl carbanion. This reactive carbanion underwent the alkylation reaction with primary alkyl chlorides, bromides and iodides (Scheme 3.13).<sup>[11]</sup>



**Scheme 3.13** Deprotonation of *gem*-trimethylsilylboryl methane followed by selective alkylation with alkyl halides.

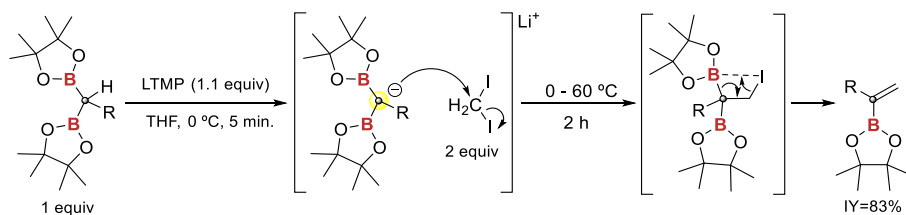
Other substrates such as the pinacolboryl (phenylthio)methane compounds could be effectively deprotonated by the use of a less hindered base, such as lithium diisopropylamide (LDA). This base is able to induce the formation of the doubly stabilized  $\alpha$ -boryl /  $\alpha$ -sulfide carbanion showed in Scheme 3.14. Subsequent addition of primary alkyl halides to the reaction mixture promoted the formation of  $\alpha$ -(phenylthio)alkane boronic esters. This methodology was able to provide a series of tetrasubstituted methane products (Scheme 3.14).<sup>[12]</sup>

## Inter and Intramolecular selective alkylations of CH(Bpin)(SiMe<sub>3</sub>)(SR) with alkyl halides



**Scheme 3.14** Selective deprotonation-alkylation sequence of pinacol (phenylthio)methaneboronates.

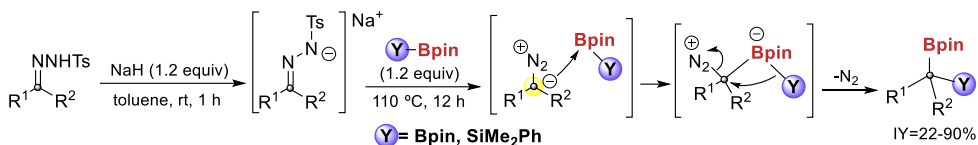
Recently, the group of Morcken<sup>[13]</sup> developed the idea to explore the reactivity of a series of *gem*-lithiated bis(boronates) anions towards the diiodomethane reagent. In this way a family of 1,1-disubstituted vinyl boronates could be accessed. From the mechanistic point of view, the lithiated substrate first undergoes alkylation with the diiodomethane, and subsequent B-I elimination results in formation of the vinyl boronate product (Scheme 3.15).



**Scheme 3.15** Synthesis of vinyl boronates by deprotonative-alkylation/B-I elimination sequence.

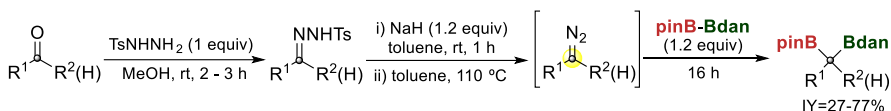
### 3.1.4 Synthesis of *geminal* diboryl alkanes by insertion of diazo compounds into boron containing reagents

One of the possible synthesis of *gem*-containing boryl species point to the insertion of diazo compounds into B-X  $\sigma$ -bonds. Aliphatic diazo compounds are not always easy to handle. Hence, one interesting way to use these reactive species is to generate them *in situ* by thermal decomposition of *N*-tosylhydrazone salts. Research along this line, led to Wang and co-workers<sup>[14]</sup> to develop a highly and efficient transition metal-free insertion of aliphatic diazo species into diboron reagents such as B<sub>2</sub>pin<sub>2</sub> (**1**) or Me<sub>2</sub>PhSiBpin. In this way a series of *gem*-bis(boronate) esters have been prepared (Scheme 3.16). From the mechanistic point of view, in this transformation are involved three important steps: the *in situ* generation of the diazo reagent, followed by the coordination of the diazo compound to the boron reagents (B<sub>2</sub>pin<sub>2</sub> (**1**) or Me<sub>2</sub>PhSiBpin) and the consequent 1,2-migration of one of the boryl or silyl fragment of the dimetalloid reagent to the adjacent carbon.



**Scheme 3.16** Generation of *gem*-bis(metalloids) by *in situ* generation of diazo compounds.

Our group has also contributed to the field of the insertion of non-stabilized diazo compound into the B–B  $\sigma$ -bond.<sup>[15]</sup> In fact, we reported the insertion of a series of aliphatic diazo compounds generated by decomposition of *N*-tosylhydrazone salts into the non-symmetrical B–B  $\sigma$ -bond of pinB-Bdan (Bdan = 1,8-naphthalenediaminoboryl). The *N*-tosylhydrazones employed in such study were derived either from aliphatic aldehydes or cyclic ketones (Scheme 3.17). Noteworthy, high diastereoselectivity can be achieved in the case of unsymmetrical substituted cyclohexanones.



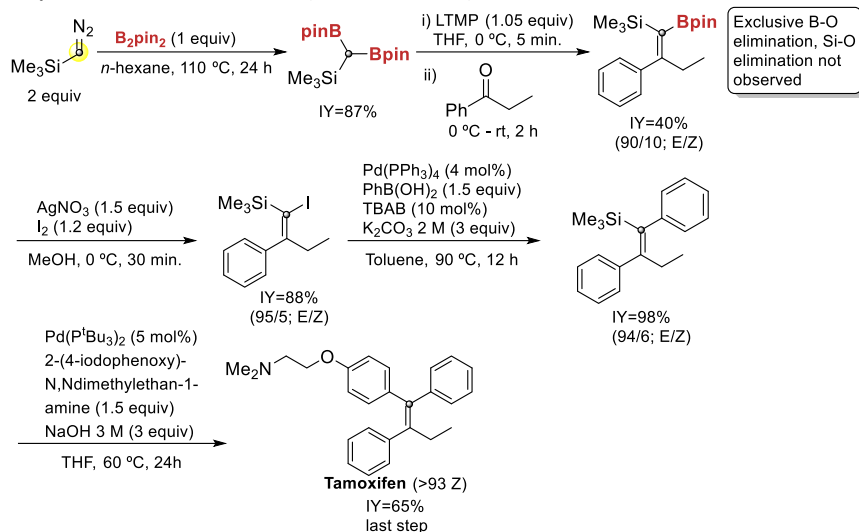
**Scheme 3.17** Diazo insertion into unsymmetrical diboron reagents such as Bpin-Bdan.

In the field of nucleophilic diazo species, the trimethylsilyl diazomethane [ $\text{CH}(\text{N}_2)(\text{SiMe}_3)$ ] (**7**) is particularly interesting since is a stable liquid (b.p. 96 °C) recognized as a safe diazomethane surrogate, with its enhanced stability rationalized by the  $\alpha$ -silyl carbanion stabilization ( $\alpha$ -silicon effect).<sup>[16]</sup> Such diazo compound contains an additional  $\text{SiMe}_3$  fragment that could be introduced in the insertion reaction with diboranes. This kind of transformation, opened the door to the introduction of many functional and reactive groups for further derivatizations.<sup>[17]</sup>

Hence our group expanded this reactivity by performing the insertion of trimethylsilyldiazomethane into the boron-boron  $\sigma$ -bond of  $\text{B}_2\text{pin}_2$  (**1**).<sup>[18]</sup> Such reaction rendered a very versatile multisubstituted [ $\text{CH}(\text{Bpin})_2(\text{SiMe}_3)$ ] (**5**) species. The synthesis of this new reagent can be efficiently performed on gram scale simply by mixing  $\text{B}_2\text{pin}_2$  (**1**) and [ $\text{CH}(\text{N}_2)(\text{SiMe}_3)$ ] (**7**) under heating. The [ $\text{CH}(\text{Bpin})_2(\text{SiMe}_3)$ ] (**5**) can be deprotonated in the presence of bulky lithiated bases to generate a boron- and silicon-stabilized carbanion able to add to ketones to form a series of *gem*-silyl borylalkenes following a B–O elimination. Through this methodology several different *gem*-( $sp^2$ )-silylboronates were prepared, most of them with high degree of *Z/E*-diastereoselection.<sup>[18]</sup> This methodology allowed for modular and

Inter and Intramolecular selective alkylations of CH(Bpin)(SiMe<sub>3</sub>)(SR) with alkyl halides

stereocontrolled synthesis of all carbon tetrasubstituted alkenes, as was illustrated by the synthesis of Tamoxifen (Scheme 3.18).

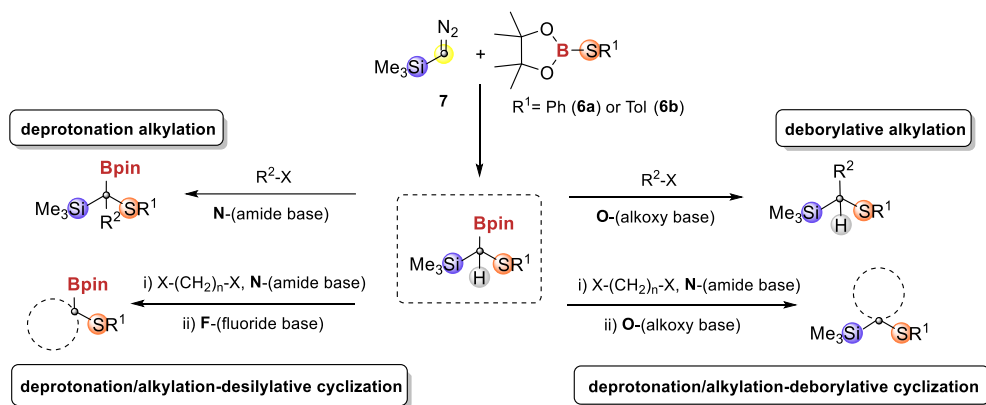


**Scheme 3.18** Insertion of trimethylsilyl diazomethane into B-B  $\sigma$ -bond followed by Boron-Wittig-type olefination of ketones. Simple access to Tamoxifen drug.

### 3.2. Aim of the Chapter

With all these precedents in mind, and based on the experience of our group in the insertion of diazo compounds into the pinB-Bdan  $\sigma$ -bond, as well as the insertion of trimethylsilyldiazomethane into  $B_2pin_2$  (**1**), we became interested in the insertion of this commercially available diazomethane equivalent into B-S  $\sigma$ -bond.

More specifically, due to the efficient insertion of  $[CH(N_2)(SiMe_3)]$  (**7**) in the B-X  $\sigma$ -bond in a transition metal-free context, we propose to explore the insertion of trimethylsilyldiazomethane (**7**) into pinB-SPh (**6a**) and pinB-STol (**6b**) bonds. This approach could represent a straight forward access to the formation of multisubstituted  $sp^3$  carbons (Si, B, S). If successful, the study would help to prepare a series of structurally diverse molecules endowed with high synthetic potential. In fact, subsequent selective base-mediated functionalizations that includes intermolecular or intramolecular cyclizative alkylations, could be envisaged (Scheme 3.19).



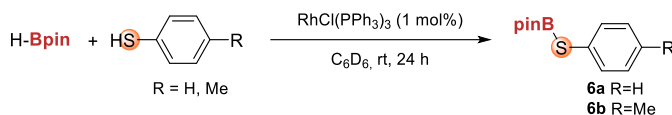
**Scheme 3.19** Strategic trimethylsilyldiazomethane insertion into pinB-S-  $\sigma$ -bond followed by selective functionalizations.



## Inter and Intramolecular selective alkylations of CH(Bpin)(SiMe<sub>3</sub>)(SR) with alkyl halides

### 3.3. Results and discussion

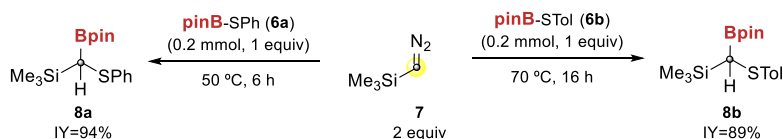
On the basis of the previously described main objective of this chapter we started the study by exploring the insertion of the commercially available [CH(N<sub>2</sub>)(SiMe<sub>3</sub>)] (**7**) with pinB-SPh (**6a**). This B-S reagent was supplied by the group of Prof. Westcott, within a collaborative project. This group prepared series of B-S reagents by means of rhodium catalysis mixing HBpin and the benzenethiol derivative (Scheme 3.20).<sup>[19]</sup>



**Scheme 3.20** Preparation of pinB-SR reagents.

The initial insertion experiments were carried out working at 0.2 mmol scale and, on the bases of some preliminary experiments carried out in the group with similar insertion reactions, it was found that the use of an excess of the diazo compound **7** (2 equiv) in the reaction along with 1 equiv of **6a** (diazo/borane = 2/1) was beneficial for the reaction completion. By means of this stoichiometry, full conversion of **6a** towards the insertion product was observed. When the reaction was performed at 50 °C during 16 hours, compound CH(Bpin)(SiMe<sub>3</sub>)(SPh) (**8a**) was obtained in almost quantitative yield. Nevertheless, we found that decreasing the reaction time to 6 hours the conversion was not significantly affected (94%) (Scheme 3.21, left).

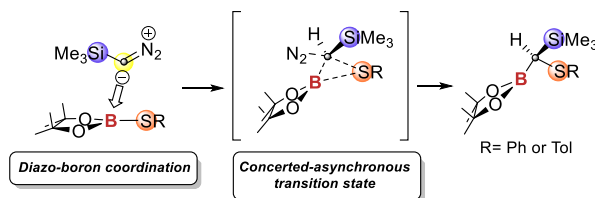
Similarly, the reaction was also performed with pinB-STol (**6b**), also supplied by the group of Prof. Westcott.<sup>[19]</sup> The inserted product [CH(Bpin)(SiMe<sub>3</sub>)(STol)] (**8b**) was also isolated in high yield (89%). However, for this B-S reagent, slightly higher temperatures (70 °C) were required to achieve full conversion towards the formation of **8b** (Scheme 3.21, right).



**Scheme 3.21** Optimized reactions conditions for the insertion of CH(N<sub>2</sub>)(SiMe<sub>3</sub>) into pinB-SR.  
 Conditions: pinB-SR (0.2mmol, 1 equiv), **7** (2 equiv), 50 – 70 °C, 6 - 16 h.

From the mechanistic point of view, the insertion of **7** into the interelement B-S  $\sigma$ -bond might be understood as an initial interaction of the nucleophilic diazo carbon to the electron deficient boron of the Bpin moiety. Subsequently, the polarization of the boron-sulfur  $\sigma$ -bond would give rise to the 1,2-migration of the adjacent SR moiety to yield the  $\alpha,\alpha$ -substituted methane product with concomitant dinitrogen

release (Scheme 3.22). An analogous mechanism was already postulated by Dr. J. Carbó through DFT calculations<sup>[20]</sup> using pinB–Bpin or pinB–Bdan and CH(N<sub>2</sub>)(CH<sub>3</sub>) as the model diazo alkane, suggesting a concerted asynchronous mechanism.<sup>[15]</sup>



**Scheme 3.22** Suggested concerted mechanism for the insertion of CH(N<sub>2</sub>)(SiMe<sub>3</sub>) into pinB-SR.

Moreover, it was possible to scale up the insertion of **7** into B-S  $\sigma$ -bonds to a gram quantities, thus providing the formation of reagent **8a** in 95% isolated yield and **8b** in 89% isolated yield. In this case, for safety reasons, a careful evaluation of reaction set up was applied since higher volumes of nitrogen were generated.

At this point, we considered that these new polysubstituted species **8a-b** could serve as an interesting entry point towards selective alkylative functionalizations. In fact, as mentioned in the *Aim of the Chapter* section, this type of *gem*-silyl boryl sulfides could, in principle, be selectively functionalized following different strategies. In first place, as mentioned in section 3.1.1, bis(boronate) esters exhibit a well established ability to coordinate to alkoxides and undergo deboryative alkylation due to the well established affinity of trigonal boron compounds to coordinate to oxygenated bases. Based on this premise, we sought to explore whether this reactivity could be ascribed to compounds of type of **8a-b** that present a silyl group in their structure. This transformation was considered challenging, since the retention of the silyl group could be compromised in the presence of the alkoxide. If successful, this two-step sequence would constitute an unprecedented protocol for the synthesis of  $\alpha$ -silyl sulfides.

Initially, and based on the work of Morken and co-workers,<sup>[2]</sup> sodium *tert*-butoxide was selected to induce the deborylation process.

The initial experiments were carried out employing **8a-b** as substrates and 1-bromotetradecane (**9**) as alkylating reagent. The reaction conditions entailed the mixing of **9** (1 equiv) with an excess of **8a-b** (1.3 equiv) in THF and subsequent addition of NaO<sup>*t*</sup>Bu (4 equiv). The excess of **8a-b** *versus* the alkylating reagent was used to discard any potential decomposition along the reaction. Within 3 hours, at room temperature the alkylated  $\alpha$ -silyl sulfide **10a** was observed in 84% yield and **10b** in 73% yield (Scheme 3.23). Longer reaction times did not result in higher yields.

## Inter and Intramolecular selective alkylations of CH(Bpin)(SiMe<sub>3</sub>)(SR) with alkyl halides

---

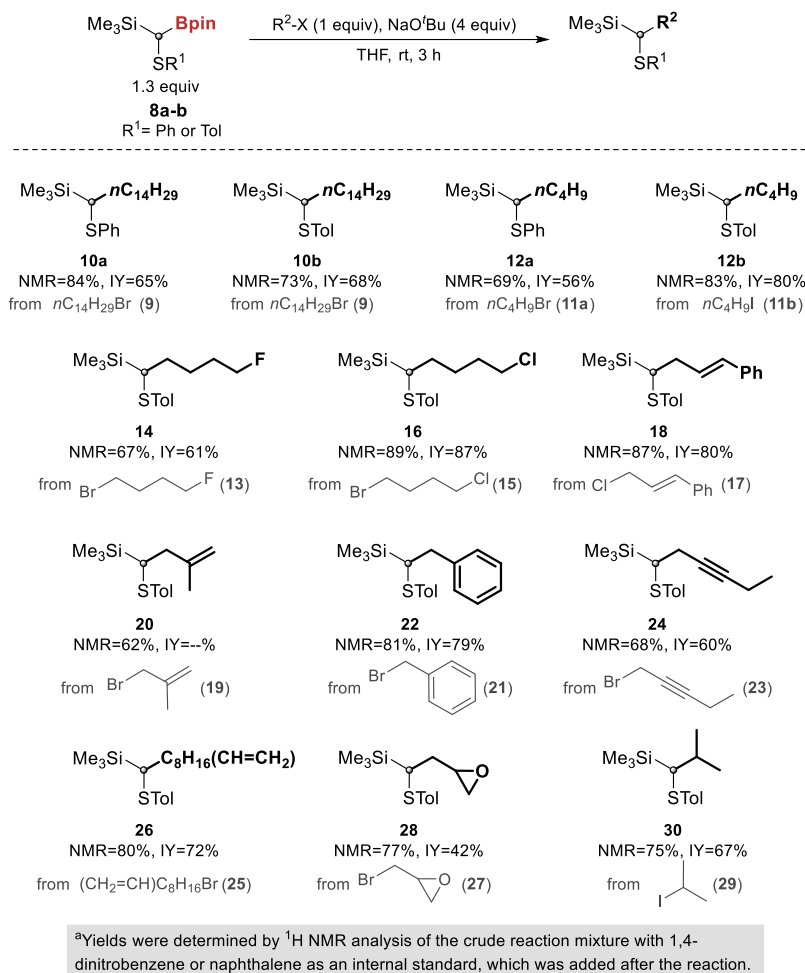
When a shorter alkyl halide was used instead, such as 1-bromobutane (**11a**), the alkylated product **12a** was obtained in moderate yield. Nevertheless, the use of 1-iodobutane (**11b**) containing a better leaving group, resulted in a more efficient reaction. In this way the  $\alpha$ -silyl sulfide **12b** was isolated in 80% yield (Scheme 3.23). Then we performed the reaction with 1-bromo-4-chlorobutane (**13**) and 1-bromo-4-fluorobutane (**15**) with substrate **6b**. The deborylative alkylation reaction took place selectively in both cases in the C-Br bond, giving rise to products **14** in 61% and **16** in 87% isolated yield, respectively (Scheme 3.23). Due to the superior leaving group ability of Br, the reaction allows selectively the formation of the new C-C bond at the C-Br site, leaving the C-F and the C-Cl bonds intact (Scheme 3.23).

Interestingly, the S<sub>N</sub>2-type alkylation of the more activated cinnamyl chloride (**17**) was easily performed to generate *E*-trimethyl(4-phenyl-1-(*p*-tolylthio)but-3-en-1-yl)silane (**18**) in 80% isolated yield. The lower ability of chloride as leaving group was this time compensated by the better transition state stabilization by the allylic nature of the electrophile (Scheme 3.23).

In agreement with this last result, other activated allylic, benzylic or propargylic halides, such as 3-bromo-2-methylprop-1-ene (**19**), benzyl bromide (**21**) and 1-bromopent-2-yne (**23**), nicely provided the alkylated  $\alpha$ -silyl sulfides **20**, **22** and **24** in moderate to high yields (Scheme 3.23). Unfortunately, product **20** could not be isolated due to decomposition during the purification process, even though, its efficient generation was undoubtable proved by NMR spectroscopy (Scheme 3.23).

The compatibility of unsaturated functional groups with respect to the base-mediated deborylative alkylation was demonstrated with the use of a substrate containing a double bond in the terminal position of the alkyl chain, substrate **25**. Hence, the efficient preparation of the corresponding *gem*-silyl sulfide derivative **26** was performed in 72% isolated yield (Scheme 3.23).

Even more remarkable is the example with 2-(bromomethyl)oxirane (**27**), where the alkylated product (**28**) was isolated in 42% yield leaving the epoxide functional group unaltered (Scheme 3.23).



**Scheme 3.23** Substrate scope of deborylative alkylation of derivatives **8a-b** via  $\text{S}_{\text{N}}2$  pathway.

We also conducted the deborylative alkylation with a secondary alkyl halide, a more challenging substrate due to the steric hindrance present around the halogen. Nevertheless, when isopropyl iodide (**29**) was chosen as alkylating agent, the anticipated lower reactivity due to the steric effects seemed to be balanced by the better leaving group ability of the iodide group, and trimethyl(2-methyl-1-(p-tolylthio)propyl)silane (**30**) was isolated in 67% yield (Scheme 3.23).

Overall, the results shown in Scheme 3.23 demonstrate that the deborylative alkylation of **8a-b** tolerates a broad substrate scope, even combining different functional groups in the same substrate as well as the use of more challenging and sterically hindered secondary alkyl halides.

## Inter and Intramolecular selective alkylations of CH(Bpin)(SiMe<sub>3</sub>)(SR) with alkyl halides

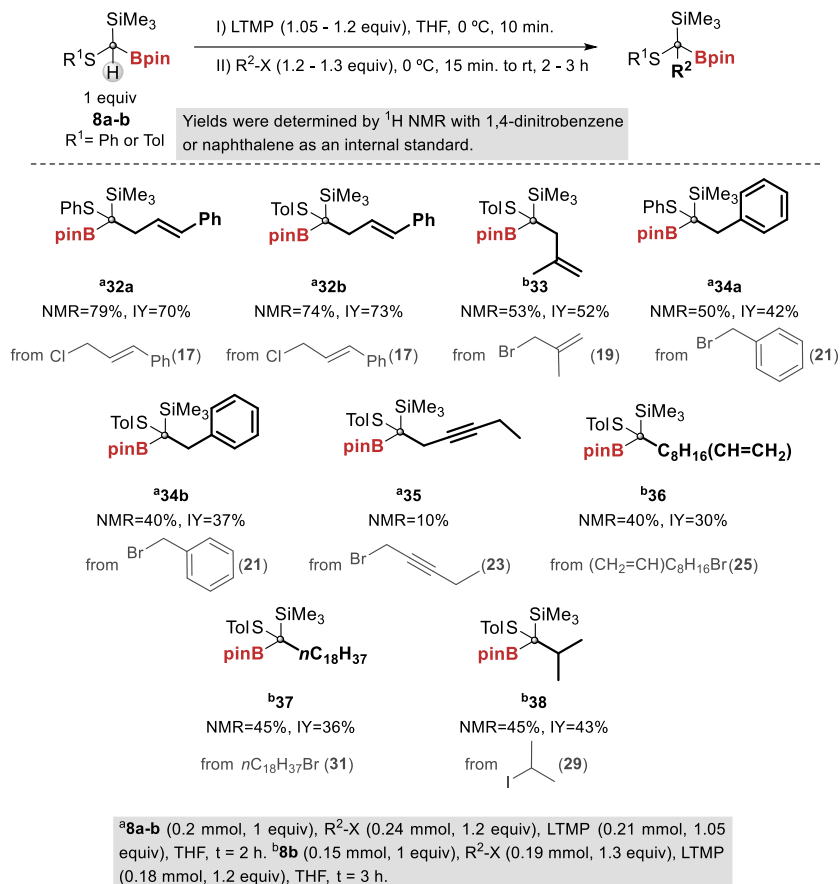
---

The two-step insertion/base-assisted deborylative alkylation constitutes an unprecedented protocol for the synthesis of alkylated  $\alpha$ -silyl sulfides in a very straightforward manner.

Next, we turned our attention to the alkylations involving the generation of double stabilized  $\alpha$ -boron /  $\alpha$ -silyl carbanions engendered through deprotonation of *gem*-polymetalloid **8a-b**. As introduced above (section 3.1.3), the switch from an alkoxide base to a bulky lithium amide, comparatively less borophilic, might influence the reaction outcome. In this case, a simple deprotonation of any  $\alpha$ -proton to the metalloid fragments could be achieved.

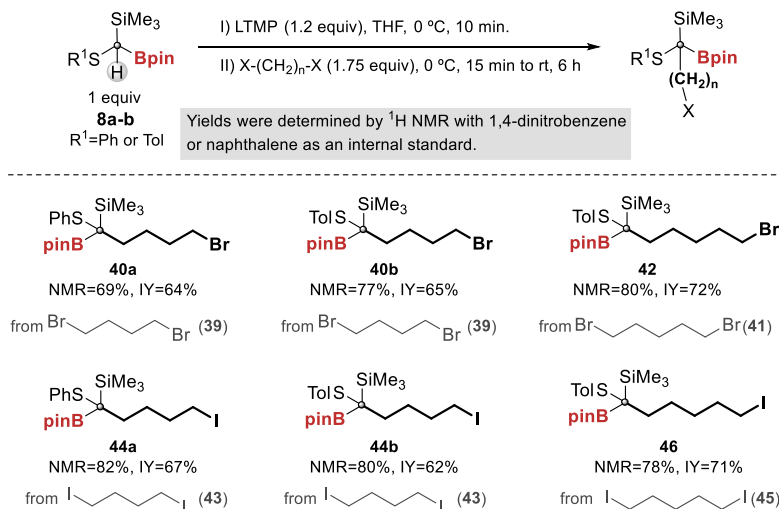
Hence, substrates **8a-b** can be efficiently deprotonated by the presence of lithium tetramethylpiperidide (LTMP) and subsequently alkylated with cinnamyl chloride. In this way, the alkylated  $\alpha$ -boryl silyl sulfides **32a** and **32b** could be obtained in 79% and 74% yield, respectively (Scheme 3.24). The reaction proved to be feasible with a series of substrates featuring allylic (**19**) and benzylic (**21**) electrophiles albeit providing the formation of **33**, **34a** and **34b** only in moderate yields (Scheme 3.24). Nevertheless, the alkylation reaction with propargylic systems proved sluggish and the corresponding tetrafunctionalized methane was only observed by NMR (10% NMR yield) (Scheme 3.24). Nonetheless, the alkylation was compatible with the presence of a monosubstituted terminal double bond, substrate **25**, giving access to the desired derivative **36** in 30% isolated yield (Scheme 3.24). The use of longer alkyl chain in substrate **31** provided the formation of the alkylated product **37** in moderate yield (Scheme 3.24).

Noteworthy is the use of more hindered secondary halides. In this case, isopropyl iodide (**29**) lead to the formation of the alkylated compound **38** in a good 43% isolated yield (Scheme 3.24).



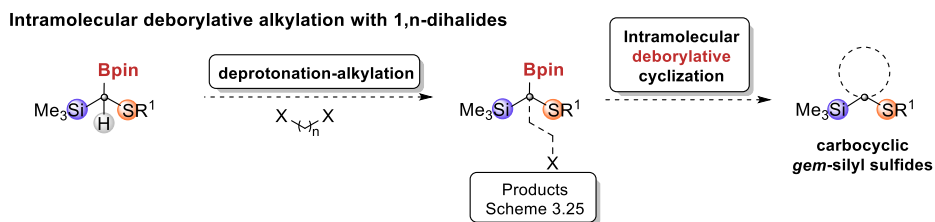
**Scheme 3.24** Substrate scope of deprotonation-alkylation of derivatives **8a-b** via  $\text{S}_{\text{N}}2$  pathway.

Encouraged by these results, we turned our attention to the use of dihalogenated alkanes, such as dibromo and diiodo alkyl derivatives. With the objective to prevent the double incorporation of **8a-b** at both ends of the alkyl chain, a higher excess of the electrophile was employed (1.75 equiv). The reaction proved to be quite efficient, affording exclusively the mono-alkylated products. When butyl dihalides were used such as **39** ( $\text{X} = \text{Br}$ ) or **43** ( $\text{X} = \text{I}$ ) products **40a**, **40b**, **44a**, and **44b** were obtained in high yields (Scheme 3.25). Moreover, extending the alkyl chain one atom (**41**  $\text{X} = \text{Br}$  and **45**  $\text{X} = \text{I}$ ) did not have an effect on the reaction outcome, and the corresponding mono-alkylated products **42** and **46** could be isolated in good yields (Scheme 3.25).

Inter and Intramolecular selective alkylations of CH(Bpin)(SiMe<sub>3</sub>)(SR) with alkyl halides

**Scheme 3.25** Substrate scope of deprotonation-alkylation of derivatives **8a-b** via S<sub>N</sub>2 pathway with dihaloalkanes.

Interestingly, when 1,*n*-dihalides are employed in these alkylation reactions, the reaction products (compounds **40a-b**, **42**, **44a-b** and **46** in Scheme 3.25) are suitable substrates for an intramolecular ring forming deborylative alkylation. As depicted in Scheme 3.26, this strategy would enable a straightforward synthesis of cyclic *gem*-silyl sulfides that are not readily available by other methods.



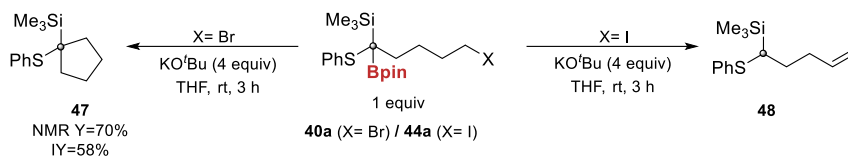
**Scheme 3.26** Intramolecular deborylative alkylation with 1,*n*-dihalides: construction of cyclic *gem*-silyl sulfides.

To study this possibility, substrate **44a** containing an iodine leaving group was treated with 4 equiv of KO<sup>t</sup>Bu in THF at room temperature. Unfortunately, the desired cyclized product was not detected after 3 hours of reaction and only the product **48** was clearly observed. The formation of **48** could be explained as a result of the presence of different competitive reactions, the E2 elimination to give an alkene, the protodeborylation and the desired alkylation pathways. Based on the

experimental result, in the reaction with substrate **44a** the intramolecular  $S_N2$  alkylation seems to be the less favoured reaction.

To our delight, when the corresponding C(Bpin)((CH<sub>2</sub>)<sub>4</sub>Br)(SiMe<sub>3</sub>)(SPh) (**40a**) was subjected to the same deborylative conditions, the five-membered ring  $\alpha$ -silyl sulfide was nicely produced and compound **47** was isolated in 70% yield (Scheme 3.27).

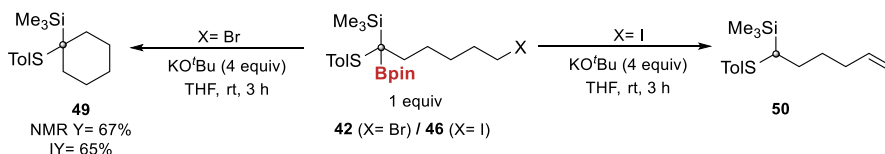
Deborylative cyclization towards five-membered ring cycle



**Scheme 3.27** Intramolecular deborylative cyclization. Reaction conditions: **40a/44b** (0.2 mmol, 1 equiv), KO<sup>t</sup>Bu (4 equiv), THF (1 mL), rt, 3 h.

Moreover, the transformation could be extended to the formation of the analogous six-membered ring *gem*-silyl sulfides. Thus, when substrate **42** was treated with 4 equiv of KO<sup>t</sup>Bu in THF at room temperature the corresponding six-membered ring  $\alpha$ -silyl sulfide **49** was isolated in 65% yield (Scheme 3.28). Once more, however, the reaction with the iodo-substrate **46** provided the unwanted product **50** as observed previously in the formation of the five-membered ring. The better leaving group ability of iodine compared to the bromine atom seems to accelerate the participation of **46** into the side elimination reaction.

Deborylative cyclization towards six-membered ring cycle



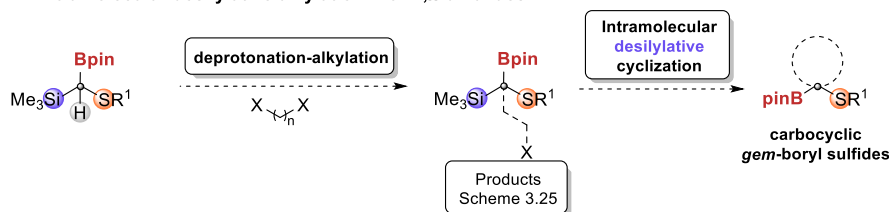
**Scheme 3.28** Intramolecular deborylative cyclization. Reaction conditions: **42/46** (0.2 mmol, 1 equiv), KO<sup>t</sup>Bu (4 equiv), THF (1 mL), rt, 3 h.

Additionally, we decided investigate the analogous, but more challenging and rather unprecedented, desilylative intramolecular cyclization. As detailed in Scheme 3.29, this strategy would yield an straightforward route to cyclic *gem*-boryl sulfides, compounds that are not readily prepared by other methods.



## Inter and Intramolecular selective alkylations of CH(Bpin)(SiMe<sub>3</sub>)(SR) with alkyl halides

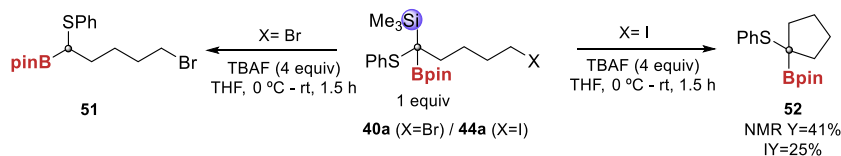
### Intramolecular desilylative alkylation with 1,*n*-dihalides



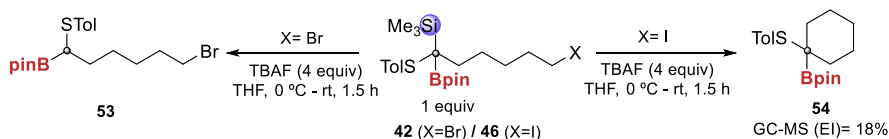
**Scheme 3.29** Intramolecular desilylative alkylation with 1,*n*-dihaloalkanes: construction of cyclic *gem*-boryl sulfides.

Based on this premise, we selected Br-substrates **40a** and **42** and I-substrates **44a** and **46** to test the potential desilylative cyclization. As in the case of the deborylative cyclization, a significant effect of the leaving group was observed. Thus, when bromo derivatives (**40a/42**) were subjected to desilylative cyclization conditions using tetra-*n*-butylammonium fluoride (TBAF), only proto-desilylated products (**51/53**) were observed, leaving the bromine atom unreacted. On the other hand, the more activated iodine-containing substrates **44a** and **46** underwent desilylative cyclization leading to the corresponding five- and six-membered carbocycles. More specifically, in the case of substrate **44a**, after addition of 4 equiv of TBAF at 0 °C and stirring during 1.5 hours, the desired five-membered ring product **52** was observed in 41% NMR yield (Scheme 3.30a). The formation of the cyclohexane derivative **54** was found to be more challenging, and under the same reaction conditions the product could only be observed in 18% yield by GC-MS analysis (Scheme 3.30b).

#### a) Desilylative cyclization towards five-membered ring cycle



#### b) Desilylative cyclization towards six-membered ring cycle



**Scheme 3.30** Intramolecular desilylative cyclization. Conditions: Substrate (0.2 mmol, 1 equiv), TBAF (1 M, 4 equiv), THF (0.3 mL), 0 °C - rt, 1.5 h.

In summary, a series of selective functionalizations of *gem*-silyl boryl sulfides have been explored. These reactions included innovative demetallative cyclizations that allowed access to new boryl containing cyclopentane and cyclohexane derivatives.

## Inter and Intramolecular selective alkylations of CH(Bpin)(SiMe<sub>3</sub>)(SR) with alkyl halides

---

### 3.4. Conclusions

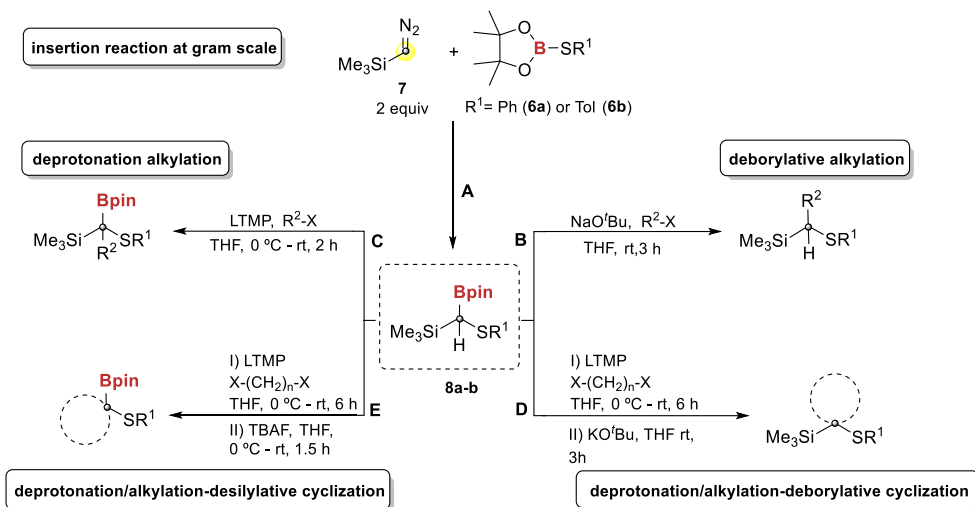
The insertion of trimethylsilyldiazomethane into B-S  $\sigma$ -bond of pinB-SPh (**6a**) and pinB-STol (**6b**) has been achieved in quantitative yield. The reaction is amenable to scale up (gram scale) in a very efficient manner (Scheme 3.31A).

A careful selection of the base has allowed the selective alkylation of trisubstituted methanes of molecular formula CH(Bpin)(SiMe<sub>3</sub>)(SR) (**8a-b**):

- NaO<sup>t</sup>Bu assisted deborylative alkylation of CH(Bpin)(SiMe<sub>3</sub>)(SR) (**8a-b**) was nicely performed in a series of alkyl halides promoted by the high boron-oxygen affinity (Scheme 3.31B).
- The deprotonation-alkylation of CH(Bpin)(SiMe<sub>3</sub>)(SR) (**8a-b**) with a series of alkyl halides and 1,*n*-dihalides was carried out under mild conditions. The use of a bulky lithium amide base alters the outcome of the reaction allowing for a boron-retentive alkylation reaction. In this way, a range of tetrasubstituted methanes can be accessed. (Scheme 3.31C).

The use of 1,*n*-dihaloalkanes as electrophiles, allowed for the synthesis of series of functionalized carbocyclic compounds from the first deborylative alkylation intermediate.

- An intramolecular ring forming deborylative alkylation was developed by the use of an alkoxide base. Through this method, a series of cyclic  $\alpha$ -silyl sulfides have been prepared (Scheme 3.31D)
- An intramolecular desilylative cyclization procedure has been achieved in the presence of a more silicophilic fluoride base. This new methodology, albeit in moderate yields, gives access to the synthesis of  $\alpha$ -boryl sulfides (Scheme 3.31E).



**Scheme 3.31** Graphical conclusions of trimethylsilyldiazomethane insertion and selective functionalizations.

## Inter and Intramolecular selective alkylations of CH(Bpin)(SiMe<sub>3</sub>)(SR) with alkyl halides

---

### 3.5. References Chapter 3

- [1] a) N. Miralles, R. J. Maza, E. Fernández, *Adv. Synth. Catal.* **2018**, *360*, 1306-1327; b) J. Royes, A. B. Cuenca, E. Fernández, *Eur. J. Org. Chem.* **2018**, *2018*, 2728-2739; c) R. Nallagonda, K. Padala, A. Masarwa, *Org. Biomol. Chem.* **2018**, *16*, 1050-1064; d) C. Wu, J. Wang, *Tetrahedron Lett.* **2018**, *59*, 2128-2140.
- [2] K. Hong, X. Liu, J. P. Morken, *J. Am. Chem. Soc.* **2014**, *136*, 10581-10584.
- [3] J. R. Coombs, L. Zhang, J. P. Morken, *J. Am. Chem. Soc.* **2014**, *136*, 16140-16143.
- [4] L. Zhang, Z. Huang, *J. Am. Chem. Soc.* **2015**, *137*, 15600-15603.
- [5] X. Liu, T. M. Deaton, F. Haeffner, J. P. Morken, *Angew. Chem. Int. Ed.* **2017**, *56*, 11485-11489.
- [6] I. H. Krouse, P. G. Wenthold, *J. Am. Soc. Mass Spectrom.* **2005**, *16*, 697-707.
- [7] M. Fiorenza, A. Mordini, S. Papaleo, S. Pastorelli, A. Ricci, *Tetrahedron Lett.* **1985**, *26*, 787-788.
- [8] T. K. Sarkar, S. Basak, *Org. Lett.* **2004**, *6*, 2925-2927.
- [9] D. S. Matteson, R. J. Moody, *J. Am. Chem. Soc.* **1977**, *99*, 3196-3197.
- [10] D. S. Matteson, R. J. Moody, *Organometallics* **1982**, *1*, 20-28.
- [11] a) D. S. Matteson, D. Majumdar, *J. Chem. Soc., Chem. Commun.* **1980**, 39-40; b) D. S. Matteson, D. Majumdar, *Organometallics* **1983**, *2*, 230-236.
- [12] D. S. Matteson, K. Arne, *J. Am. Chem. Soc.* **1978**, *100*, 1325-1326.
- [13] J. R. Coombs, L. Zhang, J. P. Morken, *Org. Lett.* **2015**, *17*, 1708-1711.
- [14] a) H. Li, X. Shanguan, Z. Zhang, S. Huang, Y. Zhang, J. Wang, *Org. Lett.* **2014**, *16*, 448-451; b) H. Li, L. Wang, Y. Zhang, J. Wang, *Angew. Chem. Int. Ed.* **2012**, *51*, 2943-2946.
- [15] A. B. Cuenca, J. Cid, D. García-López, J. J. Carbó, E. Fernández, *Org. Biomol. Chem.* **2015**, *13*, 9659-9664.
- [16] D. M. Wetzel, J. I. Brauman, *J. Am. Chem. Soc.* **1988**, *110*, 8333-8336.
- [17] a) C. H. Burgos, E. Canales, K. Matos, J. A. Soderquist, *J. Am. Chem. Soc.* **2005**, *127*, 8044-8049; b) A. Sekiguchi, W. Ando, *Organometallics* **1987**, *6*, 1857-1860; c) D. Seyferth, T. C. Flood, *J. Organometal. Chem.* **1971**, *29*, C25-C28.

- [18] E. La Cascia, A. B. Cuenca, E. Fernández, *Chem. Eur. J.* **2016**, *22*, 18737-18741.
- [19] S. A. Westcott, J. D. Webb, D. I. Mclsaac, C. M. Vogels, **2006/089402 A1 Patent**.
- [20] Calculations were performed using a Gaussian09 (B03LYP functional) and 06-31g(d,p) basis set.

UNIVERSITAT ROVIRA I VIRGILI  
COMPLEMENTARY SYNTHESIS OF ORGANOBORANES TO POPULATE THE CHEMICAL  
FUNCTIONALITY TO A GIVEN AREA OF BIOMEDICAL INTEREST  
Jordi Royes Buisan

# **Chapter 4**

## **Intramolecular borylative ring-closing C-C coupling toward spiro- and dispiro- heterocycles**

---



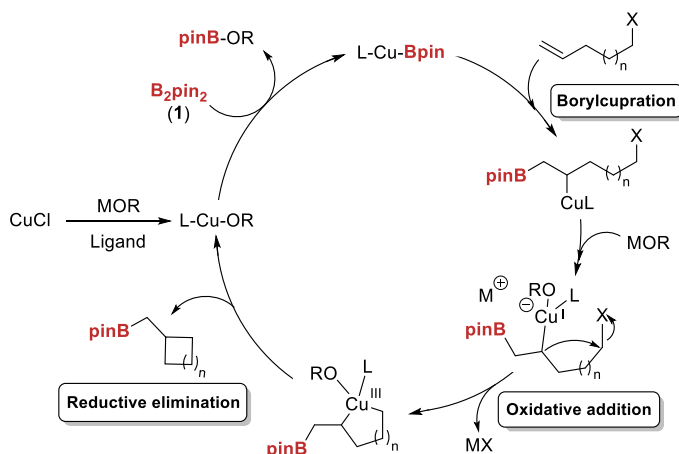
UNIVERSITAT ROVIRA I VIRGILI  
COMPLEMENTARY SYNTHESIS OF ORGANOBORANES TO POPULATE THE CHEMICAL  
FUNCTIONALITY TO A GIVEN AREA OF BIOMEDICAL INTEREST  
Jordi Royes Buisan

## 4.1. State of the art

### 4.1.1. Intramolecular carboboration

Within the borylative ring-closing reactions, the 1,2-carboboration reaction has been the most widespread explored. Copper (I) salts are able to activate diboron reagents in a specific manner to transfer one boryl unit to unsaturated substrates favoring the concomitant cross-coupling pathway.<sup>[1]</sup> Borylative cyclization of alkenes containing good leaving groups in their structure is considered an intramolecular 1,2-carboboration reaction, that provides highly substituted 3- to 5-membered rings. The stereoselectivity in the transformation can be efficiently controlled by the nature of the catalyst. In fact, this is a highly efficient methodology for the synthesis of organoboronates with complex carbon skeletons.<sup>[2]</sup>

Over the last decades, many efforts have been devoted to the development of catalytic borylative cyclization reactions and, in particular, to understand their reaction mechanisms. The reaction sequence for such transformations starts with the boryl cupration of the unsaturated double bond, followed by oxidative addition to afford the corresponding metallocyclic intermediate that generates the cyclic organoboron product via reductive elimination sequence (Scheme 4.1).

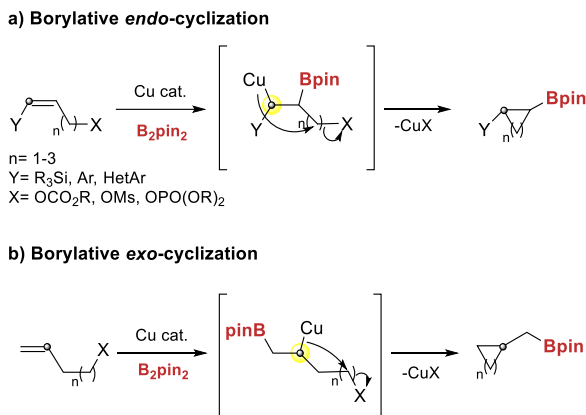


**Scheme 4.1** General borylative cyclization mechanism catalyzed by copper (I) salt.

The borylcupration step can lead to two possible cyclizations: *endo*- and *exo*-cyclization. The reaction outcome is fixed by the substrate.<sup>[3]</sup> Thus, alkene containing electron rich substituents favor the coordination of the copper close to that substituent and the boron to the internal position of the C=C, promoting the *endo*-cyclization pathway (Scheme 4.2a).

## Intramolecular borylative ring closing C-C coupling toward spiro- and dispiro-heterocycles

On the other hand, when non-activated alkenes are used, as reported by Ito and co-workers,<sup>[4]</sup> the coordination of the copper goes to the internal position of the alkene leaving the boryl group placed at the more external position of the unsaturated substrate, leading to the formation of the *exo*-cyclic product upon the reductive elimination step (Scheme 4.2b).



**Scheme 4.2** Possible borylative cyclizations pathways depending on the nature of the substrate.

### 4.1.2. The interest of spiro-bicyclic motifs

Recently, advances in molecular sciences have exerted an enormous influence in the availability of new molecular entities.<sup>[5]</sup> The key for the success in the investigations in different areas, is the identification of the targets and their synthesis. Due to the infinite number of combinations and structures, this big range of possibilities opens a broad chemical space to be discovered. Organic chemistry, has been always working to provide routes of access to new synthetic building blocks.

Traditionally, spiro-bicyclic motifs have been scarcely explored in drug discovery, mostly due to their challenging synthesis.<sup>[6]</sup> Design and availability of new spiro-bicycles is a challenging task, since it involves the synthesis of a quaternary carbon as intersection point between the two cycles.<sup>[7]</sup>

Spiro-bicyclic compounds are characterized by their compactness and their potential for spatial diversification through isomerism. The tetrahedral carbon in the spiro-linked center positions the planes of the two rings nearly perpendicular. This characteristic spatial disposition of the molecule, could be an important aspect in biological activities. Careful design of spiro-compounds could offer a wide range of possibilities for diversification, such as, the presence of defined exiting vectors, different ring size combinations, different point of intersection between the two

rings, a center of diastereoisomerism and a wide variety of substituents and functional groups.<sup>[8]</sup>

Due to their well-defined exit vectors, spiro-bicyclic molecules are considered to have reduced symmetry, that results in more divers coverage of space around the scaffold. Moreover, this is directly expressed as their compactness, engendering shape diversity looking to access to uncharted pharmacological space.<sup>[6]</sup>

Nowadays, the design of new spiro-bicyclic molecules is a growing area in modern organic synthesis. Spiro-compounds are present in the structures of many natural products and pharmaceutical companies consider them privileged scaffolds due to their biological activities and possibilities for modulation in terms of physicochemical properties and hence optimization of pharmacokinetic properties.<sup>[9]</sup>

## Intramolecular borylative ring closing C-C coupling toward spiro- and dispiro-heterocycles

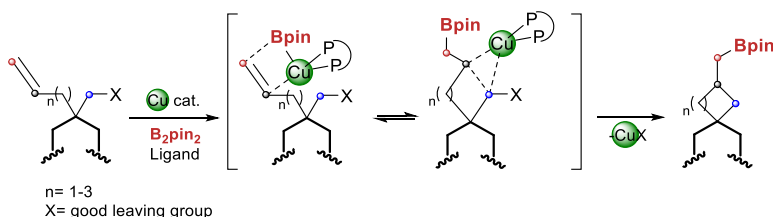
### 4.2. Aim of the Chapter

Based on the growing interest towards the synthesis of new spiro-bicyclic molecules, in this work we focus our efforts in the preparation of  $[m.n]$ -spiro-heterobicyclic structures ( $m,n = 3-5$ ) with a methylene boronate unit bound to an all-carbon cyclic backbone, aiming to expand the pharmacopeia library.

For the preparation of the target spiro-heterocyclic structures, we envisaged a synthetic strategy whereby an O- or N-containing heterocycle is already present in the starting material. The mentioned heterocycle would contain a quaternary carbon substituted with an alkene function and a leaving group, such as, an halide. The spiro-bicycle would then be formed through a Cu-catalyzed intramolecular borylative ring-closing C-C coupling of the alkenyl halide moiety (Scheme 4.3).

Even though Cu-catalyzed borylative *exo*-cyclization had been previously explored to build spiro-cyclobutane rings onto saturated carbocycles, only one example leading to a spiro-heterocyclic based skeleton has been reported.

In addition to cover the gap on the synthesis of heterocyclic spiro-compounds, we decided to explore the challenging formation of 5- and 6-membered spiro-bicyclic rings.



**Scheme 4.3** Graphical objectives of the chapter.

### 4.3. Results and discussion

Our studies started with the selection of *O*- or *N*- containing heterocyclic ester derivatives to be used as precursors of the required haloalkenes. Figure 4.1 shows diverse 5- and 6-membered heterocyclic rings (**55-60**) with *O*- or *N*- located on position 2, 3 or 4 with respect to the ester function. Substrates **55**, **56**, **59** and **60** were commercially available. Compounds **57** and **58** were synthesized from the commercially available piperidine hydrochloric salts by reaction with the corresponding sulphonyl chloride using *N,N*-diisopropylethylamine (DIPEA) as base (See Experimental Part in Chapter 8).<sup>[10]</sup>

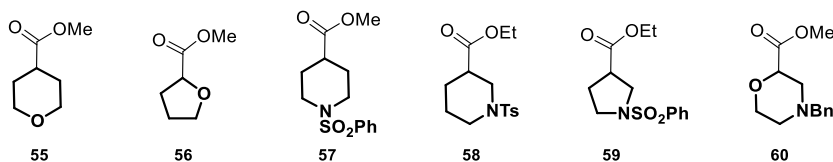
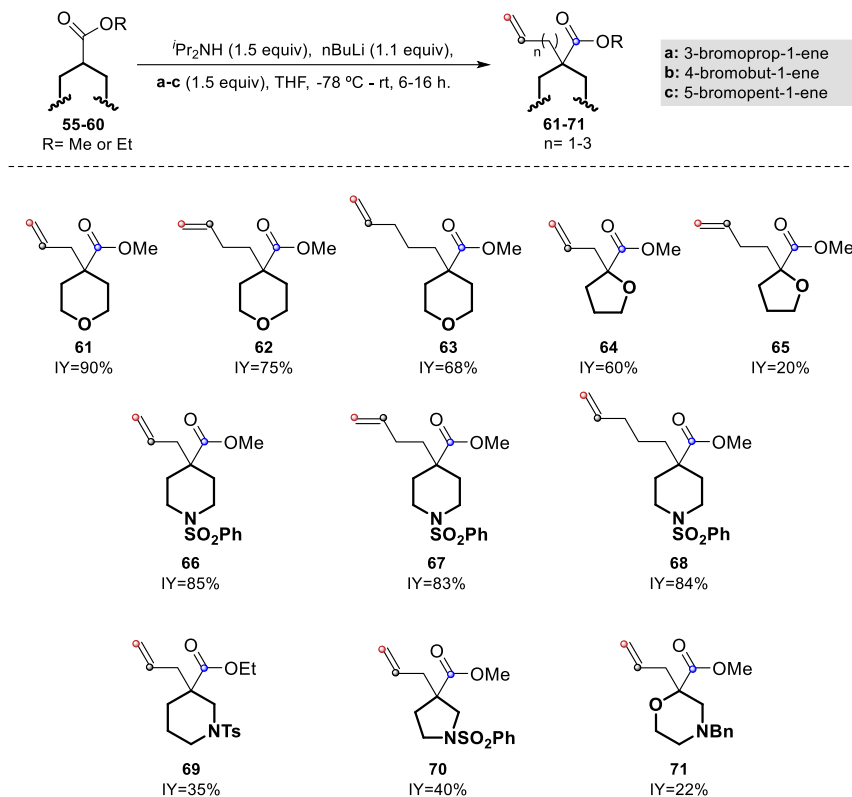


Figure 4.1 Heterocyclic carboxylic esters.

The next step was the alkylation of substrates **55-60** from Figure 4.1. This transformation was performed using *in situ* generated lithium diisopropyl amine (LDA) to deprotonate on  $\alpha$ -position to the ester group (Scheme 4.4). The carbanion was then trapped with several alkenyl halides of different chain length (**a-c**) allowing access to a variety of spiro-bicycles after ring-closing.<sup>[11]</sup> Substrate **55** was alkylated with 3-bromoprop-1-ene (**a**), 4-bromobut-1-ene (**b**) and 5-bromopent-1-ene (**c**) providing the corresponding alkylated products (**61-63**) in good to excellent yields. Then, methyl tetrahydrofuran-2-carboxylate (**56**) was satisfactorily alkylated with **a** providing methyl 2-allyltetrahydrofuran-2-carboxylate (**64**) in 60% isolated yield. The reaction with **b** proved to be more challenging and product **65** could only be isolated in 20% yield. Moreover, methyl 1-(phenylsulfonyl)piperidine-4-carboxylate (**57**) presented similar behavior as substrate **55**, allowing the formation of **66**, **67** and **68** in high isolated yields (83-85%). Other systems containing the nitrogen atom at 3-position with respect to the ester (**58-60**) only tolerated the alkylation with **a** forming the corresponding allyl-intermediates **69-71** in moderate yields. Attempts of alkylation on **58** with **b** and **c** were unsuccessful, recovering in all cases the starting material.

## Intramolecular borylative ring closing C-C coupling toward spiro- and dispiro-heterocycles

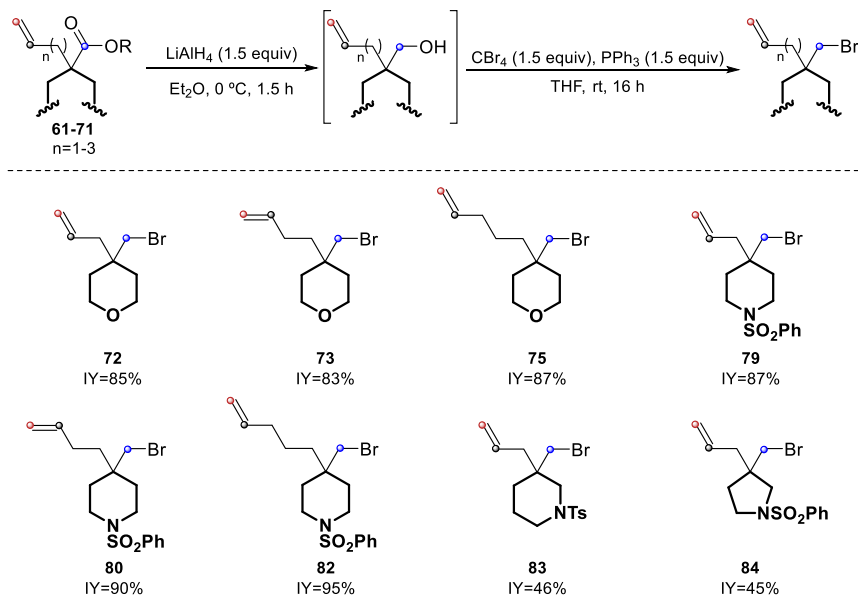


Scheme 4.4 General procedure and scope of the alkylation step.

Next the reduction of the carboxylic ester functions in **61-71** was explored. For this purpose,  $\text{LiAlH}_4$  was used as reducing agent in anhydrous  $\text{Et}_2\text{O}$  at  $0^\circ\text{C}$  (Scheme 4.5). Short reaction times of about 1.5 h were required to obtain the hydroxymethyl compounds in quantitative yields. These alcohols were used for the next reaction step without need to be purified.<sup>[12]</sup> At this point, aiming to study the effect of the leaving group in the borylative cyclization step, a number of alcohol containing scaffolds were converted to their corresponding brominated (Scheme 4.5) and / or iodinated substrates (Scheme 4.6).

Thus, the bromination of the hydroxymethyl intermediates (Scheme 4.5)<sup>[13]</sup> was achieved by the use of  $\text{CBr}_4$  and  $\text{PPh}_3$  in THF as solvent. In general, the expected brominated derivatives were isolated in excellent yields. The chain length and the heteroatom present in the heterocycle did not have a significant effect on the reaction efficiency. Substrates **61**, **62**, **63** containing a tetrahydropyran ring were converted into **72**, **73** and **75** in high yields. Also the 4-piperidine substrates were satisfactorily transformed to the bromo derivatives **79**, **80** and **82**. However, the reaction was sensitive to the presence of a nitrogen atom in position 3 respect to

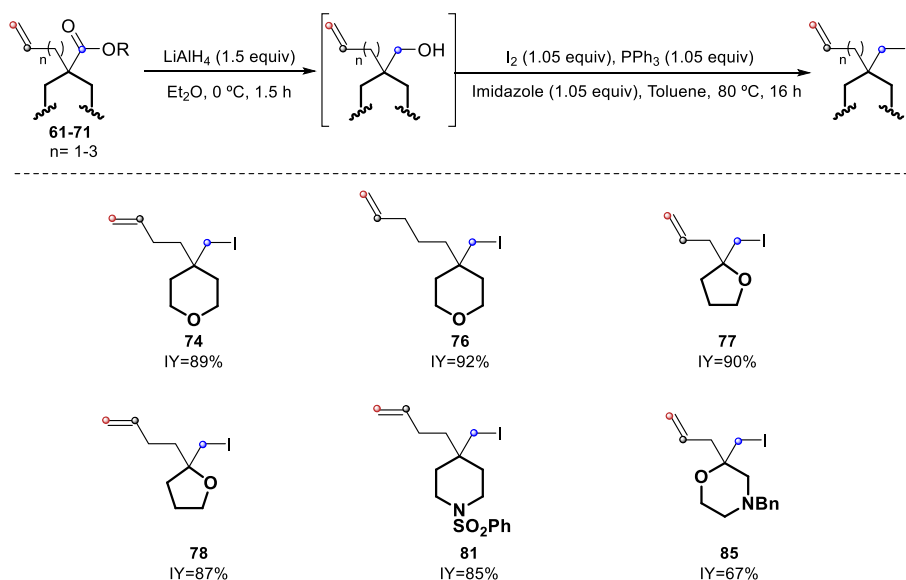
the quaternary carbon, and the alkylated 3-piperidine **83** and 3-pyrrolidine **84**, were obtained in only moderate yields. We hypothesized that this decrease in the reaction yields could be attributed to the steric hindrance created by the nitrogen protecting groups, hence hampering the bromination reaction.



Scheme 4.5 Sequential reduction/ bromination reactions

In addition several iodo derivatives were prepared for the alkylated products **61-71** (Scheme 4.6).<sup>[14]</sup> In this procedure the iodinated compounds derived from tetrahydropyrane, tetrahydrofuran and piperidine were obtained in excellent yields. Only in the case of the morpholine derivative a slight decrease in yield was observed, with product **85** in 67% isolated yield.

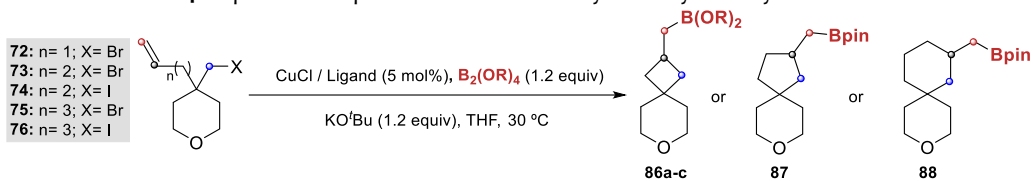


Intramolecular borylative ring closing C-C coupling toward spiro- and dispiro-  
heterocycles

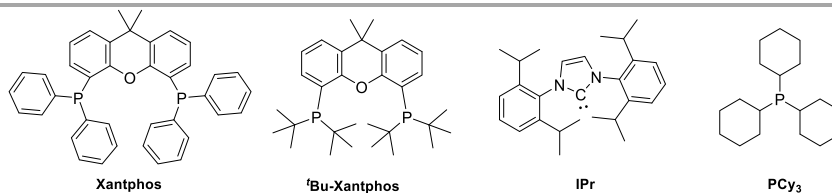
Scheme 4.6 Sequential reduction-iodination reactions

With the alkenyl halide derivatives in hand we conducted the preliminary studies on the copper catalyzed borylative ring-closing reaction. We selected as model substrates those based on the tetrahydropyran architecture (**72-76**) to find the optimal reaction conditions (Table 4.1). This reaction optimization phase was done in collaboration with the master student Albert Farré.

**Table 4.1** Optimization process for the Cu-catalyzed borylative cyclization.<sup>a</sup>



Entry	Time (h)	n	X	Substrate	Boron source (B <sub>2</sub> (OR) <sub>2</sub> )	Ligand	Product	IY [%] <sup>b</sup>
1	4	1	OH		B <sub>2</sub> pin <sub>2</sub>	Xantphos	<b>86a</b>	--
2	4	1	Br	<b>72</b>	B <sub>2</sub> pin <sub>2</sub>	Xantphos	<b>86a</b>	93%
3	4	1	Br	<b>72</b>	B <sub>2</sub> hex <sub>2</sub>	Xantphos	<b>86b</b>	65%
4	4	1	Br	<b>72</b>	B <sub>2</sub> neop <sub>2</sub>	Xantphos	<b>86c</b>	54%
5	4	2	Br	<b>73</b>	B <sub>2</sub> pin <sub>2</sub>	Xantphos	<b>87</b>	45%
6	4	2	I	<b>74</b>	B <sub>2</sub> pin <sub>2</sub>	Xantphos	<b>87</b>	65%
7	16	2	I	<b>74</b>	B <sub>2</sub> pin <sub>2</sub>	Xantphos	<b>87</b>	80%
8	16	2	I	<b>74</b>	B <sub>2</sub> pin <sub>2</sub>	PCy <sub>3</sub>	<b>87</b>	80%
9	16	2	I	<b>74</b>	B <sub>2</sub> pin <sub>2</sub>	<sup>t</sup> Bu-Xantphos	<b>87</b>	85%
10	16	2	I	<b>74</b>	B <sub>2</sub> pin <sub>2</sub>	IPr	<b>87</b>	67%
11	4	3	Br	<b>75</b>	B <sub>2</sub> pin <sub>2</sub>	Xantphos	<b>88</b>	20%
12	4	3	I	<b>76</b>	B <sub>2</sub> pin <sub>2</sub>	Xantphos	<b>88</b>	28%
13	16	3	I	<b>76</b>	B <sub>2</sub> pin <sub>2</sub>	Xantphos	<b>88</b>	36%



<sup>a</sup>Reaction conditions: CuCl (5 mol%), Xantphos (5 mol%), B<sub>2</sub>(OR)<sub>4</sub> (1.2 equiv), KO<sup>t</sup>Bu (1.2 equiv), THF (1 M), 30 °C, 4 - 16 h.

<sup>b</sup>IY= isolated yields.

## Intramolecular borylative ring closing C-C coupling toward spiro- and dispiro-heterocycles

---

First, the Cu / Xantphos catalyzed borylative ring-closing C-C coupling reaction was not successful on the hydroxyalkene derivative obtained from the reduction of ester **61**. In this case the corresponding spiro-bicycle **86** was not observed (Table 4.1, entry 1). Gladfully, the borylative ring-closing took place with the corresponding bromo derivative **72** using Xantphos as copper ligand and B<sub>2</sub>pin<sub>2</sub> (**1**) as the boron source. The desired product **86a** was isolated in excellent yield (93%) after 4 hours reaction time (Table 4.1, entry 2). The use of a different boron source, such as, B<sub>2</sub>hex<sub>2</sub> (**3**) or B<sub>2</sub>neop<sub>2</sub> (**2**) did not provide better results than those obtained with **1**, affording the desired spiro-cyclized products **86b** and **86c** in 65% and 54% isolated yield respectively (Table 4.1, entries 3,4). The lower yields observed with diboron reagents **2** and **3** might be related to a lower stability of products **86b** and **86c** under the purification conditions.

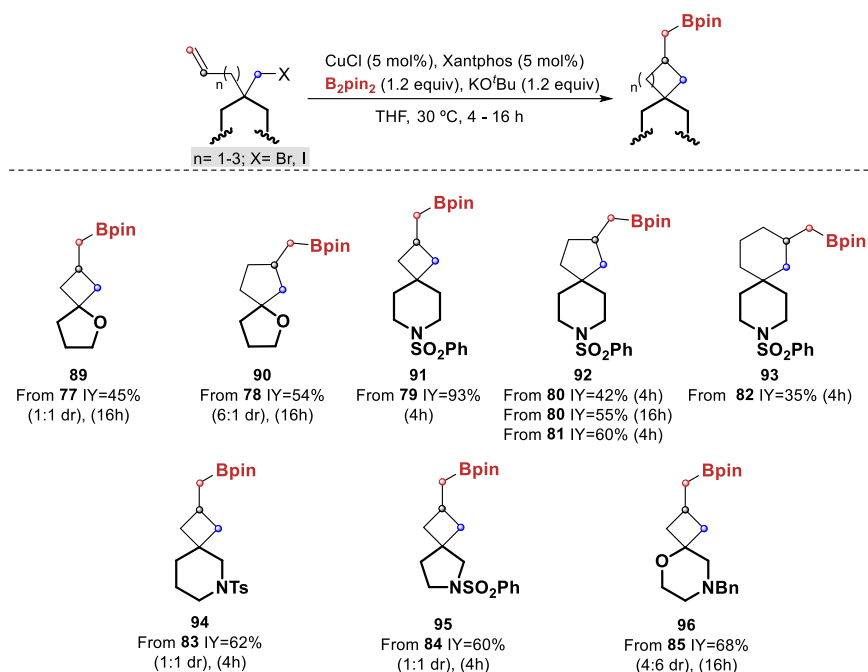
Since the formation of the 4-membered spiro-bicyclic ring was almost quantitative, we turned our attention to the borylative ring-closing reaction leading to 5-membered spiro-bicyclic compounds. The first trial with substrate **73** using B<sub>2</sub>pin<sub>2</sub> as the boron source, the C-C coupling reaction was successful and the 5-membered spiro-bicyclic scaffold **87** was obtained, albeit in moderate 45% isolated yield (Table 4.1, entry 5). Slightly better results were obtained when using substrate **74** having an iodine instead of a bromine as leaving group, and compound **87** could be obtained in 65% isolated yield after 4 hours (Table 4.1, entry 6). This result was further improved after a prolonged reaction time of 16 hours leading to a 80% isolated yield (Table 4.1, entry 7). A similar effect has been reported in the palladium-catalyzed ring forming aromatic C-H alkylations with unactivated alkyl halides.<sup>[14]</sup>

Switching from Xantphos to PCy<sub>3</sub> or <sup>t</sup>Bu-Xantphos led to comparable isolated yields of spiro-bicycle **87** (Table 4.1, entries 8-9). The use of a carbene ligand, such as 1,3-bis(2,6-diisopropylphenyl)-1*H*-imidazol-3-ium-2-ide (IPr), was detrimental for the borylative spiro-cyclization, lowering the performance of the reaction to 67% isolated yield (Table 4.1, entry 10).

As it could be anticipated, the C-C coupling reaction to form spiro-bicyclic products containing 6-membered ring such as 8-methylboryl-3-oxaspiro [5.5]undecane (**88**) proved to be more challenging. Both brominated (**75**) and iodinated (**76**) alkenyl substrates provided the formation of the targeted product under standard reaction conditions, however in only 20% and 28% isolated yields respectively (Table 4.1, entries 11-12). In the case of substrate **76** longer reaction times slightly increased the efficiency of the transformation up to 36% isolated yield (Table 4.1, entry 13). A plausible explanation accounting for the lower yields observed on the formation of the 6-membered spiro-bicyclic rings would be the required formation of an unfavoured 7-membered metallocycle prior to the reductive elimination step. It has

to be highlighted that the formation of product **88** represents the first example of a copper catalyzed borylative ring-closing C-C coupling leading to the formation of a 6-membered spiro-bicyclic ring.

With the optimized reaction conditions in hand, we then proceeded to extend the scope of the transformation using the different substrates prepared in Scheme 4.5 and Scheme 4.6. The results obtained are presented in Scheme 4.7.



**Scheme 4.7** Substrate scope of the borylative spiro-cyclization transformation.

Thus, the iodo derivative precursor **77** provided 2-methylboryl-5-oxaspiro [3.4]octane (**89**) in moderate yield (45%) as a 1 to 1 mixture of diastereoisomers (Scheme 4.7). Similarly, compound **78** having a longer spacer, provided the formation of the spiro-bicycle **90** in 54% on a diastereomeric ratio of 6:1. We hypothesized that the major flexibility of the longer alkene chain might favor a more stable conformation towards one of the diastereoisomers in the transition state intermediate. The nitrogen containing heterocycles as the bromo alkenyl piperidine derivative **79** were also suitable substrates in the spiro-cyclization process and the spiro-fused 4-membered-bicycle **91** was isolated in excellent yield (Scheme 4.7).

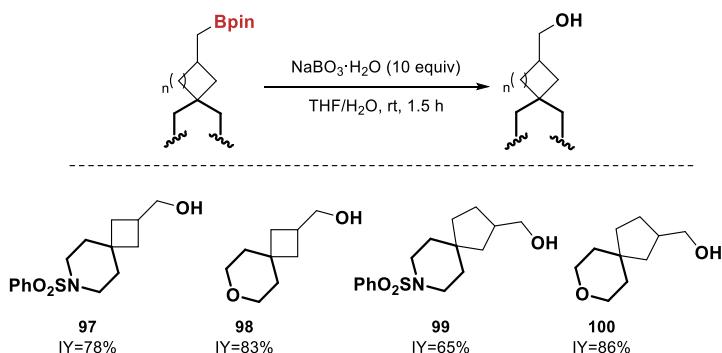
Several reaction conditions were tested for the synthesis of the 5-membered ring spiro-fused piperidine. The use of the alkenyl bromo derivative **80** under standard reaction conditions (4 h) provided the desired product **92** in moderate 42% isolated

## Intramolecular borylative ring closing C-C coupling toward spiro- and dispiro-heterocycles

yield. Again, longer reaction times increased the yield of **92** up to 55%. Moreover, the use of the alkenyl iodo derivative **81** favored the process towards the formation of the 5-membered spiro-bicycle **92** in 60% isolated yield, within 4 hours (Scheme 4.7). The longer chain alkene **82** was also successfully converted into the 6-membered spiro-bicycle **93**, however the yield of this transformation was moderate (35%) (Scheme 4.7). Additionally, the alkenyl bromo 3-piperidine (**83**) and 3-pyrrolidine (**84**) derivatives underwent the borylative ring-closing reaction providing the corresponding spiro-bicyclic derivatives **94** and **95**, in good isolated yields as 1:1 mixtures of diastereoisomers (Scheme 4.7). Finally, the spiro-cyclization reaction also took place on the iodo morpholine derivative **85**, affording compound **96** in 68% yield as a 4:6 mixture of diastereoisomes.

From the previous synthetic study it could be concluded that the efficiency of the spiro-cyclization process decreases as the size of the new ring increases from a 4- to a 6-membered ring carbocycle.  $\text{KO}^t\text{Bu}$  was found to be the optimal base, since  $\text{NaO}^t\text{Bu}$  favored the borylative debromination byproducts and  $\text{LiO}^t\text{Bu}$  gave negligible conversion toward the spiro-cyclization process. From the results obtained it can also be concluded that Cu-catalyzed borylative ring-closing C-C coupling is favored for alkenyl iodides over the matched pair alkenyl bromides. This could be attributed to the properties of iodide as better leaving group than bromide.

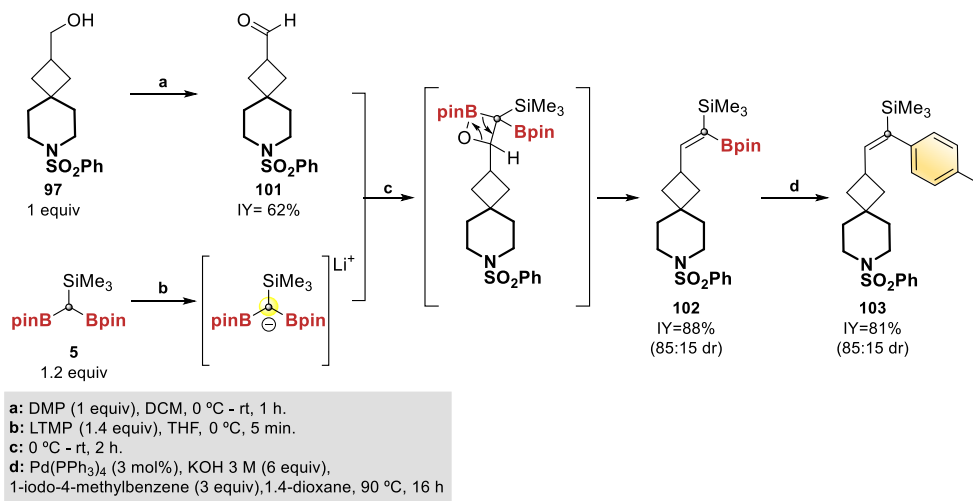
To prove the synthetic versatility of the synthesized spiro-boronate compounds further functionalizations of the C-B bond were explored. First, simple oxidative reaction conditions using  $\text{NaBO}_3 \cdot \text{H}_2\text{O}$ ,<sup>[15]</sup> gave access to the corresponding hydroxylated products **97-100** in high isolated yields (Scheme 4.8).



**Scheme 4.8** Selective oxidation of the spiro-heterocyclic boronate compounds.

Furthermore, product **97** was selectively oxidized to the corresponding aldehyde **101** using Dess-Martin periodinane (DMP) (Scheme 4.9).<sup>[16]</sup> The aldehyde **101** was transformed into the tri-substituted alkene **102** following a new olefination reaction developed in our group. This strategy is based on the deprotonation of

[CH(Bpin)<sub>2</sub>(SiMe<sub>3</sub>)] (**5**) with LTMP to generate an  $\alpha$ -boron /  $\alpha$ -silyl stabilized carbanion capable of adding to the carbonyl group in compound **101**.<sup>[17]</sup> Then, upon addition, the B-O elimination takes place through the Boron-Wittig pathway to generate the *gem*-silylborane spiro-bicycle **102** in 88% isolated yield in a 85 (*E*) to 15 (*Z*) diastereomeric ratio. Finally, the tethered boronate was subjected to Suzuki-Miyaura cross coupling conditions in the presence of 1-iodo-4-methyl benzene, Pd(PPh<sub>3</sub>)<sub>4</sub>, KOH in 1,4-dioxane as solvent at 90 °C for 16 hours, providing the desired tri-substituted alkene **103** with total stereocontrol, in a 85 (*E*) to 15 (*Z*) diastereomeric ratio (Scheme 4.9).<sup>[18]</sup>

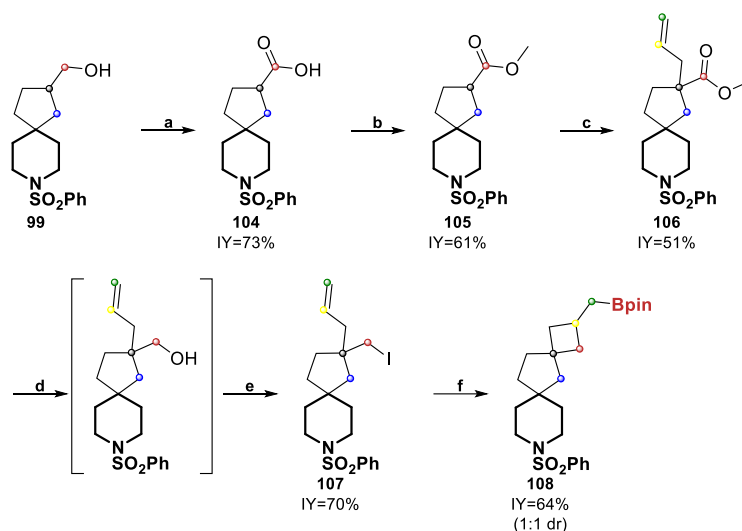


**Scheme 4.9** Selective olefination / arylation of spiro-heterobicyclic **97**.

Finally, since spiro-tricyclic structures are also present in many bioactive natural products<sup>[19]</sup> and to prove the value of this methodology we explored an iterative Cu-catalyzed borylative ring-closing C-C coupling for the preparation of a dispiro-heterotricyclic scaffold with a pendant methyl boronate. The targeted molecule would have three spiro-cyclic rings of different size, one of which would be heterocyclic. Our reaction sequence started with the Jones oxidation of the spiro-bicyclic compound **99**.<sup>[20]</sup> The oxidation product **104** has now a pendant carboxylic acid that was transformed into the methyl ester derivative **105** in moderate yield (61%).<sup>[21]</sup> Next, the spiro-bicyclic ester **105** was further elaborated into compound **106** by alkylation with allyl bromide following the procedure reported in Scheme 4.4.<sup>[11]</sup> Reduction of the ester function in **106** to the alcohol derivative<sup>[12]</sup> with concomitant iodination into compound **107**, which was achieved using the reaction conditions reported in Scheme 4.6.<sup>[14]</sup> The obtained spiro-bicyclic iodo derivative **107** successfully underwent intramolecular borylative cyclization to form the spiro-

## Intramolecular borylative ring closing C-C coupling toward spiro- and dispiro-heterocycles

tricyclic structure **108** in 64% isolated yield in a 1 to 1 diastereomeric ratio (Scheme 4.10).



- a:** Jones Reagent (0.7 equiv), acetone, H<sub>2</sub>O, 0 °C, 1 h.  
**b:** H<sub>2</sub>SO<sub>4</sub> (cat. 30 mL / mmol), MeOH (2 mL / mmol), 70 °C, 12 h.  
**c:** <sup>t</sup>Pr<sub>2</sub>NH (1.5 equiv), nBuLi (1.1 equiv), 3-bromoprop-1-ene (1.5 equiv), THF, -78 °C - rt, 6 - 16 h.  
**d:** LiAlH<sub>4</sub> (1.5 equiv), Et<sub>2</sub>O, 0 °C, 1.5 h.  
**e:** I<sub>2</sub> (1.05 equiv), PPh<sub>3</sub> (1.05 equiv), Imidazole (1.05 equiv), Toluene, 80 °C, 16 h.  
**f:** CuCl (5 mol%), Xantphos (5 mol%), B<sub>2</sub>pin<sub>2</sub> (1.2 equiv), KO<sup>t</sup>Bu (1.2 equiv), THF, 30 °C, 16 h.

**Scheme 4.10** Stepwise sequence for the synthesis of the dispiro-heterocycle scaffold.

The tricyclic structure of product **108**, was fully characterized by standard analysis and X-Ray diffraction techniques (Figure 4.2), confirming the presence of the spiro-fused four-, five-, and six-membered rings. Notably the piperidine core is an heterocycle motif commonly found in several spiro-tricycles employed in medicinal chemistry and agrochemicals.<sup>[19]</sup> The spiro-bicyclic derivative ester intermediate **105**, represents an attractive precursor for the synthesis of potent preclinical candidates used for prevention and treatment of hemorrhage.<sup>[22]</sup>

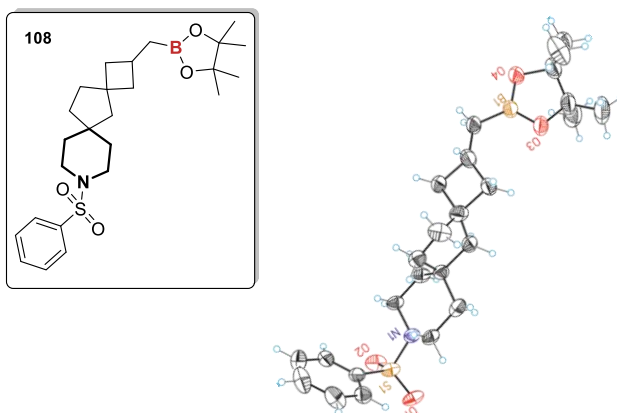


**Figure 4.2** ORTEP of the X-Ray diffraction analysis for dispiro-tricycle **108**.

With the aim to fully understand the mechanistic aspects of this transformation we established a collaboration with Prof. Feliu Maseras and Mr. Shaofei Ni from Institut Català d'Investigació Química (ICIQ), who carried out a DFT study<sup>[23]</sup> on the reaction mechanism.

A total of 28 different free energy profiles were computed varying the nature of the organic substrate, the leaving group, the counter ion from the base as well as the number of explicit THF molecules in the calculations. Figure 4.3 shows a representative free energy profile and the general features of the mechanism for the synthesis of the 5-membered ring spiro-bicyclic product **87**.

The starting point of the free energy profile is intermediate **I1**, this diposphine copper (I) alkoxide complex should be readily formed upon mixing CuCl, the alkoxy base and the ligand, Xantphos. Then by the subsequent addition of B<sub>2</sub>pin<sub>2</sub>, through  $\sigma$ -bond metathesis, the Cu-B species **I2** would then be readily formed. The first key step of this free energy profile might involve the coordination and insertion of the C=C double bond of the substrate **73** into the Cu-B specie (**I2**) via transition state **TS1**. The second key step of this transformation involves mostly a concerted step consisting in the halogen abstraction and ring closure facilitated by the copper through transition state **TS2**. Remarkably, it was possible to optimize the Cu (III) intermediate proposed previously by Ito and co-workers.<sup>[4, 24]</sup> This intermediate is shown as **I6** in Figure 4.3, since its energetic barrier is lower than 2 kcal mol<sup>-1</sup> for a reductive elimination, hence it could not be considered kinetically relevant. The highest energetic barrier in the free energy profile (Figure 4.3) is measured between **TS2** and **I4**, and is the one that affects directly to the overall efficiency of the process.



## Intramolecular borylative ring closing C-C coupling toward spiro- and dispiro-heterocycles

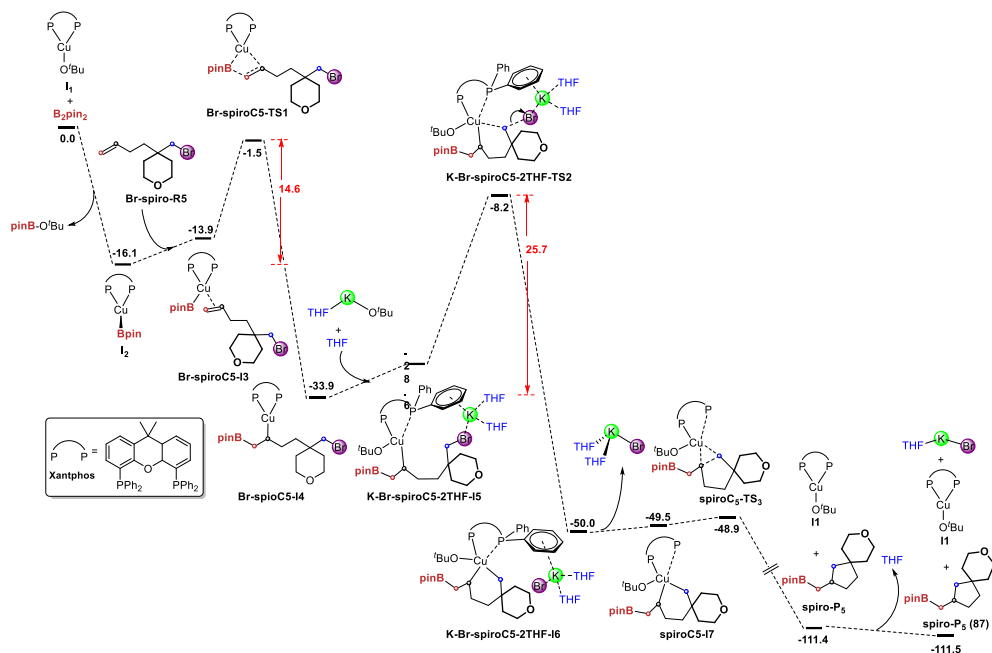


**Figure 4.3** Computed free energy profile (in kcal mol<sup>-1</sup>) for the formation of the 5-membered ring spiro-bicycle **87** with Br as the leaving group and KO<sup>t</sup>Bu as base (with the coordination of two THF solvation molecules). Energy profile calculated by Prof. Maseras and Mr. Ni at ICIQ.

A Heck-type mechanism was also considered<sup>[25]</sup> in the first activation of the C-X bond rather than activation from the C=C double bond. Much higher energetic barriers were obtained for the activation of the C-Br bond than for the mechanism on the activation of the C=C double bond.

The model energetic profile was validated with the introduction of different number of THF solvation molecules. It was found that the most favorable situation involves two molecules of THF, with an associated free energy barrier as illustrated in Figure 4.3 between **I4-TS2** of 25.7 kcal·mol<sup>-1</sup>.

## 4.4. Conclusions

In this study we evaluated diverse borylative cyclizations on unactivated alkenes through regioselective borylcupration followed by intramolecular ring-closing via halide displacement. The reaction exhibited high functional group tolerance, with central cores containing oxygen or nitrogen heteroatoms. The efficiency of the spiro-cyclization process was dependent on the size of the ring formed, with smaller rings (4-membered) being more favorable than larger ones (6-membered). This reactivity pattern was attributed to the required formation of the Cu (III) metallocyclic intermediate preceding the reductive elimination step. The present methodology enables the synthesis of new spiro-bicyclic cores, with different ring sizes in the new spiro-bicyclic motif formed. An iterative process gave access to a new dispiro-heterotricyclic structure fully characterized by X-Ray diffraction.

## Intramolecular borylative ring closing C-C coupling toward spiro- and dispiro-heterocycles

---

### 4.5. References Chapter 4

- [1] E. Buñuel, D. J. Cárdenas, *Eur. J. Org. Chem.* **2016**, 2016, 5446-5464.
- [2] K. Kubota, H. Iwamoto, H. Ito, *Org. Biomol. Chem.* **2017**, 15, 285-300.
- [3] a) H. Ito, Y. Kosaka, K. Nonoyama, Y. Sasaki, M. Sawamura, *Angew. Chem. Int. Ed.* **2008**, 47, 7424-7427; b) H. Ito, T. Toyoda, M. Sawamura, *J. Am. Chem. Soc.* **2010**, 132, 5990-5992; c) C. Zhong, S. Kunii, Y. Kosaka, M. Sawamura, H. Ito, *J. Am. Chem. Soc.* **2010**, 132, 11440-11442; d) Y. J. Zuo, X. T. Chang, Z. M. Hao, C. M. Zhong, *Org. Biomol. Chem.* **2017**, 15, 6323-6327.
- [4] K. Kubota, E. Yamamoto, H. Ito, *J. Am. Chem. Soc.* **2013**, 135, 2635-2640.
- [5] V. Uskoković, *Found. Sci.* **2010**, 15, 303-344.
- [6] E. M. Carreira, T. C. Fessard, *Chem. Rev.* **2014**, 114, 8257-8322.
- [7] S. Kotha, N. R. Panguluri, R. Ali, *Eur. J. Org. Chem.* **2017**, 2017, 5316-5342.
- [8] Y. Zheng, C. M. Tice, S. B. Singh, *Bioorg. Med. Chem. Lett.* **2014**, 24, 3673-3682.
- [9] F. Voss, S. Schunk, H. Steinhagen, in *Privileged Scaffolds in Medicinal Chemistry: Design, Synthesis, Evaluation*, The Royal Society of Chemistry, **2016**, pp. 439-458.
- [10] N. B. Palakurthy, B. Mandal, *Tetrahedron Lett.* **2011**, 52, 7132-7134.
- [11] V. Y. Stolyarenko, A. A. Evdokimov, V. I. Shishkin, *Mendeleev Commun.* **2013**, 23, 233-234.
- [12] F. X. Tavares, D. N. Deaton, A. B. Miller, L. R. Miller, L. L. Wright, H. Q. Zhou, *J. Med. Chem.* **2004**, 47, 5049-5056.
- [13] H. Li, S. S. Babu, S. T. Turner, D. Neher, M. J. Hollamby, T. Seki, S. Yagai, Y. Deguchi, H. Möhwald, T. Nakanishi, *J. Mater. Chem.* **2013**, 1, 1943-1951.
- [14] A. R. O. Venning, P. T. Bohan, E. J. Alexanian, *J. Am. Chem. Soc.* **2015**, 137, 3731-3734.
- [15] E. Yamamoto, Y. Takenouchi, T. Ozaki, T. Miya, H. Ito, *J. Am. Chem. Soc.* **2014**, 136, 16515-16521.
- [16] Y. Yamano, M. V. Chary, A. Wada, *Chem. Pharm. Bull.* **2010**, 58, 1362-1365.
- [17] E. La Cascia, A. B. Cuenca, E. Fernández, *Chem. Eur. J.* **2016**, 22, 18737-18741.

- [18] a) J. R. Coombs, L. Zhang, J. P. Morken, *Org. Lett.* **2015**, *17*, 1708-1711; b) K. Endo, M. Hirokami, T. Shibata, *J. Org. Chem.* **2010**, *75*, 3469-3472; c) K. Endo, A. Sakamoto, T. Ohkubo, T. Shibata, *Chem. Lett.* **2011**, *40*, 1440-1442.
- [19] a) J. R. Kesting, L. Olsen, D. Staerk, M. V. Tejesvi, K. R. Kini, H. S. Prakash, J. W. Jaroszewski, *J. Nat. Prod.* **2011**, *74*, 2206-2215; b) N. Kim, M.-J. Sohn, H. Koshino, E.-H. Kim, W.-G. Kim, *Bioorg. Med. Chem. Lett.* **2014**, *24*, 83-86; c) A. A. Salim, B. N. Su, H. B. Chai, S. Riswan, L. B. S. Kardono, A. Ruskandi, N. R. Farnsworth, S. M. Swanson, A. Douglas Kinghorn, *Tetrahedron Lett.* **2007**, *48*, 1849-1853; d) X. Wang, Q. Zhao, M. Vargas, Y. Dong, K. Sriraghavan, J. Keiser, J. L. Vennerstrom, *Bioorg. Med. Chem. Lett.* **2011**, *21*, 5320-5323.
- [20] K. E. Harding, L. M. May, K. F. Dick, *J. Org. Chem.* **1975**, *40*, 1664-1665.
- [21] R. Moumne, S. Lavielle, P. Karoyan, *J. Org. Chem.* **2006**, *71*, 3332-3334.
- [22] J. Orbe, J. A. Rodríguez, J. A. Sánchez, A. Salicio, M. Belzunce, A. Ugarte, H. C. Y. Chang, O. Rabal, J. Oyarzabal, J. A. Páramo, *J. Med. Chem.* **2015**, *58*, 2941-2957.
- [23] Calculations in solution (THF) were performed with the  $\omega$ B97X-D functional and a valence triple- $\zeta$  basis set complemented with polarization and diffuse functions.
- [24] H. Iwamoto, S. Akiyama, K. Hayama, H. Ito, *Org. Lett.* **2017**, *19*, 2614-2617.
- [25] a) D. Balcells, F. Maseras, B. A. Keay, T. Ziegler, *Organometallics* **2004**, *23*, 2784-2796; b) J. H. Li, D. P. Wang, Y. X. Xie, *Tetrahedron Lett.* **2005**, *46*, 4941-4944.

UNIVERSITAT ROVIRA I VIRGILI  
COMPLEMENTARY SYNTHESIS OF ORGANOBORANES TO POPULATE THE CHEMICAL  
FUNCTIONALITY TO A GIVEN AREA OF BIOMEDICAL INTEREST  
Jordi Royes Buisan

# **Chapter 5**

## **Synthesis and application of novel spiro- boronate compounds for the treatment of Alzheimer's disease**

---

UNIVERSITAT ROVIRA I VIRGILI  
COMPLEMENTARY SYNTHESIS OF ORGANOBORANES TO POPULATE THE CHEMICAL  
FUNCTIONALITY TO A GIVEN AREA OF BIOMEDICAL INTEREST  
Jordi Royes Buisan

## 5.1. State of the art

Among the most facing challenges for medicinal chemists is the discovery and development of compounds for the prevention and treatment of fatal diseases. An intense area of research focusses on Alzheimer's disease (AD), a devastating age-related neurodegenerative disorder. AD is characterized by common symptoms related with a slow but inexorable loss of memory and cognition.<sup>[1]</sup>

AD affects over 40 million people worldwide and currently there is no an available cure. Current pharmacological treatments have a temporarily mild effect in slowing down the progression of cognitive decline. This makes of AD one of the main unmet medical needs of the 21<sup>st</sup> century, hence there is an urgent need to identify disease modifying therapies, which should slowdown or treat the neurodegenerative process.<sup>[2]</sup>

### 5.1.1 Alzheimer's disease

The concept of dementia had been generally recognized over a thousand years. Alois Alzheimer, a German pathologist and neuropsychiatrist, changed the understanding of dementia after studying the evolution of symptoms of his patient Auguste Deter, a 51 years old woman that was admitted in the Frankfurt asylum on November 25<sup>th</sup> 1901. Dr. Alzheimer, after an initial examination, described the first neuropsychological characterization of this demented patient as follows:<sup>[3]</sup>

*“Her memory is seriously impaired. If objects are shown to her, she names them correctly, but almost immediately afterwards she has forgotten everything. When reading a text, she skips from line to line or reads by spelling the words individually, or by making them meaningless through her pronunciation. In writing she repeats separate syllables many times, omits others and quickly breaks down completely. In speaking, she uses gap-fills and a few paraphrased expressions (“milk-pourer” instead of cup); sometimes it is obvious she cannot go on. Plainly, she does not understand certain questions. She does not remember the use of some objects.”*

Dr. Alzheimer (Figure 5.1 left) followed the case of Auguste (Figure 5.1 right), over a period of four and a half years until April 8<sup>th</sup> 1906 when she passed away. Postmortem analysis of Auguste's brain using a new histological staining technique allowed Dr. Alzheimer to identify by the first time the presence of two different classes of protein aggregates. These aggregates are now recognized as the two main pathophysiological characteristics of the disease: amyloid plaques and neurofibrillary tangles.<sup>[4]</sup>



## Synthesis and application of novel spiro-boronate compounds for the treatment of Alzheimer's disease

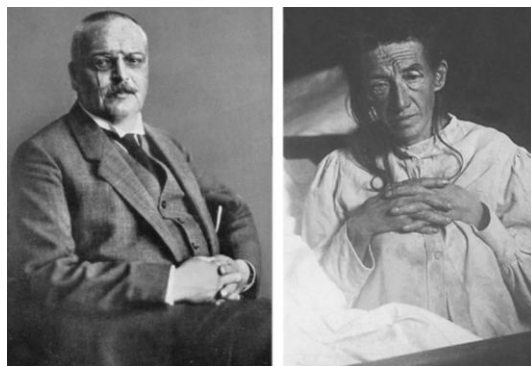


Figure 5.1 Dr. Alois Alzheimer (left) and his patient Auguste Deter (right).

### 5.1.2 Epidemiology

Epidemiology studies have proven that AD it is not a contagious disease, even though an exponential increase in the number of AD patients has been observed. Currently, 40 million people over 60 years old suffer from dementia. This figure is expected to triple and reach over 131 million in 2050 (Figure 5.2). An equal distribution of AD around the world has been observed, with non-differentiation in terms of proportion for each continent.<sup>[5]</sup>

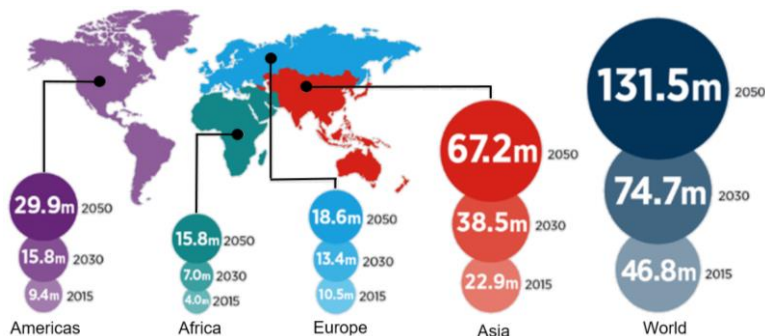


Figure 5.2 Prevalence of AD around the world and estimation in the future.

In 2018 the total estimated worldwide cost of AD was 1 trillion of dollars, which is expected to triple in 2050. If no treatment becomes available in the coming years the prevalence of AD will create a social and economic problem worldwide.

In terms of gender, AD has higher incidence in women than men, with two-thirds of new cases being diagnosed in women.<sup>[6]</sup> Moreover, related with the diet, it has been observed that people who developed type II diabetes are more prone to develop AD, even though there are not clear associations between the two diseases.<sup>[7]</sup>

A confirmed evidence is that the age is the most notable risk factor. Based on age, when the first symptoms of AD appear, the disease is classified in early-onset AD (EOAD, people younger than 65 years old) and late-onset AD (LOAD, people older than 65 years old). Commonly, EOAD is often related to mutations in specific genes, meanwhile LOAD is more associated to a combination of factors, as the ones previously commented.<sup>[8]</sup>

### 5.1.3 Pathophysiology

Since the discovery of the protein aggregates by Alöis Alzheimer, the main focus for researches has been to identify the protein(s) or enzyme(s) responsible for the accumulation of these deposits, ultimately though to be a contributing factor to the appearance of AD. From all these studies, it has been concluded that the two major neuropathological hallmarks of AD are the presence of extracellular  $\beta$ -amyloid ( $A\beta$ ) plaques made of  $A\beta$  peptides of variable length and the formation of intracellular neurofibrillary tangles (NFTs) (Figure 5.3), constituted by paired helical filaments (PHFs) of abnormally hyperphosphorylated Tau protein.

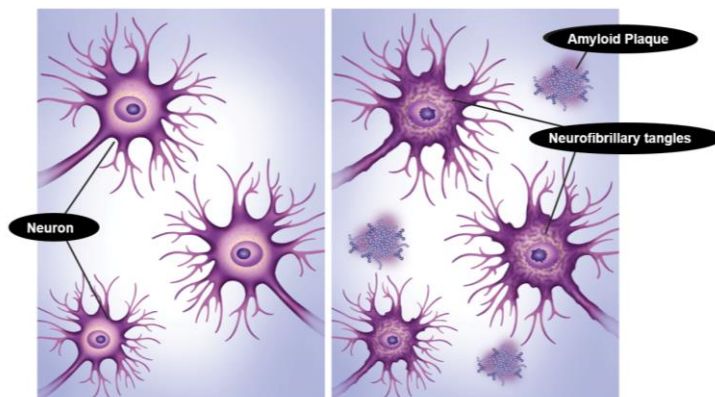


**Figure 5.3** Healthy neurons (**left**) and neurons in AD surrounded by  $A\beta$  plaques and containing intracellular NFTs (**right**).

In addition to the abnormal accumulation of protein aggregates, there are other events that aggravate the course of the disease, like neuro-inflammation processes, a great neuronal loss resulting in a diminished cerebral volume (Figure 5.4), and failure in the vascular system.<sup>[9]</sup>

## Synthesis and application of novel spiro-boronate compounds for the treatment of Alzheimer's disease

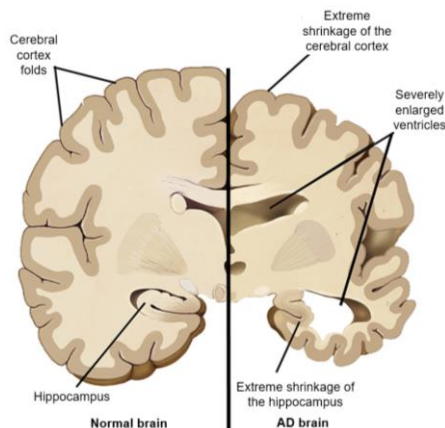


**Figure 5.4** Graphical comparative between a healthy brain (**left**) and a brain with severe AD (**right**).

Initially, most research was based in preventing the production and accumulation of  $A\beta$  peptides leading to the formation of extracellular senile plaques.<sup>[10]</sup> Amyloid  $\beta$  accumulation (red curve, Figure 5.5) starts early in life and has reached close to maximum levels when the first clinical symptoms of the disease are observed and signs of mild cognitive decline start.<sup>[10]</sup> However,  $A\beta$  accumulation alone does not correlate well with the progression of the disease, as maximum levels are present well before mild cognitive impairment (MCI) is diagnosed (purple curve, Figure 5.5). Tau deposition also starts early in life, but it is when  $A\beta$  deposition starts reaching maximum levels that an accelerated Tau deposition is observed (blue curve, Figure 5.5).

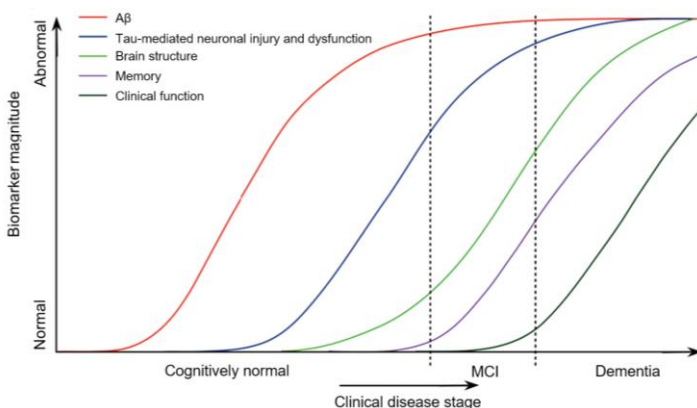


**Figure 5.5** Correlation between the accumulations of  $A\beta$  peptides and Tau protein and the clinical stage of AD.

Early stages of AD are characterized by the accumulation of amyloid  $\beta$ -protein in the brain. Then, several years after, Tau aggregates start accumulating and spreading from the entorhinal cortex throughout outer brain regions. At the point that the  $A\beta$  accumulation reaches almost the maximum level, and significant Tau pathology has developed, the first symptoms of AD, MCI stage, can be observed.

Considering that  $A\beta$  accumulation is the initiator of the disease and that Tau deposition occurs downstream, most pharmacological approaches have focused on preventing or halting the formation of senile  $A\beta$  plaques. Inhibiting beta-secretase 1 (BACE-1), a protease that performs the initial cleavage of the amyloid precursor protein (APP) which ultimately leads to the production of  $A\beta$  peptides, has been the focus of research for mayor pharmaceutical companies over the last two decades. However, despite of all efforts all BACE-1 inhibitors reaching the clinic have fallen short in phase III clinical trials.<sup>[11]</sup>

Nowadays it is recognized that blocking  $A\beta$  production at this late disease stage, were the accumulation of plaques in brain is already at maximum levels, could be analogous to treat with cholesterol lowering statins a congestive heart failure in the emergency room. For that reason, targeting a population of asymptomatic individuals but at high risk of developing AD is crucial to intersect the progression of the disease. Patient selection based on early biomarkers of the disease is a critical element to the design of appropriate clinical trials.<sup>[2]</sup>

In the last decade, interfering with the progression of Tau pathology has become an important area of research in AD due to the better correlation between Tau pathology with neurodegeneration than the one of  $A\beta$  deposition.

#### 5.1.4 Tau hypothesis

Tau is an intraneuronal unfolded and highly soluble protein. Its principal function is the assembly and stabilization of the microtubules in the axons of neurons (Figure 5.6). The microtubules are essential in neurons for the distribution of proteins and nutrients along them.<sup>[12]</sup>

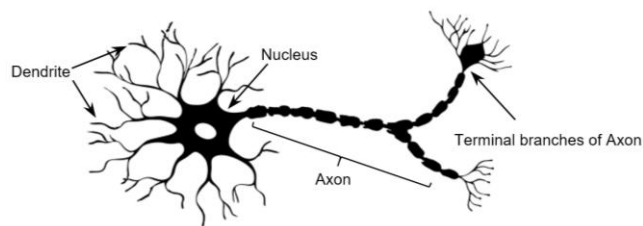
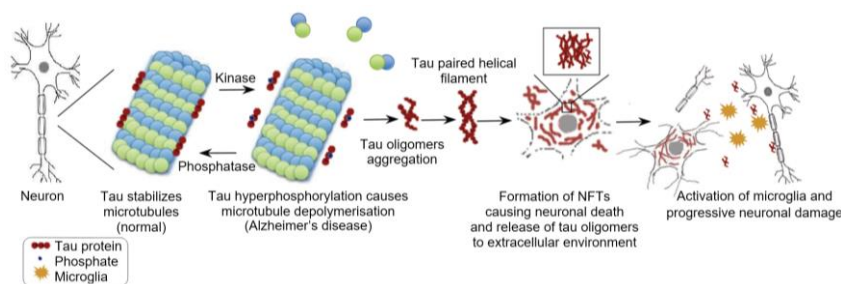


Figure 5.6 Illustration of the different general parts from healthy neuron.

## Synthesis and application of novel spiro-boronate compounds for the treatment of Alzheimer's disease

The accumulation of neurofibrillary tangles (NFTs) in the brain is a hallmark of AD. Postmortem analysis of AD brains has shown abnormal levels of hyperphosphorylated Tau protein. In a healthy brain Tau contains around 2-3 moles of phosphates per mole of protein, whereas an AD brain it contains 3- to 4-fold more phosphates.<sup>[13]</sup> Hence, it is believed that in the course of AD Tau gets hyperphosphorylated, which causes its detachment from the microtubules rendering phospho-Tau in the cytosol. This phosphorylated Tau protein starts templating and aggregating additional Tau monomers and oligomers, ultimately leading to the formation of pair helical filaments (PHFs) that subsequently aggregate to form the characteristic NFTs found in AD brain. (Figure 5.7).<sup>[14]</sup> The formation of NFTs and accumulation in the neuronal cell body eventually leads to apoptosis.<sup>[15]</sup>



**Figure 5.7** Process of Tau hyperphosphorylation causing the apoptosis of the neuron cell.

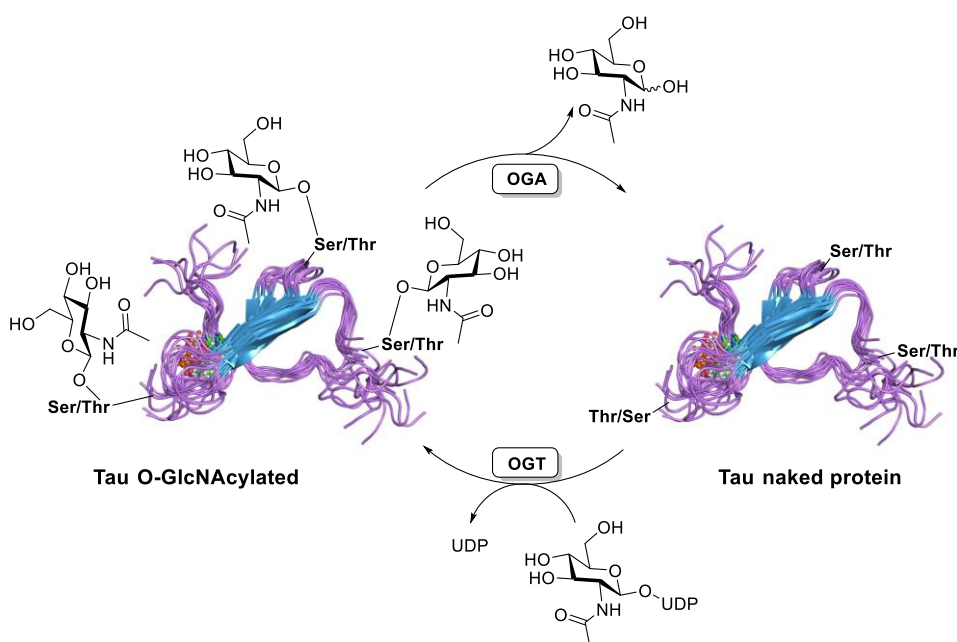
Great efforts have been made to understand and regulate Tau phosphorylation. The inhibition of kinases responsible for installing phosphate groups in Tau has been considered a fundamental therapeutic strategy to rescue Tau mediated neurodegeneration.<sup>[16]</sup> However, this strategy has proven challenging, which suggest that there might be other underlying mechanisms regulating the number of sites phosphorylated that remain unknown.<sup>[17]</sup>

Recent studies have shown that Tau protein is hypo-*O*-GlcNAcylated in AD brains, suggesting that the presence of *O*-linked- $\beta$ -*N*-acetylglucosamine (*O*-GlcNAc) residues on Tau in healthy brains could be protective.<sup>[18]</sup> *O*-GlcNAcylation and phosphorylation are mutually exclusive on the same residue, hence an amino acid residue cannot be phosphorylated once a molecule of *O*-linked- $\beta$ -*N*-acetylglucosamine is present. As consequence, in AD brains where hypo-*O*-GlcNAcylation occurs, Tau phosphorylation sites are freely exposed to kinases, as described previously in Figure 5.7, resulting in Tau abnormal hyperphosphorylation, detachment from microtubules and subsequent aggregation.

*O*-GlcNAcylation is a posttranslational modification that affects hundreds of proteins. Opposed to phosphorylation, where hundreds of kinases and phosphatases are known to add and remove a phosphate molecule, GlcNAcylation

is mediated by two enzymes: *O*-GlcNAc transferase (OGT) responsible for adding the sugar residue and *O*-GlcNAcase (OGA) which removes the *O*-linked-*N*-acetylglucosamine (*O*-GlcNAc) residue. The reciprocal relationship between the removal of *O*-GlcNAc and the hyperphosphorylation state of Tau, has encouraged researchers to identify OGA inhibitors as an approach to keep phosphorylation sites in Tau unavailable for the action of kinases.<sup>[19]</sup>

OGT, OGA and *O*-GlcNAcylated proteins are particularly abundant in the brain, suggesting they could be the key regulatory modifications which contribute to neuronal communications, memory, and the responsible players of the apparition of neurodegenerative diseases (Scheme 5.1).<sup>[20]</sup>



**Scheme 5.1** Regulation of Tau *O*-GlcNAcylation by OGT and OGA enzymes (UDP= uridine diphosphate).

Therefore, maintaining “healthy levels” of *O*-GlcNAcylation in Tau proteins by the cooperation of small-molecule inhibitors of OGA, could represent a potential approach to decrease the levels of hyperphosphorylated Tau protein. Thereby, rendering Tau less prone to detaching from the microtubules, avoiding its aggregation into neurotoxic tangles and ultimately blocking the neurotoxicity and apoptosis of the neuron.<sup>[12]</sup>

Preventing the formation of Tau aggregates may also reduce the cell-to-cell spreading of Tau-aggregates released by neurons, which has been discussed to increase the velocity of propagation in Tau related dementias.<sup>[21]</sup>

## Synthesis and application of novel spiro-boronate compounds for the treatment of Alzheimer's disease

---

Treatment with sub-optimal OGA inhibitors has already demonstrated in preclinical studies a decrease in Tau phosphorylation by preventing the removal of *O*-GlcNAc from Tau protein. These observations spurred the interest of the scientific community to identify an optimal OGA inhibitor able to control Tau phosphorylation.

### 5.1.5 Spiro-bicyclic scaffolds as source of OGA inhibitors: rationale

Several OGA inhibitors have been developed during the last years and profiled *in vitro* and *in vivo* models of neurodegenerative diseases. Thiamet G (**109**) (Figure 5.8), a potent and highly selective sugar-based inhibitor (hOGA  $K_i = 0.41$  nM, rOGA cell  $EC_{50} = 13.5$  nM),<sup>[22]</sup> has been used as a good tool compound for hypothesis validation. Compound **109** has demonstrated to increase Tau *O*-GlcNAcylation levels, with a concomitant decrease in Tau phosphorylation, reducing the formation of Tau aggregates and neuronal cell loss *in vivo*.<sup>[23]</sup>

However, Thiamet G is a poorly brain penetrant compound and preclinical efficacy studies in rodents have required chronic administration of doses of 500 mg/kg to significantly increase Tau *O*-GlcNAcylation levels.<sup>[24]</sup>

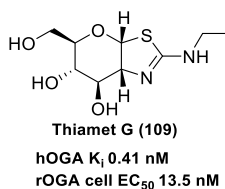
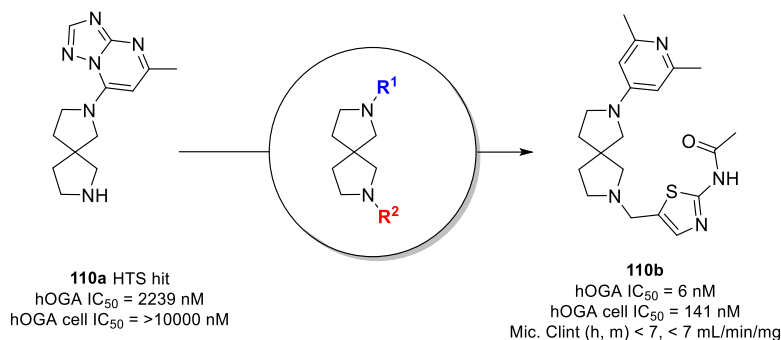


Figure 5.8 Structure of Thiamet-G a potent inhibitor of OGA.

Given the increasing interest in identifying OGA inhibitors Janssen performed a high throughput screening (HTS) of the corporate compound collection using an enzymatic assay. Among other hits identified the diazaspino-nonane (**110a**) as a weak OGA inhibitor with a  $IC_{50}$  of 2239 nM in the OGA enzymatic assay. Compound **110a** was inactive in the OGA cellular assay at the highest concentration tested (10  $\mu$ M) (Figure 5.9).



**Figure 5.9** HTS hit **110a** and advanced lead **110b** from an early SAR exploration.

The early Medicinal Chemistry strategy to improve the activity of hit **110a** consisted in the preparation of a library of compounds exploring a variety of substituents on the spiro-cyclic core nitrogen atoms. Aromatic and heteroaromatic groups on  $R^1$  were combined with a diverse set of alkyl-, (het)aryl- and benzyl like substituents in  $R^2$ .

Interestingly, when a 4-pyridyl  $R^1$  substituent was combined with an acetamidothiazolyl-containing substituent in  $R^2$  the single-digit nanomolar inhibitor **110b** was obtained (hOGA  $IC_{50}$  = 6 nM). Moreover, **110b** presented a much improved activity in the cellular assay with an  $IC_{50}$  of 141 nM (Figure 5.9) and was stable in human and mouse liver microsomes.<sup>[25]</sup>

Compound **111** from the same chemical series, where the south spiro-pyrrolidine has been replaced by a spiro-azetidine ring (Figure 5.10) could be co-crystallized with CpOGA, a bacterial orthologue from *C. perfringens* of hOGA.<sup>[26]</sup>

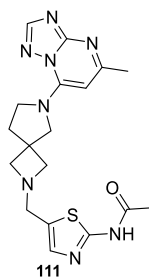


**Figure 5.10** Spiro-azetidine compound **111**.

The co-crystal obtained provided useful information on the ligand interactions in the catalytic pocket of the bacterial enzyme, which shows a very high sequence homology with the one of hOGA. The spiro-cyclic core distributes the two



## Synthesis and application of novel spiro-boronate compounds for the treatment of Alzheimer's disease

heteroaromatic substituents along the right vectors. Thus, the acetamidothiazole group in **111** goes deep into the catalytic pocket, where the *O*-GlcNAc residue in OGA client substrates is hydrolyzed, and the triazolopyrimidine ring occupies an open area of the protein where the enzyme accommodates the backbone of the natural substrates bearing the *O*-GlcNAc residue (Figure 5.11a)

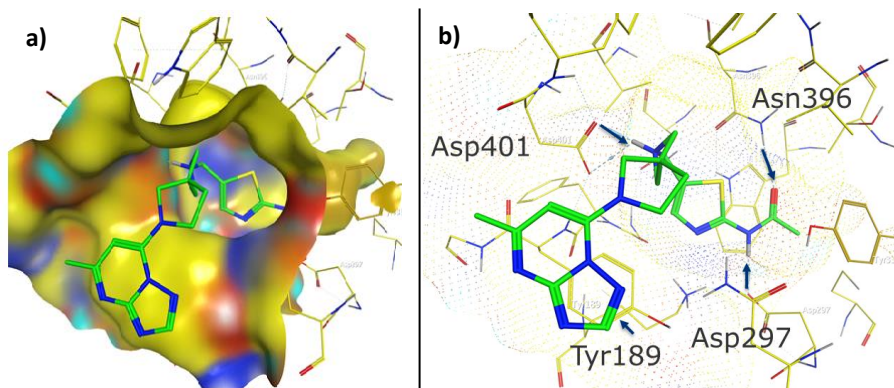


**Figure 5.11** X-Ray co-crystal of compound **111** and CpOGA. a) Protein surface; b) Key interactions between compound **111** and protein amino acid residues.

In Figure 5.11b, are highlighted the key interactions between compound **111** and the enzyme. As it can be seen there are two hydrogen-bond interactions between the acetamide substituent, and Asn396 and Asp297. Moreover, the basic nitrogen of the azetidinium ring, which is protonated at the physiological pH, establishes a dominant ionic interaction with Asp401 that anchors the core in the catalytic pocket. An extra  $\pi$ - $\pi$  stacking interaction between the triazolopyrimidine ring and Tyr189 can also be observed. Interestingly, the pyrrolidine nitrogen does not seem to make any interactions in the co-crystal structure.

## 5.2. Aim of the Chapter

With all these precedents in mind and encouraged by the results obtained with Thiamet G (**109**), as well as with the interesting *in vitro* activity of the diazospirononane **110b**, a collaboration with the Medicinal Chemistry team of Janssen in Toledo was started. The aim of this collaboration was to apply the methodology described in Chapter 4 for the synthesis of target spiro-compounds and expand the available structure activity relationship (SAR) around the novel series of OGA spiro-bicyclic inhibitors.

The research plan consisted on the preparation of novel spiro-compounds applying our reported methodology, which would enable several modifications on the spiro-bicyclic core while deleting the nitrogen atom of the diazospirononane scaffolds that does not make an interaction with the protein (Figure 5.12). In addition, the nitrogen deletion could contribute to increase the permeability and penetration in the brain-cell matrix of these inhibitors, while maintaining the good response on the enzymatic and cellular assays.

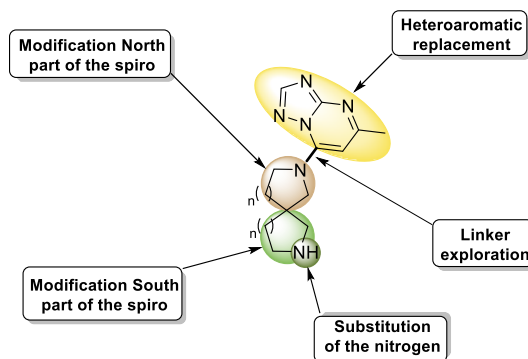


Figure 5.12 Graphical objectives of the chapter.

## Synthesis and application of novel spiro-boronate compounds for the treatment of Alzheimer's disease

### 5.3. Results and discussion

Since the hit **110a** and a good number of derivatives from this chemical series presented low cellular permeability and limited brain penetration we hypothesized that a reduction in the number of nitrogen atoms in the central spiro-bicyclic core could be beneficial for these properties. For this purpose, five different spiro-bicyclic motifs having different ring sizes and heteroatoms were designed (Figure 5.13).

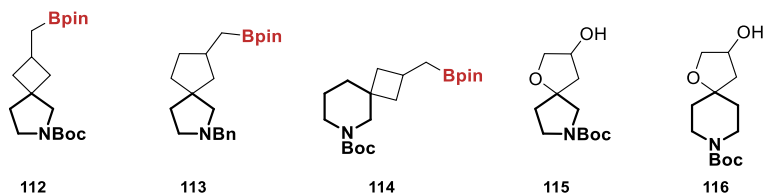


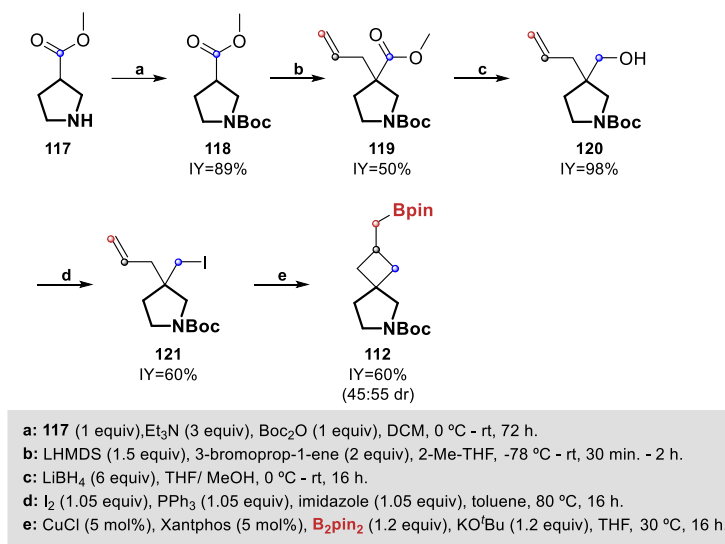
Figure 5.13 Designed spiro-bicyclic motifs.

The synthesis of scaffolds **112**, **113**, and **114** could be possible via the copper borylative cyclization reaction reported in Chapter 4. However, this methodology cannot be applied to the synthesis of compounds **115** and **116** and these were accessed following a iodo-cyclization method reported in the literature.<sup>[27]</sup>

#### 5.3.1 Synthesis of spiro-bicyclic central scaffolds

Our studies started with the synthesis of compound **112** (Figure 5.13). Since a very close analogue (**95**) of compound **112** was synthesized in Chapter 4, the same synthetic route was explored introducing slight changes to increase the efficiency of the process. Thus, pyrrolidine **117** was *N*-Boc protected with excellent yield by treatment with Boc<sub>2</sub>O in the presence of triethylamine (TEA) as a base, leading to compound **118** in excellent yield (Scheme 5.2).<sup>[28]</sup> The reason for changing the nitrogen protecting group from phenylsulfonyl in **59** to Boc in **118** was the easier removal on the later stages under acidic conditions. Then, allylation on the  $\alpha$ -position to the ester was achieved in 50% isolated yield by treatment with lithium bis(trimethylsilyl)amide and allylbromide to give compound **119** (Scheme 5.2).<sup>[29]</sup> Reduction of the ester function in **119** to the alcohol was performed with LiBH<sub>4</sub> using a mixture of THF / MeOH providing *tert*-butyl 3-allyl-3-(hydroxymethyl)pyrrolidine-1-carboxylate (**120**) in quantitative yield (Scheme 5.2).<sup>[30]</sup> Aiming to improve the copper (I) borylative cyclization pathway, alcohol **120** was converted into the iodomethyl pyrrolidine **121**, using reaction conditions previously reported in Chapter 4 (Scheme 5.2).<sup>[31]</sup> Finally, the copper borylative spiro-cyclization of **121** applying the optimal conditions identified in Chapter 4 afforded the target *tert*-butyl

2-methylboryl-6-azaspiro[3.4]octane-6-carboxylate (**112**) in a 60% isolated yield in a diastereomeric ratio of 45:55.<sup>[32]</sup>

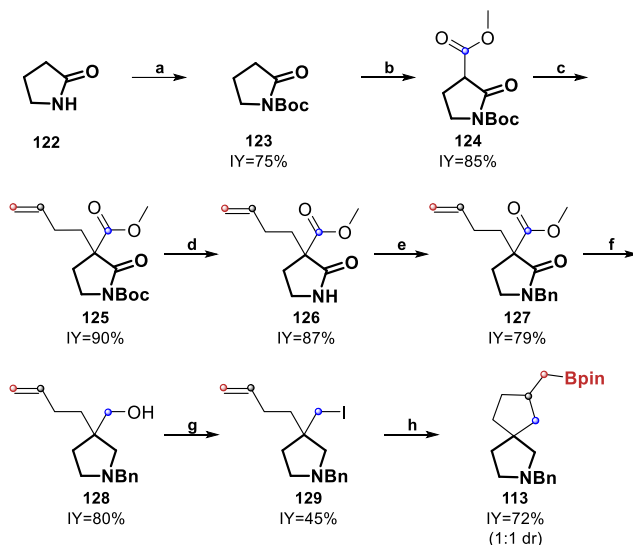


**Scheme 5.2** Synthetic route for obtaining spiro-bicyclic scaffold **112**.

Then, the synthesis of compound **113** bearing a spiro-bicyclic cyclopentane ring was attempted. This spiro-bicyclic compound has not been previously reported, neither by using the methodology described in Chapter 4 or by other methods.<sup>[32]</sup> Since the  $\alpha$ -alkylation to the ester function in pyrrolidine **118** with 4-bromo-1-butene failed to form the expected compound in satisfactory yield, a different synthetic strategy was designed (Scheme 5.3). The synthesis started with pyrrolidin-2-one (**122**), which was protected with Boc<sub>2</sub>O using DMAP as base to give the *N*-Boc-protected pyrrolidin-2-one (**123**) in good yield (Scheme 5.3).<sup>[33]</sup> Then functionalization at position 3 of the pyrrolidone core with methyl chloroformate in the presence of LHMDS gave access to the 1,3-dicarbonylic compound **124** in excellent yield.<sup>[34]</sup> Subsequent alkylation of **124** with 4-bromo-1-butene afforded the desired pyrrolidone **125** in 90% yield.<sup>[35]</sup> Of note is the importance of the nucleophilicity and stability of the carbanion formed in the reaction with 4-bromo-1-butene, going from no reaction in the case of **118** (Scheme 5.2) to almost quantitative yield for **124** (Scheme 5.3). The reduction of the two carbonyl groups in **125** proved to be a challenging process. Different reducing agents were tested affording only the *N*-methylated compound, resultant of the carbamate reduction, and different byproducts with decomposition of the starting material being the most observed reaction outcome. For these reasons, we decided to change the Boc protecting

## Synthesis and application of novel spiro-boronate compounds for the treatment of Alzheimer's disease

group of the lactam nitrogen by a simple benzyl substituent, a group expected to be unreactive under the reduction conditions of a carbonyl function. Thus treatment of **125** with an acidic solution of HCl 4 N in 1,4-dioxane, led compound **126** in excellent yield within 2 hours (Scheme 5.3).<sup>[36]</sup> *N*-benzylation of **126** with benzylbromide using Cs<sub>2</sub>CO<sub>3</sub> in acetonitrile at 90 °C gave access to the *N*-benzyl protected lactam **127** (Scheme 5.3).<sup>[37]</sup>



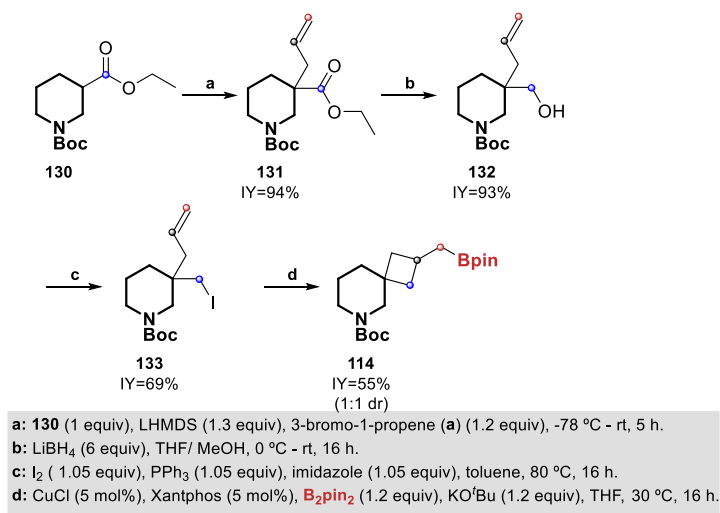
a: **122** (1 equiv), DMAP (0.1 equiv), Boc<sub>2</sub>O (1.2 equiv), ACN, 0 °C - rt, 16 h.  
 b: LHMDS (2.1 equiv), methyl chloroformate (1 equiv), THF, -78 °C, 5 min.  
 c: K<sub>2</sub>CO<sub>3</sub> (3.6 equiv), tetrabutylammonium bromide (0.2 equiv), 4-bromo-1-butene (6 equiv), acetone, rt - 60 °C, 16 h.  
 d: HCl (6 equiv), 1,4-dioxane, rt, 2 h.  
 e: Cs<sub>2</sub>CO<sub>3</sub> (2.5 equiv), benzyl bromide (1.5 equiv), ACN, 90 °C, 16 h.  
 f: LiAlH<sub>4</sub> (3 equiv), 0 °C - rt, 16 h.  
 g: I<sub>2</sub> ( 1.05 equiv), PPh<sub>3</sub> (1.05 equiv), imidazole (1.05 equiv), toluene, 80 °C, 16 h.  
 h: CuCl (5 mol%), Xantphos (5 mol%), **B<sub>2</sub>pin<sub>2</sub>** (1.2 equiv), KO<sup>t</sup>Bu (1.2 equiv), THF, 30 °C, 16 h.

**Scheme 5.3** Synthetic route for obtaining spiro-bicyclic central core **113**.

Then the use of an excess of the reducing agent such as LiAlH<sub>4</sub>, demonstrated high ability to reduce the ester and the ketone in one step giving access to compound **128** in 80% isolated yield after flash chromatography.<sup>[38]</sup> Transformation of the hydroxy group in **128** to the iodo derivative **129** under standard Appel reaction conditions occurred with moderate yield.<sup>[31]</sup> Gladly, the formation of the 5-membered ring spiro-bicycle was successfully achieved under copper (I) borylative conditions leading to compound **113** in 73% isolated yield in a 1 to 1 diastereomeric ratio (Scheme 5.3).<sup>[32]</sup>

Finally, the last spiro-bicyclic motif prepared under copper (I) borylative conditions was product **114** (Scheme 5.4). This spiro-bicyclic scaffold was synthesized following

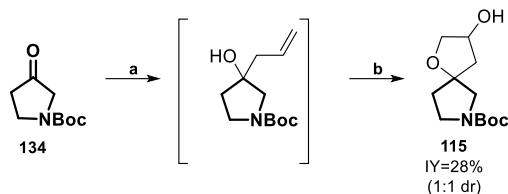
a similar procedure to the one previously described for compound **94** in Chapter 4. Thus, allylation of commercially available ethyl-*N*-Boc-piperidine-3-carboxylate (**130**) with allylbromide and LHMDS provided the piperidine **131** in nearly quantitative yield.<sup>[29]</sup> Then, the ester function in **131** was reduced using LiBH<sub>4</sub> in a mixture of THF/MeOH to give alcohol **132** that was further transformed to the iododerivative **133** in satisfactory yield.<sup>[30-31]</sup> Finally, the copper (I) borylative cyclization was performed on the corresponding alkenyl iodo derivative **133**<sup>[32]</sup> rendering the targeted spiro-bicyclic derivative **114** in moderate yield in a 1 to 1 diastereomeric ratio (Scheme 5.4).



**Scheme 5.4** Synthetic route for obtaining spiro-bicyclic central core **114**.

Additionally, compounds containing a spiro-tetrahydrofuran ring in the north part of the scaffold were synthesized following a reported procedure.<sup>[27]</sup> Thus, commercially available *tert*-butyl-3-oxopyrrolidine-1-carboxylate (**134**) was mixed with zinc dust and 3-bromo-propene in NH<sub>4</sub>Cl in THF as solvent to yield a tertiary alcohol derivative that, after reaction work up, was used for the next step without further purification. Next, addition of Na<sub>2</sub>S<sub>2</sub>O<sub>5</sub>/NaIO<sub>4</sub> in a mixture of *t*BuOH/water as solvent provided the spiro-bicycle **115** in low, but sufficient yield in a 1 to 1 diastereomeric ratio (Scheme 5.5).

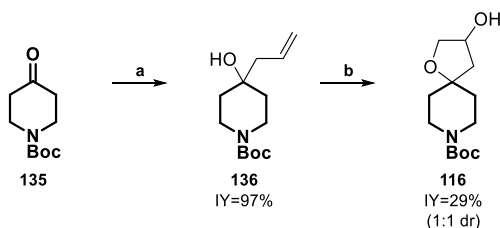
## Synthesis and application of novel spiro-boronate compounds for the treatment of Alzheimer's disease



a: **134** (1 equiv), Zn dust (2 equiv), 3-bromo-1-propene (2 equiv), THF, NH<sub>4</sub>Cl, rt, 10 h.  
b: Na<sub>2</sub>S<sub>2</sub>O<sub>5</sub> (1 equiv), NaIO<sub>4</sub> (1equiv), <sup>t</sup>BuOH, H<sub>2</sub>O, 50 °C, 10 h, then rt, 10 h.

**Scheme 5.5** Synthetic route for obtaining spiro-bicyclic scaffold **115**.

Compound **116** was synthesized starting from ketone **135** following the same reaction procedure as for the preparation of **115**.<sup>[27]</sup> Isolation and purification of the tertiary alcohol **136** did not have any influence in the outcome of the spiro-cyclization reaction and the target spiro-bicycle was obtained in 29% isolated yield in a 1 to 1 diastereomeric ratio (Scheme 5.6).



a: **135** (1 equiv), Zn dust (2 equiv), 3-bromo-1-propene (2 equiv), THF, NH<sub>4</sub>Cl, rt, 10 h.  
b: Na<sub>2</sub>S<sub>2</sub>O<sub>5</sub> (1 equiv), NaIO<sub>4</sub> (1equiv), <sup>t</sup>BuOH, H<sub>2</sub>O, 50 °C, 16 h, then rt, 16 h.

**Scheme 5.6** Synthetic route for obtaining spiro-bicyclic scaffold **116**.

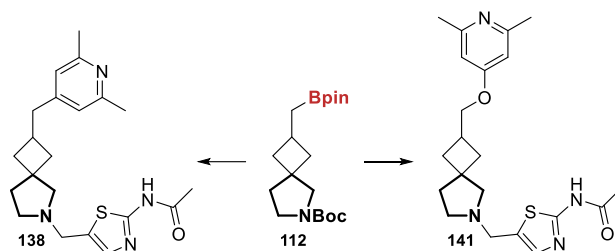
### 5.3.2 Synthesis of target molecules by derivatization of the spiro-bicyclic central scaffolds

Structure activity relationships (SAR) were initiated by modification of the spiro-bicyclic scaffolds prepared (**112-116**). The diversification strategy consisted on the introduction of preferred based on Janssen's available SAR (het)aryl-substituents in the north part of the bicycle in combination with spacers of different lengths and nature. In most cases, the acetamidothiazolyl group was kept constant as substituent on the south part of the scaffold since this substituent provided good activity in the OGA enzymatic and cellular assays.

#### a) Final targets from spiro-bicyclic central core **112**

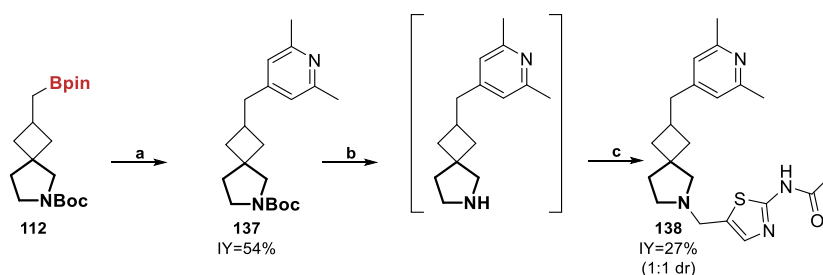
The spiro-bicyclic core **112** was used for the synthesis of the final products **138** and **141** where the linker connecting, the north heteroaryl ring and the spiro-

cyclobutane was varied (Scheme 5.7). The acetamidothiazole was kept as the preferred *N*-linked substituent for the pyrrolidine ring and a 2,6-pyridin-4-yl as distal heterocycle in the north area.



**Scheme 5.7** Final targets from spiro-bicycle **112**.

The synthesis of **138** containing a methylene spacer is outlined in (Scheme 5.8). First, arylation of the Bpin fragment with 4-bromo-2,6-dimethylpyridine under standard Suzuki-Miyaura cross-coupling conditions provided the spiro-compound **137** in moderate yield.<sup>[39]</sup> Then, *N*-Boc deprotection upon acidic treatment using a commercially available solution of HCl 4 N in 1,4-dioxane, gave access to the Boc free pyrrolidine fragment in quantitative manner.<sup>[36]</sup> This crude pyrrolidine was subjected to reductive amination with *N*-(5-formylthiazol-2-yl)acetamide using sodium triacetoxyborohydride as reductant to form the desired product **138** as a 1 to 1 mixture of diastereoisomers, albeit in low yield (Scheme 5.8).<sup>[40]</sup> Compound **138** was further purified by reverse phase HPLC to isolate the two diastereoisomers for biological testing.



**a:** **112** (1 equiv), 4-bromo-2,6-dimethylpyridine (3 equiv), Pd(PPh<sub>3</sub>)<sub>4</sub> (3mol%), KOH (6 equiv), 1,4-dioxane, 90 °C, 16 h.  
**b:** HCl (6 equiv), 1,4-dioxane, rt, 2 h.  
**c:** *N*-(5-formylthiazol-2-yl)acetamide (1.2 equiv), TEA (4 equiv), NaBH(OAc)<sub>3</sub> (3 equiv), DCM, rt, 16 h.

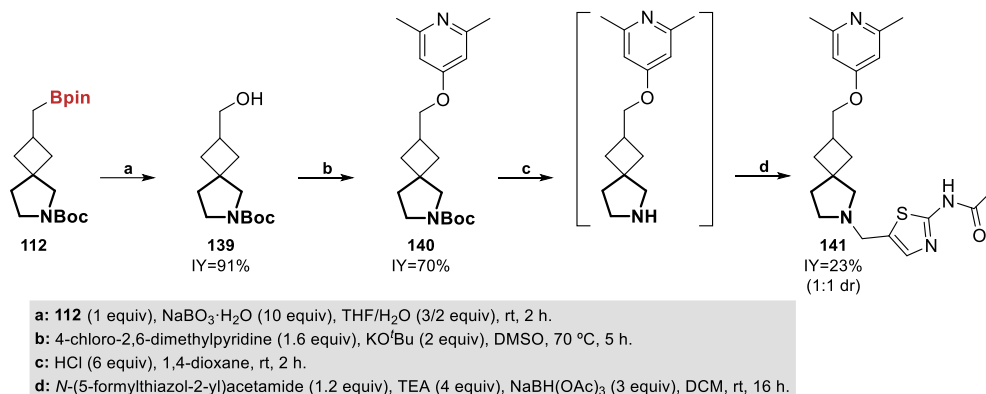
**Scheme 5.8** Synthesis of final target **138**.

Next, to explore the effect of a longer linker in the biological activity, compound **141** (Scheme 5.9) bearing a –CH<sub>2</sub>O– spacer was targeted. First, the Bpin function was transformed to the hydroxyl group under very mild oxidative conditions, giving efficient access to the desired spiro-bicyclic alcohol **139**.<sup>[41]</sup> Then, *O*-arylation with



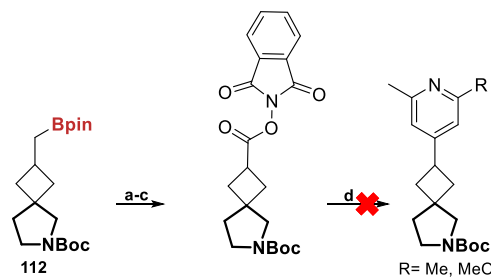
## Synthesis and application of novel spiro-boronate compounds for the treatment of Alzheimer's disease

4-chloro-2,6-dimethylpyridine under basic conditions in DMSO at 70 °C afforded compound **140** in 70% isolated yield.<sup>[42]</sup> Finally, Boc cleavage under acidic conditions<sup>[36]</sup> followed by reductive amination of the deprotected pyrrolidine hydrochloric salt with *N*-(5-formylthiazol-2-yl)acetamide afforded spiro-compound **141** in 23% isolated yield in a 1 to 1 diastereomeric ratio.<sup>[40]</sup> The diastereomeric mixture was separated by reverse-phase HPLC (Scheme 5.9).



**Scheme 5.9** Synthesis of final target **141**.

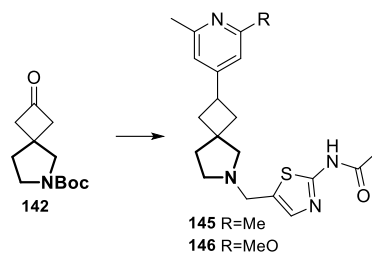
Moreover, the preparation of analogues where the distal heteroaryl substituent is directly linked to the spiro-bicyclic core was also envisaged. For that purpose, several synthetic approaches were tested from compound **112**. Derivatizations towards the alcohol derivative (reaction **a**) followed by further oxidation to the corresponding carboxylic acid (reaction **b**)<sup>[43]</sup> and the activation of the carboxylic acid by reaction with *N*-hydroxyphthalimide (reaction **c**) followed by decarboxylative arylation coupling failed in the last step reaction (reaction **d**), with no observation of the directly arylated product by LC-MS analysis of the reaction crude (Scheme 5.10).<sup>[44]</sup>



a: **112** (1 equiv), NaBO<sub>3</sub>·H<sub>2</sub>O (10 equiv), THF/H<sub>2</sub>O (3/2 equiv), rt, 2 h.  
b: Jones Reagent (0.7 equiv), acetone, H<sub>2</sub>O, 0 °C, 1h.  
c: *N*-hydroxyphthalimide (1 equiv), DMAP (0.1 equiv), DIC (1.1 equiv), DCM, rt, 16 h.  
d: NiCl<sub>2</sub> (20 mol%), di-<sup>t</sup>Bubipy (40 mol%), Py·ZnCl·LiCl (3 equiv), THF/ DMF (3:2), 25 °C, 16h.

**Scheme 5.10** Unsuccessful access to directly linked spiro-bicyclic core.

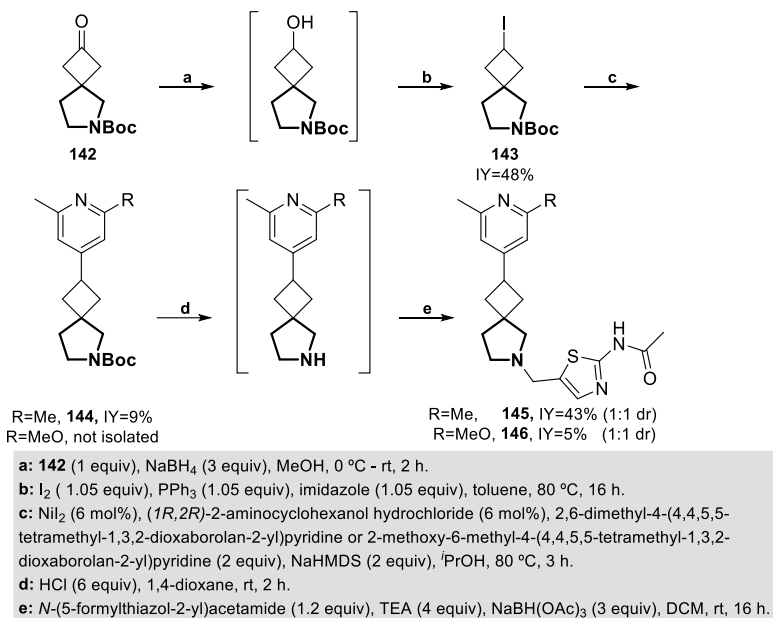
Considering these results our attention turned to commercially available *N*-Boc spiro-bicyclic ketone **142** which, gladly, could be transformed into the final target compounds **145** and **146** (Scheme 5.11).



**Scheme 5.11** Possible routes of access to directly linked heteroaryl motif.

Thus, NaBH<sub>4</sub> reduction of the ketone function in compound **142** in methanol led to alcohol **143**<sup>[45]</sup> which after aqueous work up was used for the next reaction step without purification (Scheme 5.12). Appel reaction on the alcohol group to form the iodocyclopentane derivative **143**<sup>[31]</sup> followed by cross-coupling arylation with 2,6-dimethylpyridine boronate ester under nickel catalyzed Suzuki conditions afforded compound **144** although in low yield.<sup>[46]</sup> Then, Boc cleavage<sup>[36]</sup> followed by reductive amination with *N*-(5-formylthiazol-2-yl)acetamide target compound **145** in 43% isolated yield in a diastereomeric ratio 1 to 1.<sup>[40]</sup>

## Synthesis and application of novel spiro-boronate compounds for the treatment of Alzheimer's disease

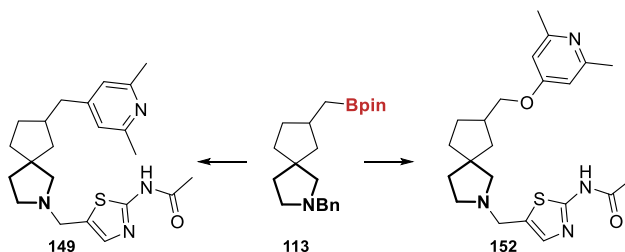


**Scheme 5.12** Synthesis of final target **145** and **146**.

Compound **146** (Scheme 5.12) was also synthesized from the corresponding pyridine boronate ester and the iodo derivative **143** following the same reaction sequence. Product **146** was obtained in a 1 to 1 diastereomeric mixture. Diastereoisomers were separated by reverse phase HPLC chromatography.

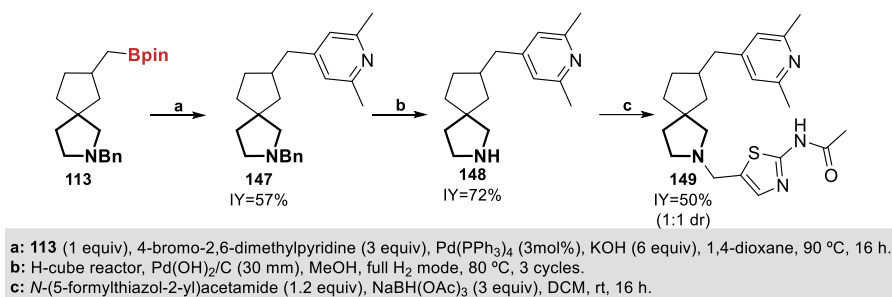
### b) Final targets from spiro-bicyclic central core **113**

Similar to scaffold **112**, the spiro-bicyclic core **113** was used for the synthesis of the final products **149** and **152** containing methylene and a -CH<sub>2</sub>O- linkers (Scheme 5.13).



**Scheme 5.13** Final products from spiro-bicycle **113**.

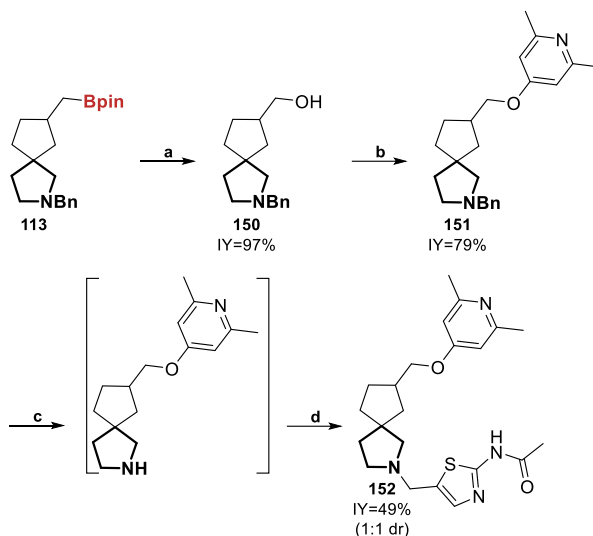
Product **149** (Scheme 5.14) was prepared from the boronate ester **113** following in the first reaction step the arylation procedure already reported in Scheme 5.8 for the synthesis of product **138**. The deprotection of the pyrrolidine nitrogen in compound **147** was achieved by cleavage of the benzyl protecting group under flow-hydrogenation conditions on a Pd(OH)<sub>2</sub>/C cartridge using an H-cube reactor. In this example, since the deprotected amine **148** is a free base, no TEA was added in the reductive amination step leading to compound **149**. Product **149** was obtained as a 1 to 1 mixture of diastereoisomers, which were separated by reverse-phase HPLC chromatography.



Scheme 5.14 Synthesis of final target **149**.

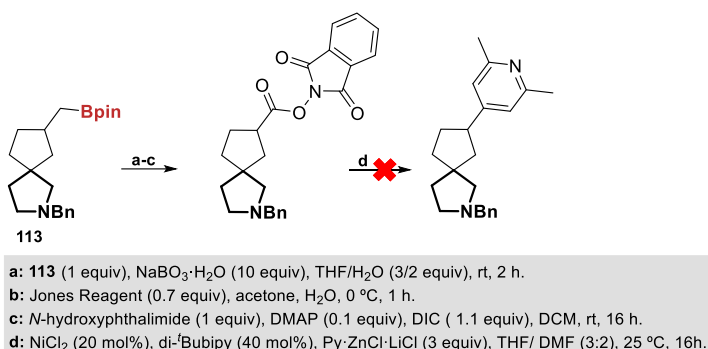
Finally target **152**, containing a –CH<sub>2</sub>O– linker (Scheme 5.15) was prepared following the procedure previously described in Scheme 5.9, the only difference being the benzyl deprotection step that was performed on H-cube reactor as in the previous example. Compound **152** was obtained in moderate yield as a 1 to 1 mixture of diastereoisomers.

## Synthesis and application of novel spiro-boronate compounds for the treatment of Alzheimer's disease



**Scheme 5.15** Synthesis of final target **152**.

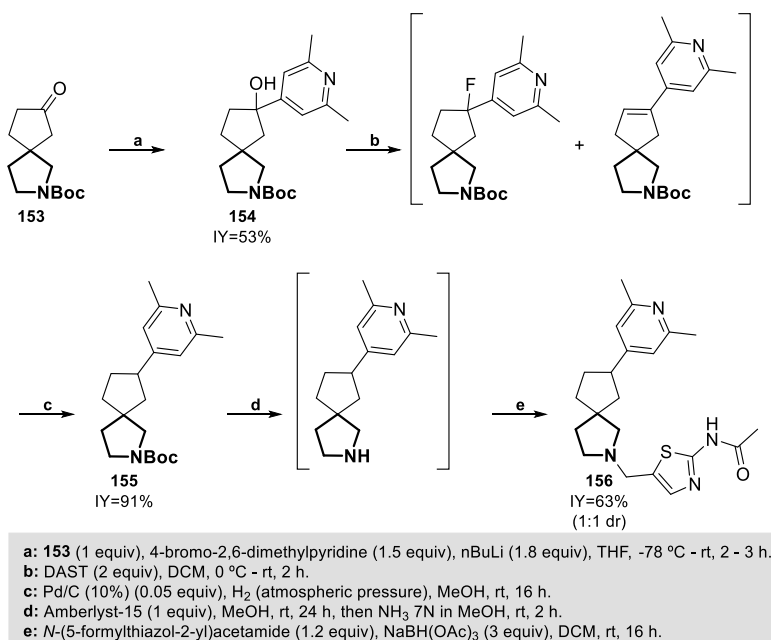
Analogous to spiro-compound **112**, the spiro-boronate **113** did not allow access to the final target **156**. Following the sequential derivatizations shown in Scheme 5.10, the reaction failed in the last step where the nickel catalyzed decarboxylative coupling was unsuccessful (Scheme 5.16).<sup>[44]</sup>



**Scheme 5.16** Unsuccessful access to directly linked spiro-bicyclic core.

A more successful approach started from commercially available *N*-Boc spiro-bicyclic ketone **153** which, gladly, could be transformed into the final target compound **156** (Scheme 5.17). Instead of following the synthesis route used with *N*-Boc spiro-bicyclic ketone **142**, a new reaction sequence was designed aiming to

increase the efficiency of the overall transformation. Thus, lithiation of 4-bromo-2,6-dimethylpyridine followed by addition to the keto-spiro-bicycle led to alcohol **154** in moderate yield.<sup>[47]</sup> To capitalize on the structure of compound **154**, the tertiary alcohol was deoxyfluorinated with (diethylamino)sulfur trifluoride (DAST).<sup>[48]</sup> The deoxyfluorination reaction was not clean and a cyclopentene derivative was formed along the expected fluorine-containing compound. The elimination can occur since the fluorination pathway proceeds through a  $S_N1$  mechanism and the attack of the fluorine to the carbocation competes with the elimination pathway. Unfortunately, we did not succeed with the purification of the mixture, hence this mixture was subjected to hydrogenation with Pd/C at atmospheric pressure.<sup>[49]</sup> Surprisingly, the mixture converged to product **155**, where the fluorinated product suffered an unpredictable hydrogenation and the unsaturated product was hydrogenated as expected. Then, as reported in previous procedures, the Boc group was cleaved. This time using an acidic modified Amberlyst-15 resin, the deprotected amine was obtained and used for the next step without purification.<sup>[50]</sup> Then, reductive amination provided compound **156** in 63% isolated yield in a diastereomeric ratio 1 to 1 (Scheme 5.17).<sup>[40]</sup> The diastereomeric mixture was sent to chiral SFC separation to get each enantiomer in a pure form. However, only the diastereomeric mixture was fully characterized.

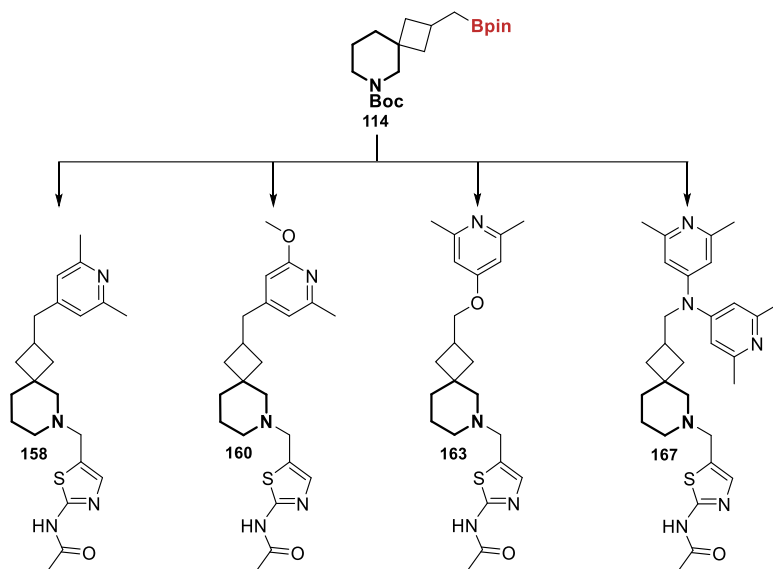


Scheme 5.17 Synthesis of final target **156**.

## Synthesis and application of novel spiro-boronate compounds for the treatment of Alzheimer's disease

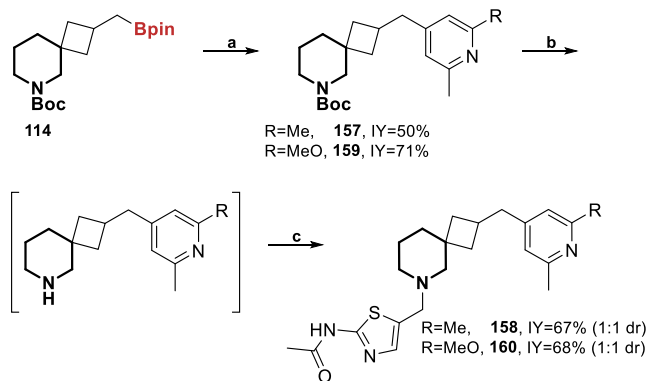
### c) Final targets from spiro-bicyclic central core **114**

Analogous to the previous central scaffolds, the spiro-bicyclic core **114** was derivatized towards the formation of **158** and **160** compounds containing a methylene linker, **163** introducing the  $-\text{CH}_2\text{O}-$  linker and, for the first time, product **167** which contains a  $-\text{CH}_2\text{N}-$  group as spacer (Scheme 5.18).



Scheme 5.18 Final targets from spiro-bicycle **114**.

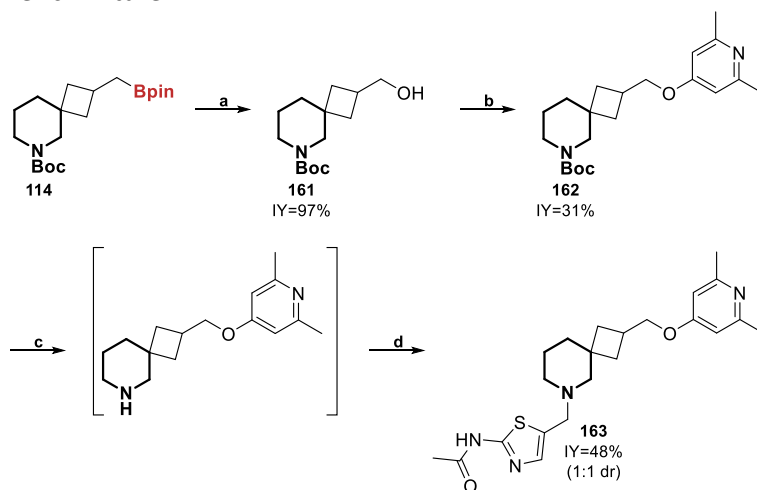
The synthesis of products **158** and **160** is outlined in Scheme 5.19. Starting from the spiro-bicyclic boronate **114** and the corresponding pyridine derivatives, following procedure reported for the synthesis of compound **138** in Scheme 5.8, intermediates **157** and **159** were obtained. The final targets **158** and **160** were synthesized in good yields after deprotection and reductive amination on intermediates **157** and **159**, respectively. In both cases products were obtained in a 1 to 1 diastereomeric ratio.



**a:** **114** (1 equiv), 4-bromo-2,6-dimethylpyridine (3 equiv), Pd(PPh<sub>3</sub>)<sub>4</sub> (3 mol%), KOH (6 equiv), 1,4-dioxane, 90 °C, 16 h.  
**b:** HCl (6 equiv), 1,4-dioxane, rt, 2 h.  
**c:** *N*-(5-formylthiazol-2-yl)acetamide (1.2 equiv), TEA (4 equiv), NaBH(OAc)<sub>3</sub> (3 equiv), DCM, rt, 16 h.

**Scheme 5.19** Synthesis of final targets **158** and **160**.

The -CH<sub>2</sub>O- linker product was also synthesized following a previously described reaction sequence as shown in Scheme 5.20. Thus, oxidation of the boronate ester **114** yielded almost quantitatively the primary alcohol **161** which was then *O*-arylated towards intermediate **162**. Finally, deprotection and subsequent reductive amination afforded the target product **163** in 48% isolated yield, as 1:1 diastereomeric mixture.



**a:** **114** (1 equiv), NaBO<sub>3</sub>·H<sub>2</sub>O (10 equiv), THF/H<sub>2</sub>O (3/2 equiv), rt, 2 h.  
**b:** 4-chloro-2,6-dimethylpyridine (1.6 equiv), KO<sup>t</sup>Bu (2 equiv), DMSO, 70 °C, 5 h.  
**c:** HCl (6 equiv), 1,4-dioxane, rt, 2 h.  
**d:** *N*-(5-formylthiazol-2-yl)acetamide (1.2 equiv), TEA (4 equiv), NaBH(OAc)<sub>3</sub> (3 equiv), DCM, rt, 16 h.

**Scheme 5.20** Synthesis of final target **163**.

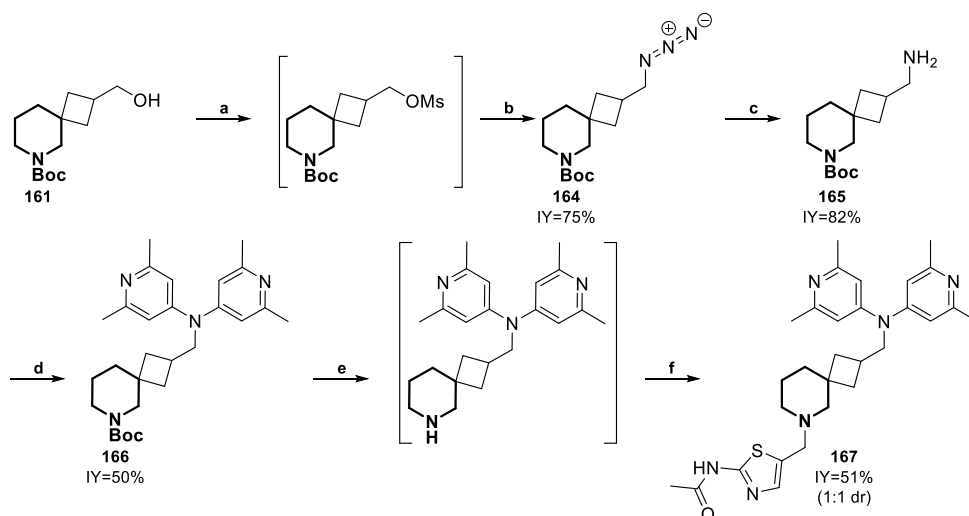


## Synthesis and application of novel spiro-boronate compounds for the treatment of Alzheimer's disease

Aiming to study the effect of linkers of different nature on the OGA inhibitory activity a -CH<sub>2</sub>NH- linker containing molecule was synthesized (Scheme 5.21).

The synthesis started from the alcohol intermediate **161** which was transformed into a mesylate derivative by treatment with mesyl chloride and DIPEA in DCM. This mesylate intermediate, after aqueous work-up, was used for the next reaction step without further purification.<sup>[51]</sup> Treatment of the mesylate intermediate with sodium azide in DMF at 70 °C for 16 hours provided the azido spiro-compound **164** that was stable enough to be isolated after column chromatography in 75% of yield.<sup>[52]</sup> Next, the azide group was reduced to the amine **165** under hydrogenation conditions using the H-cube reactor.<sup>[53]</sup> Unfortunately, due to the high reactivity demonstrated by the amine it was not possible to obtain the mono-arylation target molecule and only a compound containing two pyridine units (**166**) could be isolated.

Even though, we decided to go forward with this product and thus proceeded to the deprotection of the amine<sup>[36]</sup> and subsequent reductive amination leading to a spiro-compound with two distal pyridine units (**167**) in a diastereomeric ratio 1 to 1 (Scheme 5.21).<sup>[40]</sup> The diastereomeric mixture of product **167** was separated by reverse-phase HPLC chromatography.

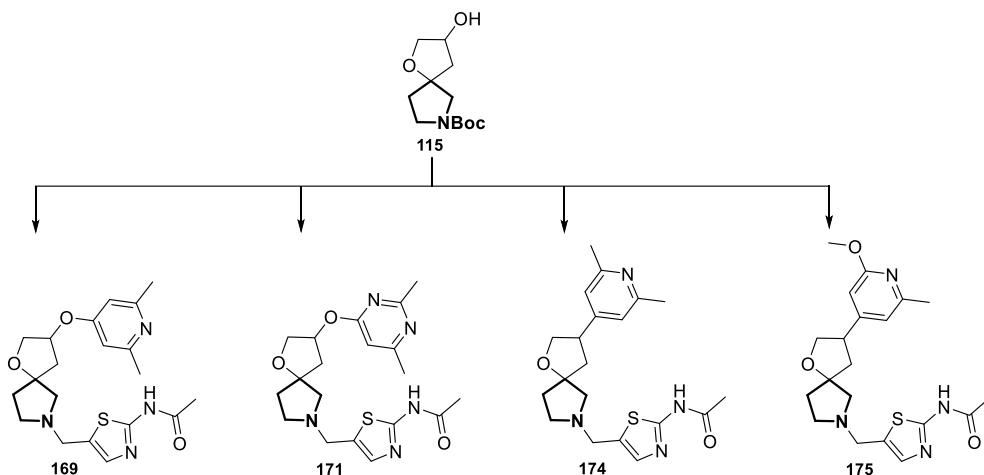


- a: **161** (1 equiv), MsCl (1.1 equiv), DIPEA (2 equiv), DCM, 0 °C - rt, 1 h.  
 b: NaN<sub>3</sub> (3 equiv), DMF, 0 °C - 70 °C, 16 h.  
 c: H-cube reactor, Pd/C (30 mm), EtOH, full H<sub>2</sub> mode, 50 °C, 1 cycle.  
 d: 4-chloro-2,6-dimethylpyridine (2 equiv), Pd<sub>2</sub>(dba)<sub>3</sub> (5 mol%), Davephos (7 mol%), NaO<sup>t</sup>Bu (1.5 equiv), 1,4-dioxane, 100 °C, 16 h.  
 e: HCl (6 equiv), 1,4-dioxane, rt, 2 h.  
 f: N-(5-formylthiazol-2-yl)acetamide (1.2 equiv), TEA (4 equiv), NaBH(OAc)<sub>3</sub> (3 equiv), DCM, rt, 16 h.

Scheme 5.21 Synthesis of final target **167**.

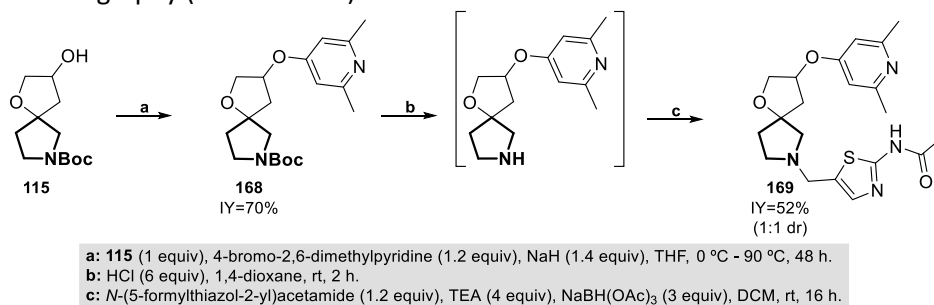
**d) Final targets from spiro-bicyclic central core 115**

Next, we turned our attention to the derivatization of the spiro-bicyclic central core **115**. Despite the fact this spiro-compound had been described in the literature, no further derivatization and functionalization towards compounds of potential pharmaceutical interest has been reported. In order to study the potential of this bicyclic core in our OGA inhibition program the final products **169**, **171**, **174** and **175** (Scheme 5.22) were prepared. Interestingly, this scaffold gives access to the new *-O-* linker not prepared previously in the program.



**Scheme 5.22** Final targets from spiro-bicycle **115**.

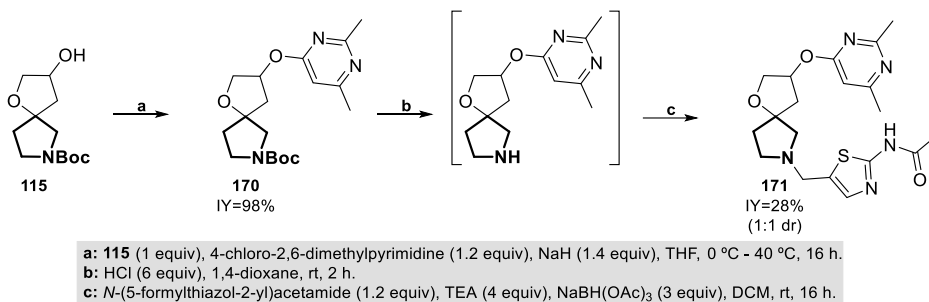
Starting from the secondary alcohol **115**, the *O*-arylation reaction was performed using NaH and 4-bromo-2,6-dimethylpyridine rendering the formation of the *O*-arylated product **168** in 70% isolated yield.<sup>[54]</sup> Then, deprotection and successive reductive amination provided the final product **169** in 52% isolated yield in a diastereomeric ratio 1 to 1, which was separated by reverse-phase HPLC chromatography (Scheme 5.23).



**Scheme 5.23** Synthesis of final target **169**.

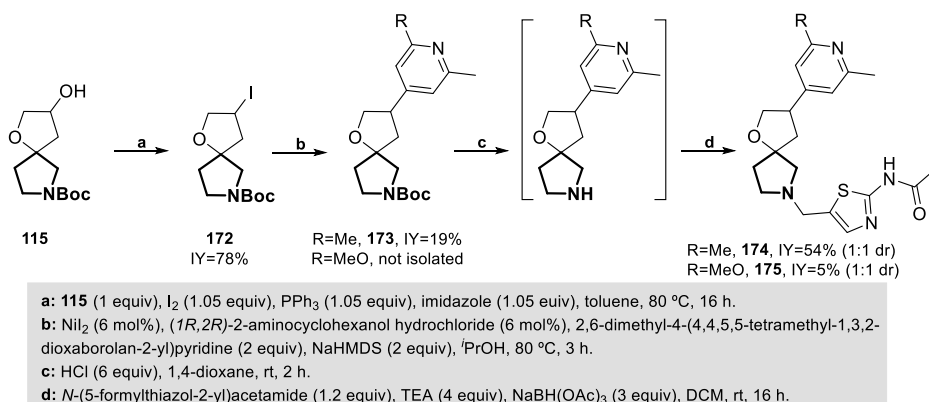
## Synthesis and application of novel spiro-boronate compounds for the treatment of Alzheimer's disease

Moreover, a new heteroaromatic ring was introduced for the first time in the north part of the scaffold. Following the conditions used for the synthesis of **169** in Scheme 5.23 and using 4-chloro-2,6-dimethylpyrimidine the corresponding *O*-arylated intermediate **170** was obtained in almost quantitative yield. Deprotection followed by reductive amination delivered the final product **171** as a 1 to 1 mixture of diastereoisomers in 28% isolated yield (Scheme 5.24).



**Scheme 5.24** Synthesis of final target **171**.

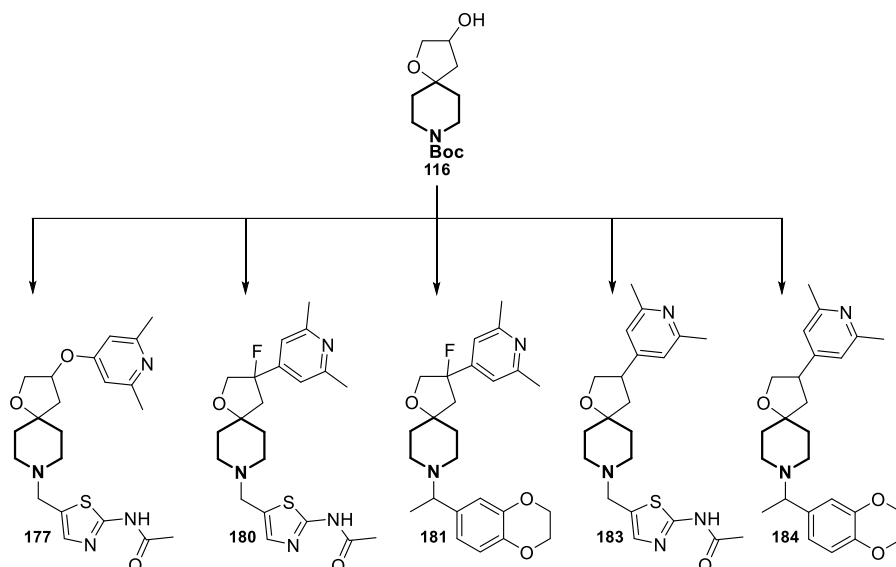
Additionally, compounds **174** and **175** in which the heteroaryl group is directly linked to the tetrahydrofuran ring were also prepared following the conditions used for the synthesis of final products **145** and **146** in Scheme 5.12. Gladly, after iodination (**178**, 78%), Suzuki-Miyaura coupling (**173**, R=Me, 19%), deprotection and subsequent reductive amination compounds **174** (54%) and **175** (5%, over three reaction steps) were isolated, in both cases products were obtained as a 1 to 1 diastereomeric mixture (Scheme 5.25).



**Scheme 5.25** Synthesis of final target **174** and **175**.

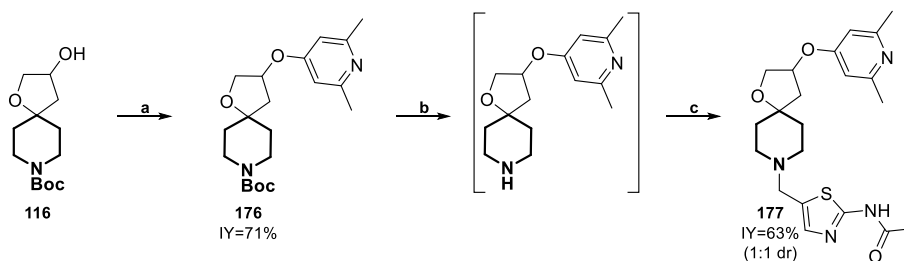
### e) Final targets from spiro-bicyclic central core **116**

Finally, the spiro-bicyclic core **116** was modified to introduce the same set of spacers installed in scaffold **115**, although alternative methodologies were applied to introduce a fluorine atom adjacent to the linker attachment point (Scheme 5.26).



Scheme 5.26 Final targets from spiro-bicycle **116**.

Firstly, the product containing an -O- linker was prepared following the conditions reported in Scheme 5.23. Thus, the final product **177** was obtained in good yield, as a 1 to 1 diastereomeric mixture, in a three step reaction sequence starting from alcohol **116**: (Reaction a) *O*-arylation (**176**, 71%), (Reaction b) deprotection and (Reaction c) reductive amination (Scheme 5.27).

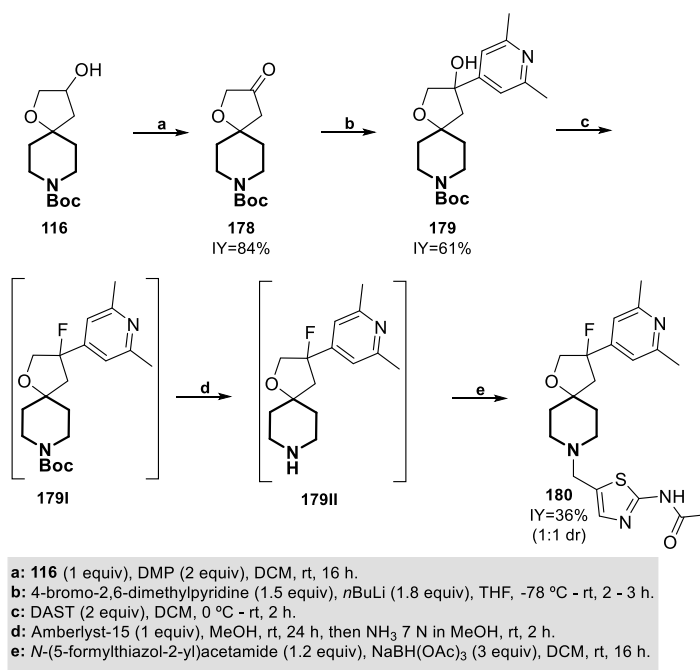


**a:** **116** (1 equiv), 4-bromo-2,6-dimethylpyridine (1.2 equiv), NaH (1.4 equiv), THF, 0 °C - 90 °C, 48 h.  
**b:** HCl (6 equiv), 1,4-dioxane, rt, 2 h.  
**c:** *N*-(5-formylthiazol-2-yl)acetamide (1.2 equiv), TEA (4 equiv), NaBH(OAc)<sub>3</sub> (3 equiv), DCM, rt, 16 h.

Scheme 5.27 Synthesis of final target **177**.

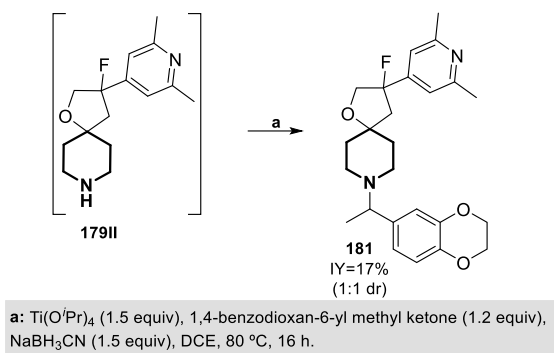
## Synthesis and application of novel spiro-boronate compounds for the treatment of Alzheimer's disease

Moreover, as described previously in Scheme 5.17, arylation of a cycloalkanone through lithiation of 4-bromo-2,6-dimethylpyridine renders a tertiary OH group susceptible to be fluorinated. Aiming to perform this transformation, oxidation of the spiro-cyclopentanol, using Dess-Martin periodinane (DMP) rendered the spiro-cyclopentanone (**178**) in excellent yield.<sup>[55]</sup> Then, organolithium addition followed by deoxyfluorination of the intermediate alcohol **179** gave access to the expected fluorocyclopentane derivative without detection of the elimination byproduct (Scheme 5.28). Finally, successive deprotection and reductive amination with *N*-(5-formylthiazol-2-yl)acetamide gave target **180** in 36% isolated yield in a diastereomeric ratio 1 to 1, obtaining for the first time a final product with a fluorine substituent on the spiro-bicyclic core (Scheme 5.28).



**Scheme 5.28** Synthesis of final target **180**.

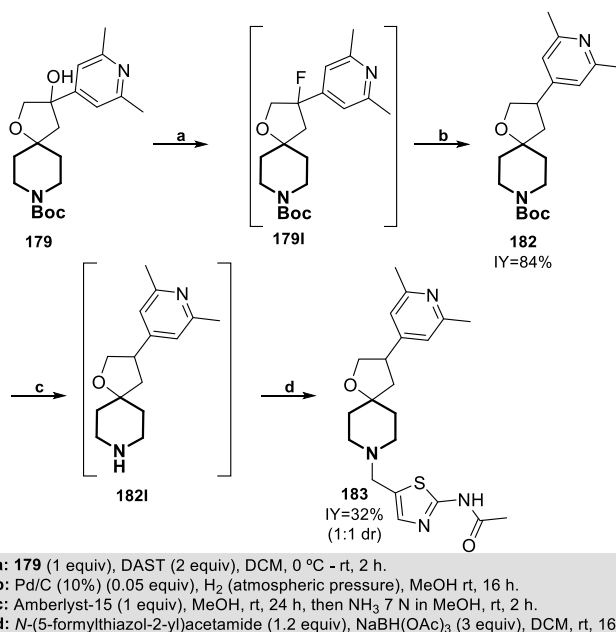
In addition, based on relevant SAR from a different OGA-chemotype, a new derivative containing a benzodioxane motif in the south part of the scaffold was prepared. Reductive amination on the fluorine-containing deprotected spiro-piperidine (**179II**) with 1,4-benzodioxan-6-yl methyl ketone, Ti(O<sup>*i*</sup>Pr)<sub>4</sub>, NaBH<sub>3</sub>CN in DCE at 80 °C, yielded the final product **181** in 17% isolated yield in a diastereomeric ratio 1 to 1 (Scheme 5.29).



**Scheme 5.29** Synthesis of final target **181**.

With the aim to study the influence of the fluorine atom on the biological activity of the molecules, the corresponding matched-pairs **183** and **184** without the fluorine atom were also prepared.

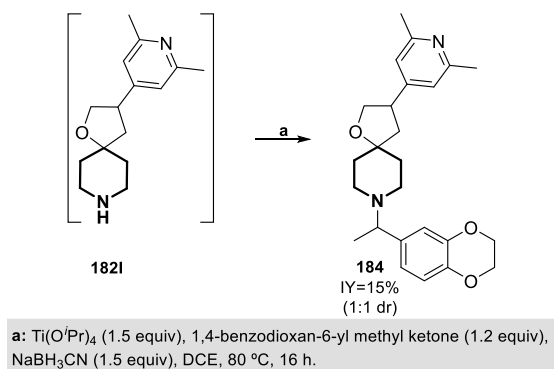
Taking into account the previous observation that the fluorine atom was cleaved under hydrogenation conditions, the *N*-Boc-fluorinated spiro-piperidine intermediate was hydrogenated using Pd/C at atmosphere pressure, affording full conversion towards the defluorinated *N*-Boc-protected piperidine (**179I**) (Scheme 5.30).<sup>[49]</sup> Consecutive deprotection and reductive amination with *N*-(5-formylthiazol-2-yl)acetamide formed product **183** in moderate yield, as a 1 to 1 mixture of diastereoisomers (Scheme 5.30).



**Scheme 5.30** Synthesis of final target **183**.

## Synthesis and application of novel spiro-boronate compounds for the treatment of Alzheimer's disease

Similarly, reductive amination of **182I** with 1,4-benzodioxan-6-yl methyl ketone led to compound **184** as 1 to 1 mixture of diastereoisomers (Scheme 5.31).<sup>[56]</sup>



Scheme 5.31 Synthesis of final target **184**.

### 5.3.3 SAR analysis from the final target spiro-compounds

In this section the structure-activity relationship (SAR) analysis from the final targets prepared in section 5.3.2 is described. The criteria of evaluation starts first by measuring their hOGA inhibitor activity in a biochemical and cellular assays. The protocols for these in vitro assays are described below:

#### a) OGA Biochemical assay:

The assay is based on the inhibition of the hydrolysis of fluorescein mono- $\beta$ -D-*N*-Acetyl-Glucosamine (FM-GlcNAc) by the recombinant human Meningioma Expressed Antigen 5 (MGEA5), also referred to as *O*-GlcNAcase (OGA). The hydrolysis FM-GlcNAc results in the formation of  $\beta$ -D-*N*-glucosamineacetate and fluorescein. The fluorescence of the latter can be measured at excitation wavelength 485 nm and emission wavelength 538 nm. An increase in enzyme activity results in an increase in fluorescence signal. Full length OGA enzyme was purchased at OriGene. The enzyme was stored in 25 mM Tris.HCl, pH 7.3, 100 mM glycine, 10% glycerol at -20 °C. Thiamet G and GlcNAcStatin were tested as reference compounds. The assay was performed in 200 mM Citrate/phosphate buffer supplemented with 0.005% Tween-20. 35.6 g  $\text{Na}_2\text{HPO}_4 \cdot 2\text{xH}_2\text{O}$  were dissolved in 1 L water to obtain a 200 mM solution. 19.2 g citric acid was dissolved in 1 L water to obtain a 100 mM solution. pH of the sodiumphosphate solution was adjusted with the citric acid solution to 7.2. The buffer to stop the reaction consists of a 500 mM carbonate (734 mg) buffer, pH 11.0.

FM-GlcNAc were dissolved in 5.48 mL DMSO to obtain a 250 mM solution and was stored at -20 °C. OGA was used at a 2 nM concentration and FM-GlcNAc at a 100 μM final concentration. Dilutions were prepared in assay buffer.

50 nL of a compound dissolved in DMSO was dispensed on Black Proxiplate™ 384 Plus Assay plates and 3 μl fl-OGA enzyme mix added subsequently. Plates were pre-incubated for 60 min. at room temperature and then 2 μl FM-GlcNAc substrate mix added. Final DMSO concentrations did not exceed 1%. Plates were briefly centrifuged for 1 min. at 1000 rpm and incubate at room temperature for 6 h. To stop the reaction 5 μl STOP buffer were added and plates centrifuge again 1 min. at 1000 rpm. Fluorescence was quantified in the Thermo Scientific Fluoroskan Ascent or the PerkinElmer EnVision with excitation wavelength 485 nm and emission wavelength 538 nm.

For analysis a best-fit curve is fitted by a minimum sum of squares method. From this an IC<sub>50</sub> value and Hill coefficient was obtained. High control (no inhibitor) and low control (saturating concentrations of standard inhibitor) were used to define the minimum and maximum values.

#### **b) OGA Cellular assay:**

HEK293 cells inducible for P301L mutant human Tau (isoform 2N4R) were established at Janssen. Thiamet-G was used for both plate validation (high control) and as reference compound (reference EC<sub>50</sub> assay validation). OGA inhibition is evaluated through the immunocytochemical (ICC) detection of *O*-GlcNAcylated proteins using a monoclonal antibody detecting *O*-GlcNAcylated residues as previously described. Inhibition of OGA will result in an increase of *O*-GlcNAcylated protein levels resulting in an increased signal in the experiment. Cell nuclei are stained with Hoechst to give a cell culture quality control and a rough estimate of immediate compounds toxicity, if any. ICC pictures are imaged with a Perkin Elmer Opera Phenix plate microscope and quantified with the provided software Perkin Elmer Harmony 4.1.

Cells were propagated in DMEM high Glucose following standard procedures. 2 days before the cell assay cells are split, counted and seeded in Poly-D-Lysine (PDL) coated 96-wells plate at a cell density of 12,000 cells per cm<sup>2</sup> (4,000 cells per well) in 100 μl of Assay Medium (Low Glucose medium is used to reduce basal levels of GlcNAcylation). At the day of compound test medium from assay plates was removed and replenished with 90 μl of fresh Assay Medium. 10 μl of compounds at a 10-fold final concentration were added to the wells. Plates were centrifuged shortly before incubation in the cell incubator for 6 hours. DMSO concentration was set to 0.2%. Medium is discarded by applying vacuum. For staining of cells medium was removed and cells washed once with 100 μl D-PBS. From next step onwards



## Synthesis and application of novel spiro-boronate compounds for the treatment of Alzheimer's disease

---

unless other stated assay volume was always 50  $\mu$ l and incubation was performed without agitation and at room temperature. Cells were fixed in 50  $\mu$ l of a 4% paraformaldehyde PBS solution for 15 min. at room temperature. The PFA PBS solution was then discarded and cells washed once in 10mM Tris Buffer, 150 mM NaCl, 0.1% Triton X, pH 7.5 (ICC buffer) before being permeabilized in same buffer for 10 minutes. Samples are subsequently blocked in ICC containing 5% goat serum for 45-60 minutes at room temperature. Samples were then incubated with primary antibody (1/1000 from commercial provider, see above) at 4°C overnight and subsequently washed 3 times for 5 min. in ICC buffer. Samples were incubated with secondary fluorescent antibody (1/500 dilution) and nuclei stained with Hoechst 33342 at a final concentration of 1  $\mu$ g/ml in ICC for 1 hour. Before analysis samples were washed 2 times manually for 5 min. in ICC base buffer.

Imaging is performed using Perkin Elmer Phenix Opera using a water 20x objective and recording 9 fields per well. Intensity readout at 488 nm is used as a measure of

O-GlcNAcylation level of total proteins in wells. To assess potential toxicity of compounds nuclei were counted using the Hoechst staining. IC<sub>50</sub> values are calculated using parametric non-linear regression model fitting. As a maximum inhibition Thiamet G at a 200  $\mu$ M concentration is present on each plate. In addition, a concentration response of Thiamet G is calculated on each plate.

The following figures show the different products prepared along with their OGA inhibitory activity in the biochemical and cellular assays. Depending on the compound, in some cases this was tested as a mixture of diastereoisomers and/or as single diastereoisomer.

The results obtained in these assays are discussed on the following paragraphs. First, we looked compounds where the distal heteroaryl ring is directly linked to the spiro-carbocyclic ring (Figure 5.14). The replacement of the central spirocyclic diamine core in **110b** (pIC<sub>50</sub> = 8.22, cell pEC<sub>50</sub> = 6.85) by the spiro-cyclopentane **156** (pIC<sub>50</sub> = 7.18, cell pEC<sub>50</sub> = 6.67) and spiro-cyclobutane **145** (pIC<sub>50</sub> = 7.44, cell pEC<sub>50</sub> = 6.74) was tolerated in terms of OGA inhibitory activity, with the compounds being about one-fold less potent in the biochemical assay. Nevertheless, it is interesting to mention that their activity in the OGA cellular assay was comparable to that of **110b**, suggesting that the deletion of the north nitrogen atom in the spirocyclic core has a pronounced effect in the physicochemical properties of the molecules resulting in an increased cellular penetration. All pure stereoisomers of compound **156** were tested, with isomer **156a'** (pIC<sub>50</sub> = 7.47, cell pEC<sub>50</sub> = 6.54) being the more potent in the OGA biochemical assay while retaining a good cellular activity. Considering the good activity levels obtained with the spiro-cyclobutane derivative **145**, two close analogues bearing a less basic pyridyl ring were tested. Unfortunately, both **146** (pIC<sub>50</sub> = 7.06, cell pEC<sub>50</sub> = 6.32) and **146a'** (pIC<sub>50</sub> = 6.48, cell pEC<sub>50</sub> = 6.04) were found

to be less active, suggesting that pKa of the pyridyl nitrogen could play a role in the inhibitory activity of the compounds.

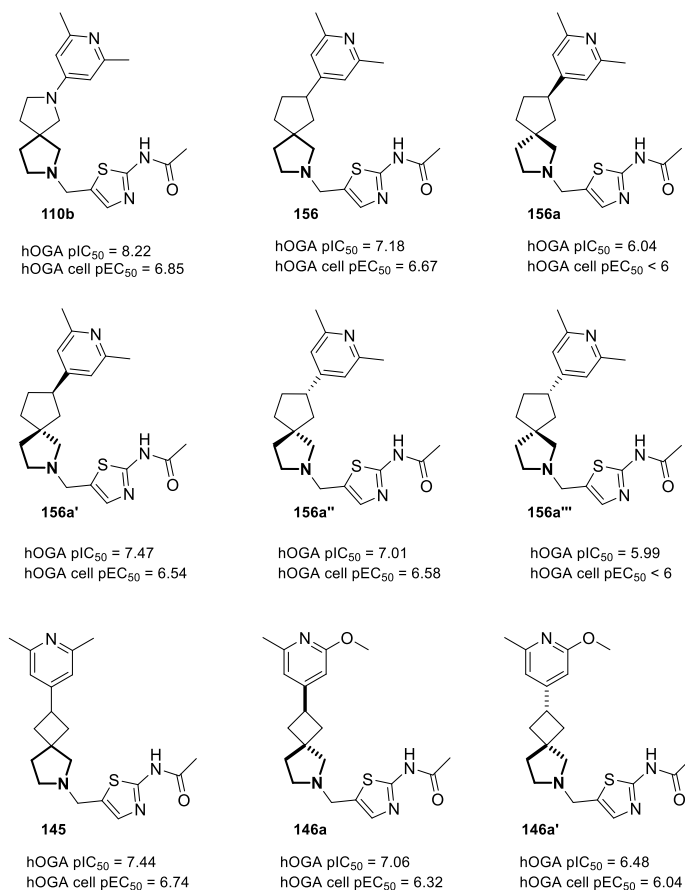


**Figure 5.14** SAR analysis from the direct linked heteroaromatic replacement in the carbocyclic spiranes.

## Synthesis and application of novel spiro-boronate compounds for the treatment of Alzheimer's disease

The spiro-tetrahydrofuran derivatives **174** ( $pIC_{50} = 7.68$ , cell  $pEC_{50} = 6.22$ ) and **175** ( $pIC_{50} = 7.22$ , cell  $pIC_{50} < 6$ ) showed comparable activity to spiro-cyclopentane **145** ( $pIC_{50} = 7.44$ , cell  $pEC_{50} = 6.74$ ) in the OGA biochemical assay, however this modification led to a reduction in the cellular activity of the compounds. Remarkably, enlarging the pyrrolidine ring to a piperidine one was clearly detrimental for the activity, with compound **183** ( $pIC_{50} = 5.60$ , cell  $pEC_{50} = 6.16$ ) being two orders of magnitude less potent than **145**. Compound **184** ( $pIC_{50} = 5.06$ , cell  $pEC_{50} < 6$ ) containing a benzodioxane substituent an active motif when placed at **110b** did not improve activity. Introduction of a fluorine substituent adjacent to the heteroaromatic ring (**180**,  $pIC_{50} = 5.74$ , cell  $pEC_{50} = 6.4$  and **181**,  $pIC_{50} = 5.17$ , cell  $pEC_{50} < 6$ ) did not have an influence on the activity of the compounds (Figure 5.15).

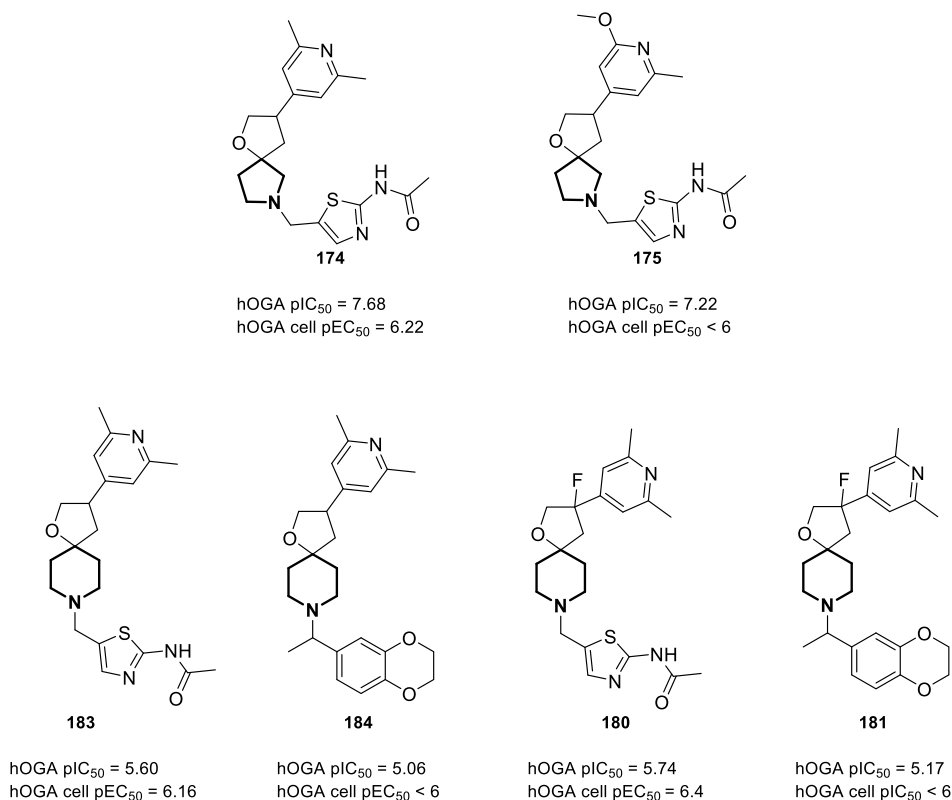


**Figure 5.15** SAR analysis from the direct linked heteroaromatic replacement in the containing THFs spiranes.

The insertion of an oxygen atom between the spiro-tetrahydrofuran scaffold and the pyridyl ring did not have an effect on the activity, with the most active diastereoisomer **169a'** ( $pIC_{50} = 7.52$ , cell  $pEC_{50} = 6.27$ ) being equipotent to the

directly linked analogue **174** ( $pIC_{50} = 7.68$ , cell  $pEC_{50} = 6.22$ ), albeit the latter being screened as a 1 to 1 mixture of diastereoisomers. Replacement of the pyridyl ring for a pyrimidine one (**171**,  $pIC_{50} = 7.11$ , cell  $pEC_{50} < 6$ ) was tolerated in terms of biochemical but not cellular activity (Figure 5.16). Moreover, as previously observed, product **177** ( $pIC_{50} = 5.97$ , cell  $pIC_{50} = 6.88$ ) containing a spiro-piperidine ring was significantly less potent than the corresponding spiro-pyrrolidine matched pair **169a'**.

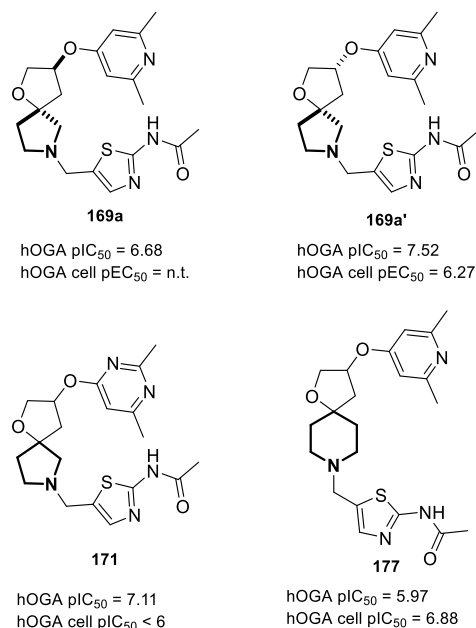
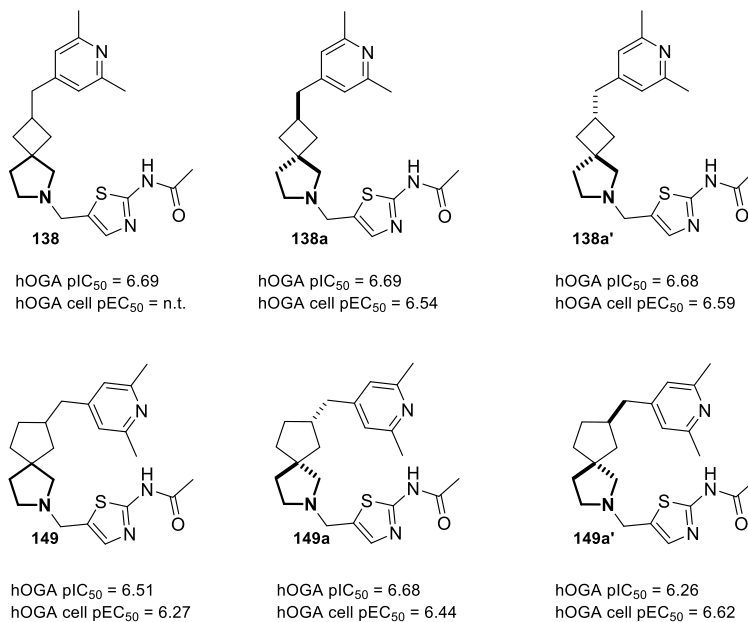


Figure 5.16 SAR analysis from the -O- linked heteroaromatic replacement.

In addition, introduction of a methylene linker between the pyridyl ring and the spiro-cycloalkane core was detrimental for activity (Figure 5.17). Compounds **138** ( $pIC_{50} = 6.69$ ) and **149** ( $pIC_{50} = 6.51$ ) were slightly less potent than their corresponding matched pairs **145** ( $pIC_{50} = 7.44$ ) and **156** ( $pIC_{50} = 7.18$ ), where the pyridyl ring is directly linked to the spiro-cycloalkane ring. The isolated diastereoisomers **138a**, **138a'**, **149a** and **149a'** were also tested leading to similar inhibitory values than the corresponding diastereoisomeric mixtures (Figure 5.17).

## Synthesis and application of novel spiro-boronate compounds for the treatment of Alzheimer's disease



**Figure 5.17** SAR analysis from the -CH<sub>2</sub>- linked heteroaromatic replacement.

Furthermore, the use of a one atom longer spacer -CH<sub>2</sub>O- led to comparable results to those obtained with the methylene linked compounds. Thus compounds **141** (pIC<sub>50</sub> = 6.89) and **152** (pIC<sub>50</sub> = 6.87) showed similar inhibitory activity than their corresponding matched pairs **138** (pIC<sub>50</sub> = 6.69) and **149** (pIC<sub>50</sub> = 6.51). Interestingly the pure diastereoisomer **141a'** showed a nice inhibitory activity in the biochemical assay (pIC<sub>50</sub> = 7.13), but more important, this activity was kept in the OGA cellular assay (cell pEC<sub>50</sub> = 7.34). To demonstrate the key role of acetamidothiazole group in the OGA inhibitory activity of the compounds, the synthesis intermediate **151**, containing a *N*-benzyl substituent in the pyrrolidine ring, was tested in the enzymatic assay and found to be inactive (pIC<sub>50</sub> < 5).

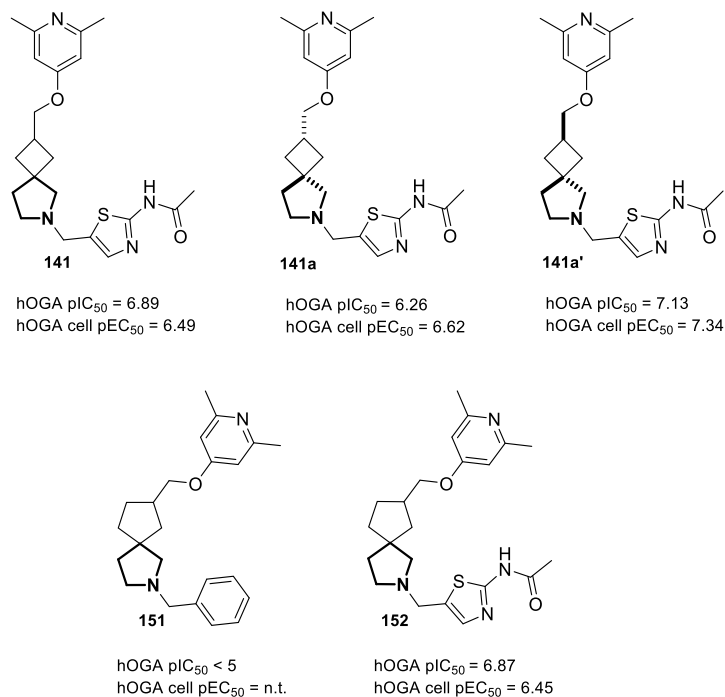


**Figure 5.18** SAR analysis from the  $-\text{CH}_2\text{O}-$  linked heteroaromatic replacement.

Finally, the spiro-bicyclic boronate **114** proved to be the central scaffold to source potent OGA inhibitors with balanced enzymatic and cellular activities. As can be seen in Figure 5.19, both, analogues containing methylene (**158**: pIC<sub>50</sub> = 7.38, cell pEC<sub>50</sub> = 7.13 and **160**: pIC<sub>50</sub> = 7.08, cell pEC<sub>50</sub> = 6.66) or  $-\text{CH}_2\text{O}-$  (**163**: pIC<sub>50</sub> = 7.13, cell pEC<sub>50</sub> = 7.34) linkers, displayed in most cases comparable enzymatic and cellular activities with pIC<sub>50</sub> and pEC<sub>50</sub> values above 7. Nevertheless, the most potent compounds identified in this collaborative project came from the introduction of a  $-\text{CH}_2\text{N}-$  linker, where the unexpected double heteroarylation of the linker led to compound **167** that after separation of diastereoisomers rendered the pure diastereoisomer **167a** (pIC<sub>50</sub> = 8.36, cell pEC<sub>50</sub> = 8.1), a single digit nanomolar inhibitor in both the enzymatic and cellular assays.

## Synthesis and application of novel spiro-boronate compounds for the treatment of Alzheimer's disease

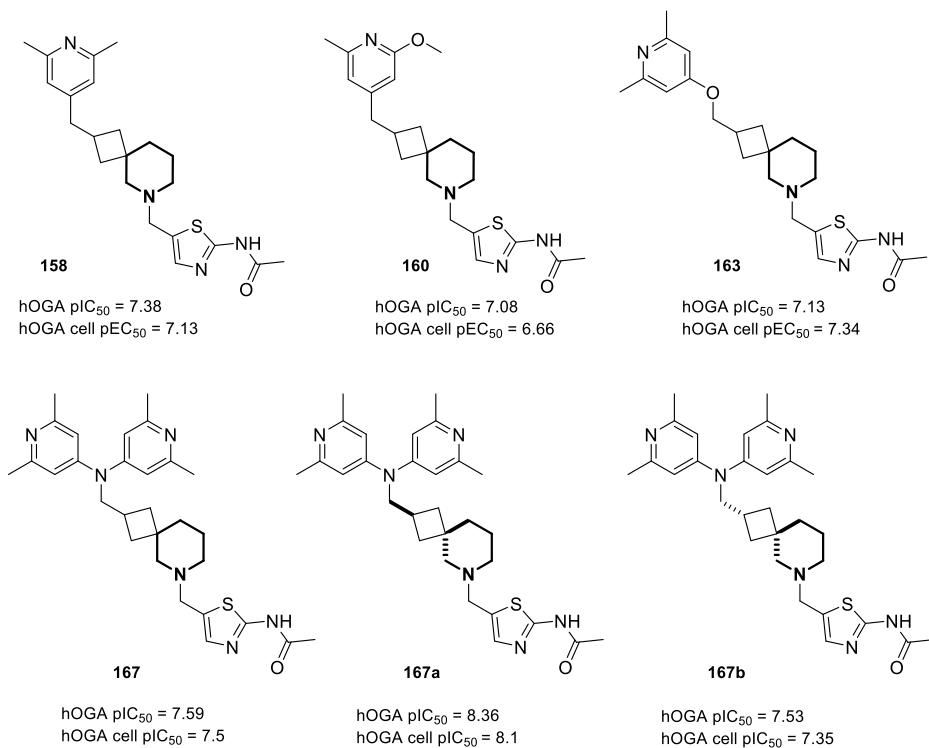


**Figure 5.19** SAR derived from the spiro-cyclobutylpiperidine scaffold **114**.

## 5.4. Conclusions

In summary, 5-central scaffolds have been synthesized in gram scale by two different spiro-cyclization methods. These scaffolds were derivatized introducing a distal heteroaromatic ring as substituent in the north cycle and in most cases an acetamidotiazole substituent on the south part of the scaffold. The boronate and hydroxy substituents on the spiro-cyclic core were used as handles to explore linkers of different length and nature as spacers between the distal heteroaromatic and the spiro-cyclic core. This exploration identified a spiro-cyclobutylpiperidine as an optimal central scaffold for the preparation of potent OGA inhibitors.



## Synthesis and application of novel spiro-boronate compounds for the treatment of Alzheimer's disease

---

### 5.5. References Chapter 5

- [1] J. Bowen, L. Teri, W. Kukull, W. McCormick, S. M. McCurry, E. B. Larson, *Lancet* **1997**, *349*, 763-765.
- [2] M. S. Wolfe, *J. Med. Chem.* **2012**, *55*, 8977-8978.
- [3] M. Strassnig, M. Ganguli, *Psychiatry (Edgmont)* **2005**, *2*, 30-33.
- [4] M. W. Bondi, E. C. Edmonds, D. P. Salmon, *J. Int. Neuropsychol. Soc.* **2017**, *23*, 818-831.
- [5] M. Prince, R. Bryce, E. Albanese, A. Wimo, W. Ribeiro, C. P. Ferri, *Alzheimers Dement.* **2013**, *9*, 63-75.
- [6] M. M. Wickens, D. A. Bangasser, L. A. Briand, *Front. Mol. Neurosci.* **2018**, *11*, 1-12.
- [7] T. Ninomiya, in *Diabetes Mellitus: A risk factor for Alzheimer's Disease* (Eds.: Y. Nakabeppu, T. Ninomiya), Springer Singapore, Singapore, **2019**, pp. 13-25.
- [8] M. F. Mendez, *Neurol. Clin.* **2017**, *35*, 263-281.
- [9] S. H. Mokhtar, M. M. Bakhuraysah, D. S. Cram, S. Petratos, *Int. J. Alzheimers Dis.* **2013**, *2013*, 1-15.
- [10] J. A. Hardy, G. A. Higgins, *Science* **1992**, *256*, 184.
- [11] a) H. Martiskainen, S. K. Herukka, A. Stančáková, J. Paananen, H. Soininen, J. Kuusisto, M. Laakso, M. Hiltunen, *Ann. Neurol.* **2017**, *82*, 128-132; b) A. Mullard, *Nat. Rev. Drug Discov.* **2019**, *18*, 656.
- [12] F. P. Chong, K. Y. Ng, R. Y. Koh, S. M. Chye, *Cell. Mol. Neurobiol.* **2018**, *38*, 965-980.
- [13] F. Liu, K. Iqbal, I. Grundke, G. W. Hart, C. X. Gong, *Proc. Natl. Acad. Sci. U.S.A.* **2004**, *101*, 10804-10809.
- [14] a) C. N. Chirita, E. E. Congdon, H. Yin, J. Kuret, *Biochemistry* **2005**, *44*, 5862-5872; b) C. A. Lasagna, D. L. Castillo, M. J. Guerrero, G. R. Jackson, R. Kayed, *Biochemistry* **2010**, *49*, 10039-10041; c) S. Mondragón, G. Basurto, I. Santa, R. Mena, L. I. Binder, J. Avila, M. A. Smith, G. Perry, F. García, *Int. J. Clin. Exp. Pathol.* **2008**, *89*, 81-90; d) N. Sahara, S. Maeda, M. Murayama, T. Suzuki, N. Dohmae, S. Yen, A. Takashima, *Eur. J. Neurosci.* **2007**, *25*, 3020-3029.
- [15] R. Fu, Q. Shen, P. Xu, J. J. Luo, Y. Tang, *Mol. Neurobiol.* **2014**, *49*, 1422-1434.
- [16] G. Lindwall, R. D. Cole, *J. Biol. Chem.* **1984**, *259*, 5301-5305.

- [17] a) M. P. Mazanetz, P. M. Fischer, *Nat. Rev. Drug Discov.* **2007**, *6*, 464-479; b) K. Mullane, M. Williams, *Biochem Pharmacol* **2013**, *85*, 289-305.
- [18] S. Wang, F. Yang, V. A. Petyuk, A. K. Shukla, M. E. Monroe, M. A. Gritsenko, K. D. Rodland, R. D. Smith, W. J. Qian, C. X. Gong, T. Liu, *J. Pathol.* **2017**, *243*, 78-88.
- [19] S. Lim, M. M. Haque, G. Nam, N. Ryoo, H. Rhim, K. Y. Kim, *Int. J. Mol. Sci.* **2015**, *16*, 20212-20224.
- [20] C. X. Gong, F. Liu, K. Iqbal, *Proc. Natl. Acad. Sci.* **2012**, *109*, 17319-17320.
- [21] a) B. Frost, R. L. Jacks, M. I. Diamond, *J. Biol. Chem.* **2009**, *284*, 12845-12852; b) N. Kfoury, B. B. Holmes, H. Jiang, D. M. Holtzman, M. I. Diamond, *J. Biol. Chem.* **2012**, *287*, 19440-19451.
- [22] H. G. Selnick, J. F. Hess, C. Tang, K. Liu, J. B. Schachter, J. E. Ballard, J. Marcus, D. J. Klein, X. Wang, M. Pearson, M. J. Savage, R. Kaul, T. S. Li, D. J. Vocadlo, Y. Zhou, Y. Zhu, C. Mu, Y. Wang, Z. Wei, C. Bai, J. L. Duffy, E. J. McEachern, *J. Med. Chem.* **2019**.
- [23] D. L. Graham, A. J. Gray, J. A. Joyce, D. Yu, J. O'Moore, G. A. Carlson, M. S. Shearman, T. L. Dellovade, H. Hering, *Neuropharmacology* **2014**, *79*, 307-313.
- [24] N. B. Hastings, X. Wang, L. Song, B. D. Butts, D. Grotz, R. Hargreaves, J. Fred Hess, K. L. K. Hong, C. R. R. Huang, L. Hyde, M. Laverty, J. Lee, D. Levitan, S. X. Lu, M. Maguire, V. Mahadomrongkul, E. J. McEachern, X. Ouyang, T. W. Rosahl, H. Selnick, M. Stanton, G. Terracina, D. J. Vocadlo, G. Wang, J. L. Duffy, E. M. Parker, L. Zhang, *Mol. Neurodegener.* **2017**, *12*, 1-16.
- [25] J. M. Bartolomé, A. A. Trabanco, C. M. Martinez, **PCT/EP2018/052901, Patent.**
- [26] F. V. Rao, H. C. Dorfmüller, F. Villa, M. Allwood, I. M. Eggleston, D. M. F. van Aalten, *EMBO J.* **2006**, *25*, 1569-1578.
- [27] A. I. Moskalenko, S. L. Belopukhov, A. A. Ivlev, V. I. Boev, *Russ. J. Organ. Chem.* **2011**, *47*, 1091-1096.
- [28] J. Mendiola, S. García, Ó. Frutos, M. L. Puente, R. L. Gu, V. V. Khau, *Org. Process Res. Dev.* **2009**, *13*, 292-296.
- [29] C. V. Stevens, T. Rammeloo, N. De Kimpe, *Synlett* **2001**, *2001*, 1519-1522.
- [30] J. E. DeLorbe, S. Y. Jabri, S. M. Mennen, L. E. Overman, F. L. Zhang, *J. Am. Chem. Soc.* **2011**, *133*, 6549-6552.
- [31] A. R. O. Venning, P. T. Bohan, E. J. Alexanian, *J. Am. Chem. Soc.* **2015**, *137*, 3731-3734.

## Synthesis and application of novel spiro-boronate compounds for the treatment of Alzheimer's disease

---

- [32] J. Royes, S. Ni, A. Farré, E. La Cascia, J. J. Carbó, A. B. Cuenca, F. Maseras, E. Fernández, *ACS Catal.* **2018**, *8*, 2833-2838.
- [33] P. Craven, A. Aimon, M. Dow, N. Fleury, R. Guilleux, R. Morgentin, D. Roche, T. Kalliokoski, R. Foster, S. P. Marsden, A. Nelson, *Bioorg. Med. Chem.* **2015**, *23*, 2629-2635.
- [34] K. M. Bogle, D. J. Hirst, D. J. Dixon, *Tetrahedron* **2010**, *66*, 6399-6410.
- [35] F. Mo, F. Li, D. Qiu, J. Wang, *Tetrahedron* **2010**, *66*, 1274-1279.
- [36] S. D. Patel, W. M. Habeski, H. Min, J. Zhang, R. Roof, B. Snyder, G. Bora, B. Campbell, C. Li, D. Hidayetoglu, D. S. Johnson, A. Chaudhry, M. E. Charlton, N. M. Kablaoui, *Bioorg. Med. Chem. Lett.* **2008**, *18*, 5689-5693.
- [37] P. D. Bailey, K. M. Morgan, D. I. Smith, J. M. Vernon, *Tetrahedron* **2003**, *59*, 3369-3378.
- [38] L. Harris, M. Gilpin, A. L. Thompson, A. R. Cowley, M. G. Moloney, *Org. Biomol. Chem.* **2015**, *13*, 6522-6550.
- [39] a) J. R. Coombs, L. Zhang, J. P. Morken, *Org. Lett.* **2015**, *17*, 1708-1711; b) K. Endo, M. Hirokami, T. Shibata, *J. Org. Chem.* **2010**, *75*, 3469-3472; c) K. Endo, A. Sakamoto, T. Ohkubo, T. Shibata, *Chem. Lett.* **2011**, *40*, 1440-1442.
- [40] S. D. Banister, L. M. Rendina, M. Kassiou, *Bioorg. Med. Chem. Lett.* **2012**, *22*, 4059-4063.
- [41] E. Yamamoto, Y. Takenouchi, T. Ozaki, T. Miya, H. Ito, *J. Am. Chem. Soc.* **2014**, *136*, 16515-16521.
- [42] K. C. Caster, in *Encyclopedia of Reagents for Organic Synthesis*.
- [43] K. E. Harding, L. M. May, K. F. Dick, *J. Org. Chem.* **1975**, *40*, 1664-1665.
- [44] J. Cornella, J. T. Edwards, T. Qin, S. Kawamura, J. Wang, C. M. Pan, R. Gianatassio, M. Schmidt, M. D. Eastgate, P. S. Baran, *J. Am. Chem. Soc.* **2016**, *138*, 2174-2177.
- [45] D. Franck, T. Kniess, J. Steinbach, S. Zitzmann, M. Friebe, L. M. Dinkelborg, K. Graham, *Bioorg. Med. Chem.* **2013**, *21*, 643-652.
- [46] M. J. Meyers, S. A. Long, M. J. Pelc, J. L. Wang, S. J. Bowen, B. A. Schweitzer, M. V. Wilcox, J. McDonald, S. E. Smith, S. Foltin, J. Rumsey, Y. S. Yang, M. C. Walker, S. Kamtekar, D. Beidler, A. Thorarensen, *Bioorg. Med. Chem. Lett.* **2011**, *21*, 6545-6553.

- [47] E. Torrente, C. Parodi, L. Ercolani, C. De Mei, A. Ferrari, R. Scarpelli, B. Grimaldi, *J. Med. Chem.* **2015**, *58*, 5900-5915.
- [48] J. J. W. Duan, Z. Lu, B. Jiang, B. V. Yang, L. M. Doweyko, D. S. Nirschl, L. E. Haque, S. Lin, G. Brown, J. Hynes, J. S. Tokarski, J. S. Sack, J. Khan, J. S. Lippy, R. F. Zhang, S. Pitt, G. Shen, W. J. Pitts, P. H. Carter, J. C. Barrish, S. G. Nadler, L. M. Salter-Cid, M. McKinnon, A. Fura, G. L. Schieven, S. T. Wroblewski, *Bioorg. Med. Chem. Lett.* **2014**, *24*, 5721-5726.
- [49] A. Mori, Y. Miyakawa, E. Ohashi, T. Haga, T. Maegawa, H. Sajiki, *Org. Lett.* **2006**, *8*, 3279-3281.
- [50] G. Sartori, R. Ballini, F. Bigi, G. Bosica, R. Maggi, P. Righi, *Chem. Rev.* **2004**, *104*, 199-250.
- [51] S. Albrecht, A. Defoin, C. Tarnus, *Synthesis* **2006**, *2006*, 1635-1638.
- [52] S. Randl, S. Blechert, *J. Org. Chem.* **2003**, *68*, 8879-8882.
- [53] Y. Fukuta, T. Mita, N. Fukuda, M. Kanai, M. Shibasaki, *J. Am. Chem. Soc.* **2006**, *128*, 6312-6313.
- [54] J. T. Welch, D. S. Lim, *Bioorg. Med. Chem.* **2007**, *15*, 6659-6666.
- [55] K. Takao, N. Hayakawa, R. Yamada, T. Yamaguchi, H. Saegusa, M. Uchida, S. Samejima, K. Tadano, *J. Org. Chem.* **2009**, *74*, 6452-6461.
- [56] S. Bhattacharyya, *J. Org. Chem.* **1995**, *60*, 4928-4929.

UNIVERSITAT ROVIRA I VIRGILI  
COMPLEMENTARY SYNTHESIS OF ORGANOBORANES TO POPULATE THE CHEMICAL  
FUNCTIONALITY TO A GIVEN AREA OF BIOMEDICAL INTEREST  
Jordi Royes Buisan

# **Chapter 6**

## **Intramolecular diastereoselective borylative spiro-cyclization through alkenyl aldehydes**

---

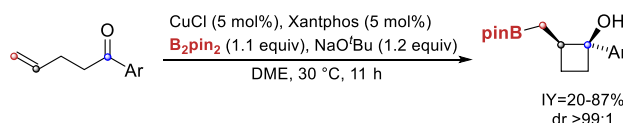
UNIVERSITAT ROVIRA I VIRGILI  
COMPLEMENTARY SYNTHESIS OF ORGANOBORANES TO POPULATE THE CHEMICAL  
FUNCTIONALITY TO A GIVEN AREA OF BIOMEDICAL INTEREST  
Jordi Royes Buisan

## 6.1. State of the art

### 6.1.1 1,2-Carboboration of alkenyl ketones

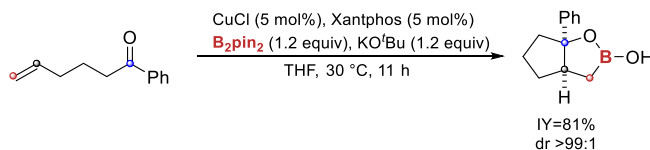
Formation of small rings through 1,2-carboboration process has fascinated organic chemists during the last decade because of their strain and rigid framework.<sup>[1]</sup> Recent works have demonstrated the efficiency of the copper mediated borylative cyclization of multiple C-C bonds through  $\gamma$ -alkenyl ketones towards the formation of cyclic products with the *in situ* incorporation of the boryl unit and the alcohol group, being considered of high interest in medicinal chemistry.

The group of Ito and co-workers<sup>[2]</sup> pioneered the field with the regioselective boryl cupration of  $\gamma$ -alkenyl aryl ketones. The alkylcopper species is formed with complete regioselectivity in the presence of CuCl, Xantphos, KO<sup>t</sup>Bu and B<sub>2</sub>pin<sub>2</sub>, placing the boryl unit at the terminal position of the olefin. The catalytic system promoted the intramolecular 1,2-addition to the carbonyl group to give 2-(borylmethyl)cyclobutanols with excellent *syn*-diastereoselectivity (Scheme 6.1).



Scheme 6.1 Borylative ring-closing of  $\gamma$ -alkenyl aryl ketones catalyzed by copper.

However, the scope of the reaction was limited to few examples, with only some modifications along the nature of the aryl group. Moreover, the authors reported one example of borylative cyclization through  $\delta$ -alkenyl aryl ketones which provided the formation of a 1,2-oxaborolane bicyclic structure in high yield and good diastereoselectivity (Scheme 6.2).



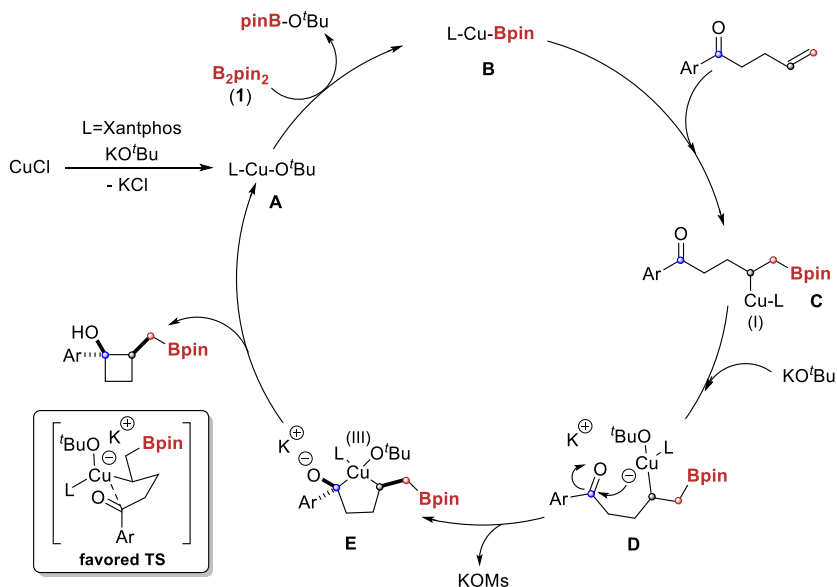
Scheme 6.2 Borylative ring-closing of  $\delta$ -alkenyl aryl ketones catalyzed by copper.

The authors proposed a reaction mechanism for this intramolecular 1,2-carboboration (Scheme 6.3). The catalytic cycle might start with the formation of the copper alkoxide complex, via  $\sigma$ -bond metathesis between LCuOR (**A**) and B<sub>2</sub>pin<sub>2</sub> affording the boryl copper (**I**) active species (**B**). Intermediate **C** might be next



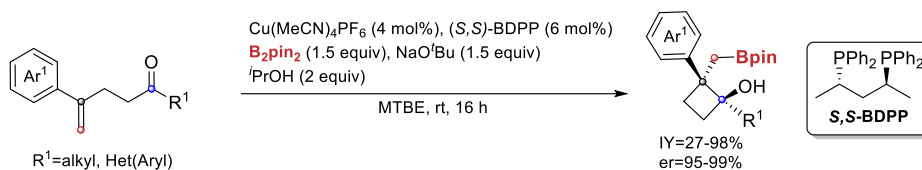
## Intramolecular diastereoselective borylative spiro-cyclization through alkenyl aldehydes

formed by chemo- and regioselective 1,2-addition of Cu-B to C=C bond. Subsequently, an extra coordination of the alkoxide base could form a more nucleophilic cuprate intermediate **D**. It has been suggested that a Cu (III) species **E**, formed via oxidative addition, evolves into the desired cyclic product via reductive elimination and closing the catalytic cycle by regenerating the species **A**. The *syn*-selectivity observed, could be explained through the less sterically hindered transition state postulated and included in Scheme 6.3.



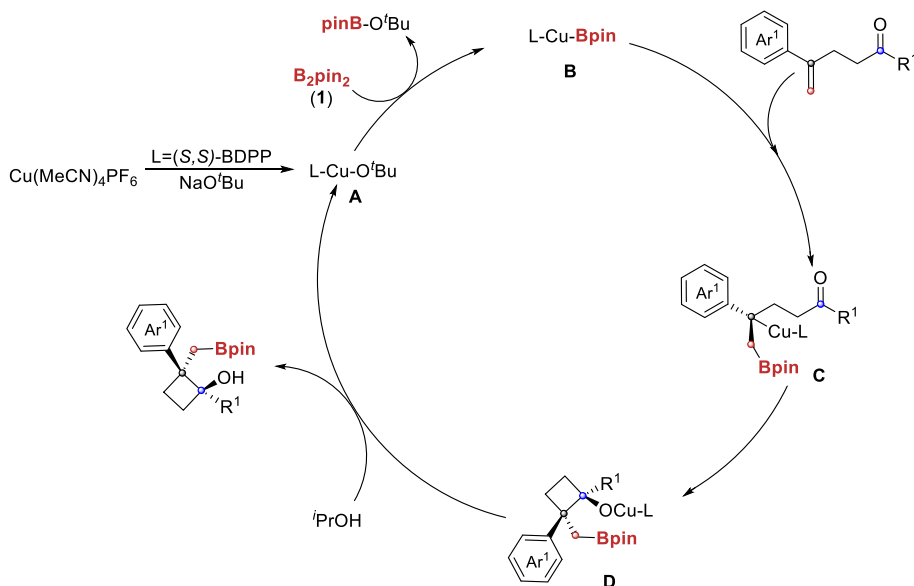
**Scheme 6.3** Suggested mechanism for the borylative cyclization of alkenyl aryl ketones.<sup>[2]</sup>

In contrast, an opposite *anti*-diastereoselection has been reported by Lautens and co-workers<sup>[3]</sup> for the borylative cyclization of  $\gamma$ -alkenyl aryl/alkyl ketones. The use of Cu(MeCN)<sub>4</sub>PF<sub>6</sub>/NaO<sup>t</sup>Bu as precursor of the catalytic system gave access to a wide variety of boryl arylated cyclobutanols. Interestingly, as the asymmetric addition of boron to alkenes is an important tool to readily introduce molecular complexity and flexibility,<sup>[4]</sup> the use of (*S,S*)-BDPP as ligand allowed for the enantioselective preparation of these cyclobutanol derivatives (Scheme 6.4).



**Scheme 6.4** Enantioselective borylative ring-closing of substituted  $\gamma$ -alkenyl aryl/alkyl ketones catalyzed by copper.

In this study, the use of MTBE (methyl *tert*-butyl ether) as the optimal solvent was reported, although comparable results were obtained with THF. Interestingly the use of *i*PrOH as additive was critical to obtain good conversions. Lautens and co-workers proposed a complementary mechanism to the one reported by Ito and co-workers.<sup>[2]</sup> However no justification of the *anti*-diastereoisomerism was provided (Scheme 6.5).



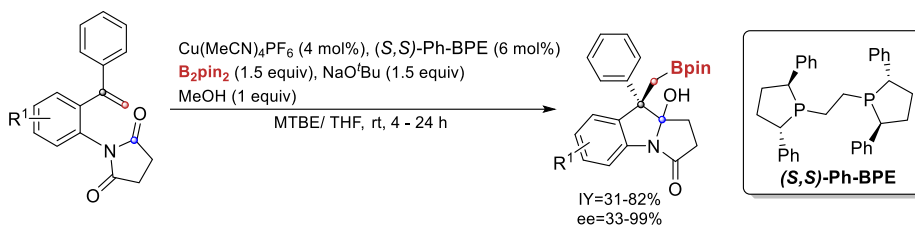
**Scheme 6.5** Suggested mechanism for the borylative cyclization of substituted  $\gamma$ -alkenyl aryl ketones.<sup>[3]</sup>

The boryl copper (I) active species **B** promotes the coordination and concomitant insertion to the styrene moiety of the substrate to give the benzylic copper species **C**. Then intramolecular cyclization to the tethered aryl ketone might form intermediate **D**. Subsequently, the intermediate **D** might undergo

## Intramolecular diastereoselective borylative spiro-cyclization through alkenyl aldehydes

protodemetalation assisted by the alcoholic additive (*i*PrOH) to furnish the arylated cycobutanol product and recycle the catalyst.

More recently this group has also developed the enantioselective copper catalyzed borylation/1,2-imide addition cascade reaction to assemble boron-containing indolines.<sup>[5]</sup> However, in this Cu (I) catalytic system (*S,S*)-Ph-BPE as chiral ligand and MeOH as additive resulted more efficient. The authors also observed that the use of bulkier alcohols as additive provided lower enantioselectivities. The transformations were found to be highly diastereoselective and enantioselective, as well as tolerant with a variety of aryl substituents (Scheme 6.6).

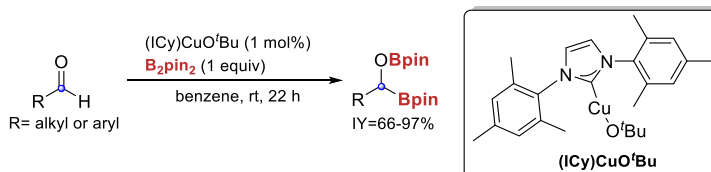


**Scheme 6.6** Enantioselective borylative ring-closing of substituted alkenyl phenyl pyrrolidindiones catalyzed by copper.

This group also reported previously the enantioselective boryl acylation process for accessing chiral 3,3-disubstituted oxindoles.<sup>[6]</sup>

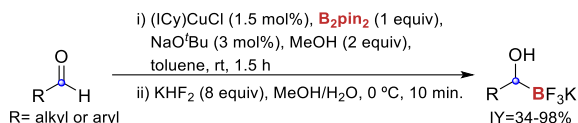
### 6.1.2 1,2-Borylation of aldehydes catalyzed by copper complexes

Copper (I) complexes can also catalyze the 1,2-diboration of aldehydes. However, the use of aldehydes as substrates have proved complex due to the lack of success in the isolation of 1,2-diborated products.<sup>[7]</sup> Sadighi and co-workers<sup>[8]</sup> reported for the first time the 1,2-diboration of aliphatic and aromatic aldehydes. The use of a carbene copper (I) complex catalyzes the formation of 1,2-diborated products in high yields (Scheme 6.7). These diborated compounds could be isolated by recrystallization and showed high stability when stored under argon. However, they have a tendency to decompose in the presence of oxygen as well as during purification by flash column chromatography.



**Scheme 6.7** 1,2-diboration of aldehydes catalyzed by copper complexes.

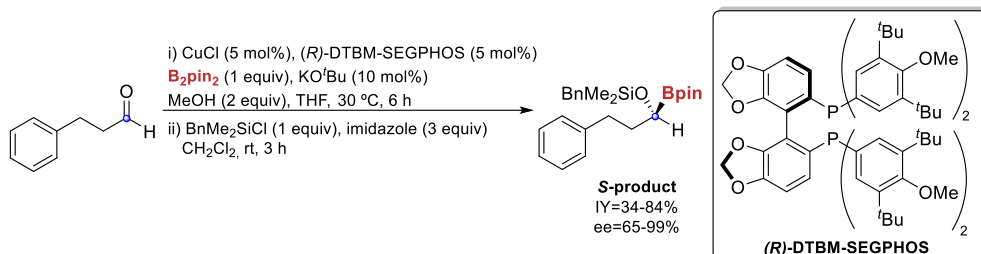
Molander and co-workers<sup>[9]</sup> improved the reaction conditions reported by Sadighi performing the reaction in toluene and using MeOH as additive. The reaction was accelerated and full converted after 1.5 hours. Subsequent addition of  $\text{KHF}_2$  provided the corresponding mono-trifluoroborated products in moderate to excellent yield (Scheme 6.8).



Scheme 6.8 . Preparation of potassium 1-(hydroxy)alkyltrifluoroborates.

In that context, Clark and co-workers<sup>[10]</sup> reported the one pot direct 1,2-diboration/ homologation to provide  $\beta$ -hydroxyboronate esters in moderate to good yields.

More recently, Ito and co-workers<sup>[11]</sup> reported the enantioselective borylation of aldehydes using a Cu (I) salt and (*R*)- or (*S*)-DTBM-SEGPHOS as chiral ligand. These studies evidenced excellent enantioselectivities and a broad substrate scope towards the formation of borylated protected alcohols (Scheme 6.9).



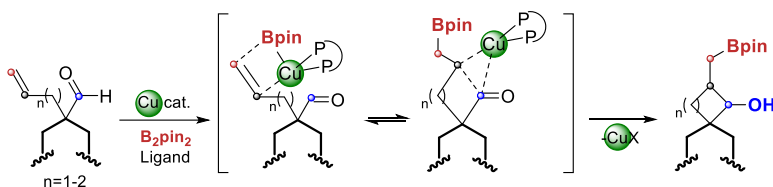
Scheme 6.9 Enantioselective borylation of aliphatic aldehydes catalyzed by copper.

## Intramolecular diastereoselective borylative spiro-cyclization through alkenyl aldehydes

### 6.2. Aim of the Chapter

With all these precedents in mind and based in our previous work, we decided to study the potential of alkenyl aldehydes as synthetic precursor to spiro-cyclic products with vicinal borylmethyl and hydroxyl functional groups (Scheme 6.10).

Despite the fact that copper catalyzed borylative addition to aldehydes or alkenes had been previously explored, to the best of our knowledge, this would be the first example of a borylcupration followed by intramolecular electrophilic trapping of the alkylcopper intermediate with an aldehyde, although intermolecular versions are already known.<sup>[12]</sup>



Scheme 6.10 Graphical objective of the chapter.

### 6.3. Results and discussion

We began with the synthesis of the alkenyl aldehydes from the corresponding derivative esters **55**, **185**, **130** and from commercially available aldehyde **186** (Figure 6.1). Substrates **185** and **130** were obtained from the commercially available hydrochloric amine salts by *N*-protection with tosylchloride/TEA<sup>[13]</sup> and Boc<sub>2</sub>O/DIPEA<sup>[14]</sup> respectively.

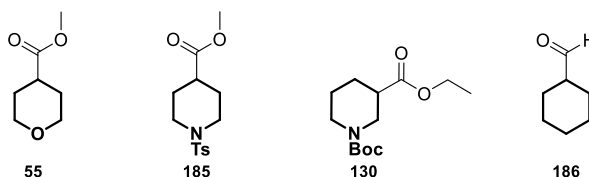
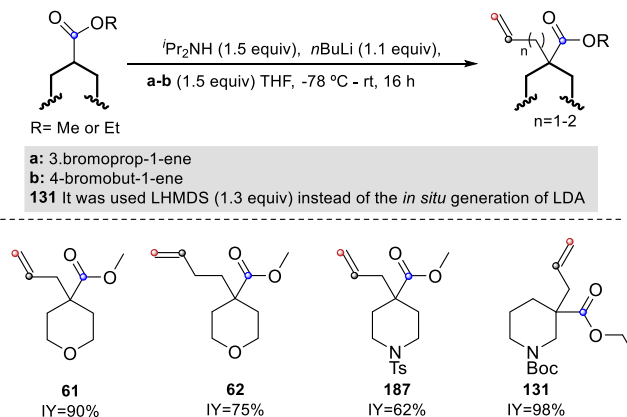


Figure 6.1 Derivative esters and aldehydes used as starting materials.

The alkylation of substrates **55** and **185** with 3-bromoprop-1-ene was performed with the *in situ* generated LDA in THF (Scheme 6.11). The desired alkylated products **61** and **187** were isolated in 90% and 62% yield respectively. Moreover substrate **55** was alkylated with 4-bromobut-1-ene under the same reaction conditions giving access to the alkylated ester **62** in 75% isolated yield. For the alkylation of ester **130** the use of lithium bistrimethylsilyl amide (LHMDS)<sup>[15]</sup> instead of LDA<sup>[16]</sup> resulted in higher isolated yields of product **131** (98%) (Scheme 6.11).

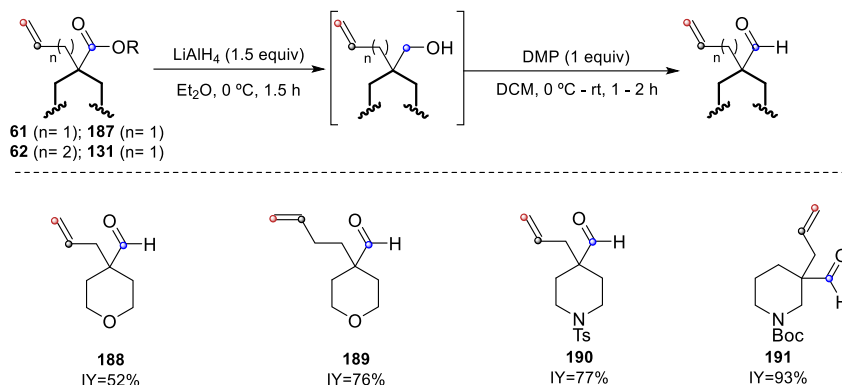


Scheme 6.11 General procedure and scope of the alkylation step.

Subsequently, the alkylated derivative ester intermediates **61**, **62**, **187** and **131** were reduced to the hydroxymethylene products with lithium aluminum hydride (LiAlH<sub>4</sub>) as reducing agent in anhydrous Et<sub>2</sub>O at 0 °C (Scheme 6.12). The hydroxylated

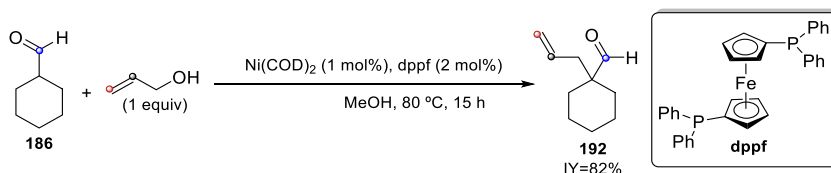
## Intramolecular diastereoselective borylative spiro-cyclization through alkenyl aldehydes

intermediates were obtained in quantitative yields after aqueous work up and were subjected to the next reaction step without further purification.<sup>[17]</sup> Oxidation of the alcohols was achieved using Dess-Martin periodinane leading to the corresponding aldehydes **188-191** in good to excellent yields (Scheme 6.12).<sup>[18]</sup> The lower 52% yield for substrate **188** was due to partial decomposition of the product during the purification step.



**Scheme 6.12** General procedure for the synthesis of alkenyl aldehydes by sequential reduction-oxidation.

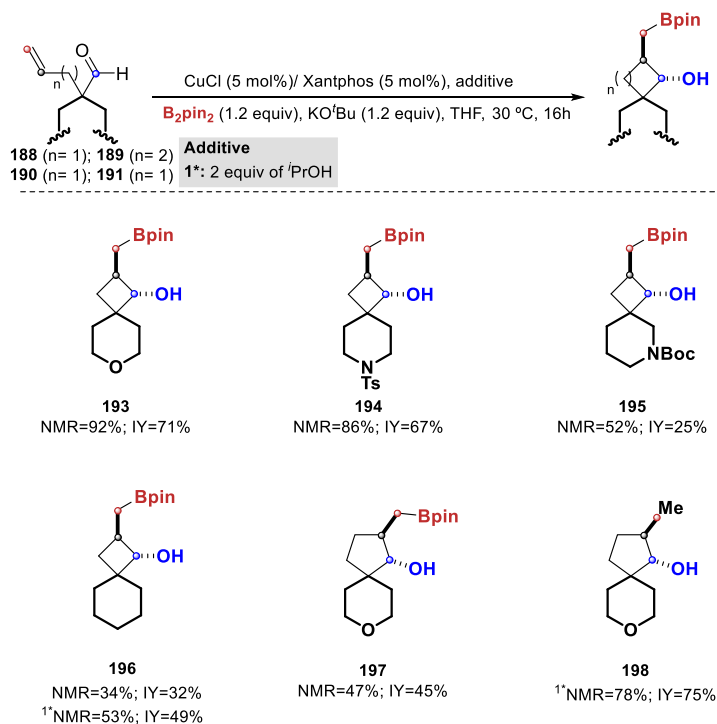
The alkenyl aldehyde **192** was prepared from substrate **186** by reaction with allyl alcohol under catalytic amounts of Ni(COD)<sub>2</sub> and dppf as ligand in MeOH. After 15 hours at 80 °C the cyclohexyl alkenyl aldehyde (**192**) was obtained in 82% isolated yield (Scheme 6.13).<sup>[19]</sup>



**Scheme 6.13** Synthesis of alkenyl aldehyde **192**.

The borylative ring-closing reaction conditions previously described were applied to substrates **188-192**. Gratifyingly, substrate **188** underwent the borylative ring-closing catalyzed by CuCl / Xantphos, in the presence of B<sub>2</sub>pip<sub>2</sub> and KO<sup>t</sup>Bu in THF. After 16 hours reaction time, the desired cyclized product **193** was isolated in high yield (Scheme 6.14). The analogous 4-piperidine alkenyl aldehyde substrate **190** exhibited similar reactivity providing the target product **194** in 67% isolated yield (Scheme 6.14). To our surprise a decrease of the reaction efficiency was observed

in the case of the 3-piperidine alkenyl aldehyde substrate **191**, obtaining the expected product **195** in only 25% isolated yield. The cyclohexyl substrate **192** was successfully transformed into the desired product **196** but in low 32% isolated yield.



**Scheme 6.14** Borylative ring-closing of alkenyl aldehydes catalyzed by copper.

Having in mind Lauten's work where the addition of  $i\text{PrOH}$  was found essential to produce the borylative cyclization of alkenyl ketones,<sup>[3]</sup> we decided to add 2 equivalents of  $i\text{PrOH}$  with the aim to accelerate the catalytic process in the protonolysis step. Interestingly, **196** was now isolated in 49% yield (Scheme 6.14). Moreover, we extend the methodology to the synthesis of 5-membered ring containing spiro-cycles. Using **189** as substrate, under the same catalytic conditions, the spiro-bicycle **197** was obtained in 45% isolated yield. The addition of  $i\text{PrOH}$  resulted in higher conversion towards the spiro-cyclized product, however the boron unit was lost during the process and compound **198** was formed in 75% isolated yield (Scheme 6.14).

Interestingly, the reaction outcome indicates that initial borylcupration takes place chemoselectively on the alkene without altering the aldehyde functionality. This is an important point to validate in the new methodology, since the present copper



## Intramolecular diastereoselective borylative spiro-cyclization through alkenyl aldehydes

catalyzed method is similar to the one reported for the 1,2-diboration of aldehydes.<sup>[8-11]</sup>

Impressively, the borylative cyclization of alkenyl aldehydes was completely diastereoselective with both the borylmethyl and hydroxyl group in *anti*-position. The relative configuration of these two groups was determined by NOE experiments of product **193** (Figure 6.2, NOE). For instance, a negative NOE between **Ha** and **Hb**, was observed upon irradiation of **Ha**. However, when **Hb** was irradiated selectively it was observed a positive NOE with the protons from the pinacol unit (Figure 6.2, NOE 2).

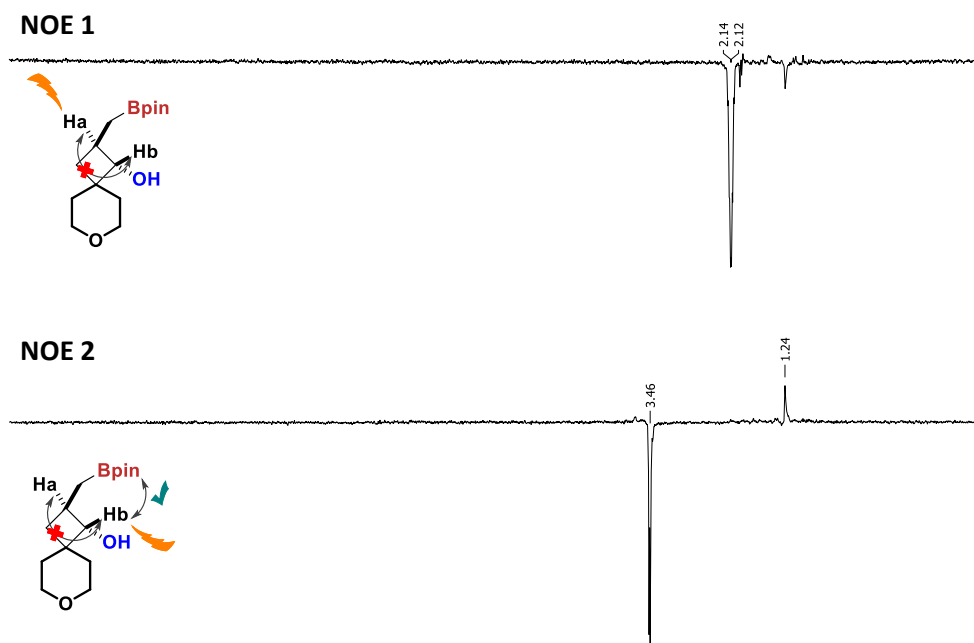
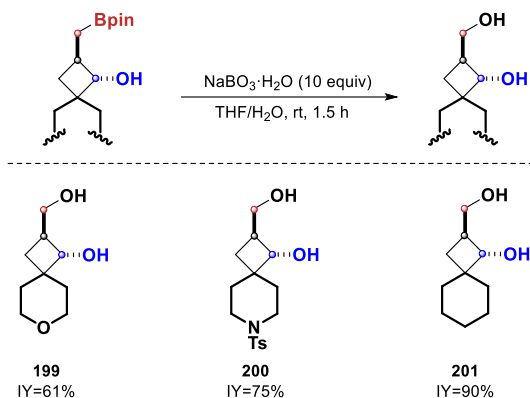


Figure 6.2 NOE experiments of product **193**.

Next, to prove the synthetic utility of this functionalized spiro-bicycles, compounds **193**, **194** and **196** were selectively oxidized with  $\text{NaBO}_3 \cdot \text{H}_2\text{O}$  under very mild conditions to form the corresponding dihydroxylated products **199**, **200** and **201** in high yields (Scheme 6.15).



**Scheme 6.15** Selective oxidation of the spiro-compounds.

X-Ray diffraction of product **200** allowed the complete characterization of the diol product and confirmed the *anti*-diastereoselectivity (Figure 6.3).

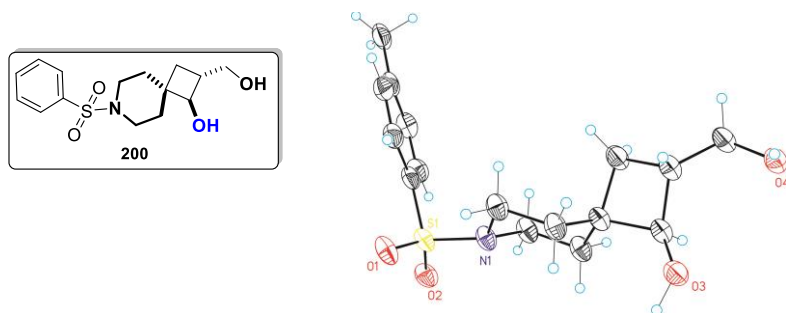


**Figure 6.3** X-Ray diffraction of *anti*-2-(hydroxymethyl)-7-(phenylsulfonyl)spiro[3.5]nonan-1-ol (**200**).

## Intramolecular diastereoselective borylative spiro-cyclization through alkenyl aldehydes

---

### 6.4. Conclusions

In this preliminary study, we have been able to synthesize a variety of alkenyl aldehyde substrates in an efficient manner. Moreover, we have gained access to a new synthetic method via borylative ring-closing catalyzed by copper complexes modified with Xantphos ligand. The present methodology has demonstrated total catalyst control in terms of chemoselectivity and diastereoselectivity, which was confirmed by X-Ray diffraction on a diol derivative. Additionally, good functional group tolerance has been proved with the successful spiro-cyclization of central cores containing oxygen or nitrogen, as well as different protecting groups. This transformation represents an unprecedented method to the preparation of new functionalized spiro-bicycles and also expands the pharmacopeia library for potential biomedical applications.

## 6.5. References Chapter 6

- [1] Z. Liu, Y. Gao, T. Zeng, K. M. Engle, *Isr. J. Chem.* **2019**, *0*.
- [2] E. Yamamoto, R. Kojima, K. Kubota, H. Ito, *Synlett* **2016**, *27*, 272-276.
- [3] A. Whyte, B. Mirabi, A. Torelli, L. Prieto, J. Bajohr, M. Lautens, *ACS Catal.* **2019**, *9*, 9253-9258.
- [4] Y. Xi, J. F. Hartwig, *J. Am. Chem. Soc.* **2017**, *139*, 12758-12772.
- [5] A. Whyte, A. Torelli, B. Mirabi, M. Lautens, *Org. Lett.* **2019**, *21*, 8373-8377.
- [6] A. Whyte, K. I. Burton, J. Zhang, M. Lautens, *Angew. Chem. Int. Ed.* **2018**, *57*, 13927-13930.
- [7] C. A. G. Carter, K. D. John, G. Mann, R. L. Martin, T. M. Cameron, R. T. Baker, K. L. Bishop, R. D. Broene, S. A. Westcott, in *Group 13 Chemistry, Vol. 822*, American Chemical Society, **2002**, pp. 70-87.
- [8] D. S. Laitar, E. Y. Tsui, J. P. Sadighi, *J. Am. Chem. Soc.* **2006**, *128*, 11036-11037.
- [9] G. A. Molander, S. R. Wisniewski, *J. Am. Chem. Soc.* **2012**, *134*, 16856-16868.
- [10] C. M. Moore, C. R. Medina, P. C. Cannamela, M. L. McIntosh, C. J. Ferber, A. J. Roering, T. B. Clark, *Org. Lett.* **2014**, *16*, 6056-6059.
- [11] K. Kubota, E. Yamamoto, H. Ito, *J. Am. Chem. Soc.* **2015**, *137*, 420-424.
- [12] a) J. C. Green, M. V. Joannou, S. A. Murray, J. M. Zanghi, S. J. Meek, *ACS Catal.* **2017**, *7*, 4441-4445; b) K. Lee, A. R. Zhugralin, A. H. Hoveyda, *J. Am. Chem. Soc.* **2009**, *131*, 7253-7255; c) C. Rasson, A. Stouse, A. Boreux, V. Cirriez, O. Riant, *Chem.: Eur. J.* **2018**, *24*, 9234-9237; d) A. Welle, V. Cirriez, O. Riant, *Tetrahedron* **2012**, *68*, 3435-3443.
- [13] P. Williamson, A. Galván, M. J. Gaunt, *Chem. Sci.* **2017**, *8*, 2588-2591.
- [14] N. B. Palakurthy, B. Mandal, *Tetrahedron Lett.* **2011**, *52*, 7132-7134.
- [15] M. Özlügedik, S. Ünalı, B. Wibbeling, D. Hoppe, *Adv. Synth. Catal.* **2005**, *347*, 1627-1631.
- [16] V. Y. Stolyarenko, A. A. Evdokimov, V. I. Shishkin, *Mendeleev Commun.* **2013**, *23*, 233-234.

## Intramolecular diastereoselective borylative spiro-cyclization through alkenyl aldehydes

---

- [17] F. X. Tavares, D. N. Deaton, A. B. Miller, L. R. Miller, L. L. Wright, H. Q. Zhou, *J. Med. Chem.* **2004**, *47*, 5049-5056.
- [18] Y. Yamano, M. V. Chary, A. Wada, *Chem. Pharm. Bull.* **2010**, *58*, 1362-1365.
- [19] Y. Bernhard, B. Thomson, V. Ferey, M. Sauthier, *Angew. Chem. Int. Ed.* **2017**, *56*, 7460-7464.

# Chapter 7

## Concluding remarks

---

UNIVERSITAT ROVIRA I VIRGILI  
COMPLEMENTARY SYNTHESIS OF ORGANOBORANES TO POPULATE THE CHEMICAL  
FUNCTIONALITY TO A GIVEN AREA OF BIOMEDICAL INTEREST  
Jordi Royes Buisan

In chapter 3, we performed for the first time the insertion of trimethylsilyldiazomethane into the B-S  $\sigma$ -bond of pinB-SPh (**6a**) and pinB-STol (**6b**). The reaction was performed efficiently and was amenable for scale up to a gram scale. The corresponding tri-substituted methanes, CH(Bpin)(SiMe<sub>3</sub>)(SR) (**8a-b**), were selectively functionalized by means of a series of selective alkylation reactions after careful choice of the base employed. The use of an alkoxy base, assisted the deborylative alkylation of CH(Bpin)(SiMe<sub>3</sub>)(SR) (**8a-b**) with a series of alkyl halides. The use of a bulky nitrogenated base altered the outcome of the reaction allowing for a boron-retentive alkylation reaction. In this way, a range of highly substituted methanes were accessed. Additionally, when 1,*n*-dihaloalkanes were employed as electrophiles, the first deborylative alkylation intermediate could be subsequently transformed into a series of functionalized carbocyclic compounds. In this sense, an intramolecular ring forming deborylative alkylation was observed when an alkoxide base is used. Furthermore, an intramolecular desilylative cyclization could be achieved in the presence of a more silicophilic fluoride base.

In chapter 4, a series of compounds containing unactivated alkenes and a C-X moiety were prepared. Those substrates were suitable substrates to conduct a borylative cyclization through a regioselective borylcupration followed by subsequent intramolecular ring closing via halide displacement. The transformation exhibited high functional group tolerance, with central cyclic substrates containing oxygen and nitrogen as heteroatoms. The transformation revealed a direct dependence on the size of ring formed, which was directly dependent on the metalocyclic intermediate based on Cu (III) species. The present methodology opened the door to the preparation of new spiro-bicyclic cores allowing for ring size variation in both cycles. Iteration of optimized protocol gave access to a structurally complex dispiro-heterotricyclic structure fully characterized by X-Ray diffraction.

In chapter 5, an application of several spiro-heterobicyclic cores synthesized in chapter 4 was explored in the context of a Medicinal Chemistry program targeting OGA inhibitors to treat Alzheimer's disease. Up to 5-central spiro-bicyclic scaffolds were prepared in multi-gram scale by two different spiro-cyclization methods. These central cores were derivatized introducing a distal heteroaromatic ring as substituent in the north cycle and in most cases an acetamidotiazole substituent on the south part of the scaffold. The boronate and hydroxy substituents on the spiro-cyclic core proved to be good synthetic handles to anchor linkers of different length and nature as spacers between the distal heteroaromatic and the spiro-cyclic core.



## Concluding remarks

This exploration identified a spiro-cyclobutylpiperidine as an optimal central scaffold for the preparation of potent OGA inhibitors.

In [chapter 6](#), the preliminary studies on a novel intramolecular borylative ring closing reaction of alkenyl aldehydes by chemoselective borylcupration followed by C=O insertion is reported. The results obtained have demonstrated a total catalyst control in terms of chemoselectivity and diastereoselectivity, which was confirmed by X-Ray diffraction of a diol containing derivative. Additionally methodology has demonstrated high functional group tolerance, with central cores containing oxygen or nitrogen, as well as different protecting groups. This transformation opens the door to new functionalized spiro-compounds and also expands the pharmacopeia library to be studied for appropriate biomedical applications.

# Chapter 8

## Experimental part

---

UNIVERSITAT ROVIRA I VIRGILI  
COMPLEMENTARY SYNTHESIS OF ORGANOBORANES TO POPULATE THE CHEMICAL  
FUNCTIONALITY TO A GIVEN AREA OF BIOMEDICAL INTEREST  
Jordi Royes Buisan

## 8.1. General considerations

**Solvents and reagents:** Solvents and reagents were obtained from commercial suppliers and dried and/or purified (if needed) by standard procedures, as specified in "Purification of Laboratory Chemicals".<sup>[1]</sup> Tetrahydrofuran was dried by distillation from sodium benzophenone ketyl. All reactions were conducted in oven and flame-dried glassware under an inert atmosphere of argon, using Schlenk-type techniques. *Flash chromatography* was performed on standard silica gel (Merck Kieselgel 60 F254 400-630 mesh). *Thin layer chromatography* was performed on Merck Kieselgel 60 F254 which was developed using standard visualizing agents: UV fluorescence (254 and 366 nm) or potassium permanganate/ $\Delta$ .

**NMR spectra** were recorded at a Varian Goku 400 or a Varian Mercury 400 spectrometer, in the work done at the URV and on Bruker DPX-400 or Bruker AV-500 spectrometers with standard pulse sequences, operating at 400 MHz and 500 MHz respectively, in the work done at Janssen Cilag center.  $^1\text{H}$  NMR and  $^{13}\text{C}\{^1\text{H}\}$  NMR chemical shifts ( $\delta$ ) are reported in ppm with the solvent resonance as the internal standard ( $\text{CHCl}_3$ : 7.26 ppm ( $^1\text{H}$ ) and  $\text{CDCl}_3$ : 77.16 ppm ( $^{13}\text{C}$ )).  $^{11}\text{B}\{^1\text{H}\}$  NMR chemical shifts ( $\delta$ ) are reported in ppm relative to  $(\text{CH}_3)_2\text{O}\cdots\text{BF}_3$ .  $^{29}\text{Si}\{^1\text{H}\}$  NMR chemical shifts ( $\delta$ ) are reported in ppm relative to  $(\text{CH}_3)_4\text{Si}$ . Data are reported as follows: chemical shift, multiplicity (s = singlet, d = doublet, t = triplet, q = quartet, hept = heptuplet, br = broad, m = multiplet), coupling constants (Hz) and integration.

**High resolution mass spectra (HRMS)** were recorded using a 6210 Time of Flight (TOF) mass spectrometer from Agilent Technologies (Waldbronn, Germany) with an ESI interface and it was performed at the Servei de Recursos Científics i Tècnics (Universitat Rovira i Virgili, Tarragona) or using a BIOTOF II Time of Flight (TOF) mass spectrometer from Bruker with an APCI interface or EI interface and it was performed at the Unidade de Espectrometría de Masas e Proteómica (Universidad de Santiago de Compostela, Santiago de Compostela). GC-MS analyses were performed on a HP6890 gas chromatograph and an Agilent Technologies 5973 Mass selective detector (Waldbronn, Germany) equipped with an achiral capillary column HP-5 (30m, 0.25mm i. d., 0.25  $\mu\text{m}$  thickness) using He as the carrier gas.

## 8.2. Experimental procedures and spectral data of Chapter 3

### 8.2.1 General procedure for the insertion of trimethylsilyldiazo methane into pinB-SR $\sigma$ -bonds.

In the glove-box, an oven-dried resealable Teflon screw-cap Schlenk reaction tube equipped with a magnetic stir bar was charged with 2 mmol of RS-Bpin (R = Ph, Tol, Bn). Then, a 2 M solution in hexanes of (trimethylsilyl)diazomethane (1 mmol, 2 equiv) was added dropwise. After stirring in the glove-box for 5 min. the Schlenk tube was sealed and heated at the corresponding temperature (PhS-Bpin at 50 °C, TolS-Bpin and BnS-Bpin at 70 °C) for the appropriated time (PhS-Bpin for 6 h, TolS-Bpin and BnS-Bpin for 16 h). The reaction was cooled down to room temperature and the solvent was evaporated to dryness. The crude residue was analyzed by GC-MS and  $^1\text{H}$  NMR. Then the products were purified by silica gel flash chromatography.

### 8.2.2 General procedure for the deborylative alkylation reaction.

In the glove box, a 7.5 mL screw cap vial equipped with a magnetic stir bar was charged with CH(Bpin)(SiMe<sub>3</sub>)(SR) (0.1 mmol, 1.3 equiv) and NaO<sup>t</sup>Bu (0.31 mmol, 4 equiv). Then, 0.5 mL of THF was incorporated and finally the halogenated reagent was added (0.077 mmol, 1 equiv). The reaction was stirring at room temperature for 3 h and quenched with 2 mL of saturated Na<sub>2</sub>S<sub>2</sub>O<sub>4</sub> and extracted 3 times with 3 mL of Et<sub>2</sub>O. All the organic layers were collected and dried over MgSO<sub>4</sub> and evaporated to dryness. The crude residue was analyzed by GC-MS and yields of products were calculated based on relative integration on the  $^1\text{H}$  NMR compared to an internal standard (1,4-dinitrobenzene or naphthalene). Then, the products were purified by silica gel flash chromatography.

### 8.2.3 General procedure for the deprotonation-alkylation reaction.

In the glove box, an oven-dried resalable Teflon screw-cap Schlenk reaction tube equipped with a magnetic stir bar was charged with LTMP (0.21 mmol, 1.05 equiv) and 0.8 mL of dried THF. The flask was sealed, removed from the glove box and the reaction mixture was cooled to 0 °C. Under Argon, a solution of *gem*-substrates (0.2 mmol, 1 equiv) in THF (0.2 mL) was added via syringe and the mixture was allowed to stir at 0 °C for 10 min. The corresponding electrophile (0.24 mmol, 1.2 equiv) was added dropwise and the reaction was allowed to stir at 0 °C for 15 min. Upon completion, the reaction mixture was warmed to room temperature, filtered through a silica gel plug, rinsed with diethyl ether and dichloromethane, and concentrated *in vacuo*. The crude reaction mixture was purified on silica gel.

#### 8.2.4 General procedure for the deborylative cyclization reaction.

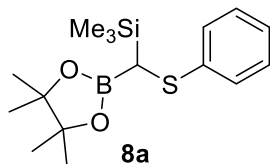
In the glove box, a 7.5 mL screw cap vial equipped with a magnetic stir bar was charged with the corresponding alkylated products (0.2 mmol, 1 equiv) and  $\text{KO}^t\text{Bu}$  (0.8 mmol, 4 equiv). Then 1.0 mL of THF was incorporated. The reaction was stirring at room temperature for 3 h and quenched with 2 mL of saturated  $\text{Na}_2\text{S}_2\text{O}_4$  and extracted 3 times with 3 mL of  $\text{Et}_2\text{O}$ . All the organic layers were collected and dried over  $\text{MgSO}_4$ , filtered and evaporated to dryness. The crude residue was analyzed by GC-MS and yields of cyclized compounds were calculated based on relative integration on the  $^1\text{H}$  NMR compared to an internal standard (1,4-dinitrobenzene). Then, the products were purified by silica gel flash chromatography.

#### 8.2.5 General procedure for the desilylative cyclization reaction.

An oven-dried resalable Teflon screw-cap Schlenk reaction tube equipped with a magnetic stir bar was charged, under Argon, with the corresponding alkylated products (0.2 mmol, 1 equiv). Then, 0.3 mL of THF was incorporated and 4 equiv (0.8 mmol) of a 1M solution of TBAF in THF were added dropwise at 0 °C. The reaction was then stirring for 1 h at 0 °C, followed by another 30 min. of stirring at room temperature. Next, the mixture was quenched with saturated  $\text{NH}_4\text{Cl}$  aq. sat. and passed over a silica gel plug. The crude residue was analyzed by GC-MS and yields of cyclic species were calculated based on relative integration on the  $^1\text{H}$  NMR compared to an internal standard (naphthalene). Then, the product was purified by silica gel flash chromatography.

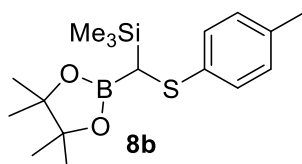
## 8.2.6 Spectral data of Chapter 3

### Trimethyl((phenylthio)(4,4,5,5-tetramethyl-1,3,2-dioxaborolan-2-yl)methyl)silane



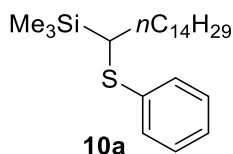
Flash column chromatography (hexane to 20:1 hexane : EtOAc) yielded **8a** (612.1 mg, 94 %) as a white solid.  $^1\text{H}$  NMR ( $\text{CDCl}_3$ , 400 MHz)  $\delta$  7.32–7.29 (m, 2H), 7.24–7.19 (m, 2H), 7.09–7.04 (m, 1H), 1.16 (s, 6H), 1.06 (s, 6H), 0.22 (s, 9H).  $^{13}\text{C}$   $\{^1\text{H}\}$  NMR ( $\text{CDCl}_3$ , 100 MHz)  $\delta$  140.2, 128.6, 126.8, 124.8, 83.9, 24.9, 24.8, -1.2.  $^{11}\text{B}$  NMR (128.3 MHz,  $\text{CDCl}_3$ )  $\delta$  33.4.  $^{29}\text{Si}$  NMR ( $\text{CDCl}_3$ , 80 MHz)  $\delta$  3.0. HRMS (ESI) for  $\text{C}_{16}\text{H}_{28}\text{BO}_2\text{SSi}$   $[\text{M}+\text{H}]^+$ : calculated: 323.1672, found: 323.1680.

### Trimethyl((4,4,5,5-tetramethyl-1,3,2-dioxaborolan-2-yl)(*p*-tolylthio)methyl)silane



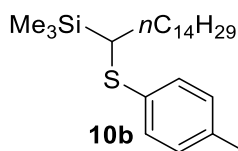
Flash column chromatography (hexane to 20:1 hexane : EtOAc) yielded **8b** (598.7 mg, 89 %) as a white solid.  $^1\text{H}$  NMR ( $\text{CDCl}_3$ , 400 MHz)  $\delta$  7.21 (d,  $J = 8.0$  Hz, 2H), 7.03 (d,  $J = 8.0$  Hz, 2H), 2.27 (s, 3H), 2.18 (s, 1H), 1.15 (s, 6H), 1.07 (s, 6H), 0.21 (s, 9H).  $^{13}\text{C}$   $\{^1\text{H}\}$  NMR ( $\text{CDCl}_3$ , 100 MHz)  $\delta$  136.3, 134.5, 129.1, 127.0, 83.6, 24.7, 24.6, 20.9, -1.4.  $^{11}\text{B}$  NMR (128.3 MHz,  $\text{CDCl}_3$ )  $\delta$  34.3.  $^{29}\text{Si}$  NMR ( $\text{CDCl}_3$ , 80 MHz)  $\delta$  2.8. HRMS (ESI) for  $\text{C}_{17}\text{H}_{30}\text{BO}_2\text{SSi}$   $[\text{M}+\text{H}]^+$ : calculated: 337.1829, found: 337.1828.

### Trimethyl(1-(phenylthio)pentadecyl)silane



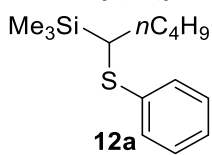
Flash column chromatography (hexane) yielded **10a** (25.5 mg, 65% yield) as a colourless oil.  $^1\text{H}$  NMR ( $\text{CDCl}_3$ , 400 MHz)  $\delta$  7.38–7.33 (m, 2H), 7.29–7.23 (m, 2H), 7.17–7.12 (m, 1H), 2.47 (dd,  $J = 6.9, 5.2$  Hz, 1H), 1.77–1.54 (m, 2H), 1.50–1.36 (m, 2H), 1.34–1.13 (m, 22H), 0.88 (t,  $J = 6.9$  Hz, 3H), 0.13 (s, 9H).  $^{13}\text{C}$   $\{^1\text{H}\}$  NMR ( $\text{CDCl}_3$ , 100 MHz)  $\delta$  138.6, 129.4, 128.8, 125.7, 34.4, 32.1, 31.9, 29.9, 29.8 (3 x C), 29.7, 29.6, 29.5, 28.4, 22.9, 14.3, -1.9.  $^{29}\text{Si}$  NMR ( $\text{CDCl}_3$ , 80 MHz)  $\delta$  4.0.

### Trimethyl(1-(*p*-tolylthio)pentadecyl)silane

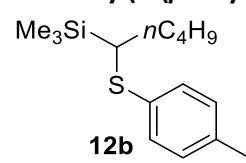


Flash column chromatography (hexane) yielded **10b** (27.6 mg, 68% yield) as a colourless oil.  $^1\text{H}$  NMR ( $\text{CDCl}_3$ , 400 MHz)  $\delta$  7.29–7.24 (m, 2H), 7.10–7.05 (m, 2H), 2.39 (dd,  $J = 6.9, 5.2$  Hz, 1H), 2.31 (s, 3H), 1.74–1.53 (m, 2H), 1.49–1.36 (m, 2H), 1.32–1.14 (m, 22H), 0.88 (t,  $J = 6.9$  Hz, 3H), 0.12 (s, 9H).  $^{13}\text{C}$   $\{^1\text{H}\}$  NMR ( $\text{CDCl}_3$ , 100 MHz)  $\delta$  135.8, 134.8, 130.2, 129.6, 35.2, 32.1, 31.8, 29.8 (4 x C), 29.6, 29.5, 28.4, 22.9, 21.2, 14.3, -1.9.  $^{29}\text{Si}$  NMR ( $\text{CDCl}_3$ , 80 MHz)  $\delta$  3.8. HRMS (APCI)  $\text{C}_{25}\text{H}_{47}\text{SSi}$   $[\text{M}+\text{H}]^+$ : calculated: 407.3162, found: 407.3151.

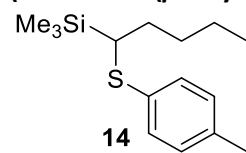
### Trimethyl(1-(phenylthio)pentyl)silane

  
**12a** Flash column chromatography (hexane) yielded **12a** (14.1 mg, 56% yield) as a colourless oil.  $^1\text{H NMR}$  ( $\text{CDCl}_3$ , 400 MHz)  $\delta$  7.37–7.33 (m, 2H), 7.28–7.23 (m, 2H), 7.17–7.11 (m, 1H), 2.47 (dd,  $J = 6.9, 5.2$  Hz, 1H), 1.77–1.56 (m, 2H), 1.47–1.36 (m, 2H), 1.28–1.19 (m, 2H), 0.83 (t,  $J = 7.3$  Hz, 3H), 0.13 (s, 9H).  $^{13}\text{C}$   $\{^1\text{H}\}$  NMR ( $\text{CDCl}_3$ , 100 MHz)  $\delta$  138.6, 129.4, 128.8, 125.6, 34.3, 31.5, 30.6, 22.9, 14.1, -1.9.  $^{29}\text{Si NMR}$  ( $\text{CDCl}_3$ , 80 MHz)  $\delta$  4.0. HRMS (EI)  $\text{C}_{14}\text{H}_{24}\text{SSi}$   $[\text{M}]^+$ : calculated: 252.1368, found: 252.1368.

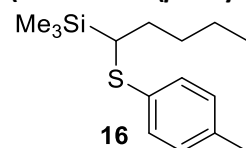
### Trimethyl(1-(*p*-tolylthio)pentyl)silane

  
**12b** Flash column chromatography (hexane) yielded **12b** (21.3 mg, 80% yield) as a colourless oil.  $^1\text{H NMR}$  ( $\text{CDCl}_3$ , 400 MHz)  $\delta$  7.27 (d,  $J = 7.9$  Hz, 2H), 7.07 (d,  $J = 7.9$  Hz, 2H), 2.40 (dd,  $J = 6.9, 5.2$  Hz, 1H), 2.31 (s, 3H), 1.74–1.54 (m, 2H), 1.51–1.32 (m, 2H), 1.30–1.17 (m, 2H), 0.84 (t,  $J = 7.3$  Hz, 3H), 0.12 (s, 9H).  $^{13}\text{C}$   $\{^1\text{H}\}$  NMR ( $\text{CDCl}_3$ , 100 MHz)  $\delta$  135.2, 134.2, 129.6, 129.1, 34.7, 31.0, 30.0, 22.4, 20.6, 13.6, -2.3.  $^{29}\text{Si NMR}$  ( $\text{CDCl}_3$ , 80 MHz)  $\delta$  3.3. HRMS (APCI) for  $\text{C}_{15}\text{H}_{27}\text{SSi}$   $[\text{M}+\text{H}]^+$ : calculated: 267.1594, found: 267.1597.

### (5-Fluoro-1-(*p*-tolylthio)pentyl)trimethylsilane

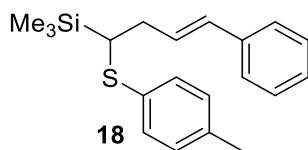
  
**14** Flash column chromatography (hexane) yielded **14** (17.3 mg, 61% yield) as a colourless oil.  $^1\text{H NMR}$  ( $\text{CDCl}_3$ , 400 MHz)  $\delta$  7.27 (d,  $J = 7.9$  Hz, 2H), 7.08 (d,  $J = 7.9$  Hz, 2H), 4.47–4.25 (m, 2H), 2.40 (q,  $J = 5.1$  Hz, 1H), 2.31 (s, 3H), 1.77–1.61 (m, 2H), 1.42 (m, 2H), 1.39–1.27 (m, 2H), 0.13 (s, 9H).  $^{13}\text{C}$   $\{^1\text{H}\}$  NMR ( $\text{CDCl}_3$ , 100 MHz)  $\delta$  135.8, 134.3, 130.1, 129.5, 83.9 (d,  $J = 164.3$  Hz), 35.1, 30.5, 30.4 (d,  $J = 19.5$  Hz), 23.7 (d,  $J = 5.4$  Hz), 21.0, -2.1.  $^{19}\text{F NMR}$  ( $\text{CDCl}_3$ , 377 MHz)  $\delta$  -217.9 (m).  $^{29}\text{Si NMR}$  ( $\text{CDCl}_3$ , 80 MHz)  $\delta$  3.4. HRMS (APCI) for  $\text{C}_{15}\text{H}_{26}\text{FSSi}$   $[\text{M}+\text{H}]^+$ : calculated: 285.1509, found: 285.1494.

### (5-Chloro-1-(*p*-tolylthio)pentyl)trimethylsilane

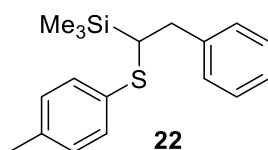
  
**16** Flash column chromatography (hexane) yielded **16** (26.1 mg, 87 % yield) as a colourless oil.  $^1\text{H NMR}$  ( $\text{CDCl}_3$ , 400 MHz)  $\delta$  7.27 (dd,  $J = 8.3, 2.1$  Hz, 2H), 7.13–7.04 (d, 2H), 3.49–3.41 (m, 2H), 2.41 (t,  $J = 5.6$  Hz, 1H), 2.32 (s, 3H), 1.76–1.65 (m, 4H), 1.64–1.52 (m, 2H), 0.17–0.09 (s, 9H).  $^{13}\text{C}$   $\{^1\text{H}\}$  NMR ( $\text{CDCl}_3$ , 100 MHz)  $\delta$  135.9, 134.2, 130.2, 129.5, 44.7, 35.0, 32.6, 30.9, 25.3, 21.0, -2.1.  $^{29}\text{Si NMR}$  ( $\text{CDCl}_3$ , 80 MHz)  $\delta$  3.9. HRMS (EI) for  $\text{C}_{15}\text{H}_{25}\text{ClSi}$   $[\text{M}]^+$ : calculated: 300.1135, found: 300.1133.



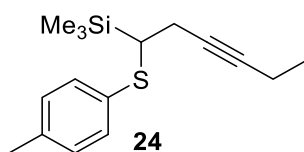
## Experimental part

**Trimethyl(4-phenyl-1-(*p*-tolylthio)but-3-en-1-yl)silane**

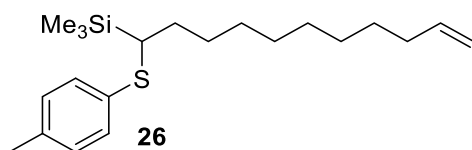
Flash column chromatography (hexane) yielded **18** (26.1 mg, 80% yield) as a colourless oil.  $^1\text{H NMR}$  ( $\text{CDCl}_3$ , **400 MHz**)  $\delta$  7.32–7.28 (m, 2H), 7.27 (q,  $J = 1.6$  Hz, 1H), 7.26–7.24 (m, 2H), 7.23 (t,  $J = 1.6$  Hz, 1H), 7.21–7.15 (m, 1H), 7.10–7.04 (m, 2H), 6.36 (d,  $J = 16.0$  Hz, 1H), 6.28–6.19 (m, 1H), 2.65–2.60 (m, 2H), 2.57–2.49 (m, 1H), 2.31 (s, 3H), 0.16 (s, 9H).  $^{13}\text{C}$   $\{^1\text{H}\}$  **NMR** ( $\text{CDCl}_3$ , **100 MHz**)  $\delta$  137.9, 137.3, 134.7, 130.5, 130.2, 128.9, 128.3, 126.6, 125.9, 25.4, 24.7, 21.0, -1.6.  $^{29}\text{Si NMR}$  ( $\text{CDCl}_3$ , **80 MHz**)  $\delta$  4.4. **HRMS (EI) for  $\text{C}_{20}\text{H}_{26}\text{SSi}$   $[\text{M}]^+$** : calculated: 326.1525, found: 326.1513.

**Trimethyl(2-phenyl-1-(*p*-tolylthio)ethyl)silane**

Flash column chromatography (hexane) yielded **22** (23.7 mg, 79% yield) as a colourless oil.  $^1\text{H NMR}$  ( $\text{CDCl}_3$ , **400 MHz**)  $\delta$  7.25–7.08 (m, 7H), 7.02–6.97 (m, 2H), 3.06–2.82 (m, 2H), 2.70–2.61 (m, 1H), 2.28 (s, 3H), 0.05–0.02 (m, 9H).  $^{13}\text{C}$   $\{^1\text{H}\}$  **NMR** ( $\text{CDCl}_3$ , **100 MHz**)  $\delta$  140.8, 135.9, 133.7, 130.6, 129.4, 129.2, 128.0, 126.0, 38.0, 37.4, 20.9, -2.2.  $^{29}\text{Si NMR}$  ( $\text{CDCl}_3$ , **80 MHz**)  $\delta$  6.5. **HRMS (APCI) for  $\text{C}_{18}\text{H}_{25}\text{SSi}$   $[\text{M}+\text{H}]^+$** : calculated: 301.1441, found: 301.1441.

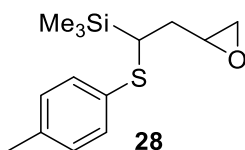
**Trimethyl(1-(*p*-tolylthio)hex-3-yn-1-yl)silane**

Flash column chromatography (hexane) yielded **24** (16.5 mg, 60% yield) as a colourless oil.  $^1\text{H NMR}$  ( $\text{CDCl}_3$ , **400 MHz**)  $\delta$  7.32–7.28 (m, 2H), 7.09 (d,  $J = 7.9$  Hz, 2H), 2.64–2.38 (m, 3H), 2.31 (s, 3H), 2.22–2.06 (m, 2H), 1.09 (t,  $J = 7.5$  Hz, 3H), 0.22–0.19 (m, 9H).  $^{13}\text{C}$   $\{^1\text{H}\}$  **NMR** ( $\text{CDCl}_3$ , **100 MHz**)  $\delta$  136.2, 134.9, 130.5, 129.5, 34.57, 30.2, 21.4, 21.2, 14.4, 12.9, -1.9.  $^{29}\text{Si NMR}$  ( $\text{CDCl}_3$ , **80 MHz**)  $\delta$  5.0. **HRMS (EI) for  $\text{C}_{16}\text{H}_{24}\text{SSi}$   $[\text{M}]^+$** : calculated: 276.1368, found: 276.1372.

**Trimethyl(1-(*p*-tolylthio)undec-10-en-1-yl)silane**

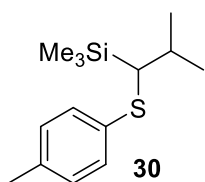
Flash column chromatography (hexane) yielded **26** (25.1 mg, 72% yield) as a colourless oil.  $^1\text{H NMR}$  ( $\text{CDCl}_3$ , **400 MHz**)  $\delta$  7.26 (dd,  $J = 4.3, 3.9$  Hz, 2H), 7.07 (d,  $J = 8.3$  Hz, 2H), 5.81 (ddt,  $J = 16.9, 10.1, 6.7$  Hz, 1H), 5.06–4.95 (m, 1H), 4.95–4.88 (m, 1H), 2.39 (dd,  $J = 6.9, 5.1$  Hz, 1H), 2.31 (s, 3H), 2.02 (dd,  $J = 14.0, 6.6$  Hz, 2H), 1.28–1.18 (m, 12H), 0.14–0.11 (m, 9H).  $^{13}\text{C}$   $\{^1\text{H}\}$  **NMR** ( $\text{CDCl}_3$ , **100 MHz**)  $\delta$  139.2, 135.6, 134.6, 130.0, 129.3, 114.0, 35.0, 33.8, 31.6, 29.6, 29.4, 29.0, 28.8, 28.1, 22.6, 14.1, -2.0.  $^{29}\text{Si NMR}$  ( $\text{CDCl}_3$ , **80 MHz**)  $\delta$  3.8. **HRMS (EI) for  $\text{C}_{18}\text{H}_{25}\text{SSi}$   $[\text{M}]^+$** : calculated: 348.2307, found: 348.2312.

### Trimethyl(2-(oxiran-2-yl)-1-(*p*-tolylthio)ethyl)silane



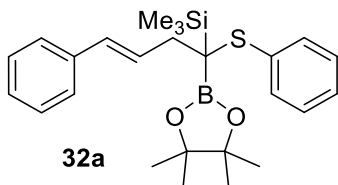
Flash column chromatography (hexane) yielded **28** (11.1 mg, 42% yield) as a colourless oil.  $^1\text{H NMR}$  ( $\text{CDCl}_3$ , 400 MHz)  $\delta$  7.29–7.26 (m, 2H), 7.21 (d,  $J$  = 8.2 Hz, 2H), 7.09 (d,  $J$  = 7.9 Hz, 2H), 7.03 (d,  $J$  = 7.8 Hz, 2H), 3.09 (m, 1H), 2.68 (m, 1H), 2.65–2.53 (m, 1H), 2.41 (dd,  $J$  = 5.0, 2.7 Hz, 1H), 2.31 (s, 3H), 2.27 (s, 3H), 1.95–1.80 (m, 4H), 0.21 (s, 9H), 0.19 (d,  $J$  = 3.3 Hz, 9H).  $^{13}\text{C}$   $\{^1\text{H}\}$  NMR ( $\text{CDCl}_3$ , 100 MHz)  $\delta$  136.1, 133.7, 130.0, 129.6, 129.1, 127.1, 50.8, 47.6, 34.5, 32.3, 31.4, 30.9, 29.7, 24.7, 24.6, 21.0, -1.3, -2.2.  $^{29}\text{Si NMR}$  ( $\text{CDCl}_3$ , 80 MHz)  $\delta$  4.4, 2.8. HRMS (EI) for  $\text{C}_{14}\text{H}_{22}\text{OSSi}$   $[\text{M}]^+$ : calculated: 266.1161, found: 266.1161.

### Trimethyl(2-methyl-1-(*p*-tolylthio)propyl)silane



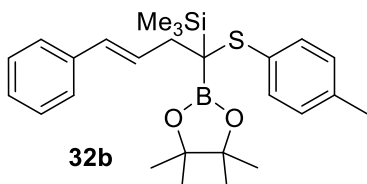
Flash column chromatography (hexane) yielded **30** (16.9 mg, 67% yield) as a colourless oil.  $^1\text{H NMR}$  ( $\text{CDCl}_3$ , 400 MHz)  $\delta$  7.27 (q,  $J$  = 2.2 Hz, 2H), 7.05 (dd,  $J$  = 11.4, 3.5 Hz, 2H), 2.45 (d,  $J$  = 3.5 Hz, 1H), 2.30 (s, 3H), 2.17–2.07 (m, 1H), 0.99 (dd,  $J$  = 6.8, 5.0 Hz, 6H), 0.18–0.15 (m, 9H).  $^{13}\text{C}$   $\{^1\text{H}\}$  NMR ( $\text{CDCl}_3$ , 100 MHz)  $\delta$  136.0, 135.4, 129.6, 129.4, 43.6, 31.2, 22.0, 20.9, -0.8.  $^{29}\text{Si NMR}$  ( $\text{CDCl}_3$ , 80 MHz)  $\delta$  2.4. HRMS (EI) for  $\text{C}_{14}\text{H}_{24}\text{SSi}$   $[\text{M}]^+$ : calculated: 252.1368, found: 252.1370.

### *E*-trimethyl(4-phenyl-1-(phenylthio)-1-(4,4,5,5-tetramethyl-1,3,2-dioxaborolan-2-yl)but-3-en-1-yl)silane



Flash column chromatography (50:1 hexane : EtOAc) yielded **32a** (61.3 mg, 70 % yield) as a colourless oil.  $^1\text{H NMR}$  ( $\text{CDCl}_3$ , 400 MHz)  $\delta$  7.58–7.53 (m, 2H), 7.31–7.25 (m, 4H), 7.22–7.16 (m, 4H), 6.57–6.40 (m, 2H), 2.89–2.72 (m, 2H), 1.19 (s, 6H), 1.17 (s, 6H), 0.20 (s, 9H).  $^{13}\text{C}$   $\{^1\text{H}\}$  NMR ( $\text{CDCl}_3$ , 100 MHz)  $\delta$  138.0, 136.0, 133.8, 130.8, 130.2, 128.5, 128.3, 127.0, 126.8, 126.1, 83.8, 37.2, 25.5, 24.9, -1.5.  $^{11}\text{B NMR}$  (128.3 MHz,  $\text{CDCl}_3$ )  $\delta$  33.9.  $^{29}\text{Si NMR}$  ( $\text{CDCl}_3$ , 80 MHz)  $\delta$  6.1. HRMS (ESI) for  $\text{C}_{25}\text{H}_{35}\text{BNaO}_2\text{SSi}$   $[\text{M}+\text{Na}]^+$ : calculated: 438.2334, found: 438.2336.

### *E*-trimethyl(4-phenyl-1-(4,4,5,5-tetramethyl-1,3,2-dioxaborolan-2-yl)-1-(*p*-tolylthio)but-3-en-1-yl)silane

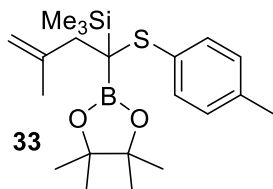


Flash column chromatography (50:1 hexane : EtOAc) yielded **32b** (66.0 mg, 73 % yield) as a colourless oil.  $^1\text{H NMR}$  ( $\text{CDCl}_3$ , 400 MHz)  $\delta$  7.50–7.46 (m, 2H), 7.31–7.26 (m, 4H), 7.22–7.15 (m, 1H), 7.04–6.98 (m, 2H), 2.82–2.67 (m, 2H), 2.28 (s, 3H), 1.20 (s, 6H), 1.19 (s, 6H), 0.18 (s, 9H).  $^{13}\text{C}$   $\{^1\text{H}\}$  NMR ( $\text{CDCl}_3$ , 100 MHz)  $\delta$  138.0, 137.4, 134.9, 131.8, 130.7, 130.4, 129.1, 128.5, 126.8, 126.0, 83.8, 37.3, 25.5, 24.9, 21.2, -1.5.  $^{11}\text{B NMR}$  (128.3 MHz,  $\text{CDCl}_3$ )  $\delta$  33.9.  $^{29}\text{Si NMR}$

## Experimental part

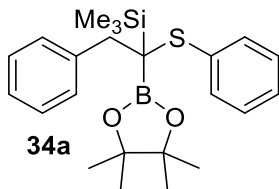
(CDCl<sub>3</sub>, 80 MHz) δ 5.9. HRMS (ESI) for C<sub>26</sub>H<sub>37</sub>BNaO<sub>2</sub>SSi [M+Na]<sup>+</sup>: calculated: 475.2270, found: 475.2274.

**Trimethyl(3-methyl-1-(4,4,5,5-tetramethyl-1,3,2-dioxaborolan-2-yl)-1-(*p*-tolylthio)but-3-en-1-yl)silane**



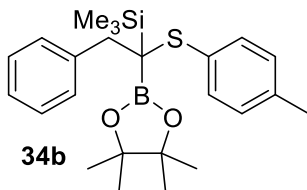
Flash column chromatography (hexane to 500:1 hexane : EtOAc) yielded **33** (40.6 mg, 52% yield) as a yellow sticky oil. <sup>1</sup>H NMR (CDCl<sub>3</sub>, 400 MHz) δ 7.51–7.45 (m, 2H), 7.01 (d, *J* = 7.9 Hz, 2H), 5.01 (s, 1H), 4.87 (s, 1H), 2.64 (d, *J* = 14.9 Hz, 1H), 2.49–2.33 (m, 1H), 2.30 (s, 3H), 1.73 (s, 3H), 1.23 (s, 6H), 1.21 (s, 6H), 0.12–0.07 (m, 9H). <sup>13</sup>C {<sup>1</sup>H} NMR (CDCl<sub>3</sub>, 100 MHz) δ 144.9, 137.3, 135.4, 131.2, 128.7, 114.0, 83.6, 40.2, 25.1, 24.0, 21.1, -1.7. <sup>11</sup>B NMR (CDCl<sub>3</sub>, 128.3 MHz) δ 33.2. <sup>29</sup>Si NMR (CDCl<sub>3</sub>, 80 MHz) δ 6.1. HRMS (ESI) for C<sub>42</sub>H<sub>70</sub>B<sub>2</sub>NaO<sub>4</sub>S<sub>2</sub>Si<sub>2</sub> [2M+Na]<sup>+</sup>: calculated: 803.4344, found: 803.4338.

**Trimethyl(2-phenyl-1-(phenylthio)-1-(4,4,5,5-tetramethyl-1,3,2-dioxaborolan-2-yl)ethyl)silane**



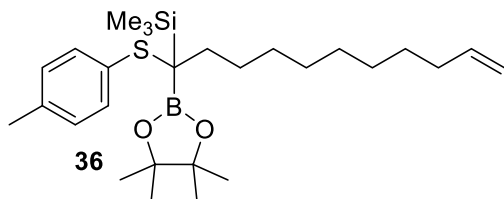
Flash column chromatography (hexane to 500:1 hexane : EtOAc) yielded **34a** (34.6 mg, 42% yield) as a colourless oil. <sup>1</sup>H NMR (CDCl<sub>3</sub>, 400 MHz) δ 7.53–7.49 (m, 3H), 7.22–7.12 (m, 2H), 7.02–6.93 (m, 3H), 6.87–6.80 (m, 2H), 3.38 (d, *J* = 13.6 Hz, 1H), 2.92 (d, *J* = 13.6 Hz, 1H), 1.18 (s, 6H), 1.09 (s, 6H), 0.16 (s, 9H). <sup>13</sup>C {<sup>1</sup>H} NMR (CDCl<sub>3</sub>, 100 MHz) δ 141.1, 137.3, 131.2, 131.1, 127.8, 127.8, 126.3, 125.6, 83.9, 38.8, 25.4, 25.1, -1.9. <sup>11</sup>B NMR (128.3 MHz, CDCl<sub>3</sub>) δ 32.8. <sup>29</sup>Si NMR (CDCl<sub>3</sub>, 80 MHz) δ 6.2. HRMS (ESI) for C<sub>23</sub>H<sub>33</sub>BNaO<sub>2</sub>SSi [M+Na]<sup>+</sup>: calculated: 435.1961, found: 435.1957.

**Trimethyl(2-phenyl-1-(4,4,5,5-tetramethyl-1,3,2-dioxaborolan-2-yl)-1-(*p*-tolylthio)ethyl)silane**



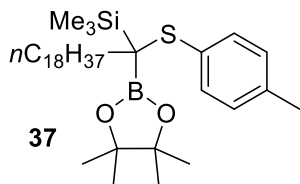
Flash column chromatography (hexane to 500:1 hexane : EtOAc) yielded **34b** (31.5 mg, 37% yield) as a yellow sticky oil. <sup>1</sup>H NMR (CDCl<sub>3</sub>, 400 MHz) δ 7.55–7.48 (m, 2H), 7.27–7.14 (m, 4H), 6.84 (t, *J* = 3.6 Hz, 3H), 3.32 (d, *J* = 13.8 Hz, 1H), 2.94 (d, *J* = 13.8 Hz, 1H), 2.22 (s, 3H), 1.17 (s, 6H), 1.10 (s, 6H), 0.13 (s, 9H). <sup>13</sup>C {<sup>1</sup>H} NMR (CDCl<sub>3</sub>, 100 MHz) δ 141.0, 135.9, 132.8, 132.4, 131.0, 128.5, 126.0, 83.6, 38.5, 25.1, 24.8, 20. -2.0. <sup>11</sup>B NMR (CDCl<sub>3</sub>, 128.3 MHz) δ 33.8. <sup>29</sup>Si NMR (CDCl<sub>3</sub>, 80 MHz) δ 5.88. HRMS (ESI) for C<sub>24</sub>H<sub>35</sub>BNaO<sub>2</sub>SSi [M+Na]<sup>+</sup>: calculated: 449.2117, found: 449.2119.

**Trimethyl(1-(4,4,5,5-tetramethyl-1,3,2-dioxaborolan-2-yl)-1-(*p*-tolylthio)undec-10-en-1-yl)silane**



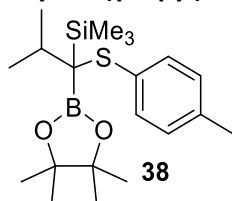
Flash column chromatography (hexane to 500:1 hexane : EtOAc) yielded **36** (28.4 mg, 30% yield) as a colourless oil.  $^1\text{H NMR}$  ( $\text{CDCl}_3$ , 400 MHz)  $\delta$  7.40 (d,  $J = 8.1$  Hz, 2H), 7.03 (d,  $J = 7.9$  Hz, 2H), 5.82 (ddt,  $J = 16.9, 10.2, 6.6$  Hz, 1H), 5.04–4.96 (m, 1H), 4.95–4.90 (m, 1H), 2.30 (s, 3H), 2.04 (dd,  $J = 14.5, 6.9$  Hz, 2H), 1.87–1.65 (m, 2H), 1.39–1.31 (m, 2H), 1.27–1.22 (m, 10H), 1.19 (s, 12H), 0.10 (s, 9H).  $^{13}\text{C}$   $\{^1\text{H}\}$  NMR ( $\text{CDCl}_3$ , 100 MHz)  $\delta$  139.2, 137.2, 134.4, 132.2, 128.9, 114.0, 83.5, 33.8, 32.9, 30.3, 29.5, 29.4, 29.1, 28.9, 27.4, 25.2, 24.8, 21.1, -1.4.  $^{11}\text{B NMR}$  ( $\text{CDCl}_3$ , 128.3 MHz)  $\delta$  30.6.  $^{29}\text{Si NMR}$  ( $\text{CDCl}_3$ , 80 MHz)  $\delta$  5.8. HRMS (ESI) for  $\text{C}_{54}\text{H}_{94}\text{B}_2\text{NaO}_4\text{S}_2\text{Si}_2$   $[\text{2M}+\text{Na}]^+$ : calculated: 971.6215, found: 971.6220.

**Trimethyl(1-(4,4,5,5-tetramethyl-1,3,2-dioxaborolan-2-yl)-1-(*p*-tolylthio)nonadecyl)silane**



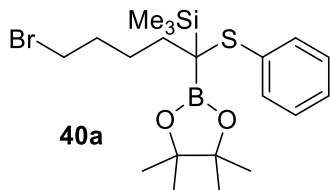
Flash column chromatography (hexane to 500:1 hexane : EtOAc) yielded **37** (43.4 mg, 36% yield) as a colourless oil.  $^1\text{H NMR}$  ( $\text{CDCl}_3$ , 400 MHz)  $\delta$  7.43–7.38 (m, 2H), 7.06–7.01 (m, 2H), 2.29 (d,  $J = 10.0$  Hz, 3H), 1.64–1.52 (m, 2H), 1.25 (s, 32H), 1.19 (s, 12H), 0.88 (t,  $J = 6.9$  Hz, 3H), 0.10 (s, 9H).  $^{13}\text{C}$   $\{^1\text{H}\}$  NMR ( $\text{CDCl}_3$ , 100 MHz)  $\delta$  137.0, 134.4, 132.1, 128.9, 83.5, 32.9, 31.9, 30.3, 29.7, 29.6, 29.3, 27.4, 25.2, 24.8, 22.6, 21.1, 14.1, -1.4.  $^{11}\text{B NMR}$  ( $\text{CDCl}_3$ , 128.3 MHz)  $\delta$  35.0.  $^{29}\text{Si NMR}$  ( $\text{CDCl}_3$ , 80 MHz)  $\delta$  4.9. HRMS (ESI) for  $\text{C}_{35}\text{H}_{65}\text{BNaO}_2\text{SSi}$   $[\text{M}+\text{Na}]^+$ : calculated: 611.4483, found: 611.4465.

**Trimethyl(2-methyl-1-(4,4,5,5-tetramethyl-1,3,2-dioxaborolan-2-yl)-1-(*p*-tolylthio)propyl)silane**

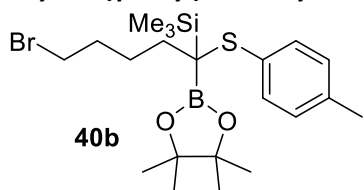


Flash column chromatography (hexane to 500:1 hexane : EtOAc) yielded **38** (32.5 mg, 43% yield) as a colourless oil.  $^1\text{H NMR}$  ( $\text{CDCl}_3$ , 400 MHz)  $\delta$  7.59–7.51 (m, 2H), 7.01 (d,  $J = 7.9$  Hz, 2H), 2.30 (s, 3H), 1.25 (m, 1H), 1.21 (d,  $J = 6.8$  Hz, 3H), 1.20 (s, 6H), 1.17 (s, 6H), 1.04 (d,  $J = 6.8$  Hz, 3H), 0.17 (s, 9H).  $^{13}\text{C}$   $\{^1\text{H}\}$  NMR ( $\text{CDCl}_3$ , 100 MHz)  $\delta$  137.1, 135.5, 132.7, 128.6, 83.3, 32.6, 25.1, 25.0, 22.9, 21.1, 21.0, 0.3.  $^{11}\text{B NMR}$  ( $\text{CDCl}_3$ , 128.3 MHz)  $\delta$  33.6.  $^{29}\text{Si NMR}$  ( $\text{CDCl}_3$ , 80 MHz)  $\delta$  4.0. HRMS (ESI) for  $\text{C}_{20}\text{H}_{35}\text{BNaO}_2\text{SSi}$   $[\text{M}+\text{Na}]^+$ : calculated: 401.2127, found: 401.2117.

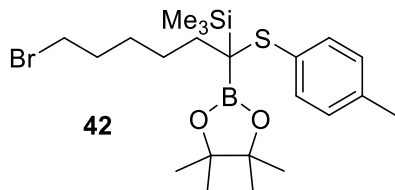
## Experimental part

**(5-bromo-1-(phenylthio)-1-(4,4,5,5-tetramethyl-1,3,2-dioxaborolan-2-yl)pentyl)trimethylsilane**

Flash column chromatography (hexane to 500:1 hexane : EtOAc) yielded **40a** (58.5 mg, 64% yield) as a pale yellow sticky oil.  $^1\text{H NMR}$  ( $\text{CDCl}_3$ , 400 MHz)  $\delta$  7.49 (m, 2H), 7.21 (m, 3H), 3.39 (t,  $J = 6.7$  Hz, 2H), 2.01–1.63 (m, 6H), 1.18 (s, 6H), 1.17 (s, 6H), 0.14 (s, 9H).  $^{13}\text{C}$   $\{^1\text{H}\}$  NMR ( $\text{CDCl}_3$ , 100 MHz)  $\delta$  136.1, 133.4, 128.2, 126.9, 83.7, 34.3, 32.1, 28.6, 25.3, 24.8, 7.2, -1.5.  $^{11}\text{B NMR}$  ( $\text{CDCl}_3$ , 128.3 MHz)  $\delta$  33.9.  $^{29}\text{Si NMR}$  ( $\text{CDCl}_3$ , 80 MHz)  $\delta$  5.4. HRMS (APCI) for  $\text{C}_{20}\text{H}_{35}\text{BBro}_2\text{SSi}$  [ $\text{M}+\text{H}$ ] $^+$ : calculated: 457.1402, found: 457.1399.

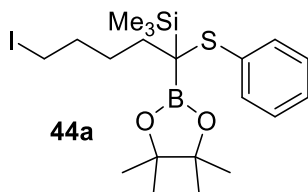
**(5-bromo-1-(4,4,5,5-tetramethyl-1,3,2-dioxaborolan-2-yl)-1-(p-tolylthio)pentyl)trimethylsilane**

Flash column chromatography (hexane to 500:1 hexane : EtOAc) yielded **40b** (61.2 mg, 65% yield) as a pale yellow sticky oil.  $^1\text{H NMR}$  ( $\text{CDCl}_3$ , 400 MHz)  $\delta$  7.41 (dd,  $J = 8.4, 1.9$  Hz, 2H), 7.05 (t,  $J = 9.3$  Hz, 2H), 3.40 (t,  $J = 6.8$  Hz, 2H), 2.30 (s, 3H), 1.91–1.64 (m, 6H), 1.19 (s, 6H), 1.18 (s, 6H), 0.12 (s, 9H).  $^{13}\text{C}$   $\{^1\text{H}\}$  NMR ( $\text{CDCl}_3$ , 100 MHz)  $\delta$  137.2, 134.4, 131.7, 129.0, 83.6, 33.5, 33.5, 32.1, 26.1, 25.2, 24.7, 21.0, -1.5.  $^{11}\text{B NMR}$  ( $\text{CDCl}_3$ , 128.3 MHz)  $\delta$  34.4.  $^{29}\text{Si NMR}$  ( $\text{CDCl}_3$ , 80 MHz)  $\delta$  5.2. HRMS (APCI) for  $\text{C}_{21}\text{H}_{37}\text{BBro}_2\text{SSi}$  [ $\text{M}+\text{H}$ ] $^+$ : calculated: 471.1559, found: 471.1559.

**(6-bromo-1-(4,4,5,5-tetramethyl-1,3,2-dioxaborolan-2-yl)-1-(p-tolylthio)hexyl)trimethylsilane**

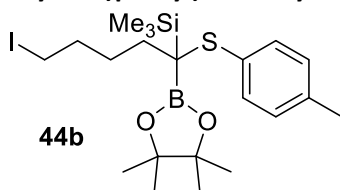
Flash column chromatography (hexane to 500:1 hexane : EtOAc) yielded **42** (69.8 mg, 72% yield) as a yellow sticky oil.  $^1\text{H NMR}$  ( $\text{CDCl}_3$ , 400 MHz)  $\delta$  7.40 (d,  $J = 7.6$  Hz, 2H), 7.04 (d,  $J = 7.6$  Hz, 2H), 3.39 (t,  $J = 6.9$  Hz, 2H), 2.30 (s, 3H), 1.94–1.52 (m, 6H), 1.48–1.36 (m, 2H), 1.19 (s, 6H), 1.18 (s, 6H), 0.16 (s, 9H).  $^{13}\text{C}$   $\{^1\text{H}\}$  NMR ( $\text{CDCl}_3$ , 100 MHz)  $\delta$  137.1, 134.3, 131.8, 128.9, 83.5, 33.9, 32.7, 32.6, 28.6, 26.4, 25.2, 24.7, 21.1, -1.5.  $^{11}\text{B NMR}$  ( $\text{CDCl}_3$ , 128.3 MHz)  $\delta$  34.3.  $^{29}\text{Si NMR}$  ( $\text{CDCl}_3$ , 80 MHz)  $\delta$  5.1. HRMS (APCI) for  $\text{C}_{22}\text{H}_{39}\text{BBro}_2\text{SSi}$  [ $\text{M}+\text{H}$ ] $^+$ : calculated: 485.1715, found: 485.1714.

**5-iodo-1-(phenylthio)-1-(4,4,5,5-tetramethyl-1,3,2-dioxaborolan-2-yl)pentyl)trimethylsilane**



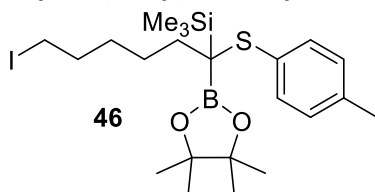
Flash column chromatography (hexane to 500:1 hexane : EtOAc) yielded **44a** (67.5 mg, 67% yield) as a yellow sticky oil.  $^1\text{H NMR}$  ( $\text{CDCl}_3$ , 400 MHz)  $\delta$  7.49 (m, 2H), 7.25–7.17 (m, 3H), 3.18 (t,  $J = 7.0$  Hz, 2H), 1.93–1.68 (m, 6H), 1.19 (s, 6H), 1.18 (s, 6H), 0.14 (s, 9H).  $^{13}\text{C}$   $\{^1\text{H}\}$  NMR ( $\text{CDCl}_3$ , 100 MHz)  $\delta$  136.1, 133.4, 128.2, 126.9, 83.7, 34.3, 32.1, 28.6, 25.3, 24.8, 7.2, -1.5.  $^{11}\text{B NMR}$  ( $\text{CDCl}_3$ , 128.3 MHz)  $\delta$  34.6.  $^{29}\text{Si NMR}$  ( $\text{CDCl}_3$ , 80 MHz)  $\delta$  5.5. HRMS (ESI) for  $\text{C}_{20}\text{H}_{34}\text{BINO}_2\text{SSi}$  [ $\text{M}+\text{Na}$ ] $^+$ : calculated: 527.1084, found: 527.1087.

**(5-iodo-1-(4,4,5,5-tetramethyl-1,3,2-dioxaborolan-2-yl)-1-(*p*-tolylthio)pentyl)trimethylsilane**



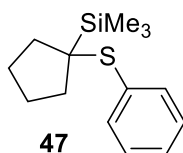
Flash column chromatography (hexane to 500:1 hexane : EtOAc) yielded **44b** (64.2 mg, 62% yield) as a yellow sticky oil.  $^1\text{H NMR}$  ( $\text{CDCl}_3$ , 400 MHz)  $\delta$  7.41 (d,  $J = 8.1$  Hz, 2H), 7.04 (d,  $J = 8.3$  Hz, 2H), 3.18 (t,  $J = 7.0$  Hz, 2H), 2.30 (s, 3H), 1.88–1.62 (m, 6H), 1.19 (s, 6H), 1.18 (s, 6H), 0.12 (s, 9H).  $^{13}\text{C}$   $\{^1\text{H}\}$  NMR ( $\text{CDCl}_3$ , 100 MHz)  $\delta$  137.2, 134.4, 131.7, 128.9, 83.5, 34.2, 31.9, 28.5, 25.2, 24.7, 21.0, 7.2, -1.5.  $^{11}\text{B NMR}$  ( $\text{CDCl}_3$ , 128.3 MHz)  $\delta$  34.8.  $^{29}\text{Si NMR}$  ( $\text{CDCl}_3$ , 80 MHz)  $\delta$  5.1. HRMS (APCI) for  $\text{C}_{21}\text{H}_{37}\text{BIO}_2\text{SSi}$  [ $\text{M}+\text{H}$ ] $^+$ : calculated: 519.1420, found: 519.1416.

**(6-iodo-1-(4,4,5,5-tetramethyl-1,3,2-dioxaborolan-2-yl)-1-(*p*-tolylthio)hexyl)trimethylsilane**



Flash column chromatography (hexane to 500:1 hexane : EtOAc) yielded **46** (75.6 mg, 71% yield) as a yellow sticky oil.  $^1\text{H NMR}$  ( $\text{CDCl}_3$ , 400 MHz)  $\delta$  7.40 (d,  $J = 8.1$  Hz, 2H), 7.04 (d,  $J = 7.9$  Hz, 2H), 3.17 (t,  $J = 7.1$  Hz, 2H), 2.30 (s, 3H), 1.87–1.51 (m, 6H), 1.44–1.32 (m, 2H), 1.19 (s, 6H), 1.18 (s, 6H), 0.15–0.07 (s, 9H).  $^{13}\text{C}$   $\{^1\text{H}\}$  NMR ( $\text{CDCl}_3$ , 100 MHz)  $\delta$  137.1, 134.3, 131.9, 128.9, 83.5, 33.3, 32.7, 31.0, 26.2, 25.2, 24.78, 21.09, 7.33, -1.55.  $^{11}\text{B NMR}$  ( $\text{CDCl}_3$ , 128.3 MHz)  $\delta$  34.4.  $^{29}\text{Si NMR}$  ( $\text{CDCl}_3$ , 80 MHz)  $\delta$  5.1. HRMS (APCI) for  $\text{C}_{22}\text{H}_{39}\text{BIO}_2\text{SSi}$  [ $\text{M}+\text{H}$ ] $^+$ : calculated: 533.1577, found: 533.1579.

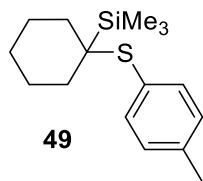
**Trimethyl(1-(phenylthio)cyclopentyl)silane**



Flash column chromatography (hexane) yielded **47** (29.0 mg, 58% yield) as a colourless oil.  $^1\text{H NMR}$  ( $\text{CDCl}_3$ , 400 MHz)  $\delta$  7.58–7.54 (m, 2H), 7.34–7.30 (m, 2H), 7.29–7.26 (m, 1H), 1.90–1.81 (m, 4H), 1.59–1.44 (m, 4H), 0.04 (s, 9H).  $^{13}\text{C}$   $\{^1\text{H}\}$  NMR ( $\text{CDCl}_3$ , 100 MHz)  $\delta$

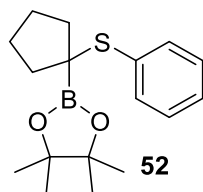
## Experimental part

137.1, 134.0, 128.4, 128.3, 45.7, 35.8, 25.8, -2.8.  $^{29}\text{Si}$  NMR ( $\text{CDCl}_3$ , 80 MHz)  $\delta$  6.7. HRMS (APCI) for  $\text{C}_{14}\text{H}_{23}\text{SSi}$  [ $\text{M}+\text{H}$ ] $^+$ : calculated: 251.1284, found: 251.1284.

**Trimethyl(1-(*p*-tolylthio)cyclohexyl)silane**

Flash column chromatography (hexane) yielded **49** (36.2 mg, 65% yield) as a colourless oil.  $^1\text{H}$  NMR ( $\text{CDCl}_3$ , 400 MHz)  $\delta$  7.41 (d,  $J = 8.0$  Hz, 2H), 7.06 (d,  $J = 8.0$  Hz, 2H), 2.33 (s, 3H), 2.06–1.89 (m, 2H), 1.73–1.66 (m, 4H), 1.48–1.42 (m, 2H), 1.29 (m, 2H), -0.10 (s, 9H).  $^{13}\text{C}$  { $^1\text{H}$ } NMR ( $\text{CDCl}_3$ , 100 MHz)  $\delta$  138.2, 136.9, 130.1, 129.1, 41.9, 31.4, 26.2, 21.2, 21.1, -2.8.  $^{29}\text{Si}$  NMR ( $\text{CDCl}_3$ , 80 MHz)  $\delta$  6.7.

HRMS (APCI) for  $\text{C}_{16}\text{H}_{27}\text{SSi}$  [ $\text{M}+\text{H}$ ] $^+$ : calculated: 279.1597, found: 279.1600.

**4,4,5,5-tetramethyl-2-(1-(phenylthio)cyclopentyl)-1,3,2-dioxaborolane**

Flash column chromatography (hexane to 200:1 hexane : EtOAc) yielded **52** (15.2 mg, 25% yield) as a colourless oil.  $^1\text{H}$  NMR ( $\text{CDCl}_3$ , 400 MHz)  $\delta$  7.45 (m, 2H), 7.26–7.21 (m, 2H), 7.19 (m, 1H), 2.16–2.04 (m, 2H), 1.90–1.75 (m, 4H), 1.62 (m, 2H), 1.15 (s, 12H).  $^{13}\text{C}$  { $^1\text{H}$ } NMR ( $\text{CDCl}_3$ , 100 MHz)  $\delta$  136.2, 131.9, 128.3, 126.4, 83.8, 36.4, 29.6, 24.8, 24.5.  $^{11}\text{B}$  NMR ( $\text{CDCl}_3$ , 128.3 MHz)  $\delta$  33.8.

HRMS (EI) for  $\text{C}_{17}\text{H}_{25}\text{BO}_2\text{S}$  [ $\text{M}$ ] $^+$ : calculated: 304.1668, found: 304.1667.

## 8.3. Experimental procedures and spectral data of Chapter 4

### 8.3.1 General procedure for the protection of amines with sulphonyl chloride derivatives<sup>[2]</sup>

*N,N*-diisopropyletilamina (DIPEA, 2 equiv, 20 mmol) and the arenesulphonyl chloride derivative (1 equiv, 10 mmol) were added to a solution of methyl piperidine-4-carboxylate (1 equiv, 10 mmol) in dry dichlorometane (0.14 M) at room temperature. The mixture was stirred for 4-16 hours until complete consumption of the corresponding arenesulphonyl chloride. The organic phase was washed with 10% of NaHCO<sub>3</sub>. The aqueous phase was extracted with ethyl acetate. The organic extracts were combined, washed with H<sub>2</sub>O and sat. NaCl, dried (MgSO<sub>4</sub>), filtered and the solvent was gently concentrated on a rotary evaporator. The crude product was purified by flash column chromatography.

### 8.3.2 General procedure for the alkylation reaction with different alkyl bromides<sup>[3]</sup>

To a 0 °C solution of *i*-Pr<sub>2</sub>NH (1.5 equiv, 15 mmol) in THF (15 mL), was added a hexane solution of *n*BuLi 2.0 M (1.1 equiv, 11 mmol) dropwise. The reaction mixture was stirred for 20 minutes and then cooled to -78 °C. The corresponding ester (1 equiv, 10 mmol) was added dropwise and the reaction mixture was stirred for 1 h at -78 °C. The corresponding alkyl halide (1.5 equiv, 15 mmol, for *n*=1, allyl bromide; *n*=2, 4-bromobut-1-ene; *n*=3, 5-bromo-1-pentene) was then added dropwise into the reaction mixture. The reaction mixture was then warmed naturally to room temperature and stirred until consumption of the starting sulphonamide. The reaction mixture was quenched by addition of saturated NH<sub>4</sub>Cl aq. and extracted with Et<sub>2</sub>O three times. The combined organic layers were then dried (MgSO<sub>4</sub>) filtered and concentrated under reduced pressure. The crude product was purified by flash column chromatography.

### 8.3.3 General procedure for the reduction of the ester to alcohols<sup>[4]</sup>

To a slurry of LiAlH<sub>4</sub> (1.5 equiv, 12 mmol) in Et<sub>2</sub>O (0.9 M) was added a solution of the methyl ester (1 equiv, 8 mmol) in Et<sub>2</sub>O (1 M) dropwise at 0 °C. The mixture was stirred for 2 h (or until consumption of the substrate). Reaction was then quenched by addition of EtOH dropwise after no observation of bubbles. Further water was added and the combination was stirred until a white solid was formed. The mixture was then filtered and extracted with EtOAc. The organic layer was separated, dried



(MgSO<sub>4</sub>), filtered and concentrated under reduced pressure to obtain the alcohol without need of further purification for the next reaction.

### 8.3.4 General procedure for the bromination reaction of alcohols<sup>[5]</sup>

In a nitrogen round-bottom flask, CBr<sub>4</sub> (1.1 equiv, 7.7 mmol) and the homoallylic alcohol (1 equiv, 7 mmol) were dissolved in dry THF (4 M). The reaction mixture was cooled to 0 °C. PPh<sub>3</sub> (1.1 equiv, 7.7 mmol) was then added portion wise and the reaction mixture was stirred for 16 h. The reaction mixture was quenched by addition of water and extracted three times with Et<sub>2</sub>O. The combined organic layers were dried (MgSO<sub>4</sub>), filtered and concentrated under reduced pressure. The crude product was purified by flash column chromatography.

### 8.3.5 General procedure for the iodination reaction of alcohols<sup>[6]</sup>

To a solution of triphenylphosphine (1.05 equiv, 7.35 mmol) and imidazole (1.05 equiv, 7.35 mmol) in toluene (0.1 M) was added iodine (1.05 equiv, 7.35 mmol) and stirred for 30 minutes at room temperature. The homoallylic alcohol (1 equiv, 7 mmol) was then added, and the reaction mixture was heated to 80 °C and stirred for 16 h. The solution was then quenched with H<sub>2</sub>O, extracted with Et<sub>2</sub>O for three times and washed with sat. Na<sub>2</sub>S<sub>2</sub>O<sub>3</sub>. The organic extracts were then dried (MgSO<sub>4</sub>), filtered and concentrated. The crude product was purified by flash chromatography.

### 8.3.6 General procedure for the borylative cyclization catalyzed by copper (I) complex

Copper chloride (5 mol%, 0.01 mmol), bis(pinacolato)diboron (1.2 equiv, 0.24 mmol) and Xantphos (5 mol%, 0.01 mmol) were placed in an oven-dried resalable Teflon screw-cap Schlenk reaction tube. The Schlenk tube was connected to a vacuum/nitrogen manifold evacuated and backfilled with nitrogen. Then THF (0.24 ml, 1 M). KO<sup>t</sup>Bu (1.2 equiv, 0.24 mmol) in THF (0.24 ml, 1 M) were added in the vial through the rubber septum. Then alkenyl halide (1 equiv, 0.2 mmol) in THF (0.2 ml, 1 M) was added dropwise at 30 °C. After the reaction was complete, the reaction mixture was filtered over celite. The organic extracts were then concentrated *in vacuo*. The crude product was purified by flash chromatography.

### 8.3.7 General procedure for the oxidation of the spiro-boronates products<sup>[7]</sup>

The oxidation was performed in a reaction vial, NaBO<sub>3</sub>·H<sub>2</sub>O (10 equiv, 2 mmol) was dissolved in THF/H<sub>2</sub>O (3:2, 0.2 M) and the boronate (1 equiv, 0.2 mmol) was then added at room temperature. After stirred for 1.5 h, the reaction mixture was extracted three times with EtOAc, dried (MgSO<sub>4</sub>), filtered and concentrated *in vacuo*. The crude mixture was further purified by flash column chromatography.

### 8.3.8 Procedure used of the selective oxidation of the spiro-cyclic alcohol to aldehyde<sup>[8]</sup>

To a solution of alcohol (1 equiv, 5 mmol) in CH<sub>2</sub>Cl<sub>2</sub> (0.3 M) was added DMP (2.120 g, 1 equiv, 5 mmol) at 0 °C. After being stirred at room temperature for 1 h, the mixture was filtered through celite. The crude was evaporated *in vacuo* and was further purified by flash column chromatography.

### 8.3.9 Procedure used for the spiro-olefination by reaction with gem-bis(boryl)silylmethane reagent<sup>[9]</sup>

An oven dried resealable Schlenk tube equipped with a stirring bar was charged with (bis(4,4,5,5-tetramethyl-1,3,2-dioxaborolan-2-yl)methyl)trimethylsilane (1.2 equiv, 3.72 mmol) and THF (0.9 M) under Argon. The mixture was then cooled to 0 °C and lithium 2,2,6,6-tetramethylpiperidide (1.4 equiv, in a 0.4 M solution in THF) was added dropwise. After 5 min., the aldehyde (1 equiv, 3.1 mmol) was added and the reaction was allowed to warm to r.t. Reaction mixture was analyzed by TLC. After substrate completion the crude was filtered through a small pad of silica gel followed by a copious washing and concentrated *in vacuo*. The crude mixture was further purified by flash column chromatography.

### 8.3.10 Procedure used for the Suzuki-Miyaura coupling reaction<sup>[10]</sup>

An oven-dried resealable Schlenk tube equipped with a stirring bar was charged with Pd(PPh<sub>3</sub>)<sub>4</sub> (3 mol%) and 1,4-dioxane (0.7 mL). To this solution the *gem*-bismetallated alkene (0.251 g, 1 equiv, 0.5 mmol), dissolved in 0.6 mL of 1,4-dioxane, 1-iodo-4-methylbenzene (3 equiv, 1.5 mmol) and a 3 M KOH solution (6 equiv, 3 mmol) were added in sequence and the reaction was heated up at 90 °C for 16 h. After completion (by TLC), the mixture was cooled to room temperature and diluted with DCM. The mixture was filtered through a small pad of celite and anhydrous MgSO<sub>4</sub>. Afterwards the solvent was concentrated *in vacuo*. The resulting

## Experimental part

crude product was purified by column chromatography to give a coupled compound.

### **8.3.11 Procedure used for the oxidation of the alcohol to the carboxylic acid<sup>[11]</sup>**

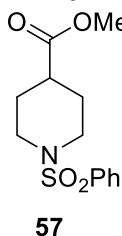
The alcohol (1 equiv, 5 mmol) was subjected to the oxidation reaction using Jones reagent (2 M, 0.7 equiv) in acetone (0.2 M) and H<sub>2</sub>O (2.5 M) at 0 °C. After 1 h, the reaction was quenched by saturated aqueous NH<sub>4</sub>Cl, extracted three times with Et<sub>2</sub>O. The combined organic layers were washed with aqueous NaOH (0.1 M) and then aqueous layer was acidified with saturated aqueous NH<sub>4</sub>Cl, extracted six times with Et<sub>2</sub>O. The combined organic layers were dried (MgSO<sub>4</sub>), filtered and concentrated *in vacuo* to obtain the corresponding carboxylic acid as a white solid.

### **8.3.12 Procedure used for the esterification of the spirocyclic acid to the ester<sup>[12]</sup>**

The carboxylic acid (1 equiv, 3.8 mmol) was treated with a solution of concentrated sulphuric acid (30 μL/mmol) in methanol (0.5 M) and refluxed for one hour. The solution was cooled to room temperature and concentrated *in vacuo*. Et<sub>2</sub>O was added and the organic layer was washed with NaHCO<sub>3</sub> (5% aq.) followed by brine. The organic layer was separated, dried (MgSO<sub>4</sub>), filtered and concentrated *in vacuo*, without need of further purification (quantitative reaction).

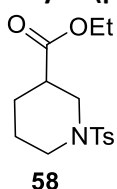
### 8.3.13 Spectral data of Chapter 4

#### Methyl 1-(phenylsulfonyl)piperidine-4-carboxylate



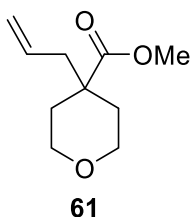
Flash column chromatography (5:1 Hexane:EtOAc to 3:1 Hexane:EtOAc) yielded **57** (85% yield) as a white solid.  $^1\text{H NMR}$  ( $\text{CDCl}_3$ , 400 MHz)  $\delta$  7.75 (m, 2H), 7.59 (m, 1H), 7.53 (m, 2H), 3.65 (s, 3H), 3.63 (m, 2H), 2.46 (m, 2H), 2.26 (m, 1H), 1.97 (m, 2H), 1.81 (m, 2H).  $^{13}\text{C}$   $\{^1\text{H}\}$  NMR ( $\text{CDCl}_3$ , 100 MHz)  $\delta$  174.2, 136.0, 132.7, 129.0, 127.5, 51.8, 45.3, 39.8, 27.3. HRMS (ESI) for  $\text{C}_{13}\text{H}_{17}\text{NNaO}_4\text{S}$   $[\text{M}+\text{Na}]^+$ : calculated: 306.0769, found: 306.0770.

#### Ethyl 1-(phenylsulfonyl)piperidine-3-carboxylate



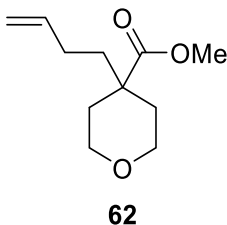
Flash column chromatography (5:1 Hexane:EtOAc) yielded **58** (88% yield) as a white solid.  $^1\text{H NMR}$  ( $\text{CDCl}_3$ , 400 MHz)  $\delta$  7.59 (d,  $J = 8.3$  Hz, 2H), 7.28 (d,  $J = 8.3$  Hz, 2H), 4.08 (q,  $J = 7.1$  Hz, 2H), 3.79 (m, 1H), 3.55 (apparent d, 1H), 2.56 (m, 1H), 2.47 (m, 1H), 2.38 (s, 3H), 2.38 (m, 1H), 1.90 (m, 1H), 1.75 (m, 1H), 1.64 – 1.51 (m, 1H), 1.36 (m, 1H), 1.20 (t,  $J = 7.1$  Hz, 3H).  $^{13}\text{C}$   $\{^1\text{H}\}$  NMR ( $\text{CDCl}_3$ , 100 MHz)  $\delta$  172.5, 143.4, 132.7, 129.5, 127.4, 60.6, 47.5, 4.13, 40.8, 26.2, 23.7, 21.3, 13.9. HRMS (ESI) for  $\text{C}_{15}\text{H}_{21}\text{NNaO}_4\text{S}$   $[\text{M}+\text{Na}]^+$ : calculated: 334.1081, found: 334.1083.

#### Methyl 4-allyltetrahydro-2H-pyran-4-carboxylate



Flash column chromatography (20:1 Hexane:EtOAc) yielded **61** (90% yield) as a colourless oil.  $^1\text{H NMR}$  ( $\text{CDCl}_3$ , 400 MHz)  $\delta$  5.63 (ddt,  $J = 16.8, 10.2, 6.5$  Hz, 1H), 5.08 – 4.94 (m, 2H), 3.74 (apparent dt, 2H), 3.67 (s, 3H), 3.40 (m, 2H), 2.20 (dd,  $J = 7.4, 1.0$  Hz, 2H), 2.02 – 1.94 (m, 2H), 1.52 (m, 2H).  $^{13}\text{C}$   $\{^1\text{H}\}$  NMR ( $\text{CDCl}_3$ , 100 MHz)  $\delta$  175.5, 132.5, 118.2, 65.2, 51.6, 45.1, 44.7, 33.7. HRMS (ESI) for  $\text{C}_{10}\text{H}_{16}\text{O}_3$   $[\text{M}]^+$ : calculated: 184.1102, found: 184.1099.

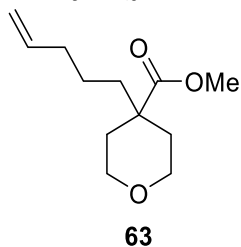
#### Methyl 4-(but-3-en-1-yl)tetrahydro-2H-pyran-4-carboxylate



Flash column chromatography (20:1 Hexane:EtOAc) yielded **62** (75% yield) as a colourless oil.  $^1\text{H NMR}$  ( $\text{CDCl}_3$ , 400 MHz)  $\delta$  5.74 (ddt,  $J = 16.8, 10.2, 6.5$  Hz, 1H), 4.97 – 4.80 (m, 2H), 3.82 (apparent dt, 2H), 3.71 (s, 3H), 3.42 (m, 2H), 2.15 (m, 2H), 1.98 – 1.90 (m, 2H), 1.67 – 1.57 (m, 2H), 1.50 (m, 2H).  $^{13}\text{C}$   $\{^1\text{H}\}$  NMR ( $\text{CDCl}_3$ , 100 MHz)  $\delta$  176.0, 137.8, 114.8, 65.4, 51.8, 44.8, 39.9, 34.2, 28.0. HRMS (ESI) for  $\text{C}_{11}\text{H}_{18}\text{O}_3$   $[\text{M}]^+$ : calculated: 198.1255, found: 198.1256.

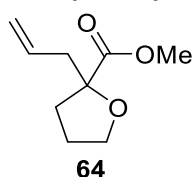
## Experimental part

### Methyl 4-(pent-4-en-1-yl)tetrahydro-2H-pyran-4-carboxylate



Flash column chromatography (20:1 Hexane:EtOAc) yielded **63** (68% yield) as a colourless oil.  $^1\text{H NMR}$  ( $\text{CDCl}_3$ , 400 MHz)  $\delta$  5.76 (ddt,  $J = 16.9, 10.2, 6.6$  Hz, 1H), 5.02 – 4.91 (m, 2H), 3.81 (apparent dt, 2H), 3.71 (s, 3H), 3.40 (m, 2H), 2.10 (m, 2H), 1.99 – 1.90 (m, 2H), 1.57 – 1.41 (m, 4H), 1.27 (m, 2H).  $^{13}\text{C}$   $\{^1\text{H}\}$  NMR ( $\text{CDCl}_3$ , 100 MHz)  $\delta$  176.2, 138.2, 114.8, 65.4, 51.7, 44.9, 40.2, 34.2, 33.8, 22.9. HRMS (ESI) for  $\text{C}_{12}\text{H}_{20}\text{O}_3$   $[\text{M}]^+$  : calculated: 212.1410, found: 212.1412.

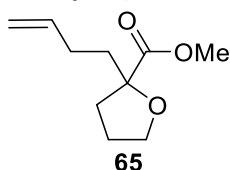
### Methyl 2-allyltetrahydrofuran-2-carboxylate



Flash column chromatography (20:1 Hexane:EtOAc) yielded **64** (60% yield) as a colourless oil.  $^1\text{H NMR}$  ( $\text{CDCl}_3$ , 400 MHz)  $\delta$  5.79 (ddt,  $J = 24.0, 10.5, 7.2$  Hz, 1H), 5.12 – 5.08 (m, 2H), 3.95 (m, 2H), 3.72 (s, 3H), 2.62 (m, 1H), 2.46 (m, 1H), 1.90 (m, 4H).  $^{13}\text{C}$   $\{^1\text{H}\}$  NMR ( $\text{CDCl}_3$ , 100 MHz)  $\delta$  175.2, 137.8, 114.6, 85.9, 68.9, 52.1, 37.3, 35.5, 28.6, 25.3. HRMS (ESI) for  $\text{C}_9\text{H}_{14}\text{O}_3$   $[\text{M}]^+$  : calculated:

170.0944, found: 170.0943.

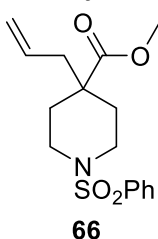
### Methyl 2-(but-3-en-1-yl)tetrahydrofuran-2-carboxylate



Flash column chromatography (20:1 Hexane:EtOAc) yielded **65** (20% yield) as a colourless oil.  $^1\text{H NMR}$  ( $\text{CDCl}_3$ , 400 MHz)  $\delta$  5.76 (ddt,  $J = 24.0, 10.5, 7.2$  Hz, 1H), 5.03 – 4.85 (m, 2H), 4.02 – 3.85 (m, 2H), 3.72 – 3.67 (m, 3H), 2.29 – 2.20 (m, 1H), 2.20 – 2.11 (m, 1H), 2.01 – 1.92 (m, 2H), 1.88 – 1.81 (m, 2H), 1.78 – 1.62 (m, 2H).  $^{13}\text{C}$   $\{^1\text{H}\}$  NMR ( $\text{CDCl}_3$ , 100 MHz)  $\delta$  175.2, 137.8,

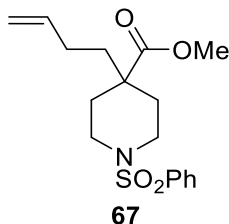
114.6, 85.9, 68.9, 52.1, 37.3, 35.5, 28.6, 25.3. HRMS (ESI) for  $\text{C}_{10}\text{H}_{16}\text{O}_3$   $[\text{M}]^+$ : calculated: 184.1099, found: 184.1012.

### Methyl 4-allyl-1-tosylpiperidine-4-carboxylate



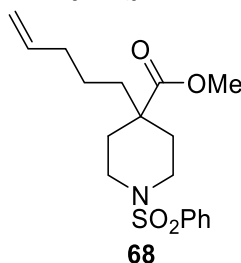
Flash column chromatography (100:0 to 60:40 pentane: EtOAc) yielded **66** (85% yield) as white solid. The  $^1\text{H NMR}$  chemical shift of product **66** is the same that the one reported in the literature.<sup>[13]</sup>

### Methyl 4-(but-3-en-1-yl)-1-(phenylsulfonyl)piperidine-4-carboxylate



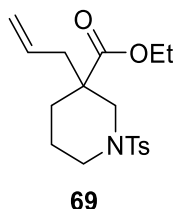
Flash column chromatography (5:1 Hexane:EtOAc to 3:1 Hexane: EtOAc) yielded **67** (83% yield) as a white solid.  $^1\text{H}$  NMR ( $\text{CDCl}_3$ , 400 MHz)  $\delta$  7.73 (dd,  $J = 8.4, 1.3$  Hz, 2H), 7.58 (t,  $J = 8.4$  Hz, 1H), 7.56 – 7.49 (m, 2H), 5.70 (m, 1H), 5.02 – 4.90 (m, 2H), 3.63 (m, 2H), 3.58 (s, 3H), 2.36 (m, 2H), 2.21 (apparent d, 2H), 1.89 (m, 2H), 1.57 (m, 4H).  $^{13}\text{C}$   $\{^1\text{H}\}$ MR ( $\text{CDCl}_3$ , 100 MHz)  $\delta$  175.2, 137.4, 136.2, 132.7, 129.0, 127.5, 115.0, 51.8, 44.9, 43.8, 39.5, 32.9, 28.2. HRMS (ESI) for  $\text{C}_{17}\text{H}_{24}\text{NO}_4\text{S}$   $[\text{M}+\text{H}]^+$ : calculated:338.1420, found: 338.1421.

### Methyl 4-(pent-4-en-1-yl)-1-(phenylsulfonyl)piperidine-4-carboxylate



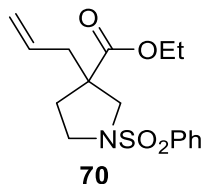
Flash column chromatography (5:1 Hexane:EtOAc to 3:1 Hexane: EtOAc) yielded **68** (84% yield) as a white solid.  $^1\text{H}$  NMR ( $\text{CDCl}_3$ , 400 MHz)  $\delta$  7.77 – 7.69 (m, 2H), 7.63 – 7.56 (m, 1H), 7.55 – 7.48 (m, 2H), 5.71 (ddt,  $J = 16.9, 10.2, 6.6$  Hz, 1H), 5.00 – 4.91 (m, 2H), 3.61 (ddd,  $J = 9.7, 6.4, 3.2$  Hz, 2H), 3.57 (s, 3H), 2.36 (m, 2H), 2.19 (apparent d, 2H), 1.97 (m, 2H), 1.53 (m, 1H), 1.47 (ddd,  $J = 9.6, 7.9, 4.2$  Hz, 2H), 1.30 – 1.17 (m, 3H).  $^{13}\text{C}$   $\{^1\text{H}\}$  NMR ( $\text{CDCl}_3$ , 100 MHz)  $\delta$  175.4, 137.9, 136.2, 132.7, 129.0, 127.5, 115.0, 51.8, 45.0, 43.9, 39.8, 33.7, 32.9, 23.1. HRMS (ESI) for  $\text{C}_{18}\text{H}_{26}\text{NO}_4\text{S}$   $[\text{M}+\text{H}]^+$ : calculated:352.1576, found: 352.1577.

### Ethyl 3-allyl-1-(phenylsulfonyl)piperidine-3-carboxylate



Flash column chromatography (5:1 Hexane:EtOAc) yielded **69** (35% yield) as a white solid.  $^1\text{H}$  NMR ( $\text{CDCl}_3$ , 400 MHz)  $\delta$  7.61 (d,  $J = 7.9$ , 2H), 7.28 (d,  $J = 7.9$  Hz, 2H), 5.62 (m, 1H), 5.01 (m, 2H), 4.11 (m, 2H), 3.39 (d,  $J = 11.5$  Hz, 1H), 3.02 (m, 1H), 2.65 (m, 2H), 2.39 (s, 3H), 2.19 (m, 1H), 1.86 (m, 1H), 1.68 (m, 2H), 1.32 (m, 2H), 1.24 (t,  $J = 7.1$  Hz, 3H).  $^{13}\text{C}$   $\{^1\text{H}\}$  NMR ( $\text{CDCl}_3$ , 100 MHz)  $\delta$  173.5, 143.3, 132.9, 132.0, 129.5, 127.4, 118.7, 60.7, 51.7, 46.4, 46.0, 40.0, 30.4, 21.5, 21.4, 14.1. HRMS (ESI) for  $\text{C}_{18}\text{H}_{25}\text{NNaO}_4\text{S}$   $[\text{M}+\text{Na}]^+$ : calculated: 374.1394, found: 374.1397.

### Ethyl 3-allyl-1-(phenylsulfonyl)pyrrolidine-3-carboxylate

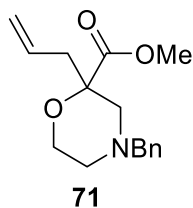


Flash column chromatography (5:1 Hexane:EtOAc) yielded **70** (40% yield) as a colorless oil.  $^1\text{H}$  NMR ( $\text{CDCl}_3$ , 400 MHz)  $\delta$  7.79 (m, 2H), 7.58 (m, 1H), 7.50 (m, 2H), 5.54 (m, 1H), 5.01 (m, 1H), 4.94 (m, 1H), 3.95 (m, 2H), 3.59 (d,  $J = 10.4$  Hz, 1H), 3.35 (m, 1H), 3.20 (m, 2H), 2.24 (m, 3H), 1.74 (m, 1H), 1.11 (t,  $J = 7.1$  Hz, 3H).  $^{13}\text{C}$   $\{^1\text{H}\}$  NMR ( $\text{CDCl}_3$ , 100 MHz)  $\delta$  173.3, 136.4, 132.6, 132.3,

## Experimental part

128.9, 127.3, 118.8, 61.0, 54.3, 52.8, 46.6, 40.4, 33.2, 13.9. HRMS (ESI) for  $C_{16}H_{21}NNaO_4S$   $[M+Na]^+$ : calculated: 346.1086, found: 346.1083.

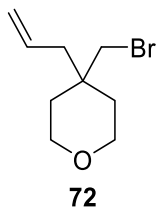
### Methyl 2-allyl-4-benzylmorpholine-2-carboxylate



Flash column chromatography (5:1 Hexane:EtOAc) yielded **71** (22% yield) as a colorless oil.  $^1H$  NMR ( $CDCl_3$ , 400 MHz)  $\delta$  7.28 (m, 5H), 5.77 (ddt,  $J = 17.3, 10.3, 7.3$  Hz, 1H), 5.04 (m, 2H), 4.03 (m, 1H), 3.80 (m, 1H), 3.73 (s, 3H), 3.53 (d,  $J = 13.3$  Hz, 1H), 3.42 (d, 13.3 Hz, 1H), 3.15 (dd,  $J = 11.3, 1.6$  Hz, 1H), 2.60 (m, 1H), 2.39 (qd,  $J = 14.1, 7.3$  Hz, 2H), 2.25 (apparent td, 1H), 2.06 (d,  $J = 11.3$  Hz, 1H).  $^{13}C$   $\{^1H\}$  NMR ( $CDCl_3$ , 100 MHz)  $\delta$  172.7, 137.5, 131.7, 128.8,

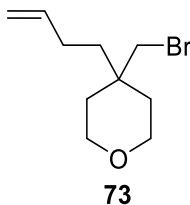
128.1, 127.1, 118.5, 79.7, 63.8, 62.6, 58.9, 52.7, 51.8, 41.6. HRMS (ESI) for  $C_{16}H_{22}NO_3$   $[M+H]^+$ : calculated: 276.1595, found: 276.1594.

### 4-Allyl-4-(bromomethyl)tetrahydro-2H-pyran



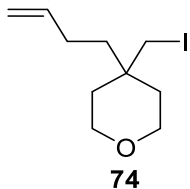
Flash column chromatography (20:1 Hexane:EtOAc) yielded **72** (85% yield) as a yellowish oil.  $^1H$  NMR ( $CDCl_3$ , 400 MHz)  $\delta$  5.72 (ddt,  $J = 16.9, 10.3, 7.6$  Hz, 1H), 5.16 (m, 2H), 3.70 – 3.60 (m, 4H), 3.39 (s, 2H), 2.27 (d,  $J = 7.6$  Hz, 2H), 1.55 (m, 4H).  $^{13}C$   $\{^1H\}$  NMR ( $CDCl_3$ , 100 MHz)  $\delta$  132.4, 119.2, 63.4, 42.3, 39.2, 34.8, 34.0.

### 4-(Bromomethyl)-4-(but-3-en-1-yl)tetrahydro-2H-pyran



Flash column chromatography (20:1 Hexane:EtOAc) yielded **73** (83% yield) as a yellowish oil.  $^1H$  NMR ( $CDCl_3$ , 400 MHz)  $\delta$  5.82 (ddt,  $J = 16.8, 10.1, 6.5$  Hz, 1H), 5.06 – 4.96 (ddd,  $J = 13.7, 12.2, 2.0$  Hz, 2H), 3.66 (m, 4H), 3.27 (s, 2H), 2.01 – 1.97 (m, 2H), 1.64 – 1.48 (m, 6H).  $^{13}C$   $\{^1H\}$  NMR ( $CDCl_3$ , 100 MHz)  $\delta$  138.2, 114.8, 63.7, 36.4, 35.2, 33.2, 26.8, 19.8.

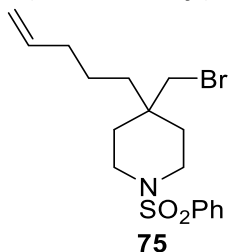
### 4-(But-3-en-1-yl)-4-(iodomethyl)tetrahydro-2H-pyran



Flash column chromatography (20:1 Hexane:EtOAc) yielded **74** (89% yield) as a yellowish oil.  $^1H$  NMR ( $CDCl_3$ , 400 MHz)  $\delta$  5.82 (ddt,  $J = 16.8, 10.1, 6.5$  Hz, 1H), 5.01 (ddd,  $J = 13.6, 11.5, 1.6$  Hz, 2H), 3.63 (m, 4H), 3.27 (s, 2H), 1.95 (m, 2H), 1.60 (m, 4H).  $^{13}C$   $\{^1H\}$  NMR ( $CDCl_3$ , 100 MHz)  $\delta$  138.1, 114.8, 65.8, 63.6, 36.4, 35.2, 33.2, 26.8, 19.7. HRMS (ESI) for  $C_{10}H_{17}IO$   $[M+H]^+$ : calculated: 281.0402, found:

281.0395.

#### 4-(Bromomethyl)-4-(pent-4-en-1-yl)-1-(phenylsulfonyl)piperidine

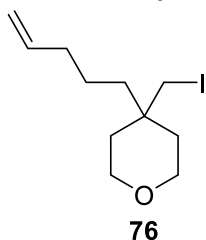


75

Flash column chromatography (5:1 Hexane:EtOAc to 3:1 Hexane: EtOAc) yielded **75** (87% yield) as a colorless oil.  $^1\text{H NMR}$  ( $\text{CDCl}_3$ , 400 MHz)  $\delta$  7.81 – 7.72 (m, 2H), 7.61 (m, 1H), 7.54 (ddd,  $J$  = 8.4, 2.3, 0.9 Hz, 2H), 5.71 (ddt,  $J$  = 16.9, 10.2, 6.6 Hz, 1H), 4.99 – 4.87 (m, 2H), 3.22 (s, 2H), 3.07 – 2.91 (m, 4H), 1.98 (m, 2H), 1.60 (m, 4H), 1.33 – 1.16 (m, 4H).  $^{13}\text{C}$   $\{^1\text{H}\}$  NMR ( $\text{CDCl}_3$ , 100 MHz)  $\delta$  138.0, 135.9, 132.7, 128.9, 127.4, 114.8, 53.4, 41.7, 41.0, 34.3, 33.7, 32.8, 32.5, 30.79, 21.4. HRMS (ESI)

for  $\text{C}_{17}\text{H}_{25}\text{BrNO}_2\text{S}$   $[\text{M}+\text{H}]^+$ : calculated: 386.0786, found: 386.0784.

#### 4-(Iodomethyl)-4-(pent-4-en-1-yl)tetrahydro-2H-pyran

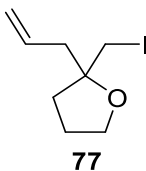


76

Flash column chromatography (20:1 Hexane:EtOAc) yielded **76** (92% yield) as a yellowish oil.  $^1\text{H NMR}$  ( $\text{CDCl}_3$ , 400 MHz)  $\delta$  5.81 (ddt,  $J$  = 16.9, 10.2, 6.7 Hz, 1H), 5.00 (ddd,  $J$  = 13.6, 12.2, 2.0 Hz, 2H). 3.67 – 3.56 (m, 4H), 3.26 (s, 2H), 2.14 – 2.00 (m, 2H), 1.62 – 1.49 (m, 4H), 1.49 – 1.34 (m, 2H), 1.32 – 1.18 (m, 2H).  $^{13}\text{C}$   $\{^1\text{H}\}$  NMR ( $\text{CDCl}_3$ , 100 MHz)  $\delta$  138.4, 114.9, 63.7, 36.5, 35.3, 34.0, 33.2, 21.6, 20.2. HRMS (ESI) for  $\text{C}_{11}\text{H}_{19}\text{IO}$   $[\text{M}+\text{Na}]^+$ : calculated:

317.0378, found: 317.0524.

#### 2-Allyl-2-(iodomethyl)tetrahydrofuran

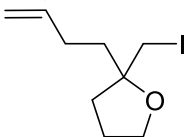


77

Flash column chromatography (20:1 Hexane:EtOAc) yielded **77** (90% yield) as a yellowish oil.  $^1\text{H NMR}$  ( $\text{CDCl}_3$ , 400 MHz)  $\delta$  5.77 (ddt,  $J$  = 17.4, 10.1, 7.3 Hz, 1H), 5.15 (ddd,  $J$  = 13.6, 12.2, 2.1 Hz, 2H), 3.95 – 3.84 (m, 2H), 3.26 (s, 2H), 2.46 (d,  $J$  = 7.4 Hz, 2H), 2.03 – 1.83 (m, 4H).  $^{13}\text{C}$   $\{^1\text{H}\}$  NMR ( $\text{CDCl}_3$ , 100 MHz)  $\delta$  133.4, 118.7, 82.6, 68.6, 42.9, 34.6, 26.4, 16.1. HRMS (ESI) for  $\text{C}_8\text{H}_{13}\text{IO}$   $[\text{M}+\text{Na}]^+$ : calculated: 252.0008, found:

252.0011.

#### 2-(But-3-en-1-yl)-2-(iodomethyl)tetrahydrofuran

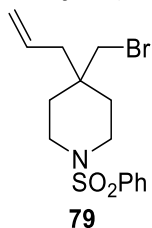


78

Flash column chromatography (20:1 Hexane:EtOAc) yielded **78** (87% yield) as a yellowish oil.  $^1\text{H NMR}$  ( $\text{CDCl}_3$ , 400 MHz)  $\delta$  5.92 – 5.76 (m, 1H), 5.08 – 4.93 (m, 2H), 3.88 (m, 2H), 3.26 (s, 2H), 2.13 – 2.04 (m, 2H), 1.96 (m, 4H), 1.8 (m, 2H).  $^{13}\text{C}$   $\{^1\text{H}\}$  NMR ( $\text{CDCl}_3$ , 100 MHz)  $\delta$  138.2, 114.6, 83.0, 68.5, 37.7, 35.0, 28.3, 26.4, 15.7. HRMS (ESI) for  $\text{C}_9\text{H}_{15}\text{IO}$   $[\text{M}+\text{Na}]^+$ : calculated: 266.0168, found: 266.0169.

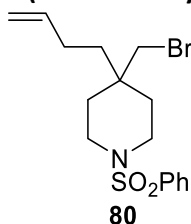


## Experimental part

**4-Allyl-4-(bromomethyl)-1-(phenylsulfonyl)piperidine**

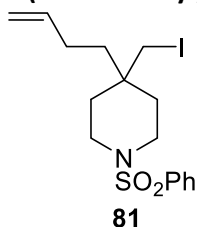
Flash column chromatography (5:1 Hexane:EtOAc) yielded **79** (87% yield) as a colourless oil.  $^1\text{H NMR}$  ( $\text{CDCl}_3$ , 400 MHz)  $\delta$  7.78 – 7.76 (m, 2H), 7.65 – 7.59 (m, 1H), 7.57 – 7.51 (m, 2H), 5.63 (ddt,  $J = 16.9, 10.2, 7.6$  Hz, 1H), 5.08 – 5.04 (m, 2H), 3.21 (s, 2H), 3.11 – 2.92 (m, 4H), 2.07 (d,  $J = 7.5$  Hz, 2H), 1.72 – 1.54 (m, 4H).  $^{13}\text{C}$   $\{^1\text{H}\}$  NMR ( $\text{CDCl}_3$ , 100 MHz)  $\delta$  136.1, 132.8, 131.9, 129.1, 127.5, 119.5, 41.8, 41.0, 39.0, 34.9, 32.7. **HRMS (ESI) for  $\text{C}_{15}\text{H}_{20}\text{BrNO}_2\text{S}$   $[\text{M}]^+$**  : calculated: 357.0408, found:

357.0398.

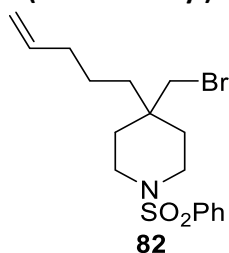
**4-(Bromomethyl)-4-(but-3-en-1-yl)-1-(phenylsulfonyl)piperidine**

Flash column chromatography (5:1 Hexane:EtOAc) yielded **80** (90% yield) as a colorless oil.  $^1\text{H NMR}$  ( $\text{CDCl}_3$ , 400 MHz)  $\delta$  7.81 – 7.72 (m, 2H), 7.66 – 7.59 (m, 1H), 7.58 – 7.52 (m, 2H), 5.74 (ddt,  $J = 16.8, 10.2, 6.5$  Hz, 1H), 4.99 (dd,  $J = 17.1, 1.6$  Hz, 1H), 4.94 (dd,  $J = 10.1, 1.1$  Hz, 1H), 3.24 (s, 2H), 3.12 – 3.02 (m, 2H), 3.02 – 2.91 (m, 2H), 1.91 (m, 2H), 1.65 (m, 4H), 1.46 – 1.35 (m, 2H).  $^{13}\text{C}$   $\{^1\text{H}\}$  NMR ( $\text{CDCl}_3$ , 100 MHz)  $\delta$  137.9, 136.1, 132.8, 129.1, 127.5, 114.9,

41.8, 40.7, 34.5, 33.0, 26.8. **HRMS (ESI) for  $\text{C}_{16}\text{H}_{23}\text{BrNO}_2\text{S}$   $[\text{M}+\text{H}]^+$** : calculated:372.0626, found: 372.0627.

**4-(But-3-en-1-yl)-4-(iodomethyl)-1-(phenylsulfonyl)piperidine**

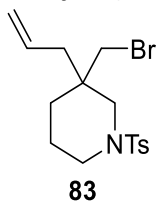
Flash column chromatography (5:1Hexane:EtOAc) yielded **81** (85% yield) as a colorless oil.  $^1\text{H NMR}$  ( $\text{CDCl}_3$ , 400 MHz)  $\delta$  7.77 (m, 2H), 7.65 – 7.59 (m, 1H), 7.58 – 7.52 (m, 2H), 5.74 (m, 1H), 5.00 (m, 1H), 4.94 (m, 1H), 3.07 (overlapped signals, s, 3H + m, 2H), 2.93 (m, 2H), 1.95 – 1.83 (m, 2H), 1.65 (m, 4H), 1.36 (m, 2H).  $^{13}\text{C}$   $\{^1\text{H}\}$  NMR ( $\text{CDCl}_3$ , 100 MHz)  $\delta$  137.7, 136.1, 132.8, 129.1, 127.5, 114.9, 41.9, 36.4, 33.7, 33.3, 26.7, 17.9. **HRMS (ESI) for  $\text{C}_{16}\text{H}_{23}\text{INO}_2\text{S}$   $[\text{M}+\text{H}]^+$** : calculated:420.0487, found: 420.0489.

**4-(Bromomethyl)-4-(pent-4-en-1-yl)-1-(phenylsulfonyl)piperidine**

Flash column chromatography (5:1 Hexane:EtOAc to 3:1 Hexane: EtOAc) yielded **82** (95% yield) as a colorless oil.  $^1\text{H NMR}$  ( $\text{CDCl}_3$ , 400 MHz)  $\delta$  7.81 – 7.72 (m, 2H), 7.61 (m, 1H), 7.54 (ddd,  $J = 8.4, 2.3, 0.9$  Hz, 2H), 5.71 (ddt,  $J = 16.9, 10.2, 6.6$  Hz, 1H), 4.99 – 4.87 (m, 2H), 3.22 (s, 2H), 3.07 – 2.91 (m, 4H), 1.98 (m, 2H), 1.60 (m, 4H), 1.33 – 1.16 (m, 4H).  $^{13}\text{C}$   $\{^1\text{H}\}$  NMR ( $\text{CDCl}_3$ , 100 MHz)  $\delta$  138.0, 135.9, 132.7, 128.9, 127.4, 114.8, 53.4, 41.7, 41.0, 34.3, 33.7, 32.8, 32.5, 30.79, 21.4. **HRMS (ESI)**

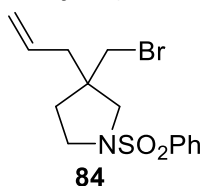
**for  $\text{C}_{17}\text{H}_{25}\text{BrNO}_2\text{S}$   $[\text{M}+\text{H}]^+$** : calculated: 386.0786, found: 386.0784.

### 3-Allyl-3-(bromomethyl)-1-(phenylsulfonyl)piperidine



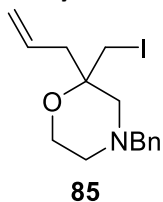
Flash column chromatography (5:1 Hexane:EtOAc to 3:1 Hexane:EtOAc) yielded **83** (46% yield) as colorless oil.  $^1\text{H NMR}$  ( $\text{CDCl}_3$ , 400 MHz)  $\delta$  7.60 (dd,  $J = 8.4, 1.7$  Hz, 2H), 7.36 – 7.28 (m, 2H), 5.70 (ddt,  $J = 17.8, 10.2, 7.6$  Hz, 1H), 5.21 – 5.10 (m, 2H), 3.43 (d,  $J = 10.5$  Hz, 1H), 3.37 (d,  $J = 10.6$  Hz, 1H), 3.03 (m, 1H), 2.91 (d,  $J = 11.6$  Hz, 1H), 2.87 – 2.76 (m, 1H), 2.72 (d,  $J = 11.6$  Hz, 1H), 2.42 (s, 3H), 2.24 – 2.17 (m, 2H), 1.74 – 1.60 (m, 2H), 1.54 – 1.27 (m, 2H).  $^{13}\text{C}$   $\{^1\text{H}\}$  NMR ( $\text{CDCl}_3$ , 100 MHz)  $\delta$  143.5, 132.8, 131.8, 129.6, 127.4, 119.5, 53.0, 46.5, 39.5, 38.8, 37.1, 31.3, 21.4, 20.8. HRMS (ESI) for  $\text{C}_{16}\text{H}_{23}\text{BrNO}_2\text{S}$   $[\text{M}+\text{H}]^+$ : calculated: 372.0627, found: 372.0627.

### 3-Allyl-3-(bromomethyl)-1-(phenylsulfonyl)pyrrolidine



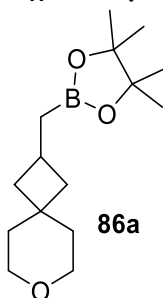
Flash column chromatography (5:1 Hexane:EtOAc to 3:1 Hexane:EtOAc) yielded **84** (45% yield) as a white solid.  $^1\text{H NMR}$  ( $\text{CDCl}_3$ , 400 MHz)  $\delta$  7.80 (m, 2H), 7.59 (m, 1H), 7.56 – 7.49 (m, 2H), 5.63 – 5.49 (m, 1H), 5.10 – 4.99 (m, 2H), 3.31 – 3.25 (m, 2H), 3.19 (d,  $J = 10.4$  Hz, 1H), 3.14 (apparent s, 2H), 3.06 (d,  $J = 10.4$  Hz, 1H), 2.14–2.08 (m, 2H), 1.75 (m, 2H).  $^{13}\text{C}$   $\{^1\text{H}\}$  NMR ( $\text{CDCl}_3$ , 100 MHz)  $\delta$  136.0, 132.7, 132.1, 129.0, 127.2, 119.5, 55.8, 46.4, 46.2, 39.2, 38.9, 33.8. HRMS (ESI) for  $\text{C}_{14}\text{H}_{19}\text{BrNO}_2\text{S}$   $[\text{M}+\text{H}]^+$ : calculated: 344.0315, found: 344.0314.

### 2-Allyl-4-benzyl-2-(iodomethyl)morpholine



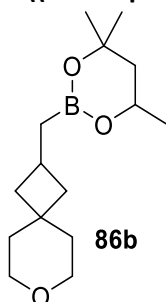
Flash column chromatography (5:1 Hexane:EtOAc to 3:1 Hexane:EtOAc) yielded **85** (67% yield) as a white solid.  $^1\text{H NMR}$  ( $\text{CDCl}_3$ , 400 MHz)  $\delta$  7.37 – 7.19 (m, 5H), 5.72 – 5.53 (m, 1H), 5.08 (m, 2H), 3.67 (m, 3H), 3.41 (s, 2H), 3.29 (d,  $J = 10.6$  Hz, 1H), 2.53 (d,  $J = 11.5$  Hz, 1H), 2.46–2.38 (m, 3H), 2.26 (d,  $J = 11.5$  Hz, 1H), 2.20 (m, 1H).  $^{13}\text{C}$   $\{^1\text{H}\}$  NMR ( $\text{CDCl}_3$ , 100 MHz)  $\delta$  137.8, 132.2, 128.8, 128.3, 127.2, 119.1, 72.7, 62.9, 61.7, 58.3, 52.9, 41.1, 13.0. HRMS (ESI) for  $\text{C}_{15}\text{H}_{21}\text{INO}$   $[\text{M}+\text{H}]^+$ : calculated: 358.0664, found: 358.0662.

### 2-((7-Oxaspiro[3.5]nonan-2-yl)methyl)-4,4,5,5-tetramethyl-1,3,2-dioxaborolane

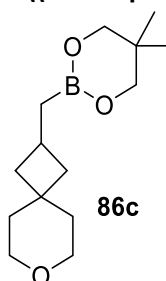


Flash column chromatography (40:1 Hexane:EtOAc) yielded **86a** (93% yield) as a yellowish oil.  $^1\text{H NMR}$  ( $\text{CDCl}_3$ , 400 MHz)  $\delta$  3.61 (m, 2H), 3.51 (m, 2H), 2.40 (sep,  $J = 8.0$  Hz, 1H), 2.03 (m, 2H), 1.60 (m, 2H), 1.48 (m, 2H), 1.39 (m, 2H), 1.22 (s, 12H), 0.95 (d,  $J = 7.8$  Hz, 2H).  $^{13}\text{C}$   $\{^1\text{H}\}$  NMR ( $\text{CDCl}_3$ , 100 MHz)  $\delta$  82.8, 64.9, 64.7, 40.8, 40.6, 37.2, 32.8, 25.1, 24.8.  $^{11}\text{B}$  NMR ( $\text{CDCl}_3$ , 128.3 MHz)  $\delta$  34.2. HRMS (ESI) for  $\text{C}_{15}\text{H}_{27}\text{BO}_3$   $[\text{M}+\text{H}]^+$ : calculated: 267.2123, found: 267.2134.

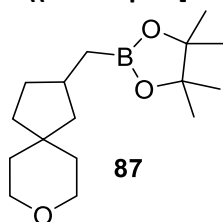
## Experimental part

**2-((7-Oxaspiro[3.5]nonan-2-yl)methyl)-4,4,6-trimethyl-1,3,2-dioxaborinane****86b**

Flash column chromatography (40:1 Hexane:EtOAc) yielded **86b** (hex) (65% yield) as a yellowish oil.  $^1\text{H NMR}$  ( $\text{CDCl}_3$ , 400 MHz)  $\delta$  4.12 (m, 1H), 3.58 (m, 2H), 3.50 (m, 2H), 2.34 (sep,  $J = 8.0$  Hz, 1H), 1.98 (m, 2H), 1.73 (apparent dd, 1H), 1.58 (m, 2H), 1.46 (m, 2H), 1.35 (m, 3H), 1.24 (s, 6H), 1.21 (d,  $J = 6.2$  Hz, 3H), 0.81 (d,  $J = 7.8$  Hz, 2H).  $^{13}\text{C}$   $\{^1\text{H}\}$  NMR ( $\text{CDCl}_3$ , 100 MHz)  $\delta$  70.3, 65.0, 64.7, 64.4, 45.9, 40.8, 40.7, 37.3, 32.8, 31.2, 28.1, 25.4, 23.2.  $^{11}\text{B NMR}$  ( $\text{CDCl}_3$ , 128.3 MHz)  $\delta$  30.2. HRMS (ESI) for  $\text{C}_{15}\text{H}_{27}\text{BO}_3$   $[\text{M}+\text{H}]^+$ : calculated: 267.2123, found: 267.2134.

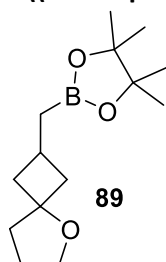
**2-((7-Oxaspiro[3.5]nonan-2-yl)methyl)-5,5-dimethyl-1,3,2-dioxaborinane****86c**

Flash column chromatography (40:1 Hexane:EtOAc) yielded **86c** (neop) (54% yield) as a yellowish oil.  $^1\text{H NMR}$  ( $\text{CDCl}_3$ , 400 MHz)  $\delta$  3.65 (m, 2H), 3.56 (s, 4H), 3.51 (m, 2H), 2.36 (sep,  $J = 8.0$  Hz, 1H), 2.92 (m, 2H), 1.62 – 1.58 (m, 2H), 1.49 (m, 2H), 1.38 (m, 2H), 0.93 (s, 6H), 0.88 (d,  $J = 7.8$  Hz, 2H).  $^{13}\text{C}$   $\{^1\text{H}\}$  NMR ( $\text{CDCl}_3$ , 100 MHz)  $\delta$  71.9, 65.0, 64.7, 63.9, 41.0, 40.7, 37.6, 37.3, 32.8, 31.6, 25.2, 21.8.  $^{11}\text{B NMR}$  ( $\text{CDCl}_3$ , 128.3 MHz)  $\delta$  34.6. HRMS (ESI) for  $\text{C}_{14}\text{H}_{25}\text{BO}_3$   $[\text{M}+\text{H}]^+$ : calculated: 253.1975, found: 253.1976.

**2-((7-Oxaspiro[3.5]nonan-2-yl)methyl)-5,5-dimethyl-1,3,2-dioxaborinane****87**

Flash column chromatography (40:1 Hexane:EtOAc) yielded **87** (85% yield) as a yellowish oil.  $^1\text{H NMR}$  ( $\text{CDCl}_3$ , 400 MHz)  $\delta$  3.62 (m, 4H), 2.09 (m, 1H), 1.82 (m, 2H), 1.51 (m, 2H), 1.43 (m, 4H), 1.23 (s, 12H), 1.18 (m, 2H), 0.83 (m, 2H).  $^{13}\text{C}$   $\{^1\text{H}\}$  NMR ( $\text{CDCl}_3$ , 100 MHz)  $\delta$  82.8, 65.7, 65.4, 47.9, 40.1, 39.8, 38.9, 37.9, 34.8, 33.7, 24.8, 24.7.  $^{11}\text{B NMR}$  ( $\text{CDCl}_3$ , 128.3 MHz)  $\delta$  34.7. HRMS (ESI) for  $\text{C}_{14}\text{H}_{25}\text{BO}_3$   $[\text{M}+\text{H}]^+$ : calculated: 298.2548, found:

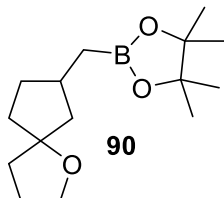
298.2557.

**2-((5-Oxaspiro[3.4]octan-2-yl)methyl)-4,4,5,5-tetramethyl-1,3,2-dioxaborolane****89**

Flash column chromatography (40:1 Hexane:EtOAc) yielded **89** (45% yield) as a yellowish oil, as a mixture of diastereoisomers 1:1 (a:a').  $^1\text{H NMR}$  ( $\text{CDCl}_3$ , 400 MHz)  $\delta$  3.75 (m, 2Ha + 2Ha'), 2.41 (m, 1Ha + 1Ha'), 2.17 (m, 1Ha + 1Ha'), 1.86 (m, 4Ha), 1.82 (m, 4Ha'), 1.70 (m, 1Ha + 1Ha'), 1.25 (apparent s, 2Ha), 1.24 (apparent s, 2Ha'), 1.22 (s, 12Ha), 1.22 (s, 12Ha'), 0.99 (d,  $J = 4.9$  Hz, 2Ha), 0.96 (d,  $J = 4.9$  Hz, 2Ha').  $^{13}\text{C}$   $\{^1\text{H}\}$  NMR ( $\text{CDCl}_3$ , 100 MHz)  $\delta$  82.9, 81.9, 79.3, 67.0, 66.2, 44.1, 42.2, 38.3, 36.4, 29.7, 25.0, 24.8, 23.2, 22.5, 1.2.  $^{11}\text{B NMR}$

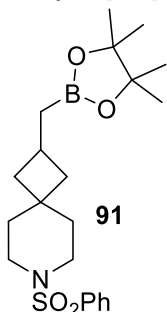
(CDCl<sub>3</sub>, 128.3 MHz) δ 34.5. HRMS (ESI) for C<sub>14</sub>H<sub>25</sub>BO<sub>3</sub> [M+H]<sup>+</sup>: calculated: 253.1975, found: 253.1976.

### 2-((1-Oxaspiro[4.4]nonan-7-yl)methyl)-4,4,5,5-tetramethyl-1,3,2-dioxaborolane



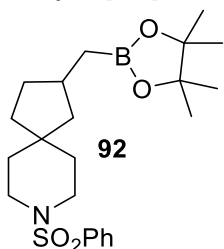
Flash column chromatography (40:1 Hexane:EtOAc) yielded **90** (54% yield) as a yellowish oil, as a mixture of diastereoisomers 6:1 (a:a'). <sup>1</sup>H NMR (CDCl<sub>3</sub>, 400 MHz) δ 3.77 (m, 2Ha + 2Ha'), 2.27 (m, 1Ha + 1Ha'), 2.00 (m, 1Ha + 1Ha'), 1.87 (m, 1Ha + 1Ha'), 1.76 (m, , 4Ha + 4Ha'), 1.52 (m, 2Ha + 2Ha'), 1.37 (m, 2Ha + 2Ha'), 1.23 (s, 12Ha + 12Ha'), 0.90 (d, J = 7.0 Hz, 2Ha), 0.83 (d, J = 7.5 Hz, 2Ha'). <sup>13</sup>C {<sup>1</sup>H} NMR (CDCl<sub>3</sub>, 100 MHz) δ 90.6, 82.8, 66.5, 66.4, 47.5, 47.2, 38.3, 37.6, 36.8, 34.7, 34.4, 33.7, 33.5, 29.7, 25.8, 25.7, 24.8. <sup>11</sup>B NMR (CDCl<sub>3</sub>, 128.3 MHz) δ 34.4. HRMS (ESI) for C<sub>17</sub>H<sub>27</sub>BO<sub>3</sub> [M+H]<sup>+</sup>: calculated: 267.2123, found: 267.2134.

### 7-(Phenylsulfonyl)-2-((4,4,5,5-tetramethyl-1,3,2-dioxaborolan-2-yl)methyl)-7-azaspiro[3.5]nonane



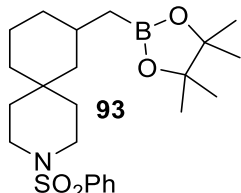
Flash column chromatography (20:1 Hexane:EtOAc) yielded **91** (93% yield) as a yellowish oil. <sup>1</sup>H NMR (CDCl<sub>3</sub>, 400 MHz) δ 7.72 (apparent d, J = 8.0 Hz, 2H), 7.57 (m, 1H), 7.50 (m, 2H), 2.95 (t, J = 5.7 Hz, 2H), 2.85 (t, J = 5.7 Hz, 2H), 2.40 – 2.25 (sep, J = 8.0 Hz, 1H), 1.85 (m, 2H), 1.67 (t, J = 5.4 Hz, 2H), 1.54 (t, J = 5.4 Hz, 2H), 1.29 – 1.21 (m, 4H), 1.18 (s, 12H), 0.88 (d, J = 7.8 Hz, 2H). <sup>13</sup>C {<sup>1</sup>H} NMR (CDCl<sub>3</sub>, 100 MHz) δ 136.4, 132.5, 128.9, 127.5, 82.8, 43.3, 43.0, 39.9, 38.9, 35.5, 32.9, 24.9, 24.7. <sup>11</sup>B NMR (CDCl<sub>3</sub>, 128.3 MHz) δ 34.2. HRMS (ESI) for C<sub>21</sub>H<sub>32</sub>BNO<sub>4</sub>S [M]<sup>+</sup>: calculated: 404.2181, found: 404.2179.

### 8-(Phenylsulfonyl)-2-((4,4,5,5-tetramethyl-1,3,2-dioxaborolan-2-yl)methyl)-8-azaspiro[4.5]decane

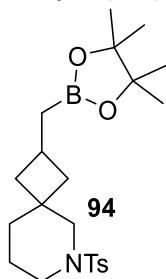


Flash column chromatography (20:1 Hexane:EtOAc to 15:1 Hexane: EtOAc) yielded **92** (60% yield) as a colorless oil. <sup>1</sup>H NMR (CDCl<sub>3</sub>, 400 MHz) δ 7.72 (d, J = 7.0 Hz, 2H), 7.55 (m, 1H), 7.53 – 7.46 (m, 2H), 3.00 – 2.83 (m, 4H), 2.06 – 1.90 (m, 1H), 1.79 – 1.68 (m, 1H), 1.60 – 1.52 (m, 2H), 1.49 (m, 3H), 1.34 (m, 1H), 1.24 (m, 2H), 1.16 (s, 12H), 1.13 – 0.95 (m, 2H), 0.77 – 0.72 (m, 2H). <sup>13</sup>C {<sup>1</sup>H} NMR (CDCl<sub>3</sub>, 100 MHz) δ 136.1, 132.5, 128.9, 127.6, 82.9, 46.9, 44.0, 43.8, 40.1, 38.1, 37.4, 37.0, 34.7, 33.6, 24.7. <sup>11</sup>B {<sup>1</sup>H} NMR (CDCl<sub>3</sub>, 128.3 MHz) δ 35.2. HRMS (ESI) for C<sub>22</sub>H<sub>35</sub>BNO<sub>4</sub>S [M+H]<sup>+</sup>: calculated: 420.2376, found: 420.2378.

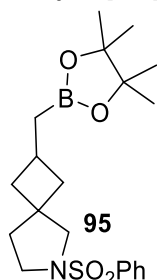
## Experimental part

**3-(Phenylsulfonyl)-8-((4,4,5,5-tetramethyl-1,3,2-dioxaborolan-2-yl)methyl)-3-azaspiro[5.5]undecane**

Flash column chromatography (20:1 pentane:EtOAc) yielded **93** (35% yield) as a colorless oil.  $^1\text{H NMR}$  ( $\text{CDCl}_3$ , 400 MHz)  $\delta$  7.76 (dd,  $J = 8.3, 1.3$  Hz, 2H), 7.61 (m, 1H), 7.54 (m, 2H), 3.00 (m, 4H), 1.61 (m, 4H), 1.36 (m, 4H), 1.23 (s, 12H), 0.88 (m, 4H), 0.72 (m, 3H).  $^{13}\text{C}$   $\{^1\text{H}\}$  NMR ( $\text{CDCl}_3$ , 100 MHz)  $\delta$  136.2, 132.8, 129.1, 127.5, 82.9, 41.8, 41.2, 35.1, 34.4, 32.9, 32.7, 29.7, 29.3, 24.8, 23.8, 22.7, 22.0.  $^{11}\text{B}$   $\{^1\text{H}\}$  NMR ( $\text{CDCl}_3$ , 128.3 MHz)  $\delta$  35.0. HRMS (ESI) for  $\text{C}_{23}\text{H}_{37}\text{BNO}_4\text{S}$   $[\text{M}]^+$ : calculated: 434.2538, found: 434.2535.

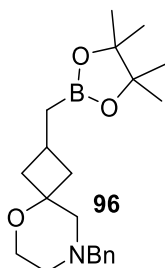
**2-((4,4,5,5-Tetramethyl-1,3,2-dioxaborolan-2-yl)methyl)-6-tosyl-6-azaspiro[3.5]nonane**

Flash column chromatography (20:1 pentane:EtOAc) yielded **94** (62% yield) as a white solid, as a mixture of diastereoisomers 1:1 (a:a').  $^1\text{H NMR}$  ( $\text{CDCl}_3$ , 400 MHz)  $\delta$  7.60 (m, 2Ha + 2Ha'), 7.29 (m, 2Ha + 2Ha'), 2.82 (m, 2Ha + 2Ha'), 2.45 (m, 1Ha), 2.41 (s, 3Ha), 2.40 (s, 3Ha'), 2.36 (m, 1Ha'), 2.06 (m, 2Ha), 1.89 (m, 2Ha'), 1.60 (m, 2Ha), 1.52 (m, 2Ha'), 1.37 (m, 6Ha + 6Ha'), 1.21 (s, 12Ha + 12Ha'), 0.94 (apparent t, 2Ha + 2Ha').  $^{13}\text{C}$   $\{^1\text{H}\}$  NMR ( $\text{CDCl}_3$ , 100 MHz)  $\delta$  143.1, 133.3, 133.1, 129.5, 127.6, 82.9, 57.5, 55.1, 46.4, 39.0, 38.9, 37.5, 34.2, 33.9, 29.6, 25.1, 25.0, 24.8, 21.8, 21.6, 21.5.  $^{11}\text{B}$  NMR ( $\text{CDCl}_3$ , 128.3 MHz)  $\delta$  35.4. HRMS (ESI) for  $\text{C}_{22}\text{H}_{35}\text{BNO}_4\text{S}$   $[\text{M}+\text{H}]^+$ : calculated: 420.2379, found: 420.2378.

**6-(Phenylsulfonyl)-2-((4,4,5,5-tetramethyl-1,3,2-dioxaborolan-2-yl)methyl)-6-azaspiro[3.4]octane**

Flash column chromatography (20:1 pentane:EtOAc) yielded **95** (60% yield) as a white solid, as a mixture of diastereoisomers 1:1 (a:a').  $^1\text{H NMR}$  ( $\text{CDCl}_3$ , 400 MHz)  $\delta$  7.79 (m, 2Ha + 2Ha'), 7.54 (m, 1Ha + 1Ha'), 7.49 (m, 2Ha + 2Ha'), 3.25 (t,  $J = 6.8$  Hz, 2Ha), 3.21 (s, 2Ha), 3.19 (apparent t, 2Ha'), 3.09 (s, 2Ha'), 2.28 (m, 1Ha + 1Ha'), 1.83 (m, 2Ha + 2Ha'), 1.75 (t,  $J = 7.0$  Hz, 2Ha), 1.65 (t,  $J = 7.0$  Hz, 2Ha'), 1.41 (m, 2Ha + 2Ha'), 1.17 (s, 12Ha + 12Ha'), 0.85 (d,  $J = 7.7$  Hz, 2Ha), 0.83 (d,  $J = 7.6$  Hz, 2Ha').  $^{13}\text{C}$   $\{^1\text{H}\}$  NMR ( $\text{CDCl}_3$ , 100 MHz)  $\delta$  136.9, 132.4, 128.8, 127.3, 82.8, 59.2, 58.6, 46.8, 46.5, 41.2, 40.8, 39.4, 39.3, 38.5, 37.0, 29.6, 26.0, 25.4, 24.7.  $^{11}\text{B}$  NMR ( $\text{CDCl}_3$ , 128.3 MHz)  $\delta$  33.8. HRMS (ESI) for  $\text{C}_{20}\text{H}_{31}\text{BNO}_4\text{S}$   $[\text{M}+\text{H}]^+$ : calculated: 392.2064, found: 392.2065.

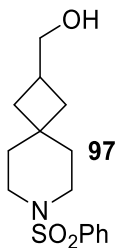
### 8-Benzyl-2-((4,4,5,5-tetramethyl-1,3,2-dioxaborolan-2-yl)methyl)-5-oxa-8-azaspiro[3.5]nonane



96

Flash column chromatography (20:1 pentane:EtOAc) yielded **96** (68% yield) as a white solid, as a pure isomer. The other isomer was isolated as a mixture of the two isomers in a ratio 4:6.  $^1\text{H NMR}$  ( $\text{CDCl}_3$ , **400 MHz**)  $\delta$  7.39 – 7.21 (m, 5H), 3.65 – 3.55 (m, 2H), 3.49 (apparent s, 2H), 2.47 – 2.20 (m, 6H), 1.91 (sep,  $J = 7.9$  Hz, 1H), 1.58 (m, 2H), 1.24 – 1.19 (s, 12H), 0.98 (d,  $J = 7.7$  Hz, 2H).  $^{13}\text{C}$  { $^1\text{H}$ }  $\text{NMR}$  ( $\text{CDCl}_3$ , **100 MHz**)  $\delta$  138.3, 128.8, 128.2, 127.0, 82.9, 72.1, 62.9, 61.9, 60.2, 53.0, 40.2, 29.7, 24.7, 22.8.  $^{11}\text{B NMR}$  ( $\text{CDCl}_3$ , **128.3 MHz**)  $\delta$  35.4. **HRMS (ESI) for  $\text{C}_{21}\text{H}_{33}\text{BNO}_3$  [ $\text{M} + \text{H}$ ] $^+$** : calculated: 358.2552, found: 358.2552.

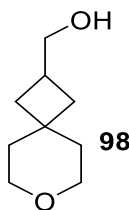
### (7-(Phenylsulfonyl)-7-azaspiro[3.5]nonan-2-yl)methanol



97

Flash column chromatography (6:1 pentane:DCM) yielded **97** (78% yield) as a white solid.  $^1\text{H NMR}$  ( $\text{CDCl}_3$ , **400 MHz**)  $\delta$  7.74 (m, 2H), 7.58 (m, 1H), 7.52 (m, 2H), 3.53 (d,  $J = 6.5$  Hz, 2H), 2.96 (m, 2H), 2.88 (m, 2H), 2.38 (sep,  $J = 7.4$  Hz, 1H), 1.75 (m, 2H), 1.70 (m, 2H), 1.59 (m, 2H), 1.42 (m, 2H).  $^{13}\text{C}$  { $^1\text{H}$ }  $\text{NMR}$  ( $\text{CDCl}_3$ , **100 MHz**)  $\delta$  136.2, 132.6, 128.9, 127.5, 67.4, 43.1, 42.87, 38.3, 36.0, 33.8, 33.1, 30.2. **HRMS (ESI) for  $\text{C}_{15}\text{H}_{22}\text{NO}_3\text{S}$  [ $\text{M} + \text{H}$ ] $^+$** : calculated: 296.1315, found: 296.1315.

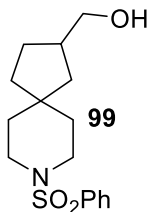
### (7-Oxaspiro[3.5]nonan-2-yl)methanol



98

Flash column chromatography (6:4 pentane:DCM) yielded **98** (83% yield) as a yellowish oil.  $^1\text{H NMR}$  ( $\text{CDCl}_3$ , **400 MHz**)  $\delta$  3.67 (m, 4H), 3.54 (m, 2H), 2.26 (sep,  $J = 7.7$  Hz, 1H), 1.81 (m, 2H), 1.51 (m, 4H), 1.34 (m, 2H).  $^{13}\text{C}$  { $^1\text{H}$ }  $\text{NMR}$  ( $\text{CDCl}_3$ , **100 MHz**)  $\delta$  67.8, 64.7, 64.4, 40.0, 37.7, 34.7, 33.2, 30.4. **HRMS (ESI) for  $\text{C}_9\text{H}_{16}\text{O}_2$  [ $\text{M} + \text{Na}$ ] $^+$** : calculated: 179.1047, found: 179.1057.

### (8-(Phenylsulfonyl)-8-azaspiro[4.5]decan-2-yl)methanol



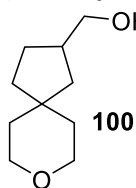
99

Flash column chromatography (6:1 pentane:DCM) yielded **99** (65% yield) a colorless oil.  $^1\text{H NMR}$  ( $\text{CDCl}_3$ , **400 MHz**)  $\delta$  7.73 (m, 2H), 7.60 (m, 1H), 7.50 (m, 2H), 3.47 (m, 2H), 3.03 (m, 2H), 2.92 (m, 2H), 2.13 (sep,  $J = 7.4$  Hz, 1H), 1.70 (m, 1H), 1.55 (m, 5H), 1.35 (m, 1H), 1.28 (m, 1H), 0.95 (m, 1H).  $^{13}\text{C}$  { $^1\text{H}$ }  $\text{NMR}$  ( $\text{CDCl}_3$ , **100 MHz**)  $\delta$  136.1, 132.6, 128.9, 127.6, 67.2, 44.0, 43.7, 40.9, 40.5, 40.4, 37.6, 37.0, 36.3, 27.3. **HRMS (ESI) for  $\text{C}_{16}\text{H}_{24}\text{NO}_3\text{S}$  [ $\text{M} + \text{H}$ ] $^+$** : calculated: 310.1472, found:

310.1471.

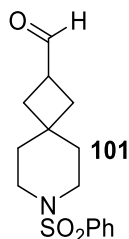
## Experimental part

### (8-Oxaspiro[4.5]decan-2-yl)methanol



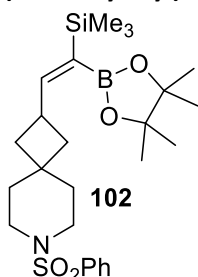
Flash column chromatography (6:4 pentane:DCM) yielded **100** (86% yield) as a yellowish oil.  $^1\text{H NMR}$  ( $\text{CDCl}_3$ , 400 MHz)  $\delta$  3.63 (m, 4H), 3.55 (m, 2H), 2.47 (sep,  $J = 7.5$  Hz, 1H), 1.92 (m, 2H), 1.63 (m, 2H), 1.53 (m, 6H).  $^{13}\text{C}$   $\{^1\text{H}\}$  NMR ( $\text{CDCl}_3$ , 100 MHz)  $\delta$  67.5, 65.6, 65.3, 41.0, 40.3, 39.1, 38.0, 27.5. HRMS (ESI) for  $\text{C}_{10}\text{H}_{18}\text{O}_2$   $[\text{M} + \text{Na}]^+$ : calculated: 193.1204, found: 193.1209.

### 7-(Phenylsulfonyl)-7-azaspiro[3.5]nonane-2-carbaldehyde



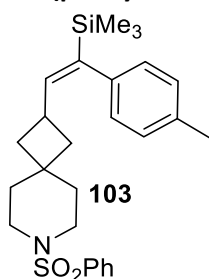
Flash column chromatography (3:1 Hexane:EtOAc) yielded **101** (62% yield) as a white solid.  $^1\text{H NMR}$  ( $\text{CDCl}_3$ , 400 MHz)  $\delta$  9.66 (d,  $J = 1.5$  Hz, 1H), 7.72 (m, 2H), 7.57 (m, 1H), 7.50 (m, 2H), 3.06 (sep,  $J = 7.6$  Hz, 1H), 2.94 (m, 2H), 2.87 (m, 2H), 1.89 (m, 4H), 1.70 (m, 2H), 1.55 (m, 2H).  $^{13}\text{C}$   $\{^1\text{H}\}$  NMR ( $\text{CDCl}_3$ , 100 MHz)  $\delta$  202.2, 136.1, 132.7, 129.0, 127.5, 42.9, 42.7, 39.0, 37.0, 36.1, 33.9, 31.3. HRMS (ESI) for  $\text{C}_{15}\text{H}_{20}\text{NO}_3\text{S}$   $[\text{M} + \text{H}]^+$ : calculated: 294.1160, found: 294.1158.

### E-7-(Phenylsulfonyl)-2-(2-(4,4,5,5-tetramethyl-1,3,2-dioxaborolan-2-yl)-2-(trimethylsilyl)vinyl)-7-azaspiro[3.5]nonane



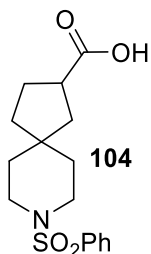
Flash column chromatography (40:1 pentane:EtOAc) yielded **102** (88% yielding in a mixture of diastereoisomers 85:15) as a colorless solid. Major isomer was possible to be isolated exclusively.  $^1\text{H NMR}$  ( $\text{CDCl}_3$ , 400 MHz)  $\delta$  7.72 (m, 2H), 7.54 (m, 1H), 7.49 (m, 2H), 6.34 (d,  $J = 8.3$  Hz, 1H), 3.16 (m, 1H), 2.94 (m, 2H), 2.85 (m, 2H), 1.94 – 1.79 (m, 2H), 1.66 (m, 2H), 1.56 (m, 2H), 1.48 (m, 2H), 1.20 (s, 12H), 0.05 (s, 9H).  $^{13}\text{C}$   $\{^1\text{H}\}$  NMR ( $\text{CDCl}_3$ , 100 MHz)  $\delta$  164.9, 160.8, 136.1, 132.5, 128.9, 128.9, 127.5, 82.9, 43.1, 42.9, 38.4, 38.2, 35.5, 33.7, 33.3, 24.7, 1.0.  $^{11}\text{B}$  NMR (129 MHz,  $\text{cdcl}_3$ )  $\delta$  32.8.  $^{29}\text{Si}$  NMR (80 MHz,  $\text{cdcl}_3$ )  $\delta$  -4.01. HRMS (ESI) for  $\text{C}_{25}\text{H}_{41}\text{BNO}_4\text{SSi}$   $[\text{M} + \text{H}]^+$ : calculated: 490.2618, found: 490.2618.

### E-7-(phenylsulfonyl)-2-(2-(p-tolyl)-2-(trimethylsilyl)vinyl)-7-azaspiro[3.5]nonane



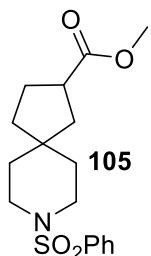
Flash column chromatography (30:1 pentane:EtOAc) yielded **103** (81% yielding in a mixture of diastereoisomers 85:15) as a white solid.  $^1\text{H NMR}$  ( $\text{CDCl}_3$ , 400 MHz)  $\delta$  7.71 (m, 2H), 7.59 (m, 1H), 7.50 (m, 2H), 7.04 (m, 2H), 6.75 (m, 2H), 5.90 (d,  $J = 8.8$  Hz, 1H), 2.88 (m, 4H), 2.75 (m, 1H), 2.30 (s, 3H), 1.75 (m, 2H), 1.58(m, 4H), 1.45 (m, 2H), 0.03 (m, 9H).  $^{13}\text{C}$   $\{^1\text{H}\}$  NMR ( $\text{CDCl}_3$ , 100 MHz)  $\delta$  150.9, 145.9, 143.4, 139.1, 136.3, 134.6, 132.6, 128.9, 128.6, 128.4, 127.5, 127.2, 43.1, 43.0, 38.8, 38.6, 35.3, 33.3, 28.5, 21.1, -1.5.  $^{29}\text{Si}$  NMR (80 MHz,  $\text{CDCl}_3$ )  $\delta$  -5.13. HRMS (ESI) for  $\text{C}_{26}\text{H}_{36}\text{NO}_2\text{SSi}$   $[\text{M} + \text{H}]^+$ : calculated: 454.2231, found: 454.2231.

### 8-(Phenylsulfonyl)-8-azaspiro[4.5]decane-2-carboxylic acid



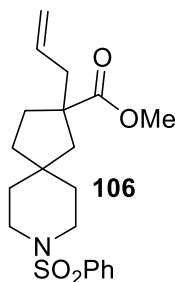
Work up purification mentioned previously yielded **104** (73% yield) as a colorless oil.  $^1\text{H NMR}$  ( $\text{CDCl}_3$ , 400 MHz)  $\delta$  7.74 (d,  $J = 7.3$  Hz, 2H), 7.60 (m, 1H), 7.53 (m, 2H), 3.02 (m, 2H), 2.91 (m, 2H), 2.80 (m, 1H), 1.90 (m, 2H), 1.86 (m, 7H), 0.90 – 0.81 (m, 1H).  $^{13}\text{C}$   $\{^1\text{H}\}$  NMR ( $\text{CDCl}_3$ , 100 MHz)  $\delta$  182.2, 136.0, 132.7, 129.0, 127.6, 44.0, 43.7, 42.5, 40.8, 40.2, 37.1, 36.7, 36.1, 28.0. HRMS (ESI) for  $\text{C}_{16}\text{H}_{22}\text{NO}_4\text{S}$   $[\text{M}+\text{H}]^+$ : calculated 324.1264, found: 324.1264.

### Methyl 8-(phenylsulfonyl)-8-azaspiro[4.5]decane-2-carboxylate



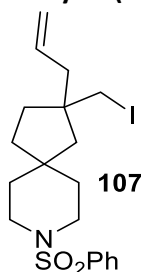
After work up, without purification it was recovered **105** (61% yield) as a colorless oil. It was only checked by  $^1\text{H NMR}$  to see if the esterification process occurred.  $^1\text{H NMR}$  ( $\text{CDCl}_3$ , 400 MHz)  $\delta$  7.73 (m, 2H), 7.58 (m, 1H), 7.53 (m, 2H), 3.61 (s, 3H), 3.04 (m, 2H), 2.90 (m, 2H), 2.77 (m, 1H), 1.83 (m, 2H), 1.49 (m, 8H).

### Methyl 2-allyl-8-(phenylsulfonyl)-8-azaspiro[4.5]decane-2-carboxylate



Flash column chromatography (5:1 Hexane:EtOAc) yielded **106** (51% yield) as a colorless oil.  $^1\text{H NMR}$  ( $\text{CDCl}_3$ , 400 MHz)  $\delta$  7.68 (dd,  $J = 8.1, 1.0$  Hz, 2H), 7.52 (m, 1H), 7.46 (m, 2H), 5.53 (m, 1H), 4.91 (m, 2H), 3.54 (s, 3H), 2.98 (m, 2H), 2.81 (m, 2H), 2.23 (m, 2H), 2.04 (m, 1H), 1.96 (d,  $J = 13.7$  Hz, 1H), 1.49 (m, 5H), 1.35 (m, 2H), 1.15 (d,  $J = 13.9$  Hz, 1H).  $^{13}\text{C}$   $\{^1\text{H}\}$  NMR ( $\text{CDCl}_3$ , 100 MHz)  $\delta$  177.4, 136.0, 134.1, 132.6, 128.9, 127.5, 117.7, 53.6, 51.8, 45.6, 44.1, 43.9, 43.7, 40.4, 37.7, 36.7, 36.5, 33.8. HRMS (ESI) for  $\text{C}_{20}\text{H}_{28}\text{NO}_4\text{S}$   $[\text{M}+\text{H}]^+$ : calculated: 378.1733, found: 378.1734.

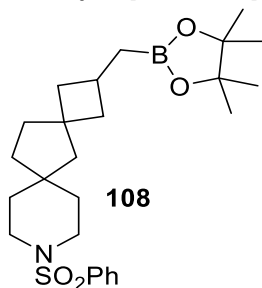
### 2-Allyl-2-(iodomethyl)-8-(phenylsulfonyl)-8-azaspiro[4.5]decane



Flash column chromatography (5:1 Hexane:EtOAc to 3:1 Hexane:EtOAc) yielded **107** (70% yield) as a colorless oil.  $^1\text{H NMR}$  ( $\text{CDCl}_3$ , 400 MHz)  $\delta$  7.72 (m, 2H), 7.57 (m, 1H), 7.51 (m, 2H), 5.60 (m, 1H), 5.07 (m, 2H), 3.16 (d,  $J = 9.8$  Hz, 1H), 3.13 (d,  $J = 9.8$  Hz, 1H), 2.99 (m, 2H), 2.89 (m, 2H), 1.61 – 1.49 (m, 6H), 1.44 (dd,  $J = 10.7, 3.7$  Hz, 2H), 1.37 (dd,  $J = 14.2$  Hz, 1H), 1.21 (t,  $J = 7.1$  Hz, 1H).  $^{13}\text{C}$   $\{^1\text{H}\}$  NMR ( $\text{CDCl}_3$ , 100 MHz)  $\delta$  136.1, 133.9, 132.7, 129.0, 127.5, 118.6, 48.0, 45.6, 44.4, 43.7, 43.7, 40.7, 37.8, 37.7, 36.6, 35.5, 22.6. HRMS (ESI) for  $\text{C}_{19}\text{H}_{27}\text{INO}_2\text{S}$   $[\text{M}+\text{H}]^+$ : calculated: 460.0806, found: 460.0802.



## Experimental part

**9-(Phenylsulfonyl)-2-((4,4,5,5-tetramethyl-1,3,2-dioxaborolan-2-yl)methyl)-9-azadispiro[3.1.56.24]tridecane**

Flash column chromatography (20:1 Hexane:EtOAc) yielded **108** (64% yield) as a yellowish oil, as a mixture of diastereoisomers 1:1 (a:a').  $^1\text{H NMR}$  ( $\text{CDCl}_3$ , 400 MHz)  $\delta$  7.76 (m, 2Ha + 2Ha'), 7.66 – 7.57 (m, 1Ha + 1Ha'), 7.57 – 7.51 (m, 2Ha + 2Ha'), 3.02 (m, 2Ha + 2Ha'), 2.97 – 2.82 (m, 2Ha + 2Ha'), 2.31 (sep,  $J = 8.5$  Hz, 1Ha + 1Ha'), 1.98 (m, 2Ha + 2Ha'), 1.65 (apparent t, 2Ha), 1.60 (s, 2Ha + 2Ha'), 1.52 (m, 6Ha + 6Ha'), 1.35 (apparent t, 2Ha'), 1.30 (m, 2Ha + 2Ha'), 1.22 (s, 12Ha + 12Ha'), 0.88 (apparent t, 2Ha + 2Ha').  $^{13}\text{C}$

$\{^1\text{H}\}$  NMR ( $\text{CDCl}_3$ , 100 MHz)  $\delta$  136.1, 132.5, 128.9, 127.6, 82.8, 52.3, 51.0, 43.9, 43.4, 43.2, 39.8, 39.6, 37.7, 37.7, 36.7, 29.6, 26.4, 24.7.  $^{11}\text{B NMR}$  ( $\text{CDCl}_3$ , 128.3 MHz)  $\delta$  34.7. HRMS (ESI) for  $\text{C}_{25}\text{H}_{39}\text{BNO}_4\text{S}$   $[\text{M}+\text{H}]^+$ : calculated: 460.2693, found: 460.2692.

## 8.4. Experimental procedures and spectral data of Chapter 5

### 8.4.1 Specific procedure for the synthesis of central core 112

To a solution of the pyrrolidine methyl ester **117** (103 mmol, 1 equiv) in DCM (171 mL), followed by the addition of Et<sub>3</sub>N (309 mmol, 3 equiv) and di-*tert*-butyl dicarbonate (103 mmol, 1 equiv,) at 0 °C. Then the mixture was stirred at room temperature for 72 h. The mixture was diluted in DCM and treated with water. The suspension was filtered over a celite pad and washed with DCM. The organic layers were separated, dried (MgSO<sub>4</sub>), filtered and evaporated *in vacuo*. The crude product was purified by flash column chromatography.<sup>[14]</sup>

To the corresponding solution of the protected methyl ester **118** (10 g, 1 equiv, 44 mmol) in 2-Me-THF (200 mL), LiHMDS 1 M in hexane (66 mL, 66 mmol, 1.5 equiv) was added dropwise at -78 °C and stirred for 10 minutes. Then allyl bromide (7.6 mL, 87 mmol, 2 equiv) was added at -78 °C and stirred for 30 min. at the same temperature. Then the mixture was warmed up to room temperature. After completion, the reaction was quenched with NH<sub>4</sub>Cl sat. at 0 °C and diluted with EtOAc. The organic layers were separated, dried (MgSO<sub>4</sub>), filtered and the solvents evaporated *in vacuo*. The crude was purified by flash column chromatography.<sup>[15]</sup>

The alkylated intermediate **119** (6 g, 1 equiv, 22 mmol) in THF (103 mL), LiBH<sub>4</sub> (11 mmol, 3 equiv) was added dropwise at 0 °C. The mixture was stirred for 2 h at room temperature. Then more LiBH<sub>4</sub> was added (11 mmol, 3 equiv) and stirred for 16 h. The mixture was treated with water and extracted with EtOAc. The organic layers were separated, dried (MgSO<sub>4</sub>), filtered and the solvents evaporated *in vacuo* to yield the product **120** as a clear oil.<sup>[16]</sup>

To a solution of triphenylphosphine (122 mmol, 1.1 equiv) and imidazole (122 mmol, 1.1 equiv) in toluene (160 mL) iodine (122 mmol, 1.1 equiv) was added and stirred for 30 min. at room temperature. Then intermediate **120** (9.9 g, 1 equiv, 41 mmol) was added, and the reaction mixture was heated to 80 °C and stirred for 16 h. The solution was quenched with H<sub>2</sub>O, extracted with EtOAc for three times and washed with Na<sub>2</sub>S<sub>2</sub>O<sub>3</sub> sat. The organic extracts were then dried (MgSO<sub>4</sub>), filtered and concentrated *in vacuo*. The crude product was purified by flash chromatography to deliver product **121** in 60% isolated yield.<sup>[6]</sup>

## Experimental part

---

Copper chloride (5 mol%, 0.147 mmol), bis(pinacolato)diboron (3.5 mmol, 1.2 equiv) and Xantphos (5 mol%, 0.147 mmol) were placed in an oven-dried reaction vial. The vial was sealed with a screw cap containing a teflon-coated rubber septum. The vial was connected to a vacuum/nitrogen manifold through a needle, evacuated and backfilled with nitrogen and THF (3.5 mL, 1 M). KO<sup>t</sup>Bu (3.5 mmol, 1.2 equiv, 1M in THF) was added to the vial through the rubber septum. Then, the alkenyl halide **121** (2.9 mmol, 1 equiv) in THF (3.5 mL, 1 M) was added dropwise at 30 °C. After the reaction was complete (around 16 h), the reaction mixture was filtered over celite. The organic extracts were then concentrated *in vacuo*. The crude product was purified by flash column chromatography to produce **112** in 60% isolated yield in a diastereomeric ratio of 45 to 55.<sup>[17]</sup>

### 8.4.2 Specific procedure for the synthesis of central core 113

To a solution of the pyrrolidin-2-one (**122**) (73 mmol, 1 equiv) in ACN (139 mL) was added di-*tert*-butyl dicarbonate (88 mmol, 1.2 equiv) at 0°C. Then the mixture was stirred at room temperature for 16 h. The reaction mixture was diluted in EtOAc and treated with water. The suspension was filtered over a celite pad and washed with EtOAc. The organic layers were separated, dried (MgSO<sub>4</sub>), filtered and evaporated *in vacuo*. The crude product was purified by flash column chromatography to yield **123** in 75%.<sup>[14]</sup>

To a solution of LHMDS (115 mmol, 2.1 equiv) 1 M in hexane in THF (40 mL) at -78°C was added dropwise intermediate **123** (55 mmol, 1 equiv) in THF (40 mL), followed immediately by the addition of methyl chloroformate (55 mmol, 1 equiv) dropwise in THF (40 mL) and stirred for 5 min. at -78°C. After full conversion of compound **123**, HCl 1 M was added, until reach pH=1 and allowed to warm to room temperature. The biphasic mixture was extracted with EtOAc. The organic layers were separated, dried (MgSO<sub>4</sub>), filtered and the solvents evaporated *in vacuo*. The crude product was purified by flash column chromatography yielding **124** in 85%.<sup>[18]</sup>

Then a solution of 1-(*tert*-butyl) 3-methyl 2-oxopyrrolidine-1,3-dicarboxylate (**124**) (47 mmol, 1 equiv) in acetone (300 mL) was added 4-bromo-1-butene (70 mmol, 1.5 equiv), K<sub>2</sub>CO<sub>3</sub> (169 mmol, 3.6 equiv), tetrabutylammonium bromide (10mmol, 2 equiv) at room temperature. Then the mixture was warmed up to 60 °C to reflux. After 2 h an extra amount of 4-bromo-1-butene (70 mmol, 1.5 equiv) was added and stirred at 60 °C for 2 h more. Then an extra amount of 4-bromo-1-butene (140 mmol, 3 equiv) was added and refluxed for 16 h (the extra addition of 4-bromo-1-butene should be added at room temperature). After full conversion of the substrate, the

volatiles were evaporated and the residue purified by flash column chromatography providing **125** in 90% isolated yield.<sup>[19]</sup>

To a solution of the alkylated product **125** (20 mmol, 1 equiv) in dioxane (24 mL) was added HCl 4 N in dioxane (120 mmol, 6 equiv) and stirred for 2 h at room temperature. After complete deprotection the solvent was evaporated *in vacuo*, the residue was dissolved in EtOAc and water and extracted with EtOAc many times. The organic layers were separated, dried (MgSO<sub>4</sub>), filtered and the solvents evaporated *in vacuo* to yield **126** in a 87%.<sup>[20]</sup>

To a solution of **126** (22 mmol, 1 equiv) in ACN (124 mL), was added Cs<sub>2</sub>CO<sub>3</sub> (56 mmol, 2.5 equiv) followed by bromomethylbenzene (33 mmol, 1.5 equiv), then the mixture was stirred at 90 °C in a sealed tube for 1h. The mixture was cool down and EtOAc was added, then the solid was filtered off through a celite pad. The solvent was evaporated *in vacuo* and the residue was purified by flash column chromatography to yield **127** in 79%.<sup>[21]</sup>

To a stirred solution of methyl 1-benzyl-3-(but-3-en-1-yl)-2-oxopyrrolidine-3-carboxylate (**127**) (12 mmol, 1 equiv) in THF (55 mL), was added LiAlH<sub>4</sub> (18 mmol, 1.5 equiv) at 0 °C and stirred for 2 h at room temperature. Then more LiAlH<sub>4</sub> (18 mmol, 1.5 equiv) was added at room temperature and stirred for 16 h more at the same temperature. The mixture was treated with water and then diluted with EtOAc. Then a solution of H<sub>2</sub>SO<sub>4</sub> (10% aq.) was added (in order to dissolve the aluminum salts). Then, it was extracted many times with EtOAc. The organic layers were separated. The aqueous phase was saturated with NaCl and extracted with EtOAc (until no observation of the product in the aqueous phase). The organic layers were combined and washed with NaHCO<sub>3</sub> sat., then the organic layers were separated, dried (MgSO<sub>4</sub>), filtered and the organic solvents removed *in vacuo* and the residue was purified by flash column chromatography.<sup>[4]</sup>

Then to a solution of triphenylphosphine (22 mmol, 1.1 equiv) and imidazole (22 mmol, 1.1 equiv) in toluene (32 mL) was added iodine (22 mmol, 1.1 equiv) and stirred for 30 minutes at room temperature. Then intermediate **128** (20 mmol, 1 equiv) was added, and the reaction mixture was heated to 80 °C and stirred for 16 h. The solution was quenched with H<sub>2</sub>O, extracted with EtOAc for three times and washed with Na<sub>2</sub>S<sub>2</sub>O<sub>3</sub> sat. The organic extracts were dried (MgSO<sub>4</sub>), filtered and concentrated *in vacuo*. The crude product was purified by flash chromatography to yield **129** in 45%.<sup>[6]</sup>

## Experimental part

---

Copper chloride (5 mol%, 0.1 mmol), bis(pinacolato)diboron (2.4 mmol, 1.2 equiv) and Xantphos (5 mol%, 0.1 mmol) were placed in an oven-dried reaction vial. The vial was sealed with a screw cap containing a teflon-coated rubber septum. The vial was connected to a vacuum/nitrogen manifold through a needle, evacuated and backfilled with nitrogen and THF (2.4 mL, 1 M). KO<sup>t</sup>Bu (2.4 mmol, 1.2 equiv, 1 M in THF) was added to the vial through the rubber septum. Then alkenyl halide **129** (2 mmol, 1 equiv) in THF (2.4 mL, 1 M) was added dropwise at 30 °C. After the reaction was complete (around 16 h), the reaction mixture was filtered over celite pad. The organic extracts were then concentrated *in vacuo*. The crude product was purified by flash column chromatography yielding **113** in 72%.<sup>[17]</sup>

### 8.4.3 Specific procedure for the synthesis of central core 114

To the corresponding solution of the *N*-Boc protected carboxylic piperidine **130** (93 mmol, 1 equiv) in THF (214 mL), LHMDS (121 mmol, 1.3 equiv, 1.06 M in hexane) was added dropwise at -78 °C and stirred for 10 min. Then allyl bromide (112 mmol, 1.2 equiv) was added at -78 °C and stirred for 30 min. at the same temperature. Then the mixture was warmed up to room temperature. After full conversion was quenched with NH<sub>4</sub>Cl sat. at 0 °C and diluted with EtOAc. The organic layers were separated, dried (MgSO<sub>4</sub>), filtered and the solvents evaporated *in vacuo*. The crude was purified by flash column chromatography providing **131** in 94% yield.<sup>[15]</sup>

The alkylated intermediate **131** (86 mmol, 1 equiv) in THF (402 mL), LiBH<sub>4</sub> (258 mmol, 3 equiv) was added dropwise at 0 °C. The mixture was stirred for 2 h at room temperature. Then more LiBH<sub>4</sub> was added (258 mmol, 3 equiv) and stirred for 16 h. The mixture was treated with water and extracted with EtOAc. The organic layer was separated, dried (MgSO<sub>4</sub>), filtered and the solvents evaporated *in vacuo* to yield the product **132** as a clear oil in 93% isolated yield.<sup>[16]</sup>

Then to a solution of triphenylphosphine (85 mmol, 1.1 equiv) and imidazole (85 mmol, 1.1 equiv) in toluene (113 mL) was added iodine (85 mmol, 1.1 equiv) and stirred for 30 min. at room temperature. Then intermediate **132** (78 mmol, 1 equiv) was added, and the reaction mixture was heated to 80 °C and stirred for 16 h. The solution was quenched with H<sub>2</sub>O, extracted with EtOAc for three times and washed with Na<sub>2</sub>S<sub>2</sub>O<sub>3</sub> sat. The organic extracts were dried (MgSO<sub>4</sub>), filtered and concentrated *in vacuo*. The crude product was purified by flash chromatography to yield **133** in 69%.<sup>[6]</sup>

Copper chloride (5 mol%, 3.1 mmol), bis(pinacolato)diboron (74 mmol, 1.2 equiv) and Xantphos (5 mol%, 3.1 mmol) were placed in an oven-dried reaction vial. The vial was sealed with a screw cap containing a teflon-coated rubber septum. The vial was connected to a vacuum/nitrogen manifold through a needle, evacuated and backfilled with nitrogen and THF (74 mL, 1 M).  $\text{KO}^t\text{Bu}$  (74 mmol, 1.2 equiv, 1 M in THF) was added to the vial through the rubber septum. Then alkenyl halide **133** (62 mmol, 1 equiv) in THF (74 mL, 1 M) was added dropwise at 30 °C. After the reaction was complete (around 16 h), the reaction mixture was filtered over celite pad. The organic extracts were then concentrated *in vacuo*. The crude product was purified by flash column chromatography yielding **114** in 55%.<sup>[17]</sup>

#### 8.4.4 General procedure for the synthesis of central core **115** and **116**<sup>[22]</sup>

Zinc dust (54 mmol, 2 equiv) was slowly added under vigorous stirring to a mixture of cyclopentanone (27 mmol, 1 equiv), allyl bromide (54 mmol, 2 equiv) in THF (8 mL, 16 M) and  $\text{NH}_4\text{Cl}$  sat. (27 mL, 5M) was added in such a way that the temperature did not exceed 40 °C. The mixture was then stirred for 10 h at room temperature. Then  $\text{H}_2\text{SO}_4$  (10% aq., 13 mL, 10M) was added, the mixture was filtered, the organic phase was separated, and the aqueous phase was saturated with NaCl and extracted with  $\text{Et}_2\text{O}$ . The extracts were combined, dried over anhydrous magnesium sulphate, then filtered and the volatiles evaporated under reduced pressure to yield a viscous black oil (for the synthesis of the central core **115** was not purified, however for the synthesis of the central core **116** was purified the intermediate **136** by flash chromatography).

Then was added  $\text{Na}_2\text{S}_2\text{O}_5$  (27 mmol, 1 equiv) in water (21 mL, 1.2 M) dropwise over a period of 2 h to a mixture of the viscous black oil,  $\text{NaIO}_4$  (1 equiv, 27 mmol), *tert*-butyl alcohol (40.5 mL), and water (35 mL) under stirring at 50 °C. The mixture was stirred for 10 h at 50 °C and for 10 h at room temperature, the dark brown organic layer was separated, and the aqueous phase was saturated with sodium chloride and extracted with ethyl acetate. The extracts were combined with the organic phase and washed with a saturated aqueous solution of sodium thiosulfate, the resulting colorless solution was dried ( $\text{MgSO}_4$ ) and the volatiles were removed under reduced pressure. The oily residue was purified by flash column chromatography.

#### 8.4.5 General procedure for the Suzuki-Miyaura coupling of methylene boronates with heteroaryl bromides catalysed by palladium<sup>[10]</sup>

On a microwave vial tube equipped with a stirring bar was charged with Pd(PPh<sub>3</sub>)<sub>4</sub> (3 mol%, 0.0159 mmol) and 1,4-dioxane (0.7 mL). To this solution the corresponding spiro-methylene boronate compound (0.53 mmol, 1 equiv), dissolved in 0.6 mL of 1,4-dioxane, 4-bromo-2,6-dimethylpyridine (1.58 mmol, 3 equiv) and a 3 M KOH solution (3 mmol, 6 equiv) were added in sequence and heated up at 90 °C for 16 h. After consumption of the substrate the mixture was cooled to room temperature and diluted in DCM. The reaction mixture was filtered through a small pad of celite and anhydrous MgSO<sub>4</sub>. Then the organic solvents were evaporated *in vacuo*. The crude was purified by flash column chromatography to yield the arylated spiro-compound.

#### 8.4.6 General procedure for the Suzuki-Miyaura coupling of secondary iodides and heteroaryl boronates catalyzed by nickel<sup>[23]</sup>

To a mixture of NiI<sub>2</sub> (6 mol%, 0.006 mmol), (1*R*,2*R*)-2-aminocyclohexanol hydrochloride (0.006 mmol, 0.06 equiv), the pyridine boronate derivative (0.229 mmol, 2 equiv,) NaHMDS (0.229 mmol, 2 equiv) in *i*PrOH (2 mL) under N<sub>2</sub> atmosphere and stirred for 10 min. at room temperature. Then the spiro-iodinated compound was added (0.114 mmol, 1 equiv) and irradiated under microwave at 80 °C for 1.5 – 3 h. After consumption of the substrate de mixture was cooled down and diluted in EtOH, filtered through a celite pad and the volatiles removed *in vacuo*. The crude was purified by flash column chromatography.

#### 8.4.7 General procedure of the arylation of ketones by lithiation<sup>[24]</sup>

To a solution of a commercially available bromo pyridine derivative (5.95 mmol, 1.5 equiv) in THF (10 mL) at -78 °C under N<sub>2</sub> atmosphere was added dropwise *n*BuLi (7.14 mmol, 1.8 equiv, 1.6 M in hexane) and stirred for 20 minutes at -78°C. Then the commercially available spiro-cyclic ketone (3.97 mmol, 1 equiv) in THF (10 mL) was added and stirred for 2 h at -78 °C. Then the reaction mixture was warmed up to room temperature and stirred for 20 minutes more. After consumption of the limiting reagent, NH<sub>4</sub>Cl sat. was added, followed by water and extracted with DCM. The organic layers were separated, dried (MgSO<sub>4</sub>), filtered and the solvent removed *in vacuo*. The crude was purified by flash column chromatography.

#### 8.4.8 General procedure for the O-arylation of alcohols with KO<sup>t</sup>Bu<sup>[25]</sup>

To a mixture of the spiro-cyclic alcohol (0.63 mmol, 1 equiv), KO<sup>t</sup>Bu (1.26 mmol, 2 equiv) in DMSO (1.26 mL) was added chloro pyridine derivative (1 mmol, 1.6 equiv) and stirred at 70 °C for 5 h. The mixture was cooled to room temperature and then water followed by EtOAc were added. The organic layer was separated, dried (MgSO<sub>4</sub>) and the volatiles evaporated *in vacuo*. The residue obtained was purified by flash column chromatography.

#### 8.4.9 General procedure for the O-arylation of alcohols with NaH<sup>[26]</sup>

To the corresponding solution spiro-cyclic alcohol (0.264 mmol, 1 equiv) in THF (1 mL) was added NaH 60% dispersion in oil (0.37 mmol, 1.4 equiv) at room temperature. The mixture was stirred during 40 min. Then chloro pyridine or pyrimidine derivative (0.31 mmol, 1.2 equiv) was added dropwise at 0 °C, and was stirred for 16 h at 40 °C. The mixture was treated with water and extracted many times with EtOAc. The organic layer was separated, dried (MgSO<sub>4</sub>), filtered and the solvents evaporated *in vacuo*. The crude was purified by flash column chromatography.

#### 8.4.10 General procedure for the deprotection of N-Boc amines with HCl<sup>[20]</sup>

The N-Boc protected spiro-compound (0.76 mmol, 1 equiv) in 1,4-dioxane (0.89 mL) at 0°C, was added HCl 4 M in 1,4-dioxane (4.61 mmol, 6 equiv) dropwise and stirred at room temperature for 2 h. After consumption of the substrate the mixture was evaporated *in vacuo* to give the corresponding N-deprotected amine spiro-cycle which was used for the next step reaction without purification.

#### 8.4.11 General procedure for the deprotection of N-Boc amines with Amberlyst-15<sup>[27]</sup>

The N-Boc protected spiro-compound (1.8 mmol, 1 equiv) was dissolved in MeOH (89 mL), the solution was introduced into a extraction funnel equipped with filter plate. Then resin Amberlyst-15 (PS-SO<sub>3</sub> (4.11 mmol/g) 1 equiv) was added and it was left shaken over 24 h. Then the solvent was removed and discarded. The resin (Amberlyst-15) was washed a three times with MeOH which was discarded. Then 7 N NH<sub>3</sub> in MeOH solution was added to the resin and left shaken over 2 h. The solvent was removed and the resin was washed two times more with 7 N NH<sub>3</sub> in MeOH. The



organic solvent (7 N NH<sub>3</sub> in MeOH) was evaporated to yield the *N*-deprotected amine spiro-cycle, which was used for the next step reaction without purification.

#### 8.4.12 General procedure for the deprotection of benzylic amines with H-cube technology

The *N*-benzylic protected spiro-compound was deprotected using H-cube reactor technology. A solution of the benzylic spiro-cycle (0.26 mmol, 1 equiv) 0.05 M in MeOH (5.2 mL) was passed through a Pd(OH)<sub>2</sub>/C 20% (30mm) cartridge in full H<sub>2</sub> mode at 80 °C (3 cycles) affording full conversion towards the desired product. Then if some impurities were present, the mixture was purified by flash column chromatography.

#### 8.4.13 General procedure for the reduction of the commercially available spiro-cyclic ketones to alcohols<sup>[28]</sup>

To a solution of a commercially available spiro-cyclic ketones (2.75 mmol, 1 equiv) in MeOH (6.2 mL) at 0 °C was added NaBH<sub>4</sub> (4.1 mmol, 1.5 equiv,). Then the mixture was warmed naturally to room temperature and stirred for 2 h. If the reaction does not complete, an extra amount of NaBH<sub>4</sub> (4.1 mmol, 1.5 equiv) should be added to get full conversion toward the reduced spiro-cyclic alcohol. After full conversion, to the mixture reaction was added water and extracted with EtOAc. The organic layer was separated, dried (MgSO<sub>4</sub>), filtered and the solvents evaporated *in vacuo* to yield the spiro-cyclic alcohol, which was used for the next step without need of purification (quantitative reaction).

#### 8.4.14 General procedure for the iodination of secondary alcohols<sup>[6]</sup>

To a solution of triphenylphosphine (8.8 mmol, 1.1 equiv) and imidazole (8.8 mmol, 1.1 equiv) in toluene (11 mL) was added iodine (8.8 mmol, 1.1 equiv) and stirred for 30 min. at room temperature. Then spiro-cyclic alcohol (8 mmol, 1 equiv) was added, and the reaction mixture was heated to 80 °C and stirred for 16 h. The solution was quenched with H<sub>2</sub>O, extracted with EtOAc for three times and washed with Na<sub>2</sub>S<sub>2</sub>O<sub>3</sub> sat. The organic extracts were then dried (MgSO<sub>4</sub>), filtered and concentrated *in vacuo*. The crude product was purified by flash chromatography.

#### 8.4.15 General procedure for the fluorination of tertiary alcohols<sup>[29]</sup>

Then to a solution of the arylated spiro-cyclic alcohols (2.02 mmol, 1 equiv) in DCM (15 mL) was added DAST (4 mmol, 2 equiv) at 0 °C under N<sub>2</sub> atmosphere and stirred at this temperature for 1 h, then it was let to warm up and stirred for 1 h more. The mixture was treated with water and NaHCO<sub>3</sub> sat. solution and extracted with DCM. The organic layer was separated, dried (MgSO<sub>4</sub>), filtered and the solvents evaporated *in vacuo*. The crude product was purified by flash chromatography.

#### 8.4.16 General procedure for the reduction of double bonds and defluorination by hydrogenation

The mixture of compounds or the fluorinated spiro-cycle (1.8 mmol, 1 equiv) were dissolved in MeOH (24.5 mL, 305 equiv, 606 mmol), followed by addition of Pd/C 10% (0.09 mmol, 0.05 equiv) at room temperature and hydrogenated with a balloon filled of hydrogen at atmospheric pressure. The mixture was stirred for 16 h at room temperature. Then, the reaction mixture was filtered through celite pad and evaporated *in vacuo*. The crude product was purified by flash chromatography.

#### 8.4.17 General procedure for the oxidation of secondary alcohols to ketones in the intermediates for the preparation of final targets<sup>[30]</sup>

To a solution of the spiro-cyclic alcohols (5 mmol, 1 equiv) in DCM (4 mL) was added DMP (10 mmol, 2 equiv) and stirred at room temperature for 16 h. Then NaHCO<sub>3</sub> sat. solution was added and extracted few times with DCM. The organic layer was separated, dried (MgSO<sub>4</sub>), filtered and the solvent removed *in vacuo*. The crude was purified by flash column chromatography.

#### 8.4.18 Procedure for the synthesis of the amino linker and the arylation protocol

To a solution of compound **161** (3.1 mmol, 1 equiv), *N,N*-diisopropylethylamine (6.3 mmol, 2 equiv) in DCM (9 mL) was added methanesulfonyl chloride (3.4 mmol, 1.1 equiv) at 0 °C and stirred for 1 h at room temperature. After consumption of the substrate (reaction monitored by TLC with eluting solution of EtOAc in Heptane 1:1) the mixture was diluted with NaHCO<sub>3</sub> sat. solution and extracted three times with DCM. The organic layer was separated and washed with water. Then the organic layer was separated from the aqueous phase, dried (MgSO<sub>4</sub>), filtered and the solvents removed *in vacuo* to provide the protected alcohol as an orange oil. The crude was used for the next step reaction without purification.<sup>[31]</sup>

## Experimental part

---

To a solution of the protected alcohol (3.35 mmol, 1 equiv) in DMF (9.5 mL) was added sodium azide (10 mmol, 3 equiv) at 0 °C. Then was heat it up at 70 °C and stirred for 16 h. The reaction mixture was then cooled to room temperature, diluted with EtOAc and water. The organic layer was separated and washed with an extra amount of water (3 x 30 mL). The organic layers were separated from the aqueous phase, dried (MgSO<sub>4</sub>), filtered and the volatiles removed *in vacuo*. The crude was purified by flash column chromatography.<sup>[32]</sup>

A solution of compound **164** (0.5 mmol, 1 equiv) in EtOH (0.9 mL) was hydrogenated using H-cube technology with Pd/C 10% cartridge in full H<sub>2</sub> mode for 1 cycle. Then, the solvent was evaporated to yield compound **165**.<sup>[33]</sup>

In a microwave vial a mixture of Pd<sub>2</sub>(dba)<sub>3</sub> (5 mol%, 0.018 mmol), Davephos (7 mol%, 0.025 mmol), NaO<sup>t</sup>Bu (0.55 mmol, 1.5 equiv) in 1,4-dioxane (1 mL) was added the spiro-compound **165** (0.37 mmol, 1 equiv) and 4-chloro-2,6-dimethylpyridine (0.74 mmol, 2 equiv), the vial was sealed and heated at 100 °C for 16 h. The mixture was cooled and filtered over a celite pad and rinsed with DCM. The filtrate was concentrated and the residue was purified by flash column chromatography.

Then to the *N*-Boc protected spiro-compound **166** (0.18 mmol, 1 equiv) in 1,4-dioxane (0.22 mL) at 0 °C, was added HCl 4 M in 1,4-dioxane (1.1 mmol, 6 equiv) dropwise and stirred at room temperature for 2 h. After consumption of the protected amine, the mixture was evaporated *in vacuo* to give the corresponding deprotected pyrrolidine spiro-compound.<sup>[20]</sup>

To a solution of the *N*-deprotected amine (0.18 mmol, 1 equiv) in DCM (2.8 mL) under N<sub>2</sub> atmosphere, was added TEA (0.75 mmol, 4 equiv) and stirred for 10 minutes at room temperature. Then *N*-(5-formylthiazol-2-yl)acetamide (0.22 mmol, 1.2 equiv) was added and stirred at room temperature for 30 min. Then sodium triacetoxyborohydride (0.56 mmol, 3 equiv) was added and stirred at room temperature for 16 h. The mixture was treated with NaHCO<sub>3</sub> sat. and extracted with DCM. The organic layer was separated, dried (MgSO<sub>4</sub>), filtered and the solvents evaporated *in vacuo*. The crude was purified by revers phase HPLC chromatography.<sup>[34]</sup>

#### 8.4.19 General procedure for the reductive amination reaction with aldehydes<sup>[34]</sup>

To a solution of the deprotected spiro-cyclic amine (0.451 mmol, 1 equiv,) in DCM (6.8 mL) under N<sub>2</sub> atmosphere, was added TEA (1.8 mmol, 4 equiv) and stirred for 10 min. at room temperature (TEA was only added when the deprotection of the amine has been performed with 4 N HCl in 1,4-dioxane). Then *N*-(5-formylthiazol-2-yl)acetamide (0.541 mmol, 1.2 equiv) was added and stirred at room temperature for 30 min. Then sodium triacetoxyborohydride (1.352 mmol, 3 equiv) was added and stirred at room temperature for 16 h. The mixture was treated with NaHCO<sub>3</sub> sat. and extracted with DCM. The organic layers were separated, dried (MgSO<sub>4</sub>), filtered and the solvents evaporated *in vacuo*. The crude was purified by flash chromatography.

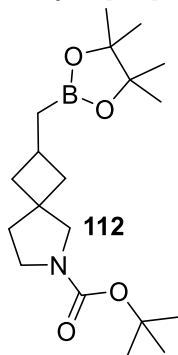
#### 8.4.20 General procedure for the reductive amination reaction with ketones<sup>[35]</sup>

To a solution of the deprotected spiro-cyclic amine (0.48 mmol, 1 equiv), 1-(2,3-dihydrobenzo[b][1,4]dioxin-6-yl)ethan-1-one (0.58 mmol, 1.2 equiv), Titanium (IV) isopropoxide (0.72 mmol, 1.5 equiv) in DCE (3.28 mL) at room temperature was added sodium cyanoborohydride (0.72 mmol, 1.5 equiv) and stirred at 80 °C for 16 h. Then the crude was cooled and filtered through a celite pad, the organic layer was separated and the aqueous phase extracted many times with EtOAc. The organic extracts were collected together, dried (MgSO<sub>4</sub>), filtered and the volatiles removed *in vacuo*. The crude was purified by flash column chromatography.

## Experimental part

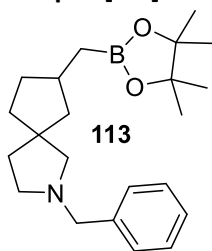
### 8.4.21 Spectral data of Chapter 5 from central cores and their intermediates

#### **Tert-butyl2-((4,4,5,5-tetramethyl-1,3,2-dioxaborolan-2-yl)methyl)-6-azaspiro[3.4]octane-6-carboxylate**

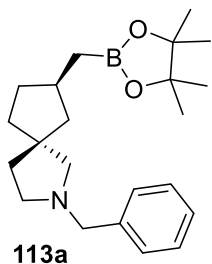


Flash column chromatography (EtOAc in Heptane 0/100 to 10/90) yielded **112** (60% yield) as a colorless oil, as a mixture of diastereoisomers 45:55 (a:a').  $^1\text{H NMR}$  ( $\text{CDCl}_3$ , 400 MHz)  $\delta$  3.33 (t,  $J = 6.7$  Hz, 2Ha), 3.27 (t,  $J = 6.6$  Hz, 2Ha'), 3.18 (s, 2Ha), 3.13 (s, 2Ha'), 2.40 (m, 1Ha + 1Ha'), 2.07 (d,  $J = 10.8$  Hz, 2Ha), 2.03 (d,  $J = 8.5$  Hz, 2Ha'), 1.85 (d,  $J = 6.8$  Hz, 2Ha), 1.83 (d,  $J = 6.8$  Hz, 2Ha'), 1.62 (m, 2Ha + 2Ha'), 1.44 (s, 9Ha + 9Ha'), 1.22 (s, 12Ha + 12Ha'), 0.94 (d,  $J = 7.7$  Hz, 2Ha + 2Ha').  $^{13}\text{C}$   $\{^1\text{H}\}$  NMR ( $\text{CDCl}_3$ , 100 MHz)  $\delta$  154.6, 82.9, 78.8, 58.2, 57.5, 44.8, 44.3, 40.7, 40.0, 39.9, 39.8, 37.2, 36.6, 29.6, 28.5, 25.7, 25.6, 24.9 (2xC), 24.8 (5xC), 24.7 (4xC), 24.6 (2xC), 19.6.  $^{11}\text{B NMR}$  (160 MHz,  $\text{CDCl}_3$ )  $\delta$  33.4. HRMS (ESI) for  $\text{C}_{38}\text{H}_{69}\text{B}_2\text{N}_2\text{O}_8$   $[\text{M}+\text{H}]^+$ : calculated: 703.1468, found: 703.5247.

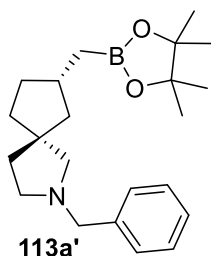
#### **2-Benzyl-7-((4,4,5,5-tetramethyl-1,3,2-dioxaborolan-2-yl)methyl)-2-azaspiro[4.4]nonane**



Flash column chromatography (EtOAc in Heptane 0/100 to 30/70) yielded **113** (72% yield) as a clear oil, as a mixture of diastereoisomers 1:1 (a:a'). Product **113** (60 mg) was sent to SFC separation (Stationary phase: Chiralpak IC  $5\mu\text{m}$  250\*21.2 mm, Mobile phase: 90%  $\text{CO}_2$ , 10% iPOH(0.3% iPrNH $_2$ )) yielding 28 mg **113a** and 38mg **113a'**.



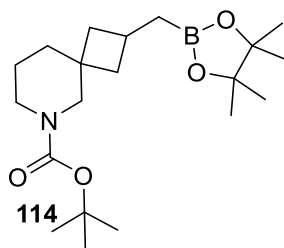
$^1\text{H NMR}$  ( $\text{CDCl}_3$ , 400 MHz)  $\delta$  7.31 (m, 4H), 7.25 – 7.20 (m, 1H), 3.61 (s, 2H), 2.60 (t,  $J = 7.0$  Hz, 2H), 2.39 (d,  $J = 9.0$  Hz, 1H), 2.36 (d,  $J = 9.0$  Hz, 1H), 2.01 (m, 1H), 1.89 (m, 1H), 1.81 (m, 1H), 1.77 (t,  $J = 7.0$  Hz, 1H), 1.61 (t,  $J = 7.0$  Hz), 1.23 (s, 12H), 1.15 (m, 1H), 0.85 (m, 1H).  $^{13}\text{C}$   $\{^1\text{H}\}$  NMR ( $\text{CDCl}_3$ , 100 MHz)  $\delta$  128.7, 128.1, 126.7, 82.8, 67.6, 60.7, 54.1, 49.8, 49.3, 40.1, 39.2, 35.1, 33.9, 24.8, 24.6, 18.5.  $^{11}\text{B NMR}$  (160 MHz,  $\text{CDCl}_3$ )  $\delta$  33.3. HRMS (ESI) for  $\text{C}_{22}\text{H}_{35}\text{BNO}_2$   $[\text{M}+\text{H}]^+$ : calculated: 356.2761, found: 356.2764.



**<sup>1</sup>H NMR (CDCl<sub>3</sub>, 400 MHz)** δ 7.31 (dt, *J* = 14.9, 7.3 Hz, 4H), 7.22 (t, *J* = 7.0 Hz, 1H), 3.61 (s, 1H), 2.65 (td, *J* = 9.3, 5.0 Hz, 1H), 2.61 – 2.54 (td, *J* = 9.3, 5.0 Hz, 1H), 2.50 (d, *J* = 9.2 Hz, 1H), 2.45 (d, *J* = 9.2 Hz, 1H), 2.09 (m, 1H), 1.83 (m, 2H), 1.69 (m, 2H), 1.54 (dt, *J* = 12.7, 7.7 Hz, 1H), 1.24 (s, 12H), 1.17 (m, 2H), 1.11 (m, 1H), 0.83 (m, 2H). **<sup>13</sup>C {<sup>1</sup>H} NMR (CDCl<sub>3</sub>, 100 MHz)** δ 128.8, 128.7, 128.1, 126.7, 82.8, 77.2, 77.0, 76.7, 67.1, 60.7, 54.1, 49.5, 49.1, 40.3, 39.8, 34.8, 34.0, 24.8, 24.7, 24.6, 18.4. **<sup>11</sup>B NMR (160 MHz,**

**CDCl<sub>3</sub>)** δ 34.0. **HRMS (ESI) for C<sub>22</sub>H<sub>35</sub>BNO<sub>2</sub> [M+H]<sup>+</sup>:** calculated: 356.2761, found: 356.2764.

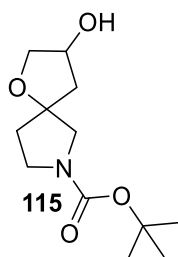
### ***Tert*-butyl-2-((4,4,5,5-tetramethyl-1,3,2-dioxaborolan-2-yl)methyl)-6-azaspiro[3.5]nonane-6-carboxylate**



Flash column chromatography (EtOAc in Heptane 0/100 to 20/80) yielded **114** (55% yield) as a clear transparent oil, as a mixture of diastereoisomers 1:1 (a:a'). **<sup>1</sup>H NMR (CDCl<sub>3</sub>, 400 MHz)** δ 3.29 (s, 2Ha), 3.27 (s, 2Ha + 2Ha'), 3.18 (s, 2Ha'), 2.36 (m, 1Ha + 1Ha'), 1.97 (m, 2Ha), 1.87 (m, 2Ha'), 1.45 (s, 9Ha), 1.44 (s, 9Ha'), 1.40 (broad s, 2Ha + 2Ha'), 1.32 – 1.23 (broad s, 4Ha + 4Ha'), 1.21 (s, 12Ha + 12Ha'), 0.94 (m, 2Ha + 2Ha'). **<sup>13</sup>C {<sup>1</sup>H} NMR (CDCl<sub>3</sub>, 100**

**MHz)** δ 155.1, 82.8, 78.9, 56.0, 53.1, 43.5, 38.6, 35.7, 34.5, 28.4, 24.7 (3xC), 22.0, 20.1. **<sup>11</sup>B NMR (160 MHz, CDCl<sub>3</sub>)** δ 33.4. **HRMS (ESI) for C<sub>20</sub>H<sub>36</sub>BNNaO<sub>4</sub> [M+Na]<sup>+</sup>:** calculated: 388.2635, found: 388.2635.

### ***Tert*-butyl 3-hydroxy-1-oxa-7-azaspiro[4.4]nonane-7-carboxylate**

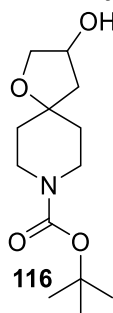


Flash column chromatography (EtOAc in Heptane 0/100 to 66/34) yielded **115** (28% yield) as a sticky brown oil, as a mixture of diastereoisomers 1:1 (a:a'). **<sup>1</sup>H NMR (CDCl<sub>3</sub>, 400 MHz)** δ 4.50 (s, 1Ha + 1Ha'), 3.93 (m, 1Ha + 1Ha'), 3.81 (m, 2Ha), 3.61 (m, 2Ha'), 3.53 – 3.36 (m, 3Ha + 3Ha'), 3.33 (d, *J* = 11.7 Hz, 1Ha), 3.20 (d, *J* = 11.5 Hz, 1Ha'), 2.25 (m, 2Ha), 2.16 (m, 2Ha'), 1.95 (m, 2Ha), 1.82 (m, 2Ha'), 1.44 (s, 9Ha + 9Ha'). **<sup>13</sup>C {<sup>1</sup>H} NMR (CDCl<sub>3</sub>, 100 MHz)** δ 164.0,

162.4, 159.4, 154.4, 107.2, 107.2, 88.2, 88.1, 87.4, 87.3, 79.3, 72.1, 72.0, 56.2, 55.7, 55.6, 55.2, 45.2, 44.8, 44.6, 44.3, 40.0, 39.9, 39.5, 37.0, 36.5, 36.4, 36.3, 35.9, 31.3, 28.4, 24.6. **HRMS (ESI) for C<sub>12</sub>H<sub>20</sub>NO<sub>4</sub> [M-H]<sup>-</sup>:** calculated: 242.1398, found: 242.1390.

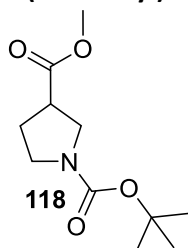
## Experimental part

### ***Tert*-butyl 3-hydroxy-1-oxa-8-azaspiro[4.5]decane-8-carboxylate**



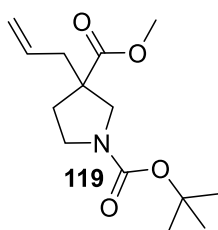
Flash column chromatography (EtOAc in Heptane 0/100 to 66/34) yielded **116** (29% yield) as a transparent oil.  $^1\text{H NMR}$  ( $\text{CDCl}_3$ , 400 MHz)  $\delta$  4.48 (s, 1H), 3.90 (dd,  $J = 9.9, 4.4$  Hz, 1H), 3.79 (m, 1H), 3.57 (broad s, 2H), 3.32 (m, 2H), 2.16 (d,  $J = 4.4$  Hz, 1H), 1.94 (dd,  $J = 13.6, 6.3$  Hz, 1H), 1.82 (m, 2H), 1.65 (m, 1H), 1.52 (m, 2H), 1.44 (s, 9H).  $^{13}\text{C}$   $\{^1\text{H}\}$  NMR ( $\text{CDCl}_3$ , 100 MHz)  $\delta$  154.8, 80.2, 79.4, 73.9, 72.6, 46.4, 37.1, 36.2, 28.4. HRMS (ESI) for  $\text{C}_{13}\text{H}_{22}\text{NO}_4$  [ $\text{M}-\text{H}$ ]: calculated: 256.1554 found: 256.1550.

### **1-(*Tert*-butyl) 3-methyl pyrrolidine-1,3-dicarboxylate**



Flash column chromatography (EtOAc in Heptane 0/100 to 15/85) yielded **118** (89% yield) as a colorless oil.  $^1\text{H NMR}$  ( $\text{CDCl}_3$ , 400 MHz)  $\delta$  3.69 (s, 3H), 3.64 – 3.38 (m, 3H), 3.38 – 2.92 (m, 2H), 2.10 (s, 2H), 1.43 (s, 9H).  $^{13}\text{C}$   $\{^1\text{H}\}$  NMR ( $\text{CDCl}_3$ , 100 MHz)  $\delta$  173.4, 154.2, 79.3, 51.9, 47.9, 45.0, 43.1, 42.2, 28.4. HRMS (ESI) for  $\text{C}_{11}\text{H}_{19}\text{NNaO}_4$  [ $\text{M}+\text{Na}$ ] $^+$ : calculated: 252.1211, found: 252.1210.

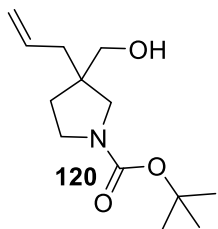
### **1-(*Tert*-butyl) 3-methyl 3-allylpyrrolidine-1,3-dicarboxylate**



Flash column chromatography (EtOAc in Heptane 0/100 to 15/85) yielded **119** (50% yield) as a yellow oil.  $^1\text{H NMR}$  ( $\text{CDCl}_3$ , 400 MHz)  $\delta$  5.68 (m, 1H), 5.06 (m, 2H), 3.74 (dd,  $J = 32.6, 11.0$  Hz, 1H), 3.69 (s, 3H), 3.46 – 3.32 (m, 2H), 3.25 (dd,  $J = 16.5, 11.3$  Hz, 1H), 2.40 (d,  $J = 7.1$  Hz, 2H), 2.35 – 1.83 (m, 2H), 1.44 (s, 9H).  $^{13}\text{C}$   $\{^1\text{H}\}$  NMR ( $\text{CDCl}_3$ , 100 MHz)  $\delta$  174.8, 154.4, 133.1, 118.6, 79.4, 79.3, 53.0, 52.1, 44.8, 44.3, 40.4, 33.4, 32.8, 31.8, 28.4,

22.6, 14.0. HRMS (ESI) for  $\text{C}_{14}\text{H}_{23}\text{NNaO}_4$  [ $\text{M}+\text{Na}$ ] $^+$ : calculated: 292.1524, found: 292.1527.

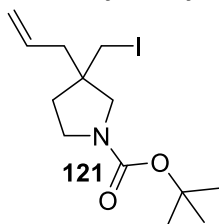
### **1-(*Tert*-butyl) 3-methyl 3-allylpyrrolidine-1,3-dicarboxylate**



After evaporation of the volatiles yielded **120** (98% yield) as a yellow oil.  $^1\text{H NMR}$  ( $\text{CDCl}_3$ , 400 MHz)  $\delta$  5.89 – 5.70 (m, 1H), 5.18 – 5.02 (m, 2H), 3.54 – 3.43 (s, 2H), 3.36 (m, 2H), 3.30 – 3.17 (m, 1H), 3.10 (m, 1H), 2.31 – 2.01 (m, 3H), 1.77 (m, 1H), 1.66 (m, 1H), 1.44 (s, 9H).  $^{13}\text{C}$   $\{^1\text{H}\}$  NMR ( $\text{CDCl}_3$ , 100 MHz)  $\delta$  154.7, 134.3, 118.1, 79.2, 65.9, 52.9, 52.5, 44.7, 44.3, 39.16, 32.0, 31.3, 28.5. HRMS (ESI) for  $\text{C}_{13}\text{H}_{22}\text{NO}_3$  [ $\text{M}-\text{H}$ ]: calculated: 240.1599, found:

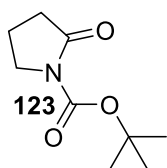
240.1599.

### **Tert-butyl 3-allyl-3-(iodomethyl)pyrrolidine-1-carboxylate**



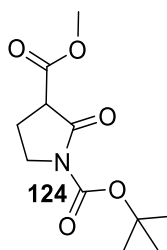
Flash column chromatography (EtOAc in Heptane 0/100 to 15/85) yielded **121** (60% yield) as a colorless oil.  $^1\text{H NMR}$  ( $\text{CDCl}_3$ , 400 MHz)  $\delta$  5.69 (m, 1H), 5.25 – 5.07 (m, 2H), 3.41 (m, 2H), 3.30 (s, 1H), 3.25 – 3.19 (s, 3H), 2.34 – 2.21 (m, 2H), 1.89 – 1.80 (m, 2H), 1.45 (s, 9H).  $^{13}\text{C}$   $\{^1\text{H}\}$  NMR ( $\text{CDCl}_3$ , 100 MHz)  $\delta$  154.5, 132.8, 119.2, 79.4, 79.4, 55.3, 54.6, 45.1, 44.6, 44.41, 44.3, 40.8, 40.7, 35.4, 34.3, 28.4, 15.9. HRMS (ESI) for  $\text{C}_{26}\text{H}_{45}\text{I}_2\text{N}_2\text{O}_4$   $[\text{MM}+\text{H}]^+$ : calculated: 703.1469, found: 703.0930.

### **Tert-butyl 2-oxopyrrolidine-1-carboxylate**



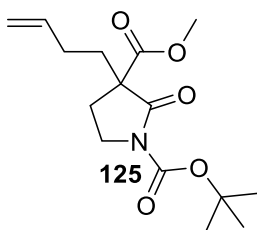
Flash column chromatography (EtOAc in Heptane 0/100 to 15/85) yielded **123** (75% yield) as a clear transparent oil.  $^1\text{H NMR}$  ( $\text{CDCl}_3$ , 400 MHz)  $\delta$  3.74 – 3.68 (t, 2H,  $J = 8.1$  Hz), 2.47 (t,  $J = 8.1$  Hz, 2H), 1.97 (tt,  $J = 15.2, 7.7$  Hz, 2H), 1.49 (s, 9H).  $^{13}\text{C}$   $\{^1\text{H}\}$  NMR ( $\text{CDCl}_3$ , 100 MHz)  $\delta$  174.2, 150.1, 82.6, 46.3, 32.8, 27.9, 17.3. HRMS (ESI) for  $\text{C}_9\text{H}_{15}\text{NNaO}_3$   $[\text{M}+\text{Na}]^+$ : calculated: 208.0950, found: 208.0945.

### **1-(Tert-butyl) 3-methyl 2-oxopyrrolidine-1,3-dicarboxylate**



Flash column chromatography (EtOAc in Heptane 0/100 to 60/40) yielded **124** (85% yield) as a viscous transparent oil that precipitates upon standing as white solid.  $^1\text{H NMR}$  ( $\text{CDCl}_3$ , 400 MHz)  $\delta$  3.86 (ddd,  $J = 10.8, 8.5, 5.4$  Hz, 1H), 3.76 (s, 3H), 3.68 (ddd,  $J = 10.8, 8.1, 6.6$  Hz, 1H), 3.53 (dd,  $J = 9.1, 7.4$  Hz, 1H), 2.37 (dddd,  $J = 13.2, 8.4, 7.4, 6.7$  Hz, 1H), 2.21 (dddd,  $J = 13.2, 9.1, 8.1, 5.4$  Hz, 1H), 1.50 (s, 9H).  $^{13}\text{C}$   $\{^1\text{H}\}$  NMR ( $\text{CDCl}_3$ , 100 MHz)  $\delta$  169.0, 168.5, 149.8, 83.3, 52.7, 50.0, 44.8, 27.8, 21.3. HRMS (ESI) for  $\text{C}_{11}\text{H}_{17}\text{NNaO}_5$   $[\text{M}+\text{Na}]^+$ : calculated: 266.1004, found: 266.1008.

### **1-(Tert-butyl) 3-methyl 3-(but-3-en-1-yl)-2-oxopyrrolidine-1,3-dicarboxylate**



Flash column chromatography (EtOAc in Heptane 0/100 to 14/86) yielded **125** (90% yield) as a viscous colourless oil.  $^1\text{H NMR}$  ( $\text{CDCl}_3$ , 400 MHz)  $\delta$  5.77 (ddt,  $J = 16.8, 10.2, 6.5$  Hz, 1H), 5.03 (dd,  $J = 17.1, 1.6$  Hz, 1H), 4.97 (dd,  $J = 10.2, 1.4$  Hz, 1H), 3.74 (s, 3H), 3.71 (dt,  $J = 8.4, 2.3$  Hz, 2H), 2.54 (ddd,  $J = 13.1, 6.4, 4.2$  Hz, 1H), 2.23 (ddd,  $J = 13.5, 11.1, 5.4$  Hz, 1H), 2.15 – 1.97 (m, 2H), 1.92 (dt,  $J = 13.1, 8.8$  Hz, 1H), 1.79 (ddd,  $J = 13.6, 10.8, 5.3$  Hz, 1H), 1.52 (s, 9H).  $^{13}\text{C}$   $\{^1\text{H}\}$  NMR ( $\text{CDCl}_3$ , 100 MHz)  $\delta$  170.9, 170.6,

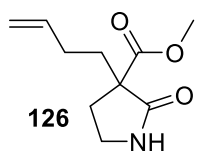


## Experimental part

150.0, 137.1, 115.3, 83.3, 57.3, 52.9, 43.8, 33.5, 31.8, 28.8, 27.9, 27.2, 22.6, 14.0.

**HRMS (ESI) for C<sub>15</sub>H<sub>22</sub>NO<sub>5</sub> [M-H]<sup>-</sup>**: calculated: 296.1503, found: 296.1170.

### Methyl 3-(but-3-en-1-yl)-2-oxopyrrolidine-3-carboxylate

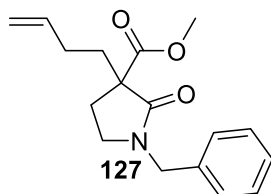


**126**

After work up yielded **126** (87% yield) as colourless oil. <sup>1</sup>H NMR (CDCl<sub>3</sub>, 400 MHz) δ 5.78 (ddt, *J* = 16.5, 10.2, 6.4 Hz, 1H), 5.02 (dd, *J* = 17.2, 1.7 Hz, 1H), 4.95 (dd, *J* = 10.3, 1.7 Hz, 1H), 3.73 (s, 3H), 3.43 (dt, *J* = 9.3, 7.6 Hz, 1H), 3.31 (tdd, *J* = 9.7, 3.4, 1.1 Hz, 1H), 2.64 (ddd, *J* = 13.0, 7.8, 3.4 Hz, 1H), 2.20 – 2.11 (m, 1H), 2.10 –

2.00 (m, 4H), 1.83 – 1.69 (m, 1H). <sup>13</sup>C {<sup>1</sup>H} NMR (CDCl<sub>3</sub>, 100 MHz) δ 175.7, 171.7, 137.4, 115.0, 54.7, 52.6, 39.7, 33.2, 30.4, 28.9. **HRMS (ESI) for C<sub>10</sub>H<sub>15</sub>NNaO<sub>3</sub> [M+Na]<sup>+</sup>**: calculated: 220.0950, found: 220.0948.

### Methyl 1-benzyl-3-(but-3-en-1-yl)-2-oxopyrrolidine-3-carboxylate

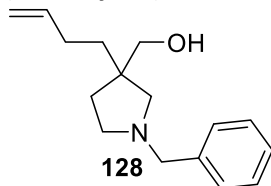


**127**

Flash column chromatography (EtOAc in Heptane 0/100 to 50/50) yielded **127** (79% yield) as a transparent oil. <sup>1</sup>H NMR (CDCl<sub>3</sub>, 400 MHz) δ 7.41 – 7.24 (m, 3H), 7.24 – 7.17 (m, 2H), 5.88 – 5.73 (m, 1H), 5.03 (dd, *J* = 17.2, 1.7 Hz, 1H), 4.96 (dd, *J* = 10.2, 1.7 Hz, 1H), 4.50 (d, *J* = 14.7 Hz, 1H), 4.44 (d, *J* = 14.7 Hz, 1H), 3.73 (s, 3H), 3.32 (dt, *J* = 9.5, 7.8 Hz, 1H), 3.15

(td, *J* = 9.2, 3.2 Hz, 1H), 2.57 – 2.41 (m, 1H), 2.23 – 2.13 (m, 1H), 2.13 – 2.00 (m, 2H), 1.95 (ddd, *J* = 13.2, 8.9, 7.6 Hz, 1H), 1.90 – 1.81 (m, 1H). <sup>13</sup>C {<sup>1</sup>H} NMR (CDCl<sub>3</sub>, 100 MHz) δ 172.0, 171.8, 137.5, 136.0, 128.6, 128.4, 128.0, 127.6, 127.5, 126.9, 115.0, 65.2, 55.6, 52.5, 47.0, 44.0, 33.2, 28.8, 27.9. **HRMS (ESI) for C<sub>17</sub>H<sub>22</sub>NO<sub>3</sub> [M+H]<sup>+</sup>**: calculated: 288.1594, found: 288.1600.

### (1-Benzyl-3-(but-3-en-1-yl)pyrrolidin-3-yl)methanol

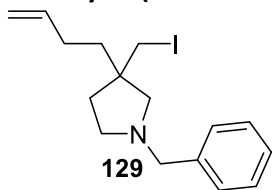


**128**

After work up yielded **128** (80% yield) as a brown oil. <sup>1</sup>H NMR (CDCl<sub>3</sub>, 400 MHz) δ 7.21 (m, 5H), 5.71 (ddt, *J* = 16.8, 10.2, 6.5 Hz, 1H), 4.93 (dd, *J* = 17.1, 1.7 Hz, 1H), 4.86 (dd, *J* = 10.2, 1.8 Hz, 1H), 3.53 (d, *J* = 9.6 Hz, 1H), 3.49 (d, *J* = 2.5 Hz, 2H), 3.35 (dd, *J* = 9.6, 1.8 Hz, 1H), 2.95 (td, *J* = 9.0, 2.9 Hz, 1H), 2.79 (d, *J* = 9.0 Hz, 1H), 2.17 (dd, *J* = 17.6, 9.4 Hz,

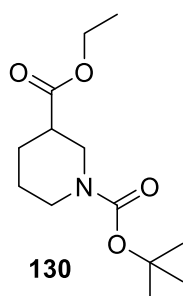
1H), 2.08 (dd, *J* = 9.1, 1.7 Hz, 1H), 1.92 (m, 3H), 1.61 (ddd, *J* = 12.8, 9.7, 3.0 Hz, 1H), 1.38 (m, 2H). <sup>13</sup>C {<sup>1</sup>H} NMR (CDCl<sub>3</sub>, 100 MHz) δ 138.7, 138.2, 128.5, 128.4, 127.1, 114.4, 71.8, 64.3, 59.9, 53.9, 45.3, 36.2, 32.8, 29.3. **HRMS (ESI) for C<sub>16</sub>H<sub>24</sub>NO [M+H]<sup>+</sup>**: calculated: 246.1858, found: 246.1863.

### 1-Benzyl-3-(but-3-en-1-yl)-3-(iodomethyl)pyrrolidine



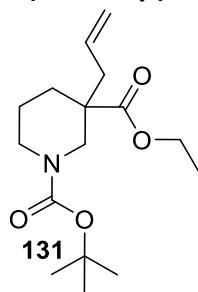
Flash column chromatography (EtOAc in Heptane 0/100 to 15/85) yielded **129** (45% yield) as a colorless oil.  $^1\text{H NMR}$  ( $\text{CDCl}_3$ , 400 MHz)  $\delta$  7.33 – 7.19 (m, 5H), 5.83 (ddt,  $J = 16.8$ , 10.2, 6.5 Hz, 1H), 5.04 (dd,  $J = 17.1$ , 1.8 Hz, 1H), 4.96 (dd,  $J = 10.2$ , 1.9 Hz, 1H), 3.57 (s, 2H), 3.41 (d,  $J = 9.7$  Hz, 1H), 3.32 (d,  $J = 9.7$  Hz, 1H), 2.77 – 2.64 (m, 1H), 2.57 (d,  $J = 9.6$  Hz, 1H), 2.50 (m, 1H), 2.35 (d,  $J = 9.6$  Hz, 1H), 2.03 – 1.91 (m, 2H), 1.82 – 1.69 (m, 2H), 1.68 – 1.53 (m, 2H).  $^{13}\text{C}$   $\{^1\text{H}\}$  NMR ( $\text{CDCl}_3$ , 100 MHz)  $\delta$  139.1, 138.4, 128.4, 128.2, 126.8, 114.5, 64.9, 60.0, 53.8, 44.8, 39.1, 36.2, 28.8, 21.3. HRMS (ESI) for  $\text{C}_{16}\text{H}_{23}\text{IN}$   $[\text{M}+\text{H}]^+$ : calculated: 353.0870, found: 356.0916.

### 1-(Tert-butyl) 3-ethyl piperidine-1,3-dicarboxylate



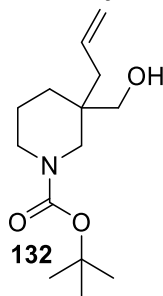
Flash column chromatography (pentane: EtOAc 100:0 to 60:40) yielded **130** (86% yield) as a colorless oil.  $^1\text{H NMR}$  ( $\text{CDCl}_3$ , 400 MHz)  $\delta$  4.07 (q,  $J = 8$  Hz, 2H), 3.84 (apparent d, 1H), 2.75 (ddd,  $J = 13.3$ , 11.4, 3.0 Hz, 1H), 2.36 (m, 1H), 1.97 (m, 1H), 1.59 (m, 2H), 1.44 (m, 3H), 1.39 (s, 9H), 1.19 (t,  $J = 7.1$  Hz, 3H).  $^{13}\text{C}$   $\{^1\text{H}\}$  NMR ( $\text{CDCl}_3$ , 100 MHz)  $\delta$  173.3, 154.5, 146.7, 85.0, 79.5, 60.3, 41.3, 28.3, 27.3, 27.2, 14.1. HRMS (ESI) for  $\text{C}_{13}\text{H}_{23}\text{NNaO}_4$   $[\text{M} + \text{Na}]^+$ : calculated: 280.1519, found: 280.1523.

### 1-(Tert-butyl) 3-ethyl 3-allylpiperidine-1,3-dicarboxylate

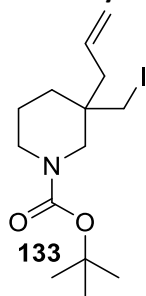


Flash column chromatography (EtOAc in Heptane 0/100 to 15/85) yielded **131** (94% yield) as a brown oil.  $^1\text{H NMR}$  ( $\text{CDCl}_3$ , 400 MHz)  $\delta$  5.89 – 5.55 (m, 1H), 5.23 – 4.93 (m, 2H), 4.11 (s, 2H), 3.77 (broad s, 1H), 3.41 (broad s, 1H), 3.22 (broad s, 2H), 2.34 (dd,  $J = 13.8$ , 7.1 Hz, 1H), 2.19 (dd,  $J = 13.8$ , 7.7 Hz, 1H), 1.99 (broad s, 1H), 1.55 (m, 3H), 1.43 (m, 9H), 1.24 (t,  $J = 7.0$  Hz, 3H).  $^{13}\text{C}$   $\{^1\text{H}\}$  NMR ( $\text{CDCl}_3$ , 100 MHz)  $\delta$  174.4, 154.7, 132.8, 118.3, 79.4, 60.4, 49.7, 46.3, 43.3, 39.8, 31.6, 28.3, 27.7, 21.7, 14.2. HRMS (ESI) for  $\text{C}_{16}\text{H}_{27}\text{NO}_4$   $[\text{M}+\text{Na}]^+$ : calculated: 320.1837, found: 320.1838.

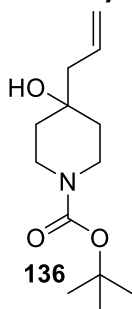
## Experimental part

**Tert-butyl 3-allyl-3-(hydroxymethyl)piperidine-1-carboxylate**

After evaporation of the volatiles yielded **132** (93% yield) as a clear transparent oil.  $^1\text{H NMR}$  ( $\text{CDCl}_3$ , 400 MHz)  $\delta$  5.81 (m, 1H), 5.03 (m, 2H), 3.77 (broad s, 1H), 3.47 (broad s, 1H), 3.21 (broad s, 1H), 2.94 (broad s, 2H), 2.56 (s, 1H), 2.16 (m, 1H), 1.99 (m, 1H), 1.48 (m, 1H), 1.43 (m, 9H), 1.33 (broad s, 4H).  $^{13}\text{C}$   $\{^1\text{H}\}$  NMR ( $\text{CDCl}_3$ , 100 MHz)  $\delta$  155.0, 132.6, 116.8, 78.7, 62.1, 48.1, 44.4, 38.9, 37.5, 29.2, 27.2, 20.3. HRMS (ESI) for  $\text{C}_{14}\text{H}_{25}\text{NNaO}_3$   $[\text{M}+\text{Na}]^+$ : calculated: 278.1732, found: 278.1735.

**Tert-butyl 3-allyl-3-(iodomethyl)piperidine-1-carboxylate**

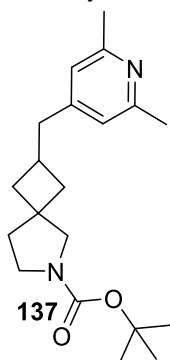
Flash column chromatography (EtOAc in Heptane 0/100 to 15/85) yielded **133** (69% yield) as a clear oil.  $^1\text{H NMR}$  ( $\text{CDCl}_3$ , 400 MHz)  $\delta$  5.70 (m, 1H), 5.15 (m, 2H), 3.44 (m, 1H), 3.32 (m, 1H), 3.20 (m, 4H), 2.09 (s, 2H), 1.56 (t,  $J = 14.9$  Hz, 4H), 1.45 (s, 10H).  $^{13}\text{C}$   $\{^1\text{H}\}$  NMR ( $\text{CDCl}_3$ , 100 MHz)  $\delta$  154.8, 132.3, 119.1, 79.7, 51.9, 43.5, 40.2, 36.1, 33.5, 31.8, 29.0, 28.4, 22.7, 21.1, 16.9, 14.1. HRMS (ESI) for  $\text{C}_{14}\text{H}_{25}\text{INO}_2$   $[\text{M}+\text{H}]^+$ : calculated: 366.09301, found: 366.0917.

**Tert-butyl 4-allyl-4-hydroxypiperidine-1-carboxylate**

Flash column chromatography (EtOAc in Heptane 0/100 to 20/80) yielded **136** (97% yield) as a colourless oil.  $^1\text{H NMR}$  ( $\text{CDCl}_3$ , 400 MHz)  $\delta$  5.84 (ddt,  $J = 17.7, 10.2, 7.5$  Hz, 1H), 5.16 (dd,  $J = 10.2, 2.1$  Hz, 1H), 5.11 (dd,  $J = 10.2, 2.1$  Hz, 1H), 3.71 (broad s, 2H), 3.14 (broad s, 2H), 2.20 (d,  $J = 7.5$  Hz, 2H), 1.53 – 1.47 (m, 4H), 1.42 (s, 9H).  $^{13}\text{C}$   $\{^1\text{H}\}$  NMR ( $\text{CDCl}_3$ , 100 MHz)  $\delta$  154.8, 132.6, 119.5, 79.3, 69.1, 47.2, 36.5, 28.4. HRMS (ESI) for  $\text{C}_{13}\text{H}_{23}\text{NNaO}_3$   $[\text{M}+\text{Na}]^+$ : calculated: 264.1575, found: 264.1582.

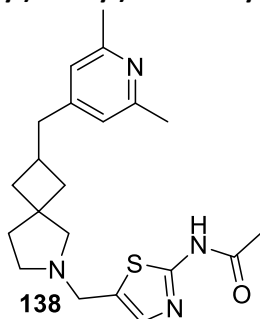
## 8.4.22 Spectral data of Chapter 5 from final targets and their intermediates

### *Tert*-butyl 2-((2,6-dimethylpyridin-4-yl)methyl)-6-azaspiro[3.4]octane-6-carboxylate

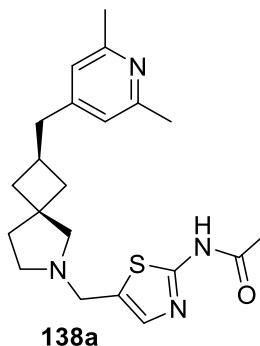


Flash column chromatography (MeOH in DCM 0/100 to 5/95) yielded **137** (54% yield) as a clear transparent oil.  $^1\text{H NMR}$  ( $\text{CDCl}_3$ , 400 MHz)  $\delta$  6.73 (s, 2Ha + 2Ha'), 3.32 (m, 4Ha + 4Ha'), 2.62 (t,  $J$  = 6.4 Hz, 2Ha + 2Ha'), 2.54 (m, 1Ha + 1Ha'), 2.48 (s, 6Ha + 6Ha'), 2.06 (m, 2Ha + 2Ha'), 1.70 (m, 4Ha + 4Ha'), 1.45 (s, 9Ha + 9Ha').  $^{13}\text{C}$   $\{^1\text{H}\}$  NMR ( $\text{CDCl}_3$ , 100 MHz)  $\delta$  157.4, 154.7, 154.5, 150.0, 121.3, 120.4, 118.2, 78.9, 57.3, 56.6, 44.6, 44.3, 44.2, 42.4, 42.3, 41.9, 41.3, 38.8, 38.1, 37.6, 37.4, 37.4, 37.2, 36.5, 30.4, 30.2, 30.0, 28.5, 24.4, 24.3. HRMS (ESI) for  $\text{C}_{20}\text{H}_{31}\text{N}_2\text{O}_2$   $[\text{M}+\text{H}]^+$ : calculated: 331.2386, found: 331.2385.

### *N*-(5-((2-((2,6-dimethylpyridin-4-yl)methyl)-6-azaspiro[3.4]octan-6-yl)methyl)thiazol-2-yl)acetamide

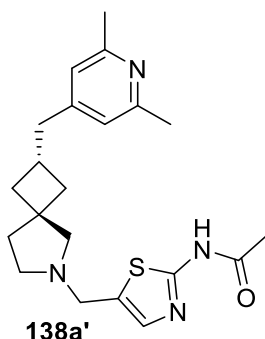


Purified by by RP HPLC (Stationary phase: XBridge  $\text{C}_{18}$  50 x 100mm, 5  $\mu\text{m}$ ), Mobile phase: Gradient from 73%  $\text{NH}_4\text{HCO}_3$  0.25% solution in Water, 27%  $\text{CH}_3\text{CN}$  to 56%  $\text{NH}_4\text{HCO}_3$  0.25% solution in Water, 44%  $\text{CH}_3\text{CN}$ ), yielded the two diastereoisomers separated. **138a** (13.5% yield) and **138a'** (13.2% yield) as a transparent oil.

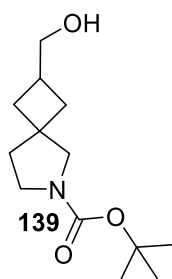


$^1\text{H NMR}$  ( $\text{CDCl}_3$ , 400 MHz)  $\delta$  12.43 (s, 1H), 7.19 (s, 1H), 6.69 (s, 2H), 3.74 (s, 2H), 2.62 (t,  $J$  = 6.8 Hz, 2H), 2.58 – 2.53 (m, 4H), 2.46 (s, 6H), 2.45 – 2.38 (m, 1H), 2.30 (s, 3H), 2.04 (m, 2H), 1.91 (t,  $J$  = 6.8 Hz, 2H), 1.77 – 1.68 (m, 2H).  $^{13}\text{C}$   $\{^1\text{H}\}$  NMR ( $\text{CDCl}_3$ , 100 MHz)  $\delta$  167.9, 159.8, 157.4, 150.3, 133.4, 130.5, 120.4, 67.1, 53.2, 51.6, 42.2, 41.0, 40.8, 39.3, 30.2, 24.3, 23.1. HRMS (ESI) for  $\text{C}_{21}\text{H}_{28}\text{N}_4\text{OS}$   $[\text{M}]^+$ : calculated: 384.1984 found: 384.1983.

## Experimental part

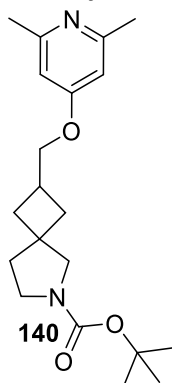
**138a'**

**<sup>1</sup>H NMR** (CDCl<sub>3</sub>, 400 MHz) δ 12.51 (s, 1H), 7.19 (s, 1H), 6.69 (s, 2H), 3.74 (s, 2H), 2.60 (s, 2H), 2.56 (dd, *J* = 7.4, 2.7 Hz, 4H), 2.46 (s, 6H), 2.34 (m, 1H), 2.30 (s, 3H), 2.10 (m, 2H), 1.82 (t, *J* = 7.1 Hz, 2H), 1.69 (m, 2H). **<sup>13</sup>C {<sup>1</sup>H} NMR** (CDCl<sub>3</sub>, 100 MHz) δ 167.9, 159.8, 157.3, 150.3, 133.3, 130.7, 120.4, 66.5, 53.3, 51.6, 42.3, 41.1, 41.0, 39.4, 31.0, 24.3, 23.1. **HRMS** (ESI) for C<sub>21</sub>H<sub>28</sub>N<sub>4</sub>OS [M]<sup>+</sup>: calculated: 384.1984, found: 384.1983.

***Tert*-butyl 2-(hydroxymethyl)-6-azaspiro[3.4]octane-6-carboxylate****139**

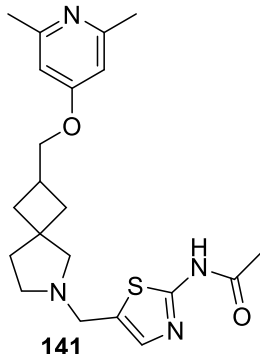
Flash column chromatography (EtOAc in Heptane 0/100; 20/80; 40/60; 100/0) yielded **139** (91% yield) as a transparent oil as a mixture of diastereoisomers 1:1 (a:a'). **<sup>1</sup>H NMR** (CDCl<sub>3</sub>, 400 MHz) δ 3.59 – 3.48 (m, 2Ha + 2Ha'), 3.34 – 3.10 (m, 4Ha + 4Ha'), 2.59 (broad s, 1Ha + 1Ha'), 2.45 – 2.34 (m, 1Ha + 1Ha'), 2.03 – 1.96 (m, 2Ha), 1.95 – 1.89 (m, 2Ha'), 1.83 (m, 2Ha), 1.77 – 1.70 (m, 2Ha + 2Ha'), 1.70 – 1.65 (m, 2Ha'), 1.39 (s, 9Ha + 9Ha'). **<sup>13</sup>C {<sup>1</sup>H} NMR** (CDCl<sub>3</sub>, 100 MHz) δ 154.8, 79.0, 66.9, 66.8, 63.0, 44.8, 44.7, 44.6, 44.5, 44.2, 44.2, 38.7, 38.0, 37.7, 37.7, 37.0, 35.6, 33.8, 33.5, 33.5, 31.8, 31.1,

30.9, 28.9, 28.4, 28.2, 24.7, 23.2, 23.1, 22.6, 14.0. **HRMS** (ESI) for C<sub>13</sub>H<sub>23</sub>NNaO<sub>3</sub> [M+Na]<sup>+</sup>: calculated: 264.1575, found: 264.1574.

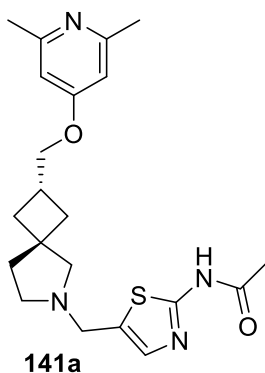
***Tert*-butyl 2-(((2,6-dimethylpyridin-4-yl)oxy)methyl)-6-azaspiro[3.4]octane-6-carboxylate****140**

Flash column chromatography (EtOAc in Heptane 0/100 to 100/0) yielded **140** (70% yield) as a colourless oil. **<sup>1</sup>H NMR** (CDCl<sub>3</sub>, 400 MHz) δ 6.48 (s, 2Ha + 2Ha'), 3.94 (m, 2Ha + 2Ha'), 3.69 (s, 2Ha), 3.37 (m, 2Ha + 2Ha'), 3.25 (m, 2Ha'), 2.72 (m, 1Ha + 1Ha'), 2.46 (s, 6Ha + 6Ha'), 2.13 (m, 2Ha), 2.08 (t, *J* = 10.3 Hz, 2Ha'), 1.92 (m, 2Ha), 1.87 (m, 2Ha'), 1.80 (m, 2Ha + 2Ha'), 1.49 (s, 9Ha + 9Ha'). **<sup>13</sup>C {<sup>1</sup>H} NMR** (CDCl<sub>3</sub>, 100 MHz) δ 165.7, 159.0, 154.6, 106.6, 78.9, 71.2, 71.2, 70.5, 67.7, 44.6, 44.5, 44.4, 44.2, 44.1, 38.6, 37.9, 37.6, 36.9, 34.0, 33.9, 33.8, 33.6, 28.4, 24.4. **HRMS** (ESI) for C<sub>20</sub>H<sub>31</sub>N<sub>2</sub>O<sub>3</sub> [M+H]<sup>+</sup>: calculated: 347.2334, found: 347.2335.

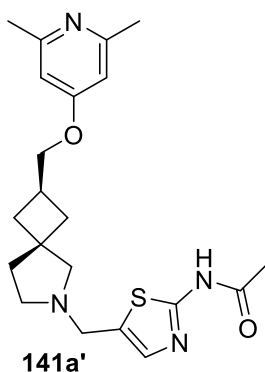
***N*-(5-((2-(((2,6-dimethylpyridin-4-yl)oxy)methyl)-6-azaspiro[3.4]octan-6-yl)methyl)thiazol-2-yl)acetamide**



Purified by RP HPLC (Stationary phase: C<sub>18</sub> XBridge 30 x 100 mm 5 μm), Mobile phase: Gradient from 81% 0.1% NH<sub>4</sub>CO<sub>3</sub>H/NH<sub>4</sub>OH pH 9 solution in Water, 19% CH<sub>3</sub>CN to 64% 0.1% NH<sub>4</sub>CO<sub>3</sub>H/NH<sub>4</sub>OH pH 9 solution in Water, 36% CH<sub>3</sub>CN), and via chiral SFC (Stationary phase: CHIRALPAK AD-H 5 μm 250\*30mm, Mobile phase: 60% CO<sub>2</sub>, 40% EtOH(0.3% iPrNH<sub>2</sub>)) yielded the two diastereoisomers separately **141a** (10% yield) and **141a'** (13% yield) both as sticky oils.

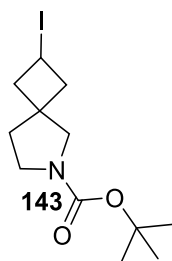


<sup>1</sup>H NMR (CDCl<sub>3</sub>, 400 MHz) δ 12.43 (s, 1Ha), 7.19 (s, 1Ha), 6.45 (s, 2Ha), 3.87 (d, *J* = 6.4 Hz, 2Ha), 3.74 (s, 2Ha), 2.66 (dt, *J* = 10.1, 6.7 Hz, 1Ha + 2Ha), 2.60 (s, 2Ha), 2.44 (s, 6Ha), 2.30 (s, 3Ha), 2.10 (m, 2Ha), 1.98 (t, *J* = 6.9 Hz, 2Ha), 1.89 (m, 2Ha). <sup>13</sup>C {<sup>1</sup>H} NMR (CDCl<sub>3</sub>, 100 MHz) δ 167.8, 165.8, 159.8, 159.0, 133.5, 130.4, 106.7, 71.5, 67.18, 53.2, 51.6, 41.0, 39.6, 37.6, 28.3, 24.4, 23.0. HRMS (ESI) for C<sub>21</sub>H<sub>29</sub>N<sub>4</sub>O<sub>2</sub>S [M+H]<sup>+</sup>: calculated: 401.2011, found: 401.2010.



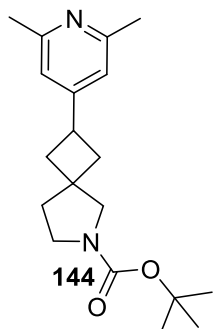
<sup>1</sup>H NMR (CDCl<sub>3</sub>, 400 MHz) δ 12.62 (s, 1Ha'), 7.22 (s, 1Ha'), 6.47 (s, 2Ha'), 3.90 (d, *J* = 6.4 Hz, 2Ha'), 3.78 (s, 2Ha'), 2.67 (s, 2Ha'), 2.62 (t, *J* = 7.1 Hz, 2Ha'), 2.56 (m, 1Ha'), 2.46 (s, 6Ha'), 2.33 (s, 3Ha'), 2.25 – 2.10 (m, 2Ha'), 1.86 (m, 4Ha'). <sup>13</sup>C {<sup>1</sup>H} NMR (CDCl<sub>3</sub>, 100 MHz) δ 168.0, 165.8, 159.9, 159.0, 133.3, 130.6, 106.7, 71.6, 66.6, 53.3, 51.5, 41.3, 39.5, 37.5, 28.9, 24.4, 23.0. HRMS (ESI) for C<sub>21</sub>H<sub>29</sub>N<sub>4</sub>O<sub>2</sub>S [M+H]<sup>+</sup>: calculated: 401.2011, found: 401.2010.

## Experimental part

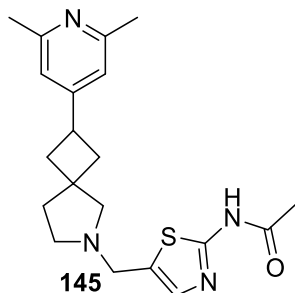
**Tert-butyl 2-iodo-6-azaspiro[3.4]octane-6-carboxylate**

675.1155, found: 675.1152.

Flash column chromatography (EtOAc in Heptane 0/100 to 15/85) yielded **143** (48% yield) as a clear transparent oil, as a mixture of diastereoisomers 1:1 (a:a').  $^1\text{H NMR}$  ( $\text{CDCl}_3$ , 400 MHz)  $\delta$  4.45 (p,  $J = 8.2$  Hz, 1Ha + 1Ha'), 3.31 (m, 4Ha + 4Ha'), 2.66 (m, 4Ha + 4Ha'), 1.96 (m, 2Ha), 1.86 (m, 2Ha'), 1.44 (s, 9Ha + 9Ha').  $^{13}\text{C}$   $\{^1\text{H}\}$  NMR ( $\text{CDCl}_3$ , 100 MHz)  $\delta$  154.6, 154.4, 79.3, 57.4, 56.9, 56.2, 55.6, 46.3, 45.9, 45.8, 45.7, 45.5, 45.2, 44.5, 44.1, 35.5, 31.8, 28.5, 22.6, 14.1, 8.5, 8.4, 8.3, 8.2. HRMS (ESI) for  $\text{C}_{24}\text{H}_{41}\text{I}_2\text{N}_2\text{O}_4$   $[\text{MM}+\text{H}]^+$ : calculated:

**Tert-butyl 2-(2,6-dimethylpyridin-4-yl)-6-azaspiro[3.4]octane-6-carboxylate**

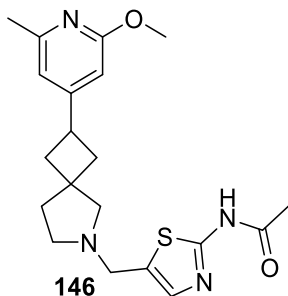
Flash column chromatography (MeOH in DCM 0/100 to 10/90) and repurified by HPLC (Stationary phase:  $\text{C}_{18}$  XBridge 30 x 100 mm 5  $\mu\text{m}$ ), Mobile phase: Gradient from 81% 0.1%  $\text{NH}_4\text{CO}_3\text{H}/\text{NH}_4\text{OH}$  pH 9 solution in Water, 19%  $\text{CH}_3\text{CN}$  to 64% 0.1%  $\text{NH}_4\text{CO}_3\text{H}/\text{NH}_4\text{OH}$  pH 9 solution in Water, 36%  $\text{CH}_3\text{CN}$ ) yielded **144** (9% yield) as a colourless oil, as a mixture of diastereoisomers 1:1 (a:a').  $^1\text{H NMR}$  ( $\text{CDCl}_3$ , 400 MHz)  $\delta$  6.76 (s, 2Ha + 2Ha'), 3.44 (m, 2Ha + 2Ha'), 3.36 (m, 1Ha + 1Ha'), 3.28 (m, 2Ha + 2Ha'), 2.48 (s, 6Ha + 6Ha'), 2.41 – 2.26 (m, 2Ha + 2Ha'), 2.20 – 2.02 (m, 2Ha + 2Ha'), 1.99 (m, 2Ha), 1.80 (m, 2Ha'), 1.48 – 1.44 (s, 9Ha + 9Ha').  $^{13}\text{C}$   $\{^1\text{H}\}$  NMR ( $\text{CDCl}_3$ , 100 MHz)  $\delta$  157.6, 154.5, 118.2, 118.2, 79.1, 57.7, 57.10, 57.0, 56.3, 44.8, 44.6, 44.4, 44.2, 41.0, 40.2, 38.4, 38.0, 37.9, 37.7, 37.0, 36.2, 33.5, 33.1, 28.5, 24.4. HRMS (ESI) for  $\text{C}_{19}\text{H}_{29}\text{N}_2\text{O}_2$   $[\text{M}+\text{H}]^+$ : calculated: 317.2229, found: 317.2229.

**N-(5-((2-(2,6-dimethylpyridin-4-yl)-6-azaspiro[3.4]octan-6-yl)methyl)thiazol-2-yl)acetamide**

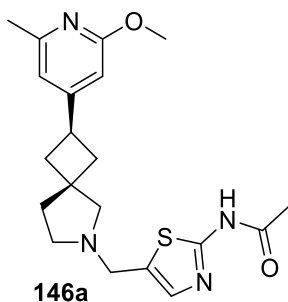
Purified by RP HPLC (Stationary phase: XBridge  $\text{C}_{18}$  50 x 100 mm, 5  $\mu\text{m}$ ), Mobile phase: Gradient from 73%  $\text{NH}_4\text{HCO}_3$  0.25% solution in Water, 27%  $\text{CH}_3\text{CN}$  to 56%  $\text{NH}_4\text{HCO}_3$  0.25% solution in Water, 44%  $\text{CH}_3\text{CN}$ ) yielded **145** (43% yield) as a colourless oil, as a mixture of diastereoisomers 1:1 (a:a').  $^1\text{H NMR}$  ( $\text{CDCl}_3$ , 400 MHz)  $\delta$  12.42 (s, 1Ha + 1Ha'), 7.23 (s, 1Ha), 7.20 (s, 1Ha'), 6.74 (s, 2Ha + 2Ha'), 3.80 (s, 2Ha), 3.75 (s, 2Ha'), 3.40 – 3.31 (m, 1Ha), 3.29 – 3.20 (m, 1Ha'), 2.74 (s, 2Ha), 2.68 (t,  $J = 6.8$  Hz, 2Ha), 2.62 (t,  $J = 7.2$  Hz, 2Ha'), 2.59 (s, 2Ha'), 2.47 (s, 6Ha + 6Ha'), 2.43 – 2.35 (m, 2Ha + 2Ha'), 2.32 (s, 3Ha + 3 Ha'), 2.17 – 2.08 (m, 2Ha + 2Ha'), 2.06 (t,  $J = 5.3$  Hz,

2Ha), 1.85 (t,  $J = 7.1$  Hz, 2Ha').  $^{13}\text{C}$   $\{^1\text{H}\}$  NMR ( $\text{CDCl}_3$ , 100 MHz)  $\delta$  167.9, 159.9, 159.8, 157.4, 155.0, 154.9, 133.5, 133.4, 130.7, 130.5, 118.2, 118.2, 66.7, 66.1, 53.4, 53.4, 53.2, 51.6, 51.6, 41.4, 41.3, 41.1, 40.7, 39.0, 34.1, 33.3, 24.3, 23.1. HRMS (ESI) for  $\text{C}_{20}\text{H}_{27}\text{N}_4\text{OS}$   $[\text{M}+\text{H}]^+$ : calculated: 371.1905, found: 371.1902.

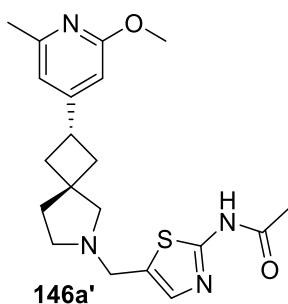
***N*-(5-((2-(2-methoxy-6-methylpyridin-4-yl)-6-azaspiro[3.4]octan-6-yl)methyl)thiazol-2-yl)acetamide**



Purified by RP HPLC (Stationary phase:  $\text{C}_{18}$  XBridge 30 x 100 mm 5  $\mu\text{m}$ ), Mobile phase: Gradient from 81% 0.1%  $\text{NH}_4\text{CO}_3\text{H}/\text{NH}_4\text{OH}$  pH 9 solution in Water, 19%  $\text{CH}_3\text{CN}$  to 64% 0.1%  $\text{NH}_4\text{CO}_3\text{H}/\text{NH}_4\text{OH}$  pH 9 solution in Water, 36%  $\text{CH}_3\text{CN}$ ), yielded the two diastereoisomers separately **146a** (2.5% yield) and **146a'** (2.5% yield) both as sticky oils.



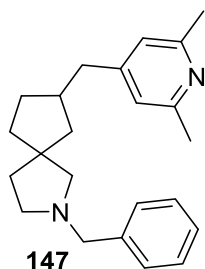
$^1\text{H}$  NMR ( $\text{CDCl}_3$ , 400 MHz)  $\delta$  11.80 (s, 1Ha), 7.23 (s, 1Ha), 6.52 (s, 1Ha), 6.32 (s, 1Ha), 3.89 (s, 3Ha), 3.81 (s, 2Ha), 3.24 (p,  $J = 9.0$  Hz, 1Ha), 2.74 (s, 2Ha), 2.63 (t,  $J = 7.2$  Hz, 2Ha), 2.40 (s, 3Ha), 2.40 – 2.36 (m, 2Ha), 2.31 (s, 3Ha), 2.09 (td,  $J = 9.6, 2.6$  Hz, 2Ha), 1.85 (t,  $J = 7.2$  Hz, 2Ha).  $^{13}\text{C}$   $\{^1\text{H}\}$  NMR ( $\text{CDCl}_3$ , 100 MHz)  $\delta$  167.9, 164.0, 159.7, 157.6, 155.9, 133.6, 130.5, 114.3, 104.4, 66.0, 53.2, 53.2, 51.5, 41.2, 41.0, 38.9, 34.1, 24.1, 23.1. HRMS (ESI) for  $\text{C}_{20}\text{H}_{27}\text{N}_4\text{O}_2\text{S}$   $[\text{M}+\text{H}]^+$ : calculated: 387.1854, found: 387.1853.



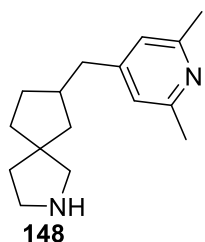
$^1\text{H}$  NMR ( $\text{CDCl}_3$ , 400 MHz)  $\delta$  11.99 (s, 1Ha'), 7.20 (s, 1Ha'), 6.52 (s, 1Ha'), 6.31 (s, 1Ha'), 3.89 (s, 3H), 3.75 (s,  $J = 5.4$  Hz, 2H), 3.34 (p,  $J = 9.0$  Hz, 1H), 2.68 (t,  $J = 6.8$  Hz, 2H), 2.59 (s, 2H), 2.40 (s, 3H), 2.36 – 2.31 (m, 2H), 2.30 (s, 4H), 2.12 (td,  $J = 9.5, 2.6$  Hz, 2H), 2.06 (t,  $J = 6.8$  Hz, 2H).  $^{13}\text{C}$   $\{^1\text{H}\}$  NMR ( $\text{CDCl}_3$ , 100 MHz)  $\delta$  167.9, 164.0, 159.7, 157.5, 155.9, 133.6, 130.4, 114.3, 104.4, 66.7, 53.4, 53.2, 51.6, 41.3, 40.7, 38.9, 33.3, 24.1, 23.1. HRMS (ESI) for  $\text{C}_{20}\text{H}_{27}\text{N}_4\text{O}_2\text{S}$   $[\text{M}+\text{H}]^+$ : calculated: 387.1854 found: 387.1853.



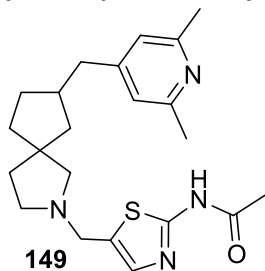
## Experimental part

**2-Benzyl-7-((2,6-dimethylpyridin-4-yl)methyl)-2-azaspiro[4.4]nonane****147**

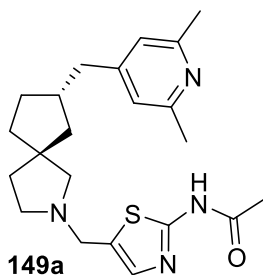
Flash column chromatography (MeOH in DCM 0/100 to 5/95) yielded **147** (57% yield) as a colourless oil as a mixture of diastereoisomers 1:1 (a:a').  $^1\text{H NMR}$  ( $\text{CDCl}_3$ , 400 MHz)  $\delta$  7.29 (m, 5Ha + 5Ha'), 6.74 (s, 2Ha + 2Ha'), 3.60 (s, 2Ha + 2Ha'), 2.62 (m, 4Ha), 2.47 (m, 6Ha + 10Ha'), 2.35 (m, 2Ha), 2.20 (m, 1Ha), 2.09 (m, 1Ha'), 1.97 – 1.75 (m, 2Ha + 2Ha'), 1.74 – 1.70 (m, 2Ha'), 1.70 – 1.61 (m, 2Ha + 2Ha'), 1.59 – 1.49 (m, 2Ha), 1.36 – 1.08 (m, 2Ha + 2Ha'), 0.83 (m, 2Ha').  $^{13}\text{C}$   $\{^1\text{H}\}$  NMR ( $\text{CDCl}_3$ , 100 MHz)  $\delta$  157.3, 151.3, 128.7, 128.7, 128.1, 126.8, 126.8, 120.7, 82.8, 67.4, 66.9, 60.7, 60.6, 54.1, 54.0, 49.0, 48.9, 47.1, 46.7, 41.9, 41.8, 40.0, 39.7, 39.6, 39.6, 39.0, 31.5, 31.4. HRMS (ESI) for  $\text{C}_{23}\text{H}_{31}\text{N}_2$   $[\text{M}+\text{H}]^+$ : calculated: 335.2482, found: 335.2481.

**7-((2,6-dimethylpyridin-4-yl)methyl)-2-azaspiro[4.4]nonane****148**

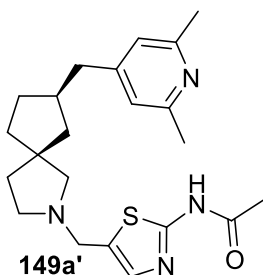
Purification by RP HPLC (Stationary phase: C18 XBridge 30 x 100 mm 5  $\mu\text{m}$ ), Mobile phase: Gradient from 81% 0.1%  $\text{NH}_4\text{CO}_3\text{H}/\text{NH}_4\text{OH}$  pH 9 solution in Water, 19%  $\text{CH}_3\text{CN}$  to 64% 0.1%  $\text{NH}_4\text{CO}_3\text{H}/\text{NH}_4\text{OH}$  pH 9 solution in Water, 36%  $\text{CH}_3\text{CN}$ ) yielded **148** (72% yield) as a colourless oil as a mixture of diastereoisomers 1:1 (a:a').  $^1\text{H NMR}$  ( $\text{CDCl}_3$ , 400 MHz)  $\delta$  6.72 (s, 2Ha + 2Ha'), 3.31 – 3.16 (m, 2Ha + 2Ha'), 3.01 (dd,  $J$  = 23.4, 11.2 Hz, 2Ha), 2.91 (s, 2Ha'), 2.51 (m, 2Ha + 2Ha'), 2.46 (s, 6Ha + 6Ha'), 2.19 (m, 1Ha + 1Ha'), 1.85 (m, 2Ha + 2Ha'), 1.79 (m, 2Ha + 2Ha'), 1.75 (2Ha), 1.65 (m, 2Ha'), 1.55 (dt,  $J$  = 13.1, 8.4 Hz, 1H), 1.27 (m, 2Ha + 2Ha').  $^{13}\text{C}$   $\{^1\text{H}\}$  NMR ( $\text{CDCl}_3$ , 100 MHz)  $\delta$  169.5, 157.5, 120.6, 55.2, 49.5, 49.4, 43.9, 43.2, 42.9, 41.2, 40.2, 40.1, 38.0, 37.9, 36.2, 35.8, 31.6, 31.4, 24.3. HRMS (ESI) for  $\text{C}_{16}\text{H}_{25}\text{N}_2$   $[\text{M}+\text{H}]^+$ : calculated: 245.2012, found: 245.2015.

**N-(5-((7-((2,6-dimethylpyridin-4-yl)methyl)-2-azaspiro[4.4]nonan-2-yl)methyl)thiazol-2-yl)acetamide****149**

Purification by RP HPLC (Stationary phase: C18 XBridge 30 x 100 mm 5  $\mu\text{m}$ ), Mobile phase: Gradient from 74% 0.1%  $\text{NH}_4\text{CO}_3\text{H}/\text{NH}_4\text{OH}$  pH 9 solution in Water, 26%  $\text{CH}_3\text{CN}$  to 58% 0.1%  $\text{NH}_4\text{CO}_3\text{H}/\text{NH}_4\text{OH}$  pH 9 solution in Water, 42%  $\text{CH}_3\text{CN}$ ) yielded the two diastereoisomers separately **149a** (24% yield) and **149a'** (26%) both as sticky colorless oils (relative configuration not determined). A low amount was sent to SFC chiral separation to get the pure enantiomers, which were analyzed in the biological assays.

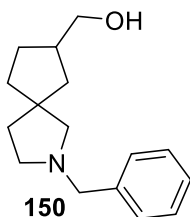


**$^1\text{H}$  NMR (CDCl<sub>3</sub>, 400 MHz)**  $\delta$  7.16 (s, 1Ha), 6.69 (s, 2Ha), 3.74 (s, 2Ha), 2.64 (dtd,  $J = 16.2, 9.2, 7.1$  Hz, 2Ha), 2.50 (dd,  $J = 28.1, 9.0$  Hz, 2Ha), 2.44 (dd,  $J = 7.5, 2.6$  Hz, 2Ha), 2.42 (s, 6Ha), 2.24 (s, 3Ha), 2.18 – 2.10 (m, 1Ha), 1.75 – 1.65 (m, 2Ha), 1.65 – 1.60 (m, 3Ha), 1.49 (dt,  $J = 12.8, 7.6$  Hz, 1Ha), 1.22 – 1.14 (m, 2Ha).  **$^{13}\text{C}$  { $^1\text{H}$ } NMR (CDCl<sub>3</sub>, 100 MHz)**  $\delta$  167.9, 159.7, 157.3, 151.3, 133.9, 120.8, 66.1, 53.3, 51.4, 49.0, 46.3, 41.7, 39.7, 39.3, 31.5, 24.2, 23.1. **HRMS (ESI) for C<sub>22</sub>H<sub>31</sub>N<sub>4</sub>OS [M+H]<sup>+</sup>**: calculated: 399.2213, found: 399.2220.



**$^1\text{H}$  NMR (CDCl<sub>3</sub>, 400 MHz)**  $\delta$  7.25 (s, 1H), 6.76 (s, 2H), 3.87 (d,  $J = 2.5$  Hz, 2H), 2.79 (td,  $J = 7.1, 3.0$  Hz, 2H), 2.54 (dd,  $J = 13.8, 6.0$  Hz, 4H), 2.49 (s, 5H), 2.29 (s, 3H), 2.18 – 2.07 (m, 1H), 1.86 – 1.77 (m, 3H), 1.73 (dt,  $J = 13.0, 7.1$  Hz, 1H), 1.67 – 1.61 (m, 2H), 1.34 – 1.26 (m, 1H), 1.22 (dd,  $J = 12.8, 9.7$  Hz, 1H).  **$^{13}\text{C}$  { $^1\text{H}$ } NMR (CDCl<sub>3</sub>, 100 MHz)**  $\delta$  168.1, 167.1, 160.0, 157.1, 151.7, 134.8, 121.0, 65.8, 52.9, 50.9, 49.1, 46.3, 41.7, 40.0, 38.9, 38.6, 31.4, 23.8, 23.0. **HRMS (ESI) for C<sub>22</sub>H<sub>31</sub>N<sub>4</sub>OS [M+H]<sup>+</sup>**: calculated: 399.2213, found: 399.2220.

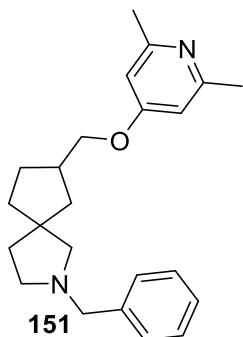
### (2-Benzyl-2-azaspiro[4.4]nonan-7-yl)methanol



Flash column chromatography (EtOAc in Heptane 0/100 to 66/44 to 100/0) yielded **150** (97% yield) as a white solid as a mixture of diastereoisomers 1:1 (a:a').  **$^1\text{H}$  NMR (CDCl<sub>3</sub>, 400 MHz)**  $\delta$  7.35 – 7.28 (m, 4Ha + 4Ha'), 7.26 – 7.19 (m, 1Ha + 1Ha'), 3.60 (s, 2Ha), 3.60 (s, 2Ha'), 3.47 (d,  $J = 6.9$  Hz, 2Ha), 3.45 (d,  $J = 6.9$  Hz, 2Ha'), 2.61 (m, 3Ha + 3Ha'), 2.47 (q,  $J = 9.2$  Hz, 2Ha), 2.40 (d,  $J = 2.0$  Hz, 2Ha'), 2.19 (m, 1Ha), 2.09 (m, 1Ha'), 1.89 – 1.81 (m, 1Ha'), 1.78 (m, 2Ha + 2Ha'), 1.73 – 1.67 (m, 2Ha + 1Ha'), 1.67 – 1.53 (m, 2Ha + 2Ha'), 1.39 – 1.27 (m, 2Ha + 2Ha').  **$^{13}\text{C}$  { $^1\text{H}$ } NMR (CDCl<sub>3</sub>, 100 MHz)**  $\delta$  139.1, 139.0, 128.7, 128.6, 128.0, 126.7, 67.2, 67.1, 66.8, 66.3, 60.7, 60.6, 54.0, 53.9, 49.1, 49.0, 43.3, 43.1, 41.0, 40.8, 39.3, 38.8, 38.2, 27.9, 27.8. **HRMS (ESI) for C<sub>16</sub>H<sub>24</sub>NO [M+H]<sup>+</sup>**: calculated: 246.1852, found: 246.1857.

## Experimental part

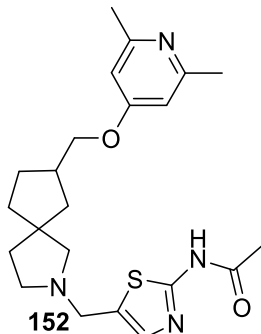
### 2-Benzyl-7-(((2,6-dimethylpyridin-4-yl)oxy)methyl)-2-azaspiro[4.4]nonane



Flash column chromatography (EtOAc in Heptane 0/100 to 100/0) yielded **151** (79% yield) as brown oil as a mixture of diastereoisomers 1:1 (a:a'). <sup>1</sup>H NMR (CDCl<sub>3</sub>, 400 MHz) δ 7.34 – 7.27 (m, 4Ha + 4Ha'), 7.25 – 7.20 (m, 1Ha + 1Ha'), 6.46 (s, 2Ha), 6.44 (s, 2Ha'), 3.82 (m, 2Ha + 2Ha'), 3.61 (s, 2Ha), 3.60 (s, 2Ha'), 2.67 – 2.59 (m, 2Ha + 2Ha'), 2.53 – 2.46 (m, 2Ha + 2Ha'), 2.45 (s, 6Ha + 6Ha'), 2.42 – 2.30 (m, 2Ha + 2Ha'), 1.98 – 1.81 (m, 1Ha + 1Ha'), 1.79 (t, *J* = 7.0 Hz, 2Ha), 1.73 (t, *J* = 7.0 Hz, 2Ha'), 1.70 – 1.65 (m, 2Ha), 1.61 (m, 2Ha'), 1.49 – 1.32 (m, 2Ha + 2Ha'). <sup>13</sup>C {<sup>1</sup>H} NMR (CDCl<sub>3</sub>, 100 MHz) δ 165.9,

159.0, 139.3, 128.6, 128.1, 126.7, 120.8, 106.6, 71.8, 71.8, 66.7, 66.3, 60.6, 60.5, 54.0, 53.9, 49.3, 49.2, 43.4, 43.2, 39.3, 39.2, 38.8, 38.2, 37.9, 37.6, 28.2, 28.2, 24.5. HRMS (ESI) for C<sub>23</sub>H<sub>31</sub>N<sub>2</sub>O [M+H]<sup>+</sup>: calculated: 351.2431, found: 351.2454.

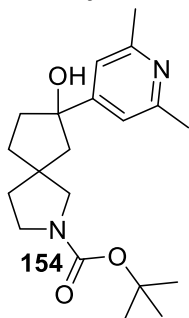
### *N*-5-(((7-(((2,6-dimethylpyridin-4-yl)oxy)methyl)-2-azaspiro[4.4]nonan-2-yl)methyl)thiazol-2-yl)acetamide



Flash column chromatography (MeOH in DCM 0/100 to 6/94) yielded **152** (49% yield) as a colourless oil as a mixture of diastereoisomers 1:1 (a:a'). <sup>1</sup>H NMR (CDCl<sub>3</sub>, 400 MHz) δ 12.64 (s, 1Ha + 1Ha'), 7.19 (s, 1Ha + 1Ha'), 6.46 (s, 2Ha), 6.44 (s, 2Ha'), 3.85 – 3.79 (m, 2Ha + 2Ha'), 3.75 (s, 2Ha + 2Ha'), 2.65 (m, 2Ha + 2Ha'), 2.51 (d, *J* = 3.1 Hz, 2Ha), 2.44 (s, 6Ha + 2Ha'), 2.43 (s, 6Ha'), 2.36 (m, 2Ha + 2Ha'), 2.30 (s, 3Ha), 2.29 (s, 3Ha'), 1.92 (m, 1Ha), 1.84 (m, 1Ha'), 1.78 (t, *J* = 7.0 Hz, 2Ha), 1.71 (t, *J* = 7.0 Hz, 2Ha'), 1.68 – 1.54 (m, 2Ha + 2Ha'), 1.50 – 1.30 (m, 2Ha + 2Ha'). <sup>13</sup>C {<sup>1</sup>H} NMR (CDCl<sub>3</sub>, 100

MHz) δ 168.0, 165.8, 159.9, 158.9, 133.2, 130.8, 106.6, 71.7, 66.2, 65.8, 53.5, 53.4, 51.6, 51.6, 49.3, 49.2, 43.1, 43.0, 39.1, 39.0, 38.6, 38.1, 37.8, 37.6, 28.1, 24.4, 23.0. HRMS (ESI) for C<sub>22</sub>H<sub>31</sub>N<sub>4</sub>O<sub>2</sub>S [M+H]<sup>+</sup>: calculated: 415.2162, found: 415.2166.

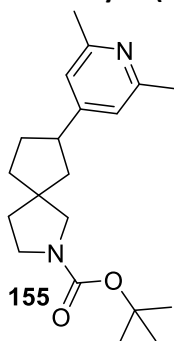
**Tert-butyl 7-(2,6-dimethylpyridin-4-yl)-7-hydroxy-2-azaspiro[4.4]nonane-2-carboxylate**



Flash column chromatography (EtOAc in Heptane 0/100 to 30/70) yielded **154** (53% yield) as a white solid as a mixture of diastereoisomers 1:1 (a:a').  $^1\text{H NMR}$  ( $\text{CDCl}_3$ , 400 MHz)  $\delta$  7.02 (s, 2Ha + 2Ha'), 3.50 – 3.29 (m, 4Ha + 4Ha'), 2.52 (s, 6Ha + 6Ha'), 2.20 – 2.07 (m, 2Ha + 2Ha'), 2.06 – 1.94 (m, 4Ha + 4Ha'), 1.90 – 1.69 (m, 4Ha + 4Ha'), 1.46 (s, 9Ha + 9Ha').  $^{13}\text{C}$   $\{^1\text{H}\}$  NMR ( $\text{CDCl}_3$ , 100 MHz)  $\delta$  157.9, 156.2, 155.8, 154.7, 116.6, 116.5, 79.1, 59.2, 58.5, 58.0, 52.5, 52.5, 52.0, 51.9, 48.0, 45.6, 45.2, 45.2, 44.8, 41.5, 41.3, 41.3, 39.7, 39.2, 39.1, 38.5, 36.2, 36.0, 35.9, 35.9, 28.5, 24.5. HRMS (ESI) for  $\text{C}_{20}\text{H}_{31}\text{N}_2\text{O}_3$   $[\text{M}+\text{H}]^+$ : calculated: 347.2334, found:

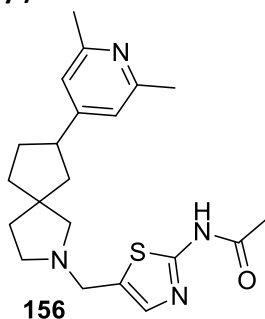
347.2335.

**Tert-butyl 7-(2,6-dimethylpyridin-4-yl)-2-azaspiro[4.4]nonane-2-carboxylate**



After filtration and evaporation yielded **155** (91% yield) as a colourless oil as a mixture of diastereoisomers 1:1 (a:a').  $^1\text{H NMR}$  ( $\text{CDCl}_3$ , 400 MHz)  $\delta$  6.85 (s, 2Ha + 2Ha'), 3.39 (m, 2Ha + 2Ha'), 3.23 (m, 2Ha + 2Ha'), 3.08 (broad m, 1Ha + 1Ha'), 2.53 (s, 6Ha + 6Ha'), 2.12 (m, 2Ha), 2.03 (m, 2Ha'), 1.80 (m, 4Ha + 4Ha'), 1.67 (m, 2Ha + 2Ha'), 1.46 (s, 9Ha + 9Ha').  $^{13}\text{C}$   $\{^1\text{H}\}$  NMR ( $\text{CDCl}_3$ , 100 MHz)  $\delta$  157.2, 154.6, 119.3, 79.1, 58.1, 57.9, 57.4, 49.5, 49.3, 48.7, 48.5, 45.4, 45.0, 44.7, 44.1, 44.1, 38.4, 38.3, 37.7, 36.9, 36.3, 36.0, 33.1, 32.8, 32.7, 32.5, 28.5, 23.9. HRMS (ESI) for  $\text{C}_{20}\text{H}_{31}\text{N}_2\text{O}_2$   $[\text{M}+\text{H}]^+$ : calculated: 331.2380, found: 331.2390.

**N-(5-((7-(2,6-dimethylpyridin-4-yl)-2-azaspiro[4.4]nonan-2-yl)methyl)thiazol-2-yl)acetamide**

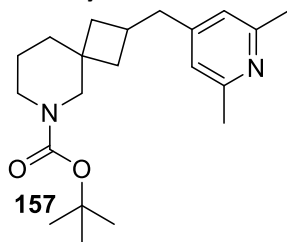


Purification by RP HPLC (Stationary phase: XBridge  $\text{C}_{18}$  50 x 100 mm, 5  $\mu\text{m}$ ), Mobile phase: Gradient from 73%  $\text{NH}_4\text{HCO}_3$  0.25% solution in Water, 27%  $\text{CH}_3\text{CN}$  to 56%  $\text{NH}_4\text{HCO}_3$  0.25% solution in Water, 44%  $\text{CH}_3\text{CN}$ ), yielded **156** (63% yield) as a colourless oil as a mixture of diastereoisomers 1:1 (a:a').  $^1\text{H NMR}$  ( $\text{CDCl}_3$ , 400 MHz)  $\delta$  12.80 (s, 1Ha + 1Ha'), 7.18 (s, 1Ha + 1Ha'), 6.76 (s, 2Ha + 2Ha'), 3.76 (s, 2Ha + 2Ha'), 3.00 (m, 1Ha), 2.90 (m, 1Ha'), 2.67 (m, 2Ha + 2Ha'), 2.53 (m, 2Ha), 2.47 (m, 2Ha'), 2.44 (s, 6Ha + 6Ha'), 2.29 (s, 3Ha + 3Ha'), 2.05 (m, 2Ha + 2Ha'), 1.88 – 1.79 (m, 2Ha + 2Ha'), 1.79 – 1.72 (m, 2Ha + 2Ha'), 1.68 (m, 2Ha), 1.64 (m, 2Ha'), 1.60 (m, 2Ha + 2Ha').  $^{13}\text{C}$   $\{^1\text{H}\}$  NMR ( $\text{CDCl}_3$ , 100 MHz)  $\delta$  167.9, 159.9, 159.9, 157.3,

## Experimental part

155.5, 155.4, 133.1, 133.1, 130.8, 130.7, 118.9, 66.7, 66.2, 53.4, 53.2, 51.6, 51.5, 49.3, 49.2, 47.6, 47.3, 43.9, 43.5, 39.8, 39.6, 39.4, 38.5, 32.5, 32.5, 24.2, 22.9. **HRMS (ESI) for C<sub>21</sub>H<sub>29</sub>N<sub>4</sub>OS [M+H]<sup>+</sup>**: calculated: 385.2062, found: 385.2061.

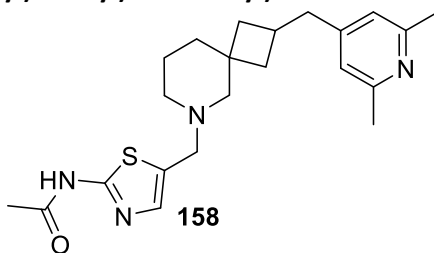
**Tert-butyl 2-((2,6-dimethylpyridin-4-yl)methyl)-6-azaspiro[3.5]nonane-6-carboxylate**



Flash column chromatography (MeOH in DCM 0/100 to 5/95) yielded **157** (50% yield) as a colourless oil as a mixture of diastereoisomers 1:1 (a:a'). **<sup>1</sup>H NMR (CDCl<sub>3</sub>, 400 MHz)** δ 6.67 (s, 2Ha + 2Ha'), 3.24 (m, 4Ha + 4Ha'), 2.56 (m, 2Ha + 2Ha'), 2.45 (m, 1Ha), 2.41 (s, 6Ha + 6Ha'), 2.38 – 2.30 (m, 1Ha'), 1.87 (t, *J* = 9.2 Hz, 2Ha), 1.76 (t, *J* = 9.9 Hz, 2Ha'), 1.54 – 1.46 (m, 2Ha + 2Ha'), 1.40 (s, 9Ha +

2Ha), 1.38 (s, 9Ha' + 2Ha'), 1.33 – 1.25 (m, 2Ha), 1.20 (m, 2Ha'). **<sup>13</sup>C {<sup>1</sup>H} NMR (CDCl<sub>3</sub>, 100 MHz)** δ 157.3, 154.9, 150.2, 120.4, 118.2, 79.1, 38.5, 36.3, 36.1, 29.4, 28.4, 28.4, 28.3, 24.3, 22.0, 14.0. **HRMS (ESI) for C<sub>21</sub>H<sub>33</sub>N<sub>2</sub>O<sub>2</sub> [M+H]<sup>+</sup>**: calculated: 345.2542, found: 345.2546.

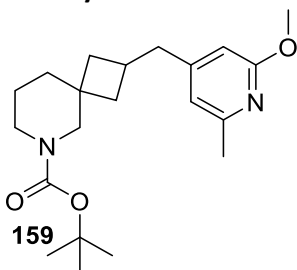
**N-(5-((2-((2,6-dimethylpyridin-4-yl)methyl)-6-azaspiro[3.5]nonan-6-yl)methyl)thiazol-2-yl)acetamide**



Flash column chromatography (MeOH in DCM 0/100 to 6/94) yielded **158** (67% yield) as a colourless oil as a mixture of diastereoisomers 1:1 (a:a'). **<sup>1</sup>H NMR (CDCl<sub>3</sub>, 400 MHz)** δ 12.80 (s, 1Ha + 1Ha'), 7.16 (s, 1Ha), 7.15 (s, 1Ha'), 6.68 (s, 2Ha + 2Ha'), 3.61 (s, 2Ha + 2Ha'), 2.56 (d, *J* = 7.6 Hz, 2Ha), 2.53 (d, *J* = 7.6 Hz, 2Ha'), 2.43 (s, 6Ha + 6Ha'), 2.40

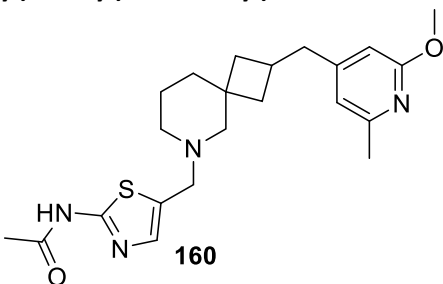
– 2.34 (m, 1Ha + 1Ha'), 2.32 (broad m, 3Ha), 2.29 (broad m, 4Ha + 4Ha'), 2.22 (broad s, 3Ha'), 1.95 (m, 2Ha), 1.89 – 1.79 (m, 2Ha'), 1.55 – 1.28 (m, 6Ha + 6Ha'). **<sup>13</sup>C {<sup>1</sup>H} NMR (CDCl<sub>3</sub>, 100 MHz)** δ 167.9, 160.1, 157.2, 157.2, 150.5, 133.6, 133.3, 130.6, 130.0, 120.3, 120.3, 103.6, 65.4, 62.8, 54.6, 54.6, 53.5, 53.4, 42.8, 38.3, 37.5, 37.3, 35.1, 35.0, 34.8, 29.9, 29.4, 24.1, 23.0, 22.3, 22.2. **HRMS (ESI) for C<sub>22</sub>H<sub>29</sub>N<sub>4</sub>OS [M-H]<sup>-</sup>**: calculated: 397.2062, found: 397.2057.

**Tert-butyl 2-((2-methoxy-6-methylpyridin-4-yl)methyl)-6-azaspiro[3.5]nonane-6-carboxylate**



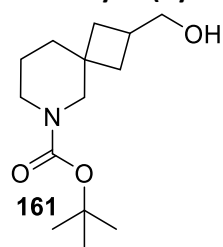
Flash column chromatography (MeOH in DCM 0/100 to 5/95) yielded **159** (71% yield) as a colourless oil as a mixture of diastereoisomers 1:1 (a:a'). **<sup>1</sup>H NMR (CDCl<sub>3</sub>, 400 MHz)** δ 6.46 (s, 1Ha + 1Ha'), 6.28 (s, 1Ha + 1Ha'), 3.85 (s, 3Ha + 3Ha'), 3.34 – 3.10 (m, 4Ha + 4Ha'), 2.64 – 2.52 (m, 2Ha + 2Ha'), 2.42 (m, 1Ha + 1Ha'), 2.39 – 2.31 (s, 3Ha + 3Ha'), 1.84 (m, 2Ha + 2Ha'), 1.41 (broad s, 9Ha + 9Ha'), 1.20 (broad s, 6Ha + 6Ha'). **<sup>13</sup>C {<sup>1</sup>H} NMR (CDCl<sub>3</sub>, 100 MHz)** δ 163.8, 163.8, 155.6, 152.6, 116.4, 116.3, 106.5, 106.4, 82.7, 79.0, 53.0, 42.6, 38.5, 38.5, 36.2, 31.7, 29.2, 28.9, 28.3, 28.3, 24.7, 24.7, 23.9, 22.5, 21.9, 14.0. **HRMS (ESI) for C<sub>21</sub>H<sub>33</sub>N<sub>2</sub>O<sub>3</sub> [M+H]<sup>+</sup>**: calculated: 361.2491, found: 361.2491.

**N-(5-((2-((2-methoxy-6-methylpyridin-4-yl)methyl)-6-azaspiro[3.5]nonan-6-yl)methyl)thiazol-2-yl)acetamide**



Flash column chromatography (MeOH in DCM 0/100 to 6/94) yielded **160** (68% yield) as a colourless oil as a mixture of diastereoisomers 1:1 (a:a'). **<sup>1</sup>H NMR (CDCl<sub>3</sub>, 400 MHz)** δ 12.80 (s, 1Ha + 1Ha'), 7.17 (s, 1Ha), 7.16 (s, 1Ha'), 6.47 (s, 2Ha), 6.26 (s, 2Ha'), 3.86 (s, 3Ha + 3Ha'), 3.62 (s, 2Ha + 2Ha'), 2.55 (m, 2Ha + 2Ha'), 2.46 – 2.39 (m, 1Ha + 1Ha'), 2.37 (s, 3Ha + 3Ha'), 2.33 – 2.30 (broad s, 3Ha + 2Ha + 3Ha' + 2Ha'), 2.01 – 1.89 (m, 2Ha), 1.89 – 1.81 (m, 2Ha'), 1.58–1.38 (m, 6Ha + 6Ha'), 1.19 (s, 2Ha + 2Ha'). **<sup>13</sup>C {<sup>1</sup>H} NMR (CDCl<sub>3</sub>, 100 MHz)** δ 167.9, 163.8, 163.8, 160.2, 155.6, 152.9, 133.6, 133.3, 130.6, 130.0, 116.4, 106.4, 106.3, 82.7, 65.5, 62.8, 54.6, 54.6, 53.6, 53.5, 53.1, 42.8, 42.8, 38.3, 37.6, 37.3, 35.1, 35.0, 34.8, 29.8, 29.4, 24.7, 24.7, 23.9, 23.0, 22.4, 22.2. **HRMS (ESI) for C<sub>22</sub>H<sub>31</sub>N<sub>4</sub>O<sub>2</sub>S [M+H]<sup>+</sup>**: calculated: 415.21677, found: 415.2169.

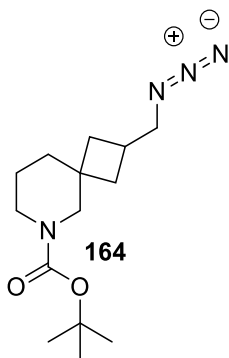
**Tert-butyl 2-(hydroxymethyl)-6-azaspiro[3.5]nonane-6-carboxylate**



Flash column chromatography (EtOAc in Heptane 0/100 to 66/44 to 100/0) yielded **161** (97% yield) as a transparent oil as a mixture of diastereoisomers 1:1 (a:a'). **<sup>1</sup>H NMR (CDCl<sub>3</sub>, 400 MHz)** δ 3.59 (m, 2Ha + 2Ha'), 3.32 (s, 2Ha), 3.28 (d, *J* = 3.8 Hz, 2Ha + 2Ha'), 3.22 (s, 2Ha'), 2.41 (m, 1Ha + 1Ha'), 1.86 (t, *J* = 11.4 Hz, 2Ha), 1.81 – 1.72 (t, *J* = 11.4 Hz, 2Ha'), 1.59 (dd, *J* = 7.3, 4.2 Hz, 1H), 1.50 – 1.46 (m, 1H), 1.45 (s, 2H), 1.44 (s, 9Ha), 1.44 (s,

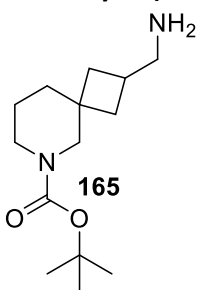


**Tert-butyl 2-(azidomethyl)-6-azaspiro[3.5]nonane-6-carboxylate**



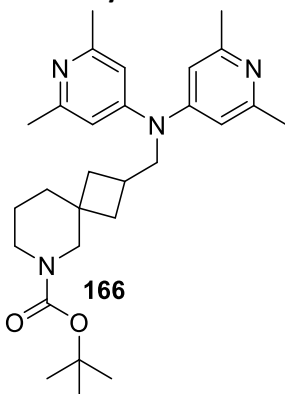
Flash column chromatography (EtOAc in Heptane 0/100 to 15/85) yielded **164** (75% yield) as a colourless oil as a mixture of diastereoisomers 1:1 (a:a').  $^1\text{H NMR}$  ( $\text{CDCl}_3$ , 400 MHz)  $\delta$  3.32 (s, 2Ha), 3.28 (m, 4Ha + 4Ha'), 3.23 (s, 2Ha'), 2.51 (m, 1Ha + 1Ha'), 1.94 (m, 2Ha), 1.85 (m, 2Ha'), 1.59 (m, 2Ha + 2Ha'), 1.51 – 1.47 (m, 2Ha + 2Ha'), 1.44 (s, 9Ha + 9Ha'), 1.42 (m, 2Ha + 2Ha').  $^{13}\text{C}$   $\{^1\text{H}\}$  NMR ( $\text{CDCl}_3$ , 100 MHz)  $\delta$  155.0, 79.3, 56.9, 56.8, 55.2, 54.6, 53.1, 52.1, 44.2, 43.3, 38.2, 35.0, 33.9, 28.4, 27.9, 22.0, 21.9. HRMS (ESI) for  $\text{C}_{14}\text{H}_{24}\text{N}_4\text{NaO}_2$   $[\text{M}+\text{H}]^+$ : calculated: 303.1796, found: 303.1795.

**Tert-butyl 2-(aminomethyl)-6-azaspiro[3.5]nonane-6-carboxylate**



After evaporation yielded **165** (82% yield) as a transparent oil as a mixture of diastereoisomers 1:1 (a:a').  $^1\text{H NMR}$  ( $\text{CDCl}_3$ , 400 MHz)  $\delta$  3.29 (s, 1H), 3.21 (s, 2Ha), 3.17 (d,  $J = 4.8$  Hz, 2Ha + 2Ha'), 3.10 (s, 2Ha'), 2.60 (m, 2Ha + 2Ha'), 2.52 (s, 2Ha + 2Ha'), 2.17 (m, 1Ha + 1Ha'), 1.81 (m, 2Ha), 1.73 – 1.66 (m, 2Ha'), 1.48 (m, 2Ha), 1.40 – 1.35 (m, 2Ha + 2Ha'), 1.34 (s, 9Ha), 1.34 (s, 9Ha'), 1.27 (m, 2Ha + 2Ha'), 1.22 – 1.14 (m, 2Ha').  $^{13}\text{C}$   $\{^1\text{H}\}$  NMR ( $\text{CDCl}_3$ , 100 MHz)  $\delta$  154.9, 78.9, 57.3, 55.3, 54.2, 53.2, 49.5, 48.1, 44.1, 43.1, 38.1, 35.8, 35.1, 33.6, 33.4, 30.9, 28.1, 21.8, 21.7. HRMS (ESI) for  $\text{C}_{14}\text{H}_{27}\text{N}_2\text{O}_2$   $[\text{M}+\text{H}]^+$ : calculated: 255.2072 found: 255.2072.

**Tert-butyl 2-((bis(2,6-dimethylpyridin-4-yl)amino)methyl)-6-azaspiro[3.5]nonane-6-carboxylate**

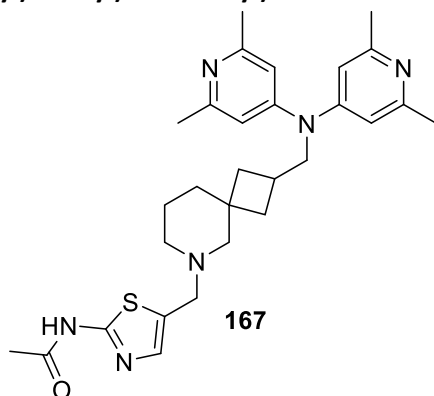


Flash column chromatography ( $(\text{NH}_3$  7N in MeOH) in DCM 0/100 to 5/95) yielded **166** (50% yield) as a colourless oil as a mixture of diastereoisomers 1:1 (a:a').  $^1\text{H NMR}$  ( $\text{CDCl}_3$ , 400 MHz)  $\delta$  6.52 (s, 4Ha + 4Ha'), 3.71 (m, 2Ha + 2Ha'), 3.25 (s, 2Ha + 2Ha'), 3.23 – 3.20 (m, 2Ha), 3.17 (m, 2Ha'), 2.60 (m, 1Ha + 1Ha'), 2.43 (s, 12Ha + 12Ha'), 1.84 (m, 2Ha), 1.76 (m, 2Ha'), 1.53 (m, 2Ha), 1.42 (broad s, 2Ha + 2Ha'), 1.40 (s, 9Ha + 9Ha'), 1.30 (s, 2Ha'), 1.22 (m, 2Ha + 2Ha').  $^{13}\text{C}$   $\{^1\text{H}\}$  NMR ( $\text{CDCl}_3$ , 100 MHz)  $\delta$  158.8, 154.9, 153.6, 112.0, 79.2, 79.2, 57.2, 57.1, 57.0, 55.7, 54.6, 52.8, 51.9, 44.4, 43.5, 38.4, 35.3, 35.0, 34.8, 28.4, 28.4, 28.0, 24.5, 22.0, 21.9. HRMS (ESI) for  $\text{C}_{28}\text{H}_{41}\text{N}_4\text{O}_2$   $[\text{M}+\text{H}]^+$ : calculated: 465.3229, found: 465.3227.

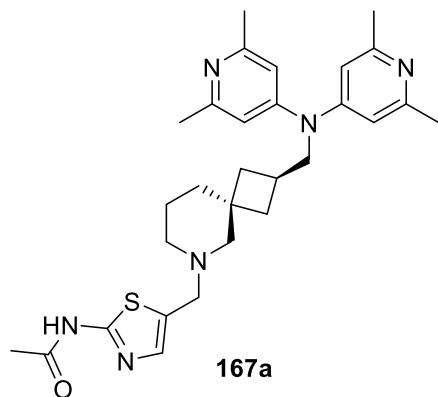


## Experimental part

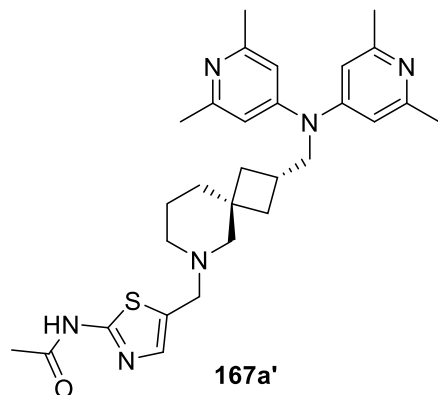
### *N*-(5-((2-((bis(2,6-dimethylpyridin-4-yl)amino)methyl)-6-azaspiro[3.5]nonan-6-yl)methyl)thiazol-2-yl)acetamide



Purification by RP HPLC (Stationary phase: C<sub>18</sub> XBridge 30 x 100 mm 5 μm), Mobile phase: Gradient from 81% 0.1% NH<sub>4</sub>CO<sub>3</sub>H/NH<sub>4</sub>OH pH 9 solution in Water, 19% CH<sub>3</sub>CN to 64% 0.1% NH<sub>4</sub>CO<sub>3</sub>H/NH<sub>4</sub>OH pH 9 solution in Water, 36% CH<sub>3</sub>CN) yielded the two diastereoisomers separately **167a** (22% yield) and **167a'** (29%) both as clear transparent oils.

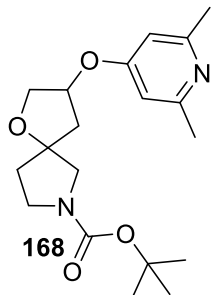


<sup>1</sup>H NMR (CDCl<sub>3</sub>, 400 MHz) δ 12.02 (s, 1Ha), 7.16 (s, 1Ha), 6.53 (s, 4Ha), 3.67 (d, *J* = 7.0 Hz, 2Ha), 3.65 – 3.61 (s, 2Ha), 2.58 (m, 1Ha), 2.44 (s, 12Ha), 2.33 (m, 2Ha), 2.30 (s, 3Ha), 2.18 (broad s, 2Ha), 1.83 (m, 2Ha), 1.54 (m, 2Ha), 1.40 (m, 4Ha). <sup>13</sup>C {<sup>1</sup>H} NMR (CDCl<sub>3</sub>, 100 MHz) δ 167.7, 159.7, 158.8, 153.6, 133.9, 130.1, 112.0, 65.3, 57.1, 54.6, 53.4, 36.3, 35.2, 34.7, 28.1, 24.6, 23.1, 22.4. HRMS (ESI) for C<sub>29</sub>H<sub>39</sub>N<sub>6</sub>OS[M+H]<sup>+</sup>: calculated: 519.2906, found: 519.2914.



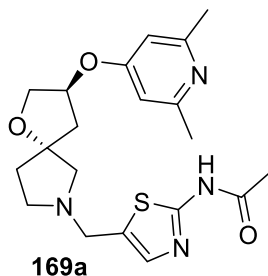
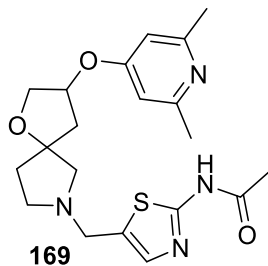
<sup>1</sup>H NMR (CDCl<sub>3</sub>, 400 MHz) δ 12.37 (s, 1Ha'), 7.15 (s, 1Ha'), 6.53 (s, 4Ha'), (d, *J* = 7.0 Hz, 2Ha'), 3.62 (s, 2Ha'), 2.53 (m, 1Ha'), 2.44 (s, 12Ha'), 2.32 (broad s, 2Ha'), 2.29 (s, 3Ha'), 2.24 (broad s, 2Ha'), 1.94 (m, 2Ha'), 1.46 (m, 2Ha'), 1.32 (m, 4Ha'). <sup>13</sup>C {<sup>1</sup>H} NMR (CDCl<sub>3</sub>, 100 MHz) δ 167.8, 160.0, 158.8, 153.6, 133.6, 130.6, 112.0, 62.5, 57.2, 54.7, 53.4, 38.3, 35.9, 35.5, 27.9, 24.5, 23.1, 22.1. HRMS (ESI) for C<sub>29</sub>H<sub>39</sub>N<sub>6</sub>OS[M+H]<sup>+</sup>: calculated: 519.2906, found: 519.2914.

**Tert-butyl 3-((2,6-dimethylpyridin-4-yl)oxy)-1-oxa-7-azaspiro[4.4]nonane-7-carboxylate**



Flash column chromatography (MeOH in DCM 0/100 to 5/95) and repurified by RP HPLC (Stationary phase: C18 XBridge 30 x 100 mm 5  $\mu$ m), Mobile phase: Gradient from 67% 0.1%  $\text{NH}_4\text{CO}_3\text{H}/\text{NH}_4\text{OH}$  pH 9 solution in Water, 33%  $\text{CH}_3\text{CN}$  to 50% 0.1%  $\text{NH}_4\text{CO}_3\text{H}/\text{NH}_4\text{OH}$  pH 9 solution in Water, 50%  $\text{CH}_3\text{CN}$ ), yielding **168** (70% yield) as a colourless oil.  $^1\text{H NMR}$  ( $\text{CDCl}_3$ , 400 MHz)  $\delta$  6.42 (s, 2Ha + 2Ha'), 4.96 (d,  $J = 4.9$  Hz, 1Ha + 1Ha'), 4.21 – 4.08 (m, 1Ha + 1Ha'), 4.06 – 3.97 (m, 1Ha + 1Ha'), 3.52 (m, 1Ha + 1Ha'), 3.44 (broad s, 2Ha + 2Ha'), 3.26 (m, 1Ha + 1Ha'), 2.45 (s, 6Ha + 6Ha'), 2.37 – 2.20 (m, 2Ha), 2.20 – 2.08 (m, 2Ha'), 2.05 – 1.93 (m, 2Ha), 1.86 (m, 2Ha'), 1.43 (s, 9Ha + 9Ha').  $^{13}\text{C}$   $\{^1\text{H}\}$  NMR ( $\text{CDCl}_3$ , 100 MHz)  $\delta$  164.0, 162.5, 159.4, 159.3, 154.4, 107.3, 107.2, 106.2, 88.3, 88.15, 87.4, 87.4, 79.3, 79.2, 72.2, 72.1, 72.0, 56.2, 55.8, 55.6, 55.3, 45.2, 44.8, 44.7, 44.3, 40.1, 39.9, 39.7, 39.6, 37.0, 36.5, 36.4, 36.3, 35.9, 31.4, 28.4, 24.6. HRMS (ESI) for  $\text{C}_{19}\text{H}_{29}\text{N}_2\text{O}_4$   $[\text{M}+\text{H}]^+$ : calculated: 349.2127, found: 349.2127.

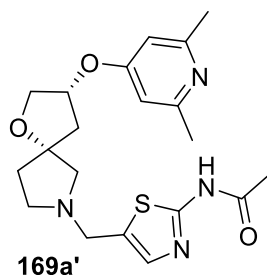
**N-(5-((3-((2,6-dimethylpyridin-4-yl)oxy)-1-oxa-7-azaspiro[4.4]nonan-7-yl)methyl)thiazol-2-yl)acetamide**



Purified by by RP HPLC (Stationary phase: XBridge C18 50 x 100 mm, 5  $\mu$ m), Mobile phase: Gradient from 73%  $\text{NH}_4\text{HCO}_3$  0.25 solution in Water, 27%  $\text{CH}_3\text{CN}$  to 56%  $\text{NH}_4\text{HCO}_3$  0.25% solution in Water, 44%  $\text{CH}_3\text{CN}$ ), yielded the two diastereoisomers separated. **169a** (26.6% yield) and **169a'** (25.1%) as a transparent oil.

$^1\text{H NMR}$  ( $\text{CDCl}_3$ , 400 MHz)  $\delta$  12.52 (s, 1H), 7.20 (s, 1H), 6.39 (s, 2H), 4.92 (m, 1H), 4.13 (dd,  $J = 10.4, 5.0$  Hz, 1H), 3.92 (dd,  $J = 10.4, 1.9$  Hz, 1H), 3.79 (s, 2H), 2.76 (s, 2H), 2.71 – 2.64 (m, 2H), 2.43 (s, 6H), 2.29 (s, 3H), 2.24 (d,  $J = 1.9$  Hz, 1H), 2.23 (d,  $J = 5.8$  Hz, 1H), 2.09 (m, 1H), 1.92 (m, 1H).  $^{13}\text{C}$   $\{^1\text{H}\}$  NMR ( $\text{CDCl}_3$ , 100 MHz)  $\delta$  168.1, 166.6, 164.7, 160.1, 158.8, 134.4, 128.5, 107.8, 88.6, 72.0, 63.6, 52.8, 51.1, 50.5, 42.3, 37.8, 23.7, 23.0. HRMS (ESI) for  $\text{C}_{20}\text{H}_{27}\text{N}_4\text{O}_3\text{S}$   $[\text{M}+\text{H}]^+$ : calculated: 403.1804, found: 403.1808.

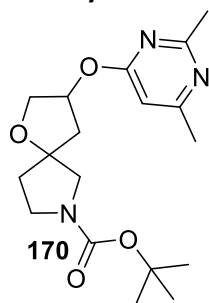
## Experimental part

**169a'**

**$^1\text{H}$  NMR (CDCl<sub>3</sub>, 400 MHz)**  $\delta$  12.41 (broad s, 1H), 7.21 (s, 1H), 6.41 (s, 2H), 4.91 (m, 1H), 4.14–4.05 (m, 1H), 3.96 (dd,  $J$  = 10.4, 1.9 Hz, 1H), 3.80 (s, 2H), 2.80–2.74 (m, 2H), 2.71–2.64 (m, 2H), 2.45 (s, 6H), 2.30 (s, 3H), 2.29–2.24 (m, 1H), 2.18–2.10 (m, 2H), 2.01–1.91 (m, 1H).  **$^{13}\text{C}$  { $^1\text{H}$ } NMR (CDCl<sub>3</sub>, 100 MHz)**  $\delta$  168.1, 166.8, 164.5, 160.0, 158.9, 134.2, 128.9, 107.6, 88.6, 72.0, 64.3, 52.1, 51.0, 50.3, 42.7, 37.6, 23.9, 23.1. **HRMS (ESI) for C<sub>20</sub>H<sub>27</sub>N<sub>4</sub>O<sub>3</sub>S [M+H]<sup>+</sup>:**

calculated: 403.1804, found: 403.1808.

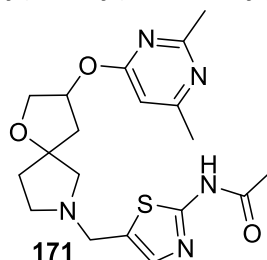
***Tert*-butyl 3-((2,6-dimethylpyrimidin-4-yl)oxy)-1-oxa-7-azaspiro[4.4]nonane-7-carboxylate**

**170**

Flash column chromatography (MeOH in DCM 0/100 to 10/90) yielded **170** (98% yield) as a colorless oil as mixture of diastereoisomers.  **$^1\text{H}$  NMR (CDCl<sub>3</sub>, 400 MHz)**  $\delta$  6.37 (s, 1H + 1Ha'), 5.69–5.55 (m, 1Ha + 1Ha'), 4.23–4.10 (m, 1Ha + 1Ha'), 3.97 (dd,  $J$  = 13.2, 12.5 Hz, 1Ha + 1Ha'), 3.54 (m, 1Ha + 1Ha'), 3.45 (m, 2Ha + 2Ha'), 3.30 (m, 1Ha + 1Ha'), 2.55 (s, 3Ha + 3Ha'), 2.39 (s, 3Ha + 3Ha'), 2.22 (m, 2Ha + 2Ha'), 1.92 (m, 2Ha + 2Ha'), 1.45 (s, 9Ha + 9Ha').  **$^{13}\text{C}$  { $^1\text{H}$ } NMR (CDCl<sub>3</sub>, 100 MHz)**  $\delta$  168.6, 167.4, 154.5, 118.0, 117.3, 104.3, 104.0, 103.6, 88.1, 87.2, 79.2,

72.6, 72.3, 56.2, 55.8, 55.7, 55.3, 45.5, 45.2, 44.8, 44.7, 44.4, 40.9, 40.1, 40.0, 39.8, 39.6, 37.0, 36.5, 36.3, 35.9, 28.4, 25.9, 23.8. **HRMS (ESI) for C<sub>18</sub>H<sub>27</sub>N<sub>3</sub>NaO<sub>4</sub> [M+Na]<sup>+</sup>:** calculated: 372.1899, found: 372.1903.

***N*-(5-((3-((2,6-dimethylpyrimidin-4-yl)oxy)-1-oxa-7-azaspiro[4.4]nonan-7-yl)methyl)thiazol-2-yl)acetamide**

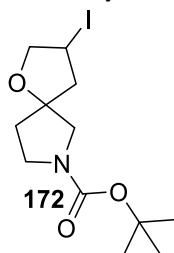
**171**

Flash column chromatography (MeOH in DCM 0/100 to 10/90) yielded **171** as mixture of diastereoisomers (28% yield) as a transparent oil as mixture of diastereoisomers.  **$^1\text{H}$  NMR (CDCl<sub>3</sub>, 400 MHz)**  $\delta$  12.22 (s, 1Ha + 1Ha'), 7.22 (s, 1Ha + 1Ha'), 6.36 (s, 1Ha), 6.34 (s, 1Ha'), 5.57 (m, 1Ha + 1Ha'), 4.16 (dd,  $J$  = 10.6, 5.1 Hz, 1Ha), 4.12 (dd,  $J$  = 10.6, 5.2 Hz, 1Ha'), 3.88 (dd,  $J$  = 10.7, 2.3 Hz, 1Ha + 1Ha'), 3.82 (s, 2Ha + 2Ha'), 2.83–2.79 (m, 2Ha + 2Ha'), 2.74–2.65 (m,

2Ha + 2Ha'), 2.54 (s, 3Ha + 3Ha'), 2.38 (s, 3Ha), 2.37 (s, 3Ha'), 2.35–2.27 (m, 2Ha), 2.30 (s, 3Ha + 3Ha'), 2.23 (m, 2Ha'), 2.15–2.09 (m, 2Ha), 2.01–1.93 (m, 2Ha').  **$^{13}\text{C}$  { $^1\text{H}$ } NMR (CDCl<sub>3</sub>, 100 MHz)**  $\delta$  168.8, 168.7, 167.8, 167.8, 167.3, 159.7, 159.6, 133.8, 130.1, 104.0, 88.6, 77.2, 76.4, 76.3, 72.4, 72.3, 64.8, 64.4, 52.9, 52.4, 51.5, 51.3, 43.1,

42.8, 38.1, 37.8, 29.7, 25.9, 23.8, 23.1. **HRMS (ESI) for C<sub>19</sub>H<sub>24</sub>N<sub>5</sub>O<sub>3</sub>S [M-H]<sup>-</sup>:**  
calculated: 402.1599 found: 402.1602.

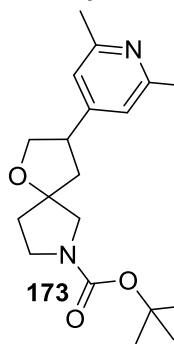
**Tert-butyl 3-iodo-1-oxa-7-azaspiro[4.4]nonane-7-carboxylate**



Flash column chromatography (EtOAc in Heptane 0/100 to 15/85) yielded **172** (78% yield) as a colourless oil. **<sup>1</sup>H NMR (CDCl<sub>3</sub>, 400 MHz)** δ 4.32 – 4.19 (m, 1Ha + 1Ha'), 4.13 (dd, *J* = 15.9, 7.7 Hz, 2Ha), 4.00 (dd, *J* = 9.8, 6.2 Hz, 2Ha'), 3.56 – 3.34 (m, 3Ha + 3Ha'), 3.21 (s, 1Ha), 3.18 (s, 1Ha'), 2.60 (dt, *J* = 15.3, 7.8 Hz, 1Ha + 1Ha'), 2.34 (d, *J* = 6.3 Hz, 1Ha), 2.31 (d, *J* = 6.4 Hz, 1Ha'), 2.25 (m, 1Ha + 1Ha'), 2.02 – 1.84 (m, 1Ha + 1Ha'), 1.43 (s, 9Ha + 9Ha'). **<sup>13</sup>C {<sup>1</sup>H} NMR (CDCl<sub>3</sub>, 100 MHz)** δ 154.4, 154.3, 88.4, 87.5, 79.3, 56.5, 55.9, 45.9, 45.7,

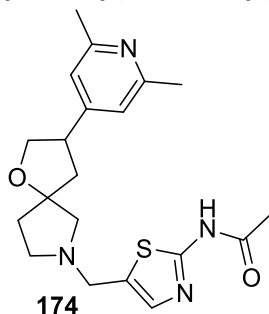
45.1, 44.7, 37.3, 36.6, 28.5, 16.7, 16.2. **HRMS (ESI) for C<sub>24</sub>H<sub>41</sub>I<sub>2</sub>N<sub>2</sub>O<sub>6</sub> [MM+H]<sup>+</sup>:**  
calculated: 707.1054, found: 707.1053.

**Tert-butyl 3-(2,6-dimethylpyridin-4-yl)-1-oxa-7-azaspiro[4.4]nonane-7-carboxylate**



Flash column chromatography (MeOH in DCM 0/100 to 10/85) yielded **173** (19% yield) as a colourless oil. **<sup>1</sup>H NMR (CDCl<sub>3</sub>, 400 MHz)** δ 6.82 (s, 2Ha + 2Ha'), 4.20 (m, 1Ha + 1Ha'), 3.78 (m, 2Ha), 3.55 (m, 2Ha'), 3.31 (m, 2Ha + 2Ha'), 2.49 (s, 6Ha + 6Ha'), 2.34 (m, 1Ha + 1Ha'), 2.15 – 2.00 (m, 3Ha + 3Ha'), 1.45 (s, 9Ha + 9Ha'), 1.24 (m, 2Ha), 1.20 (m, 2Ha'). **<sup>13</sup>C {<sup>1</sup>H} NMR (CDCl<sub>3</sub>, 100 MHz)** δ 158.5, 158.0, 146.8, 119.0, 119.0, 118.1, 88.8, 88.0, 79.4, 75.0, 72.8, 56.5, 56.2, 55.8, 45.2, 45.0, 44.7, 44.1, 41.5, 41.1, 40.8, 37.2, 36.9, 36.4, 28.5, 24.8, 24.5, 24.4. **HRMS (ESI) for C<sub>19</sub>H<sub>29</sub>N<sub>2</sub>O<sub>3</sub> [M+H]<sup>+</sup>:**  
calculated: 333.2178, found: 333.2182.

**N-(5-((3-(2,6-dimethylpyridin-4-yl)-1-oxa-7-azaspiro[4.4]nonan-7-yl)methyl)thiazol-2-yl)acetamide**

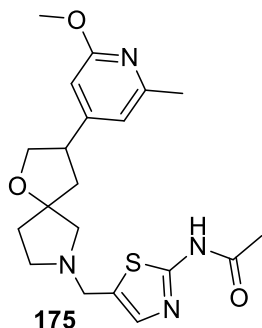


Flash column chromatography (MeOH in DCM 0/100 to 10/85) yielded **174** (54% yield) as a colourless oil. **<sup>1</sup>H NMR (CDCl<sub>3</sub>, 400 MHz)** δ 12.50 (s, 1Ha + 1Ha'), 7.23 (s, 1Ha + 1Ha'), 6.80 (s, 2Ha), 6.80 (s, 2Ha'), 4.13 (m, 1Ha + 1Ha'), 3.82 (s, 2Ha + 2Ha'), 3.77 – 3.66 (m, 1Ha + 1Ha'), 3.37 (m, 1Ha), 3.28 (m, 1Ha'), 2.89 (d, *J* = 10.1 Hz, 1Ha), 2.86 – 2.77 (m, 2Ha), 2.75 (dd, *J* = 9.9, 4.3 Hz, 1Ha + 1Ha'), 2.69 (m, 2Ha'), 2.65 (d, *J* = 9.6 Hz, 1Ha'), 2.48 (s, 6Ha), 2.47 (s, 6Ha'), 2.42 (dd, *J* = 12.6, 7.8 Hz, 1Ha), 2.33 (dd, *J* = 9.9, 5.1 Hz,

## Experimental part

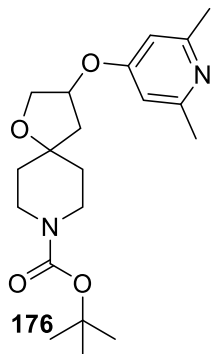
1Ha'), 2.31 (s, 3Ha), 2.30 (s, 3Ha'), 2.21 – 2.10 (m, 1Ha), 2.10 – 1.94 (m, 2Ha + 2Ha'), 1.87 (m, 1Ha').  $^{13}\text{C}$  { $^1\text{H}$ } NMR ( $\text{CDCl}_3$ , 100 MHz)  $\delta$  167.88, 167.85, 164.11, 159.72, 156.44, 153.87, 153.80, 133.84, 130.18, 130.13, 114.95, 114.92, 105.57, 103.80, 103.76, 103.69, 89.40, 89.37, 72.69, 72.60, 65.62, 64.83, 52.91, 52.77, 51.53, 51.49, 44.92, 44.41, 44.31, 44.13, 38.94, 38.27, 24.15, 23.18. HRMS (ESI) for  $\text{C}_{20}\text{H}_{27}\text{N}_4\text{O}_2\text{S}$  [ $\text{M}+\text{H}$ ] $^+$ : calculated: 387.1854, found: 387.1877.

***N*-5-((3-(2-methoxy-6-methylpyridin-4-yl)-1-oxa-7-azaspiro[4.4]nonan-7-yl)methyl)thiazol-2-yl)acetamide**



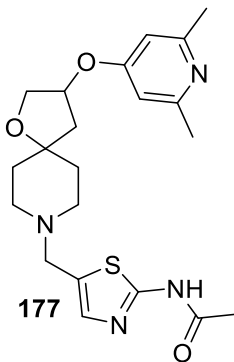
Purified by RP HPLC (Stationary phase:  $\text{C}_{18}$  XBridge 30 x 100 mm 5  $\mu\text{m}$ ), Mobile phase: Gradient from 81% 0.1%  $\text{NH}_4\text{CO}_3\text{H}/\text{NH}_4\text{OH}$  pH 9 solution in Water, 19%  $\text{CH}_3\text{CN}$  to 64% 0.1%  $\text{NH}_4\text{CO}_3\text{H}/\text{NH}_4\text{OH}$  pH 9 solution in Water, 36%  $\text{CH}_3\text{CN}$ ) yielded **175** (5% yield) as a sticky solid.  $^1\text{H}$  NMR ( $\text{CDCl}_3$ , 400 MHz)  $\delta$  12.10 (s, 1Ha + 1Ha'), 7.22 (s, 1Ha + 1Ha'), 6.58 (s, 1Ha), 6.57 (s, 1Ha'), 6.38 (s, 1Ha), 6.37 (s, 1Ha'), 4.22 – 4.05 (m, 1Ha + 1Ha'), 3.89 (s, 3Ha), 3.89 (s, 3Ha'), 3.81 (m, 2Ha + 2Ha'), 3.78 – 3.67 (m, 1Ha + 1Ha'), 3.37 (m, 1Ha), 3.27 (m, 1Ha'), 2.88 (d,  $J$  = 10.0 Hz, 1Ha), 2.83 (m, 1Ha), 2.77 (m, 1Ha'), 2.72 (m, 2Ha + 2Ha'), 2.64 (d,  $J$  = 9.5 Hz, 1Ha'), 2.41 (s, 3Ha), 2.41 (s, 3Ha'), 2.31 (s, 3Ha), 2.31 (s, 3Ha'), 2.15 (m, 1Ha), 2.11 – 1.95 (m, 2Ha + 2Ha'), 1.87 (m, 1Ha').  $^{13}\text{C}$  { $^1\text{H}$ } NMR ( $\text{CDCl}_3$ , 100 MHz)  $\delta$  167.85, 164.11, 159.71, 156.43, 153.87, 153.79, 133.84, 130.13, 114.95, 114.92, 105.56, 103.78, 89.40, 89.37, 72.69, 72.60, 65.62, 64.83, 53.31, 52.91, 52.77, 51.53, 44.92, 44.41, 44.31, 44.13, 38.94, 38.27, 24.15, 23.18. HRMS (ESI) for  $\text{C}_{20}\text{H}_{27}\text{N}_4\text{O}_3\text{S}$  [ $\text{M}+\text{H}$ ] $^+$ : calculated: 403.1803, found: 403.1806.

***Tert*-butyl 3-((2,6-dimethylpyridin-4-yl)oxy)-1-oxa-8-azaspiro[4.5]decane-8-carboxylate**



Flash column chromatography (EtOAc in Heptane 0/100 to 100/0) yielded **176** (71% yield) as a colourless oil as a mixture of diastereoisomers 1:1 (a:a').  $^1\text{H}$  NMR ( $\text{CDCl}_3$ , 400 MHz)  $\delta$  6.40 (s, 2Ha + 2Ha'), 4.93 (m, 1Ha + 1Ha'), 4.11 (dd,  $J$  = 10.5, 4.7 Hz, 2Ha), 4.02 (dd,  $J$  = 10.5, 1.7 Hz, 2Ha'), 3.65 (m, 2Ha + 2Ha'), 3.29 (m, 2Ha + 2Ha'), 2.45 (s, 6Ha + 6Ha'), 2.04 (m, 2Ha + 2Ha'), 1.86 (m, 2Ha), 1.57 (m, 2Ha + 4Ha'), 1.43 (s, 9Ha + 9Ha').  $^{13}\text{C}$  { $^1\text{H}$ } NMR ( $\text{CDCl}_3$ , 100 MHz)  $\delta$  164.1, 159.3, 154.7, 107.2, 80.6, 79.4, 71.2, 43.4, 36.4, 36.1, 31.3, 28.3, 24.5. HRMS (ESI) for  $\text{C}_{20}\text{H}_{31}\text{N}_2\text{O}_4$  [ $\text{M}+\text{H}$ ] $^+$ : calculated: 363.2283, found: 363.2282.

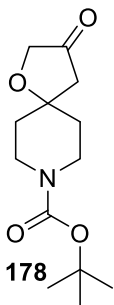
***N*-(5-((3-((2,6-dimethylpyridin-4-yl)oxy)-1-oxa-8-azaspiro[4.5]decane-8-yl)methyl)thiazol-2-yl)acetamide**



Purification by RP HPLC (Stationary phase: C<sub>18</sub> XBridge 30 x 100 mm 5 μm), Mobile phase: Gradient from 81% 0.1% NH<sub>4</sub>CO<sub>3</sub>H/NH<sub>4</sub>OH pH 9 solution in Water, 19% CH<sub>3</sub>CN to 64% 0.1% NH<sub>4</sub>CO<sub>3</sub>H/NH<sub>4</sub>OH pH 9 solution in Water, 36% CH<sub>3</sub>CN yielded **177** (63% yield) as a colourless oil as a mixture of diastereoisomers 1:1 (a:a'). <sup>1</sup>H NMR (CDCl<sub>3</sub>, 400 MHz) δ 12.79 (s, 1Ha + 1Ha'), 7.15 (s, 1Ha + 1Ha'), 6.38 (s, 2Ha + 2Ha'), 4.88 (broad s, 1Ha + 1Ha'), 4.06 (dd, *J* = 10.3, 4.4 Hz, 2Ha), 3.96 (m, 2Ha'), 3.64 (s, 2Ha + 2Ha'), 2.53 (broad s, 4Ha + 4Ha'), 2.41 (s, 6Ha + 6Ha'), 2.27 (s, 3Ha + 3Ha'), 2.14 – 1.78 (m, 4Ha + 2Ha'), 1.75 – 1.61 (m, 2Ha + 4Ha'). <sup>13</sup>C {<sup>1</sup>H} NMR (CDCl<sub>3</sub>, 100

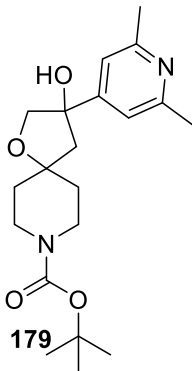
MHz) δ 167.9, 164.0, 159.9, 159.0, 133.7, 129.8, 107.1, 80.3, 77.5, 70.8, 54.0, 53.3, 50.0, 43.1, 36.1, 24.3, 22.9. HRMS (ESI) for C<sub>21</sub>H<sub>29</sub>N<sub>4</sub>O<sub>3</sub>S [M+H]<sup>+</sup>: calculated: 417.19604, found: 417.1963.

***Tert*-butyl 3-oxo-1-oxa-8-azaspiro[4.5]decane-8-carboxylate**



Flash column chromatography (EtOAc in Heptane 0/100 to 50/50) yielded **178** (84% yield) as a transparent oil. <sup>1</sup>H NMR (CDCl<sub>3</sub>, 400 MHz) δ 4.01 (s, 2H), 3.64 (m, 2H), 3.37 (m, 2H), 2.35 (s, 2H), 1.78 (m, 2H), 1.65 (m, 2H), 1.45 (s, 9H). <sup>13</sup>C {<sup>1</sup>H} NMR (CDCl<sub>3</sub>, 100 MHz) δ 214.6, 154.6, 79.6, 79.5, 69.4, 48.0, 40.2, 35.2, 28.40. HRMS (ESI) for C<sub>13</sub>H<sub>22</sub>NO<sub>4</sub> [M+H]<sup>+</sup>: calculated: 254.1392, found: 254.1393.

***Tert*-butyl 3-(2,6-dimethylpyridin-4-yl)-3-hydroxy-1-oxa-8-azaspiro[4.5]decane-8-carboxylate**

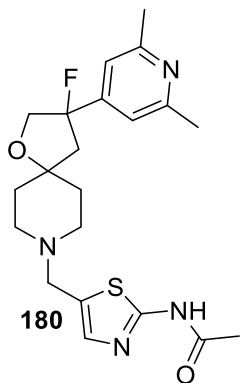


Flash column chromatography (EtOAc in Heptane 0/100 to 40/60) yielded **179** (61% yield) as a transparent oil as a mixture of diastereoisomers 1:1 (a:a'). <sup>1</sup>H NMR (CDCl<sub>3</sub>, 400 MHz) δ 7.03 (s, 2Ha + 2Ha'), 3.96 (s, 2Ha + 2Ha'), 3.61 (s, 2Ha + 2Ha'), 3.36 (m, 2Ha + 2Ha'), 2.71 (broad s, 1Ha + 1Ha'), 2.51 (s, 6Ha + 6Ha'), 2.19 (d, *J* = 13.8 Hz, 2Ha), 2.12 (d, *J* = 13.7 Hz, 2Ha'), 1.97 (m, 2Ha), 1.80 – 1.69 (m, 2Ha + 2Ha'), 1.63 (m, 2Ha'), 1.45 (s, 9Ha + 9Ha'). <sup>13</sup>C {<sup>1</sup>H} NMR (CDCl<sub>3</sub>, 100 MHz) δ 158.07, 154.78, 151.89, 116.72, 81.86, 81.31, 79.57, 78.48, 60.38, 53.35, 40.93, 37.48, 36.26,

## Experimental part

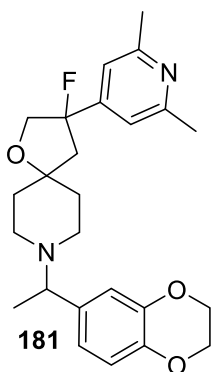
28.42, 24.54, 21.01, 14.16. **HRMS (ESI) for C<sub>20</sub>H<sub>31</sub>N<sub>2</sub>O<sub>4</sub> [M+H]<sup>+</sup>**: calculated: 363.22838, found: 363.2279.

### ***N*-(5-((3-(2,6-dimethylpyridin-4-yl)-3-fluoro-1-oxa-8-azaspiro[4.5]decan-8-yl)methyl)thiazol-2-yl)acetamide**



Purification by RP HPLC (Stationary phase: XBridge C<sub>18</sub> 50 x 100 mm, 5 μm), Mobile phase: Gradient from 73% NH<sub>4</sub>HCO<sub>3</sub> 0.25% solution in Water, 27% CH<sub>3</sub>CN to 56% NH<sub>4</sub>HCO<sub>3</sub> 0.25% solution in Water, 44% CH<sub>3</sub>CN, yielded **180** (36% yield) as a colourless oil as a mixture of diastereoisomers 1:1 (a:a'). **<sup>1</sup>H NMR (CDCl<sub>3</sub>, 400 MHz)** δ 12.72 (s, 1Ha + 1Ha'), 7.18 (s, 1Ha + 1Ha'), 6.92 (s, 2Ha + 2Ha'), 4.19 (ddd, *J* = 20.2, 10.9, 1.2 Hz, 2Ha), 3.95 (dd, *J* = 32.3, 11.0 Hz, 2Ha'), 3.68 (s, 2Ha + 2Ha'), 2.72 – 2.51 (m, 4Ha + 4Ha'), 2.50 (s, 6Ha + 6Ha'), 2.46 – 2.33 (m, 2Ha + 2Ha'), 2.29 (s, 3Ha + 3Ha'), 2.17 – 2.01 (m, 2Ha), 1.85 – 1.67 (m, 2Ha + 4Ha'). **<sup>13</sup>C {<sup>1</sup>H} NMR (CDCl<sub>3</sub>, 100 MHz)** δ 167.9, 160.1, 158.1, 158.1, 158.0, 148.5, 148.3, 140.1, 136.4, 133.7, 131.5, 130.0, 129.9, 116.7, 115.7, 115.6, 104.1, 102.3, 88.0, 81.6, 73.0, 54.3, 54.1, 51.4, 51.2, 50.1, 49.9, 49.8, 36.6, 36.3, 35.8, 24.4, 24.3, 23.0. **HRMS (ESI) for C<sub>21</sub>H<sub>28</sub>FN<sub>4</sub>O<sub>2</sub>S [M+H]<sup>+</sup>**: calculated: 419.1917, found: 419.1921.

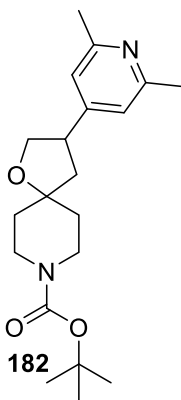
### **8-(1-(2,3-dihydrobenzo[*b*][1,4]dioxin-6-yl)ethyl)-3-(2,6-dimethylpyridin-4-yl)-3-fluoro-1-oxa-8-azaspiro[4.5]decane**



Double purification was needed: First: by flash column chromatography (MeOH in DCM 0/100 to 10/90) the desired fractions were collected and evaporated in vacuo. Second: the collected and evaporated fractions were purified by RP HPLC (Stationary phase: C<sub>18</sub> XBridge 30 x 100 mm 5 μm), Mobile phase: Gradient from 67% 0.1% NH<sub>4</sub>CO<sub>3</sub>H/NH<sub>4</sub>OH pH 9 solution in Water, 33% CH<sub>3</sub>CN to 50% 0.1% NH<sub>4</sub>CO<sub>3</sub>H/NH<sub>4</sub>OH pH 9 solution in Water, 50% CH<sub>3</sub>CN) yielded **181** (17% yield) as a colourless oil as a mixture of diastereoisomers 1:1 (a:a'). **<sup>1</sup>H NMR (CDCl<sub>3</sub>, 400 MHz)** δ 6.93 (s, 2Ha + 2Ha'), 6.83 (m, 1Ha + 1Ha'), 6.79 – 6.75 (m, 2Ha + 2Ha'), 4.23 (s, 4Ha + 4Ha'), 4.22 – 4.14 (m, 2Ha), 3.95 (m, 2Ha'), 3.37 (m, 1Ha + 1Ha'), 2.52 (s, 6Ha + 6Ha'), 2.39 (m, 4Ha + 2Ha'), 2.20 (m, 2Ha'), 2.04 (m, 2Ha + 2Ha'), 1.77 (m, 4Ha + 4Ha'), 1.33 (d, *J* = 6.7 Hz, 3Ha + 3Ha'). **<sup>13</sup>C {<sup>1</sup>H} NMR (CDCl<sub>3</sub>, 100 MHz)** δ 158.1, 158.1, 158.1, 148.8, 148.5, 143.1, 142.2, 140.3, 137.0, 136.3, 131.7, 120.5, 120.5, 120.5, 116.7, 116.7, 116.2, 116.2, 115.8, 115.7, 104.2, 102.3, 88.6, 82.2, 73.0, 64.3, 64.2, 63.9, 63.7, 51.3,

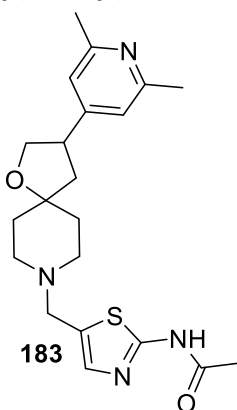
51.1, 47.7, 47.6, 47.4, 47.3, 47.2, 47.2, 37.1, 36.7, 36.3, 36.2, 24.5, 24.4, 19.3. **HRMS (ESI) for C<sub>25</sub>H<sub>32</sub>FN<sub>2</sub>O<sub>3</sub> [M+H]<sup>+</sup>**: calculated: 427.2397, found: 427.2392.

**Tert-butyl 3-(2,6-dimethylpyridin-4-yl)-1-oxa-8-azaspiro[4.5]decane-8-carboxylate**



Flash column chromatography (EtOAc in Heptane 0/100 to 40/60) yielded **182** (84% yield) as a colorless oil as a mixture of diastereoisomers 1:1 (a:a'). <sup>1</sup>H NMR (CDCl<sub>3</sub>, 400 MHz) δ 6.88 (s, 2Ha + 2Ha'), 4.20 (m, 2Ha), 3.79 (m, 2Ha'), 3.64 (broad s, 2Ha + 2Ha'), 3.44 (m, 1Ha + 1Ha'), 3.40 – 3.26 (m, 2Ha + 2Ha'), 2.55 (s, 6Ha + 6Ha'), 2.25 (m, 2Ha), 1.83 – 1.65 (m, 4Ha + 4Ha'), 1.57 (m, 2Ha'), 1.47 (s, 9Ha + 9Ha'). <sup>13</sup>C {<sup>1</sup>H} NMR (CDCl<sub>3</sub>, 100 MHz) δ 157.3, 154.7, 152.6, 119.6, 81.0, 79.4, 72.1, 44.7, 44.0, 41.0, 36.8, 36.1, 28.4, 23.5. **HRMS (ESI) for C<sub>20</sub>H<sub>31</sub>N<sub>2</sub>O<sub>3</sub> [M+H]<sup>+</sup>**: calculated: 347.23347, found: 347.2339.

**N-(5-((3-(2,6-dimethylpyridin-4-yl)-1-oxa-8-azaspiro[4.5]decan-8-yl)methyl)thiazol-2-yl)acetamide**



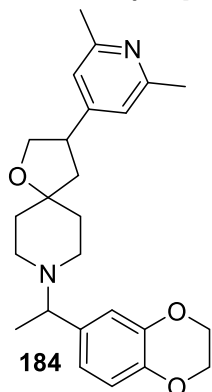
Flash column chromatography (MeOH in DCM 0/100 to 5/95) yielded **183** (32% yield) as a colourless oil as a mixture of diastereoisomers 1:1 (a:a'). <sup>1</sup>H NMR (CDCl<sub>3</sub>, 400 MHz) δ 12.68 (s, 1Ha + 1Ha'), 7.18 (s, 1Ha + 1Ha'), 6.79 (s, 2Ha + 2Ha'), 4.14 (m, 2Ha), 3.72 (m, 2Ha'), 3.67 (s, 2Ha + 2Ha'), 3.35 (m, 1Ha + 1Ha'), 2.52 (broad s, 4Ha + 4Ha'), 2.46 (s, 6Ha + 6Ha'), 2.29 (s, 3Ha + 3Ha'), 2.19 (m, 2Ha), 1.80 – 1.59 (m, 4Ha + 6Ha'). <sup>13</sup>C {<sup>1</sup>H} NMR (CDCl<sub>3</sub>, 100 MHz) δ 167.9, 160.0, 157.8, 151.3, 133.8, 130.0, 119.0, 80.7, 72.0, 54.2, 50.4, 50.1, 44.5, 43.8, 37.0, 36.4, 24.3, 23.0. **HRMS (ESI) for C<sub>21</sub>H<sub>29</sub>N<sub>4</sub>O<sub>2</sub>S [M+H]<sup>+</sup>**: calculated: 401.2011, found: 401.2041.



## Experimental part

---

### 8-(1-(2,3-Dihydrobenzo[b][1,4]dioxin-6-yl)ethyl)-3-(2,6-dimethylpyridin-4-yl)-1-oxa-8-azaspiro[4.5]decane



Double purification was needed: First: by flash column chromatography (MeOH in DCM 0/100 to 10/90) the desired fractions were collected and evaporated in vacuo. Second: the collected and evaporated fractions were purified by RP HPLC (Stationary phase: C<sub>18</sub> XBridge 30 x 100 mm 5 μm), Mobile phase: Gradient from 67% 0.1% NH<sub>4</sub>CO<sub>3</sub>H/NH<sub>4</sub>OH pH 9 solution in Water, 33% CH<sub>3</sub>CN to 50% 0.1% NH<sub>4</sub>CO<sub>3</sub>H/NH<sub>4</sub>OH pH 9 solution in Water, 50% CH<sub>3</sub>CN) yielded **184** (15% yield) as a colourless oil as a mixture of diastereoisomers 1:1 (a:a'). <sup>1</sup>H NMR (CDCl<sub>3</sub>, 400 MHz) δ 6.81 (s, 1Ha + 1Ha'), 6.79 (s, 2Ha + 2Ha'), 6.77 (s, 1Ha + 1Ha'), 6.75 (m, 1Ha + 1Ha'), 4.23 (s, 4Ha + 4Ha'), 4.13 (m, 1Ha + 1Ha'), 3.72 (m, 1Ha + 1Ha'), 3.34 (m, 2Ha

+ 2Ha'), 2.53 (broad s, 4Ha + 2Ha'), 2.47 (s, 6Ha + 6Ha'), 2.42 (broad s, 2Ha'), 2.18 (dd, *J* = 12.5, 8.3 Hz, 2Ha), 1.74 (m, 4Ha + Ha'), 1.62 (m, 2Ha'), 1.33 (d, *J* = 6.7 Hz, 3Ha + 3Ha'). <sup>13</sup>C {<sup>1</sup>H} NMR (CDCl<sub>3</sub>, 100 MHz) δ 157.8, 151.5, 143.1, 142.3, 136.8, 120.5, 119.0, 116.7, 116.2, 81.1, 72.0, 64.3, 64.2, 63.9, 63.9, 47.9, 47.7, 47.5, 44.4, 43.9, 37.4, 36.7, 24.3, 19.3, 19.2. HRMS (ESI) for C<sub>25</sub>H<sub>33</sub>N<sub>2</sub>O<sub>3</sub> [M+H]<sup>+</sup>: calculated: 409.24912, found: 409.2488.

## 8.5. Experimental procedures and spectral data of Chapter 6

### 8.5.1 General procedure for the protection of amines with sulphonyl chloride derivatives<sup>[14]</sup>

*N,N*-diisopropyletilamina (DIPEA, 2 equiv, 20 mmol) and the arenesulphonyl chloride derivative (1 equiv, 10 mmol) were added to a solution of methyl piperidine-4-carboxylate (1 equiv, 10 mmol) in dry dichlorometane (0.14 M) at room temperature. The mixture was stirred for 4-16 h until complete consumption of the corresponding arenesulphonyl chloride. The organic phase was washed with 10% of NaHCO<sub>3</sub>. The aqueous phase was extracted with ethyl acetate. The organic extracts were combined, washed with H<sub>2</sub>O and NaCl sat. solution, dried (MgSO<sub>4</sub>), filtered and the volatiles removed *in vacuo*. The crude product was purified by flash column chromatography.

### 8.5.2 General procedure for the alkylation reaction with different alkyl bromides<sup>[3, 15]</sup>

To a 0 °C solution of *i*Pr<sub>2</sub>NH (2.0 mL, 1.5 equiv, 15 mmol) in THF (15 mL), was added a hexane solution of *n*BuLi 2 M (4.4 mL, 1.1 equiv, 11 mmol) dropwise. The reaction mixture was stirred for 20 min. and then cooled to -78 °C. The corresponding ester (1.0 equiv, 10 mmol) was added dropwise and the reaction mixture was stirred for 1 h at -78 °C. The corresponding alkyl halide (1.5 equiv, 15 mmol, for *n*=1, allyl bromide; *n*=2, 4-bromobut-1-ene) was then added dropwise into the reaction mixture. The reaction mixture was then warmed naturally to room temperature and stirred until consumption of the starting sulphonamide. The reaction mixture was quenched by addition of NH<sub>4</sub>Cl sat. and extracted with Et<sub>2</sub>O three times. The combined organic layers were then dried (MgSO<sub>4</sub>) filtered and concentrated *in vacuo*. The crude product was purified by flash column chromatography.

### 8.5.3 General procedure for the reduction of the ester to alcohols<sup>[4]</sup>

To a slurry of LiAlH<sub>4</sub> (1.5 equiv, 6 mmol) in anhydrous Et<sub>2</sub>O (0.9 M) was added a solution of the methyl ester (1 equiv, 4 mmol) in Et<sub>2</sub>O (1 M) dropwise at 0 °C. The mixture was stirred for 2 h (or until consumption of the substrate). Reaction was then quenched by addition of EtOH dropwise after no observation of bubbles. Then, water was added and the mixture was stirred until a white solid was formed. The mixture was then filtered and extracted with EtOAc. The organic layers were separated, dried (MgSO<sub>4</sub>), filtered and concentrated under reduced pressure to obtain the alcohol without need of further purification for the next reaction step.

### 8.5.4 General procedure for the oxidation of primary alcohols to aldehydes<sup>[8]</sup>

To a solution of the cyclic alkenyl alcohol (2 mmol, 1 equiv) in DCM (2 mL) was added DMP (5 mmol, 2 equiv) and stirred at room temperature for 16 h. Then NaHCO<sub>3</sub> sat. solution was added and extracted few times with DCM. The organic layer was separated, dried (MgSO<sub>4</sub>), filtered and the solvent removed *in vacuo*. The crude was purified by flash column chromatography.

### 8.5.5 General procedure for the borylative cyclization catalyzed by copper (I) complex<sup>[17]</sup>

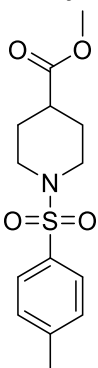
Copper chloride (5 mol%, 0.025 mmol), bis(pinacolato)diboron (1.2 equiv, 0.6 mmol) and Xantphos (5 mol%, 0.025 mmol) were placed in an oven-dried resalable Teflon screw-cap Schlenk reaction tube. The Schlenk tube was connected to a vacuum/nitrogen manifold evacuated and backfilled with nitrogen. Then THF (0.48 ml, 1 M). KO<sup>t</sup>Bu (1.2 equiv, 0.6 mmol) in THF (0.24 ml, 1 M) were added in the vial through the rubber septum. Then alkenyl aldehyde (1 equiv, 0.5 mmol) in THF (0.48 ml, 1 M) was added dropwise at 30 °C. After the reaction was complete, the reaction mixture was filtered over celite. The organic extracts were then concentrated *in vacuo*. The crude product was purified by flash chromatography.

### 8.5.6 General procedure for the oxidation of the spiroboronates products<sup>[7]</sup>

The oxidation was performed in a reaction vial, NaBO<sub>3</sub>·H<sub>2</sub>O (199.6 mg, 10 equiv, 2 mmol) was dissolved in THF/H<sub>2</sub>O (3:2, 0.2 M) and the boronate (83.8 mg, 1 equiv, 0.2 mmol) was then added at room temperature. After stirred for 1.5 h, the reaction mixture was extracted three times with EtOAc, dried (MgSO<sub>4</sub>), filtered and concentrated *in vacuo*. The crude mixture was further purified by flash column chromatography.

## 8.5.7 Spectral data of Chapter 6

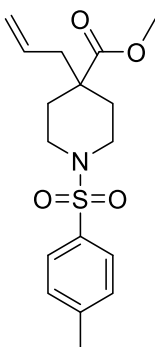
### Methyl 1-tosylpiperidine-4-carboxylate



185

Flash column chromatography (pentane: EtOAc 100:0 to 60:40) yielded **185** (60% yield) as white solid.  $^1\text{H NMR}$  ( $\text{CDCl}_3$ , 400 MHz)  $\delta$  7.62 (d,  $J = 7.9$  Hz, 2H), 7.31 (d,  $J = 7.9$  Hz, 2H), 3.64 (s, 3H), 3.61 (m, 2H), 2.43 (td,  $J = 11.4, 2.9$  Hz, 2H), 2.42 (s, 3H), 2.24 (tt,  $J = 10.7, 4.0$  Hz, 1H), 1.95 (m, 2H), 1.79 (m, 2H).  $^{13}\text{C}$   $\{^1\text{H}\}$  NMR ( $\text{CDCl}_3$ , 100 MHz)  $\delta$  174.2, 143.5, 132.9, 129.6, 127.6, 51.8, 45.3, 39.8, 27.3, 21.4. HRMS (ESI) for  $\text{C}_{28}\text{H}_{38}\text{N}_2\text{NaO}_8\text{S}_2$  [ $2\text{M} + \text{Na}$ ] $^+$ : calculated: 617.1968, found: 617.1985.

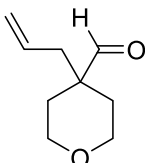
### Methyl 4-allyl-1-tosylpiperidine-4-carboxylate



187

Flash column chromatography (pentane: EtOAc 100:0 to 60:40) yielded **187** (62% yield) as white solid.  $^1\text{H NMR}$  ( $\text{CDCl}_3$ , 400 MHz)  $\delta$  7.59 (d,  $J = 8.2$  Hz, 2H), 7.28 (d,  $J = 8.2$  Hz, 2H), 5.58 (ddt,  $J = 14.9, 10.1, 7.5$  Hz, 1H), 5.06 – 4.90 (m, 2H), 3.60 – 3.50 (m, 3H), 3.55 (s, 3H), 2.40 (s, 3H), 2.37 (dd,  $J = 12.0, 2.1$  Hz, 2H), 2.19 (d,  $J = 7.5$  Hz, 2H), 2.15 (m, 2H), 1.54 (m, 2H).  $^{13}\text{C}$   $\{^1\text{H}\}$  NMR ( $\text{CDCl}_3$ , 100 MHz)  $\delta$  174.8, 143.3, 133.3, 132.1, 129.5, 127.5, 118.6, 51.7, 45.2, 44.2, 43.6, 32.4, 21.4. HRMS (ESI) for  $\text{C}_{17}\text{H}_{24}\text{NO}_4\text{S}$  [ $\text{M} + \text{H}$ ] $^+$ : calculated: 338.1421, found: 338.1425.

### 4-Allyltetrahydro-2H-pyran-4-carbaldehyde

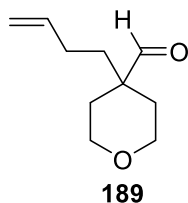


188

Flash column chromatography (pentane:  $\text{Et}_2\text{O}$  100:0 to 60:40) yielded **188** (52% yield) as a clear oil.  $^1\text{H NMR}$  ( $\text{CDCl}_3$ , 400 MHz)  $\delta$  9.50 (s, 1H), 5.66 (m, 1H), 5.10 (m, 2H), 3.81 (dt,  $J = 12.0, 4.3$  Hz, 2H), 3.43 (m, 2H), 2.25 (d,  $J = 7.5$  Hz, 2H), 1.93 (dt,  $J = 13.7, 3.9$  Hz, 2H), 1.60 (m, 3H).  $^{13}\text{C}$   $\{^1\text{H}\}$  NMR ( $\text{CDCl}_3$ , 100 MHz)  $\delta$  204.6, 131.2, 118.5, 64.0, 46.9, 40.4, 30.2. HRMS (ESI) for  $\text{C}_9\text{H}_{15}\text{O}_2$  [ $\text{M} + \text{H}$ ] $^+$ : calculated: 155.1067, found: 155.1053.

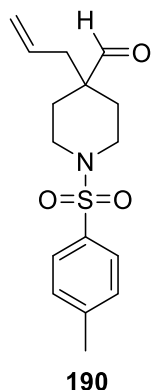
## Experimental part

### 4-(But-3-en-1-yl)tetrahydro-2H-pyran-4-carbaldehyde



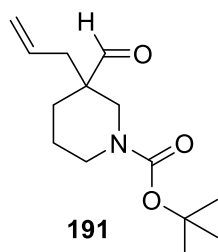
Flash column chromatography (pentane: Et<sub>2</sub>O 100:0 to 60:40) yielded **189** (76% yield) as a clear oil. <sup>1</sup>H NMR (CDCl<sub>3</sub>, 400 MHz) δ 9.42 (s, 1H), 5.67 (ddt, *J* = 16.8, 10.1, 6.5 Hz, 1H), 4.92 (m, 2H), 3.76 (dt, *J* = 11.8, 4.0 Hz, 2H), 3.36 (td, *J* = 11.5, 2.6 Hz, 2H), 1.94 – 1.81 (m, 4H), 1.59 – 1.45 (m, 4H). <sup>13</sup>C {<sup>1</sup>H} NMR (CDCl<sub>3</sub>, 100 MHz) δ 205.3, 137.4, 115.1, 64.5, 47.3, 35.9, 30.9, 27.3. HRMS (ESI) for C<sub>10</sub>H<sub>17</sub>O<sub>2</sub> [M + H]<sup>+</sup>: calculated: 169.1223, found: 169.1221.

### 4-Allyl-1-tosylpiperidine-4-carbaldehyde



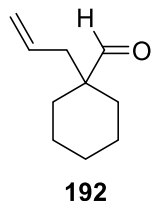
Flash column chromatography (pentane: EtOAc 100:0 to 60:40) yielded **190** (77% yield) as a clear oil. <sup>1</sup>H NMR (CDCl<sub>3</sub>, 400 MHz) δ 9.32 (s, 1H), 7.57 (d, *J* = 7.9 Hz, 2H), 7.28 (d, *J* = 7.9 Hz, 2H), 5.56 (m, 1H), 5.05 (m, 2H), 3.54 (dt, *J* = 11.8, 3.2 Hz, 2H), 2.40 (s, 3H), 2.33 (td, *J* = 12.1, 2.8 Hz, 2H), 2.16 (d, *J* = 7.5 Hz, 2H), 2.05 (m, 2H), 1.64 (m, 2H). <sup>13</sup>C {<sup>1</sup>H} NMR (CDCl<sub>3</sub>, 100 MHz) δ 204.7, 143.6, 132.8, 130.9, 129.6, 127.4, 119.5, 47.6, 43.2, 40.6, 29.6, 21.4. HRMS (ESI) for C<sub>16</sub>H<sub>22</sub>NO<sub>3</sub>S [M + H]<sup>+</sup>: calculated: 308.1315, found: 308.1315.

### Tert-butyl 3-allyl-3-formylpiperidine-1-carboxylate



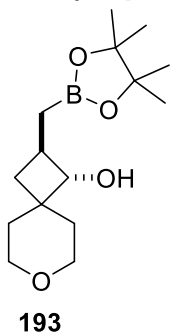
Flash column chromatography (pentane: EtOAc 100:0 to 60:40) yielded **191** (93% yield) as a clear oil. <sup>1</sup>H NMR (CDCl<sub>3</sub>, 400 MHz) δ 9.49 (s, 1H), 5.61 (m, 1H), 5.03 (m, 2H), 3.97 (m, 1H), 3.61 (broad s, 1H), 2.99 (broad s, 2H), 2.16 (m, 2H), 1.93 (broad s, 1H), 1.49 (m, 2H), 1.39 (s, 9H). <sup>13</sup>C {<sup>1</sup>H} NMR (CDCl<sub>3</sub>, 100 MHz) δ 204.7, 154.6, 131.5, 119.1, 79.8, 60.3, 49.7, 48.1, 44.1, 43.5, 38.3, 37.8, 29.0, 28.3, 21.7, 20.9, 14.1. HRMS (ESI) for C<sub>14</sub>H<sub>23</sub>NNaO<sub>3</sub> [M + Na]<sup>+</sup>: calculated: 276.1570, found: 276.1573.

### 1-Allylcyclohexane-1-carbaldehyde



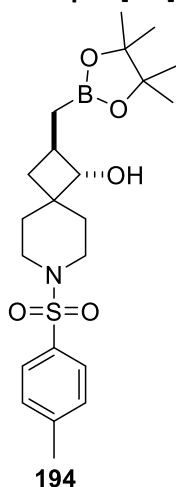
Flash column chromatography (pentane: DCM 80:20) yielded **192** (82% yield) as a colorless oil. <sup>1</sup>H NMR (CDCl<sub>3</sub>, 400 MHz) δ 9.38 (s, 1H), 5.69 – 5.48 (m, 1H), 4.97 (m, 2H), 2.11 (d, *J* = 7.5 Hz, 2H), 1.86 – 1.76 (m, 2H), 1.56 – 1.43 (m, 3H), 1.31 – 1.16 (m, 5H). <sup>13</sup>C {<sup>1</sup>H} NMR (CDCl<sub>3</sub>, 100 MHz) δ 206.8, 132.6, 118.2, 49.6, 40.7, 30.7, 29.6, 25.6, 22.4.

**Anti-2-((4,4,5,5-tetramethyl-1,3,2-dioxaborolan-2-yl)methyl)-7-oxaspiro[3.5]nonan-1-ol**



Flash column chromatography (pentane: EtOAc 100:0 to 60:40) yielded **193** (71% yield) as a clear oil.  $^1\text{H NMR}$  ( $\text{CDCl}_3$ , 400 MHz)  $\delta$  3.87 (dt,  $J = 10.8, 4.4$  Hz, 1H), 3.72 (dt,  $J = 10.9, 4.4$  Hz, 1H), 3.59 (m, 1H), 3.46 (d,  $J = 8$  Hz, 1H), 3.43 (dd,  $J = 11.5, 2.3$  Hz, 1H), 2.14 (m, 1H), 1.93 (m, 2H), 1.76 (ddd,  $J = 13.3, 9.6, 3.9$  Hz, 1H), 1.49 (m, 1H), 1.39 (m, 1H), 1.25 (s, 12H), 1.09 (dd,  $J = 16.4, 5.1$  Hz, 1H), 0.95 (t,  $J = 10.2$  Hz, 1H), 0.86 (dd,  $J = 16.4, 10.6$  Hz, 1H).  $^{13}\text{C}$   $\{^1\text{H}\}$  NMR ( $\text{CDCl}_3$ , 100 MHz)  $\delta$  83.3, 80.9, 64.9, 64.7, 39.4, 38.8, 36.3, 33.6, 30.5, 24.7, 24.7.  $^{11}\text{B NMR}$  (129 MHz,  $\text{CDCl}_3$ )  $\delta$  33.8. HRMS (ESI) for  $\text{C}_{15}\text{H}_{26}\text{BO}_3$  [ $\text{M} - \text{H}_2\text{O} + \text{H}$ ] $^+$ : calculated: 265.1975, found: 265.1964.

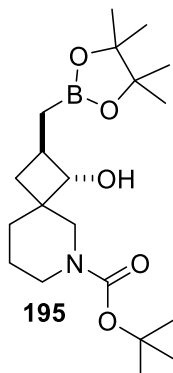
**Anti-2-((4,4,5,5-tetramethyl-1,3,2-dioxaborolan-2-yl)methyl)-7-tosyl-7-azaspiro[3.5]nonan-1-ol**



Flash column chromatography (pentane: EtOAc 100:0 to 60:40) yielded **194** (67% yield) as a clear oil.  $^1\text{H NMR}$  ( $\text{CDCl}_3$ , 400 MHz)  $\delta$  7.63 (d,  $J = 8.0$  Hz, 2H), 7.30 (d,  $J = 8.0$  Hz, 2H), 3.43 (d,  $J = 7.8$  Hz, 1H), 3.38 (m, 1H), 3.21 (m, 1H), 2.84 (s, 1H), 2.79 (m, 1H), 2.66 (m, 1H), 2.42 (s, 3H), 2.07 (m, 1H), 1.95 (m, 1H), 1.77 (m, 1H), 1.73 (t,  $J = 10.2$  Hz, 1H), 1.63 (m, 1H), 1.52 (m, 1H), 1.22 (s, 12H), 1.04 (dd,  $J = 16.7, 4.9$  Hz, 1H), 0.81 (t,  $J = 10.2$  Hz, 1H), 0.76 (m, 1H).  $^{13}\text{C}$   $\{^1\text{H}\}$  NMR ( $\text{CDCl}_3$ , 100 MHz)  $\delta$  143.1, 133.5, 129.4, 127.5, 83.4, 80.4, 43.4, 43.2, 39.4, 37.5, 36.2, 29.4, 24.7, 21.4.  $^{11}\text{B NMR}$  (129 MHz,  $\text{CDCl}_3$ )  $\delta$  33.0. HRMS (ESI) for  $\text{C}_{22}\text{H}_{35}\text{BNO}_5\text{S}$  [ $\text{M} - \text{H}_2\text{O} + \text{H}$ ] $^+$ : calculated: 436.2329, found: 436.2330.

## Experimental part

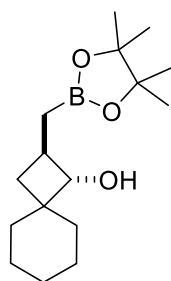
### **Anti-2-((4,4,5,5-tetramethyl-1,3,2-dioxaborolan-2-yl)methyl)-7-tosyl-7-azaspiro[3.5]nonan-1-ol**



**195**

Flash column chromatography (pentane: EtOAc 100:0 to 60:40) yielded **195** (25% yield) as a clear oil.  $^1\text{H NMR}$  (Toluene- $\text{D}_8$ ,  $95^\circ\text{C}$ , 400 MHz)  $\delta$  3.49 (dd,  $J = 42.6, 13.8$  Hz, 2H), 3.35 (broad s, 1H), 3.34 (d,  $J = 7.2$  Hz, 1H), 3.15 (m, 1H), 2.23 (m, 1H), 1.83 (t,  $J = 10.1$  Hz, 1H), 1.50 (m, 1H), 1.40 (s, 9H), 1.25 (m, 3H), 1.04 (s, 12H), 0.96 (d,  $J = 7.5$  Hz, 2H), 0.72 (t,  $J = 10.1$  Hz, 1H).  $^{13}\text{C}$   $\{^1\text{H}\}$  NMR ( $\text{CDCl}_3$ ,  $60^\circ\text{C}$ , 100 MHz)  $\delta$  155.2, 83.1, 80.9, 79.2, 48.2, 44.4, 42.1, 37.3, 37.2, 31.9, 28.4, 24.7, 24.6, 22.8, 22.6.  $^{11}\text{B NMR}$  (129 MHz,  $\text{CDCl}_3$ )  $\delta$  33.7. HRMS (ESI) for  $\text{C}_{20}\text{H}_{37}\text{BNO}_5$   $[\text{M} + \text{H}]^+$ : calculated: 382.2759, found: 382.2763.

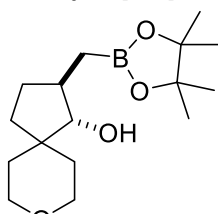
### **Anti-2-(4,4,5,5-tetramethyl-1,3,2-dioxaborolan-2-yl)spiro[3.5]nonan-1-ol**



**196**

Flash column chromatography (pentane:  $\text{Et}_2\text{O}$  60:40) yielded **196** (49% yield) as a colourless oil.  $^1\text{H NMR}$  ( $\text{CDCl}_3$ , 400 MHz)  $\delta$  3.33 (d,  $J = 7.6$  Hz, 1H), 2.09 – 1.95 (m, 1H), 1.84 – 1.76 (m, 1H), 1.64 – 1.24 (m, 10H), 1.18 (s, 12H), 0.99 (dd,  $J = 16.4, 5.6$  Hz, 1H), 0.83 – 0.79 (m, 1H), 0.77 (d,  $J = 10.5$  Hz, 1H).  $^{13}\text{C}$   $\{^1\text{H}\}$  NMR ( $\text{CDCl}_3$ , 100 MHz)  $\delta$  83.35, 81.80, 42.12, 39.41, 36.64, 34.07, 29.93, 26.40, 24.84, 23.32, 23.09, 22.55.  $^{11}\text{B NMR}$  (129 MHz,  $\text{CDCl}_3$ )  $\delta$  34.0. HRMS (ESI) for  $\text{C}_{16}\text{H}_{33}\text{BNO}_3$   $[\text{M} + \text{NH}_4]^+$ : calculated: 298.2557, found: 298.2553.

### **Anti-2-((4,4,5,5-tetramethyl-1,3,2-dioxaborolan-2-yl)methyl)-7-oxaspiro[3.5]nonan-1-ol**

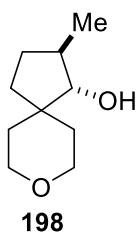


**197**

Flash column chromatography (pentane: EtOAc 100:0 to 50:50) yielded **197** (45% yield) as a clear oil.  $^1\text{H NMR}$  ( $\text{CDCl}_3$ , 400 MHz)  $\delta$  3.82 (m, 2H), 3.49 (m, 2H), 3.12 (d,  $J = 8.3$  Hz, 1H), 1.84 (m, 4H), 1.72 (m, 1H), 1.40 (m, 2H), 1.24 (s, 12H), 1.13 (m, 2H), 1.06 – 0.93 (m, 2H).  $^{13}\text{C}$   $\{^1\text{H}\}$  NMR ( $\text{CDCl}_3$ , 100 MHz)  $\delta$  87.0, 83.3, 65.3, 64.5, 42.2, 40.6, 36.9, 31.9, 30.2, 29.3, 24.7.  $^{11}\text{B NMR}$  (129 MHz,  $\text{CDCl}_3$ )  $\delta$  33.8. HRMS (ESI) for  $\text{C}_{16}\text{H}_{30}\text{BO}_4$   $[\text{M} + \text{H}]^+$ : calculated:

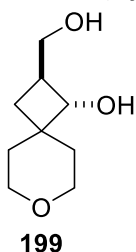
297.2237, found: 297.2238.

**Anti-2-((4,4,5,5-tetramethyl-1,3,2-dioxaborolan-2-yl)methyl)-7-oxaspiro[3.5]nonan-1-ol**



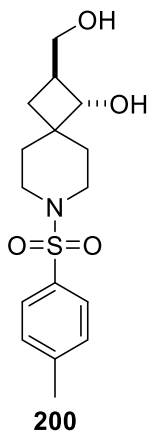
Flash column chromatography (pentane: EtOAc 100:0 to 50:50) yielded **198** (75% yield) as a clear oil.  $^1\text{H NMR}$  ( $\text{CDCl}_3$ , 400 MHz)  $\delta$  3.85 (m, 2H), 3.51 (m, 2H), 3.09 (d,  $J = 8.5$  Hz, 1H), 1.81 (m, 5H), 1.45 (m, 1H), 1.15 (m, 3H), 1.07 (d,  $J = 6.3$  Hz, 3H).  $^{13}\text{C}$   $\{^1\text{H}\}$  NMR ( $\text{CDCl}_3$ , 100 MHz)  $\delta$  87.2, 65.5, 64.4, 42.0, 39.0, 36.8, 31.7, 30.1, 27.9, 18.4. HRMS (ESI) for  $\text{C}_{10}\text{H}_{19}\text{O}_2$   $[\text{M} + \text{H}]^+$ : calculated: 171.1380, found: 171.1382.

**Anti-2-(hydroxymethyl)-7-oxaspiro[3.5]nonan-1-ol**



Flash column chromatography (pentane: EtOAc 100:0 to 0:100) yielded **199** (61% yield) as a clear oil.  $^1\text{H NMR}$  ( $\text{CDCl}_3$ , 400 MHz)  $\delta$  3.89 (dt,  $J = 11.3, 4.1$  Hz, 1H), 3.73 (m, 1H + 2H  $\text{CH}_2\text{-OH}$ ), 3.59 (m, 1H + 1H  $\text{CH-OH}$ ), 3.43 (td,  $J = 11.1, 2.6$  Hz, 1H), 2.33 (m, 1H), 1.88 (m, 2H), 1.77 (m, 1H), 1.50 (apparent d, 1H), 1.40 (m, 1H), 1.09 (t,  $J = 10.1$  Hz, 1H).  $^{13}\text{C}$   $\{^1\text{H}\}$  NMR ( $\text{CDCl}_3$ , 100 MHz)  $\delta$  77.2, 76.6, 64.9, 64.5, 42.6, 40.1, 38.1, 30.4, 29.6, 27.2. HRMS (ESI) for  $\text{C}_9\text{H}_{17}\text{O}_3$   $[\text{M} + \text{H}]^+$ : calculated: 173.1172, found: 173.1185.

**Anti-2-(hydroxymethyl)-7-tosyl-7-azaspiro[3.5]nonan-1-ol**

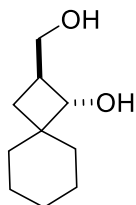


Flash column chromatography (pentane: EtOAc 100:0 to 0:100) yielded **200** (75% yield) as a clear oil.  $^1\text{H NMR}$  ( $\text{CDCl}_3$ , 400 MHz)  $\delta$  7.63 (d,  $J = 8.0$  Hz, 2H), 7.31 (d,  $J = 8.0$  Hz, 2H), 3.72 (d,  $J = 7.5$  Hz, 1H), 3.67 (dd,  $J = 10.9, 5.3$  Hz, 1H), 3.59 (dd,  $J = 10.9, 5.3$  Hz, 1H), 3.49 (m, 1H), 3.32 (m, 1H), 2.67 (td,  $J = 11.4, 3.0$  Hz, 1H), 2.53 (td,  $J = 11.4, 3.0$  Hz, 1H), 2.43 (s, 3H), 2.27 (m, 1H), 1.90 (m, 1H), 1.78 (m, 1H), 1.64 (m, 1H), 1.59 (t,  $J = 10.8$  Hz, 1H), 1.51 (m, 1H), 0.97 (t,  $J = 10.8$  Hz, 1H).  $^{13}\text{C}$   $\{^1\text{H}\}$  NMR ( $\text{CDCl}_3$ , 100 MHz)  $\delta$  143.3, 133.3, 129.6, 127.6, 75.6, 64.4, 43.3, 42.9, 42.4, 40.1, 36.7, 29.2, 26.5, 21.5. HRMS (ESI) for  $\text{C}_{16}\text{H}_{24}\text{NO}_4\text{S}$   $[\text{M} + \text{H}]^+$ : calculated: 326.1421, found: 326.1427.



Experimental part

---

**Anti-2-(hydroxymethyl)spiro[3.5]nonan-1-ol2-(hydroxymethyl)spiro[3.5]nonan-1-ol****201**

Flash column chromatography (pentane: EtOAc 100:0 to 0:100) yielded **201** (90% yield) as colourless oil.  $^1\text{H NMR}$  ( $\text{CDCl}_3$ , 400 MHz)  $\delta$  3.63 (dd,  $J = 10.9, 5.1$  Hz, 1H), 3.53 – 3.44 (m, 2H), 3.37 (s, 1H), 2.28 – 2.14 (m, 1H), 1.65 (t,  $J = 10.3$  Hz, 1H), 1.62 – 1.24 (m, 8H), 1.24 – 1.09 (m, 2H), 0.85 (t,  $J = 10.2$  Hz, 1H).  $^{13}\text{C}$   $\{^1\text{H}\}$  NMR ( $\text{CDCl}_3$ , 100 MHz)  $\delta$  78.0, 65.7, 42.7, 42.6, 38.7, 29.8, 27.4, 26.3, 23.1, 22.3. HRMS (ESI) for  $\text{C}_{10}\text{H}_{18}\text{O}_2$   $[\text{M}]^+$ :calculated: 170.1307, found: 170.1309.

## 8.6. References Chapter 8

- [1] B. Wiemer, *Acta Hydrochim. Hydrobiol.* **1989**, *17*, 632-632.
- [2] N. B. Palakurthy, B. Mandal, *Tetrahedron Lett.* **2011**, *52*, 7132-7134.
- [3] V. Y. Stolyarenko, A. A. Evdokimov, V. I. Shishkin, *Mendeleev Commun.* **2013**, *23*, 233-234.
- [4] F. X. Tavares, D. N. Deaton, A. B. Miller, L. R. Miller, L. L. Wright, H. Q. Zhou, *J. Med. Chem.* **2004**, *47*, 5049-5056.
- [5] H. Li, S. S. Babu, S. T. Turner, D. Neher, M. J. Hollamby, T. Seki, S. Yagai, Y. Deguchi, H. Möhwald, T. Nakanishi, *J. Mater. Chem.* **2013**, *1*, 1943-1951.
- [6] A. R. O. Venning, P. T. Bohan, E. J. Alexanian, *J. Am. Chem. Soc.* **2015**, *137*, 3731-3734.
- [7] E. Yamamoto, Y. Takenouchi, T. Ozaki, T. Miya, H. Ito, *J. Am. Chem. Soc.* **2014**, *136*, 16515-16521.
- [8] Y. Yamano, M. V. Chary, A. Wada, *Chem. Pharm. Bull.* **2010**, *58*, 1362-1365.
- [9] E. La Cascia, A. B. Cuenca, E. Fernández, *Chem. Eur. J.* **2016**, *22*, 18737-18741.
- [10] a) J. R. Coombs, L. Zhang, J. P. Morken, *Org. Lett.* **2015**, *17*, 1708-1711; b) K. Endo, M. Hirokami, T. Shibata, *J. Org. Chem.* **2010**, *75*, 3469-3472; c) K. Endo, A. Sakamoto, T. Ohkubo, T. Shibata, *Chem. Lett.* **2011**, *40*, 1440-1442.
- [11] K. E. Harding, L. M. May, K. F. Dick, *J. Org. Chem.* **1975**, *40*, 1664-1665.
- [12] R. Moumne, S. Lavielle, P. Karoyan, *J. Org. Chem.* **2006**, *71*, 3332-3334.
- [13] K. Kubota, E. Yamamoto, H. Ito, *J. Am. Chem. Soc.* **2013**, *135*, 2635-2640.
- [14] J. Mendiola, S. García, Ó. Frutos, M. L. Puente, R. L. Gu, V. V. Khau, *Org. Process Res. Dev.* **2009**, *13*, 292-296.
- [15] C. V. Stevens, T. Rammeloo, N. De Kimpe, *Synlett* **2001**, *2001*, 1519-1522.
- [16] J. E. DeLorbe, S. Y. Jabri, S. M. Mennen, L. E. Overman, F. L. Zhang, *J. Am. Chem. Soc.* **2011**, *133*, 6549-6552.
- [17] J. Royes, S. Ni, A. Farré, E. La Cascia, J. J. Carbó, A. B. Cuenca, F. Maseras, E. Fernández, *ACS Catal.* **2018**, *8*, 2833-2838.

## Experimental part

---

- [18] K. M. Bogle, D. J. Hirst, D. J. Dixon, *Tetrahedron* **2010**, *66*, 6399-6410.
- [19] F. Mo, F. Li, D. Qiu, J. Wang, *Tetrahedron* **2010**, *66*, 1274-1279.
- [20] S. D. Patel, W. M. Habeski, H. Min, J. Zhang, R. Roof, B. Snyder, G. Bora, B. Campbell, C. Li, D. Hidayetoglu, D. S. Johnson, A. Chaudhry, M. E. Charlton, N. M. Kablaoui, *Bioorg. Med. Chem. Lett.* **2008**, *18*, 5689-5693.
- [21] P. D. Bailey, K. M. Morgan, D. I. Smith, J. M. Vernon, *Tetrahedron* **2003**, *59*, 3369-3378.
- [22] A. I. Moskalenko, S. L. Belopukhov, A. A. Ivlev, V. I. Boev, *Russ. J. Organ. Chem.* **2011**, *47*, 1091-1096.
- [23] M. J. Meyers, S. A. Long, M. J. Pelc, J. L. Wang, S. J. Bowen, B. A. Schweitzer, M. V. Wilcox, J. McDonald, S. E. Smith, S. Foltin, J. Rumsey, Y. S. Yang, M. C. Walker, S. Kamtekar, D. Beidler, A. Thorarensen, *Bioorg. Med. Chem. Lett.* **2011**, *21*, 6545-6553.
- [24] E. Torrente, C. Parodi, L. Ercolani, C. De Mei, A. Ferrari, R. Scarpelli, B. Grimaldi, *J. Med. Chem.* **2015**, *58*, 5900-5915.
- [25] K. C. Caster, in *Encyclopedia of Reagents for Organic Synthesis*.
- [26] J. T. Welch, D. S. Lim, *Bioorg. Med. Chem.* **2007**, *15*, 6659-6666.
- [27] G. Sartori, R. Ballini, F. Bigi, G. Bosica, R. Maggi, P. Righi, *Chem. Rev.* **2004**, *104*, 199-250.
- [28] D. Franck, T. Kniess, J. Steinbach, S. Zitzmann, M. Friebe, L. M. Dinkelborg, K. Graham, *Bioorg. Med. Chem.* **2013**, *21*, 643-652.
- [29] J. J. W. Duan, Z. Lu, B. Jiang, B. V. Yang, L. M. Doweiko, D. S. Nirschl, L. E. Haque, S. Lin, G. Brown, J. Hynes, J. S. Tokarski, J. S. Sack, J. Khan, J. S. Lippy, R. F. Zhang, S. Pitt, G. Shen, W. J. Pitts, P. H. Carter, J. C. Barrish, S. G. Nadler, L. M. Salter-Cid, M. McKinnon, A. Fura, G. L. Schieven, S. T. Wroblewski, *Bioorg. Med. Chem. Lett.* **2014**, *24*, 5721-5726.
- [30] K. Takao, N. Hayakawa, R. Yamada, T. Yamaguchi, H. Saegusa, M. Uchida, S. Samejima, K. Tadano, *J. Org. Chem.* **2009**, *74*, 6452-6461.
- [31] S. Albrecht, A. Defoin, C. Tarnus, *Synthesis* **2006**, *2006*, 1635-1638.
- [32] S. Randl, S. Blechert, *J. Org. Chem.* **2003**, *68*, 8879-8882.

- [33] Y. Fukuta, T. Mita, N. Fukuda, M. Kanai, M. Shibasaki, *J. Am. Chem. Soc.* **2006**, *128*, 6312-6313.
- [34] S. D. Banister, L. M. Rendina, M. Kassiou, *Bioorg. Med. Chem. Lett.* **2012**, *22*, 4059-4063.
- [35] S. Bhattacharyya, *J. Org. Chem.* **1995**, *60*, 4928-4929.

UNIVERSITAT ROVIRA I VIRGILI  
COMPLEMENTARY SYNTHESIS OF ORGANOBORANES TO POPULATE THE CHEMICAL  
FUNCTIONALITY TO A GIVEN AREA OF BIOMEDICAL INTEREST  
Jordi Royes Buisan

# Chapter 9

## Summary

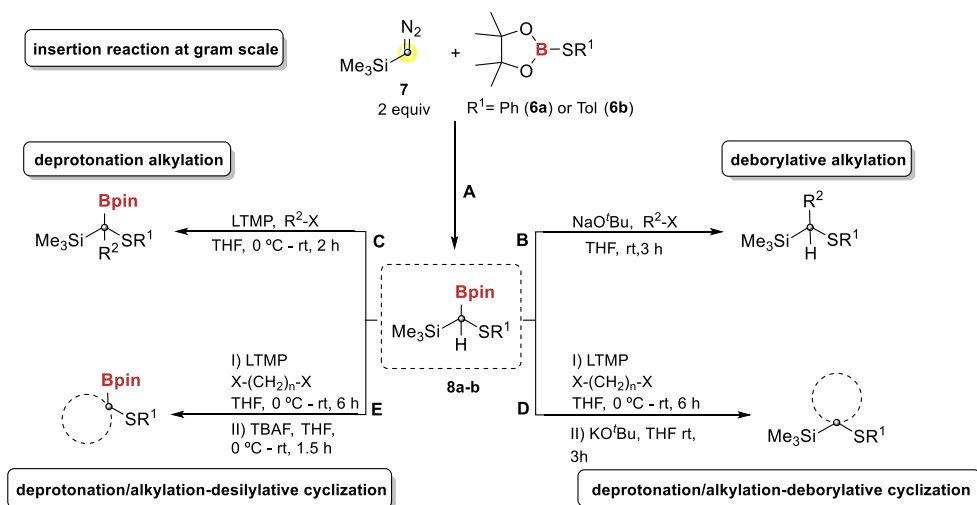
---

UNIVERSITAT ROVIRA I VIRGILI  
COMPLEMENTARY SYNTHESIS OF ORGANOBORANES TO POPULATE THE CHEMICAL  
FUNCTIONALITY TO A GIVEN AREA OF BIOMEDICAL INTEREST  
Jordi Royes Buisan

## 9.1. Summary of the thesis

The interest of the scientific community on organoborane chemistry has grown steadily over the last decades. Reported methods for the intramolecular cyclization through boron reagents have demonstrated high value to provide useful building blocks with high synthetic potential for further functionalization. In this thesis, we aimed to contribute on the development of new methodologies for the intramolecular cyclization through activation of organoborane reagents, both in metal-catalyzed<sup>[1]</sup> and transition metal-free<sup>[2]</sup> contexts.

Chapter 3 deals with the direct insertion of diazo compounds into  $\sigma$ -bonds in a transition metal-free context, as it represents an efficient process that guarantees access to complex molecular entities. Based on previous work from our group in the insertion of diazo compounds into unsymmetrical diboron reagent pinB-Bdan,<sup>[3]</sup> we proposed in the first project of the thesis to study the insertion of commercially available  $[\text{CH}(\text{N}_2)(\text{SiMe}_3)]$  (**7**) into pinB-SPh (**6a**) and pinB-STol (**6b**) reagents. This studies resulted in a straightforward methodology to access multisubstituted  $\text{sp}^3$  carbons (Si, B, S, H). The selective functionalization of the formed *gem*-polymetalloids following a selective base-mediated strategy, gave access to structurally diverse molecules of synthetic application (Scheme 9.1).



**Scheme 9.1** Strategic trimethylsilyldiazomethane insertion into pinB-SR  $\sigma$ -bonds, followed by selective functionalizations.

The insertion of **7** into the B-S  $\sigma$ -bond was examined with pinB-SPh (**6a**) and pinB-STol (**6b**) providing access to tri-substituted methanes  $[\text{CH}(\text{Bpin})(\text{SiMe}_3)(\text{SR})]$  in quantitative yields, even to a gram scale.



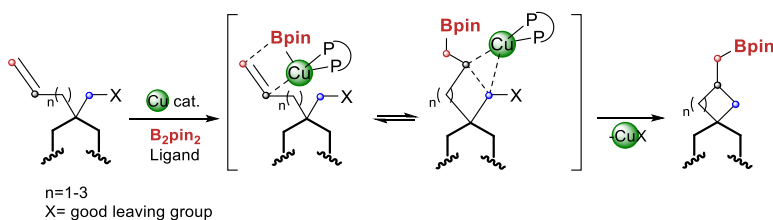
## Summary

---

Remarkably, the functionalization of the *gem*-polymetaloids was controlled by the base and exhibited not dependency on the electrophile nature. Up to twelve different electrophiles were submitted to alkylation conditions with different bases. Alkylation of the boryl fragment was facilitated by the use of sodium *tert*-butoxide providing the alkyl deborylated products. Alkyl tetra-substituted methanes with retention of the boron group were also obtained by alkylation of a carbanion formed by deprotonation with bulky lithium amide base such as LTMP. This carbanion is highly stabilized due to the three metalloid substituents in  $\alpha$ -position.

Going one step further, if 1,*n*-lineal dihaloalkanes are used in the deproto-alkylation procedure, an intermediate containing both, a geminal silyl, boryl, sulfide carbon and a distal halogen is obtained. Such intermediate can be further cyclized intramolecularly with concomitant deborylation or desilylation as a function of the employed base.

In Chapters 4 and 5 we became interested in the formation spiro-bicyclic compounds through intramolecular borylative cyclization processes and their corresponding application in Medicinal Chemistry projects. For this purpose synthesized a variety of well-designed substrates containing a haloalkene chain which under borylative cyclization conditions, mediated by copper (I), can afforded spiro-bicyclic products with a pendant methyl boryl unit (Scheme 9.2).



**Scheme 9.2** Copper (I) mediated borylative cyclization.

The substrates selected proved a high functional group tolerance for the spiro-cyclization reaction, as cyclic substrates containing oxygen or nitrogen heteroatoms and diverse functional groups underwent the transformation. Moreover, the boryl moiety installed through regioselective borylcupration step, could be selectively derivatized into different functional groups.

Additionally, this method was suitable to prepare dispiro-tricyclic structures (**108**) which are high valuable scaffolds in medicinal chemistry and agrochemicals research<sup>[4]</sup> (Figure 9.1).

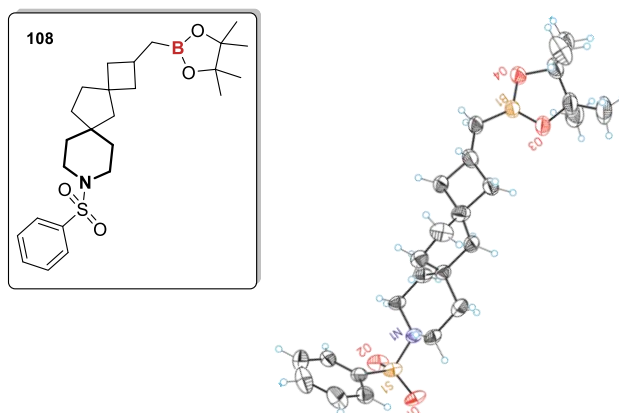


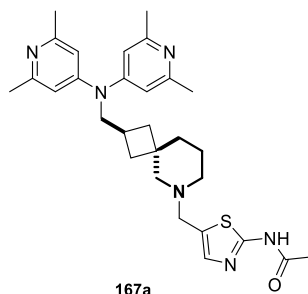
**Figure 9.1** ORTEP of the X-Ray diffraction analysis for dispiro-heterocycle **108**.

Furthermore, a mechanistic proposal supported by DFT calculations was carried out in collaboration with Prof. Maseras and Mr. Ni from ICIQ. With this studies it was possible to identify transition states that justify the reactivity observed with the different ring size spiro-bicyclic compounds, as well as, the important role of the leaving group ability of the halide in the transformation.

Next we started a collaboration with the Janssen-Cilag Medicinal Chemistry team in Toledo to study the applicability of our spiro-bicyclic cores on programs directed towards the identification of therapies to treat Alzheimer's disease. These collaborative efforts focused on intercepting, though small-molecule *O*-GlcNAcase (OGA) inhibition, the progression of the characteristic tauopathy observed in AD brains.<sup>[5]</sup>

For this purpose, five central spiro-bicyclic cores were prepared in large scale (up to 3-4 grams) and then were selectively derivatized. The exploration focused on investigating the effect of introducing different linkers, heteroaromatic replacements, and ring-size of the spiro-bicycles on the OGA inhibitory activity of this series. In this sense, we were able to synthesize 20 different final targets, which were evaluated in OGA enzymatic and cellular assays. Interestingly, compound **167a** showed high remarkable activity as OGA inhibitor with single-digit nanomolar activities in both biochemical and cellular assays (Figure 9.2).

## Summary

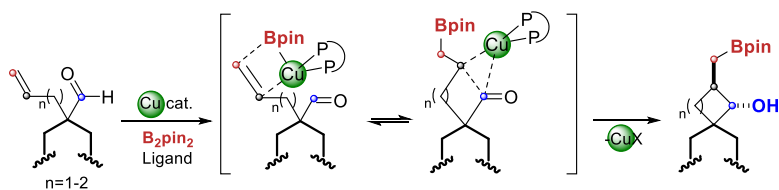


167a

hOGA pIC<sub>50</sub> = 8.36  
hOGA cell pIC<sub>50</sub> = 8.1

Figure 9.2 Compound 167a.

Finally, we wanted to develop a new methodology to cover a gap in the spiro-bicyclic library.<sup>[6]</sup> To achieve this goal, we prepared a series of heterocyclic alkenyl aldehydes and submitted them to the borylative cyclization reaction conditions that were optimized in Chapter 4. Gladly, the corresponding hydroxy-functionalized spiro-bicycles were obtained with total chemo- and diastereoselectivity (Scheme 9.3).



Scheme 9.3 Copper (I) mediated borylative cyclization of alkenyl aldehydes.

Moreover, this transformation showed a good group tolerance as well as easy functionalization under mild oxidative conditions rendering the formation of spiro-bicyclic diols with potential for further derivatization. The oxidized product (**200**) was crystallized and fully characterized by X-Ray diffraction, confirming the *anti*-diastereoselective transformation through the borylative cyclization of alkenyl aldehydes (Figure 9.3).

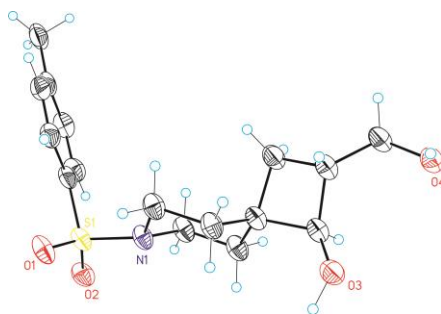
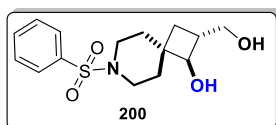


**Figure 9.3** X-Ray diffraction of *anti*-2-(hydroxymethyl)-7-(phenylsulfonyl)spiro[3.5]nonan-1-ol (**200**).

## 9.2. References Chapter 9

- [1] E. C. Neeve, S. J. Geier, I. A. I. Mkhaliid, S. A. Westcott, T. B. Marder, *Chem. Rev.* **2016**, *116*, 9091-9161.
- [2] A. B. Cuenca, R. Shishido, H. Ito, E. Fernández, *Chem. Soc. Rev.* **2017**, *46*, 415-430.
- [3] A. B. Cuenca, J. Cid, D. García-López, J. J. Carbó, E. Fernández, *Org. Biomol. Chem.* **2015**, *13*, 9659-9664.
- [4] N. Kim, M. J. Sohn, H. Koshino, E. H. Kim, W. G. Kim, *Bioorg. Med. Chem. Lett.* **2014**, *24*, 83-86.
- [5] F. V. Rao, H. C. Dorfmüller, F. Villa, M. Allwood, I. M. Eggleston, D. M. F. van Aalten, *EMBO J.* **2006**, *25*, 1569-1578.
- [6] E. M. Carreira, T. C. Fessard, *Chem. Rev.* **2014**, *114*, 8257-8322.

# **Chapter 10**

## **List of publications, conferences and research collaboration**

---

UNIVERSITAT ROVIRA I VIRGILI  
COMPLEMENTARY SYNTHESIS OF ORGANOBORANES TO POPULATE THE CHEMICAL  
FUNCTIONALITY TO A GIVEN AREA OF BIOMEDICAL INTEREST  
Jordi Royes Buisan

## List of publications

M. G. Civit, J. Royes, C. M. Vogels, S.A. Westcott, A. B. Cuenca, E. Fernández "Strategic trimethylsilyldiazomethane insertion into pinB-SR followed by selective alkylations" *Org. Lett.* **2016**, *18*, 3830-3833.

J. Royes, A. B. Cuenca, E. Fernández "Access to 1,1-Diborylalkenes and Concomitant Stereoselective Reactivity" *Eur. J. Org. Chem.* **2018**, 2728–2739.

J. Royes, S. Ni, A. Farré, E. La Cascia, J. J. Carbó, A. B. Cuenca, F. Maseras, E. Fernández "Copper-Catalyzed Borylative Ring Closing C-C Coupling toward Spiro- and Dispiroheterocycles" *ACS Catal.* **2018**, *8*, 2833-2838.

C. Martínez, J. Bartolomé, A. Trabanco, A. Ebnet, A. Bretteville G. Tresadern, M. Somers, E. Fernández, J. Royes, J. Vega, A. Cerro, F. Delgado, M. Sola, A. Garcia "Discovery of JNJ-67483676, a novel non-saccharide O-GLCNAcase (OGA) inhibitor for the treatment of Alzheimer's disease (AD)" *In writing process*; 2019.

R. Maza, J. Royes, J. Carbó, E. Fernández "Borylcupration of alkenes towards intramolecular trapping with aldehydes: a rational chemo and stereo preference" *In writing process*; 2019.



## Posters and presentations

**XXVI Reunión Bienal Química Orgánica**, Huelva, España, Junio 2016 - Poster presentation.

**IUPAC 2017 - 46th World Chemistry Congress**, São Paulo, Brazil, Julio 2017 - Poster presentation.

**Girona Seminar 2018**, Girona, España, Abril 2018 - Poster presentation.

**TRAPCAT2, Second Trans Pyrenean Meeting in Catalysis**, Tarragona, España, Octubre 2018 - Poster presentation.

**EUROBORON VIII**, Montpellier, Francia - Poster and oral communication.

## Research collaboration

Project: Synthesis and application of novel spiro-boronate compounds for the treatment of Alzheimer's disease.

Center: Janssen Cilag, from Johnson & Johnson, Toledo, Spain.

Supervisor: Dr. Andrés Avelino Trabanco Suárez.

Period: September (2017) – August (2018).

UNIVERSITAT ROVIRA I VIRGILI  
COMPLEMENTARY SYNTHESIS OF ORGANOBORANES TO POPULATE THE CHEMICAL  
FUNCTIONALITY TO A GIVEN AREA OF BIOMEDICAL INTEREST  
Jordi Royes Buisan

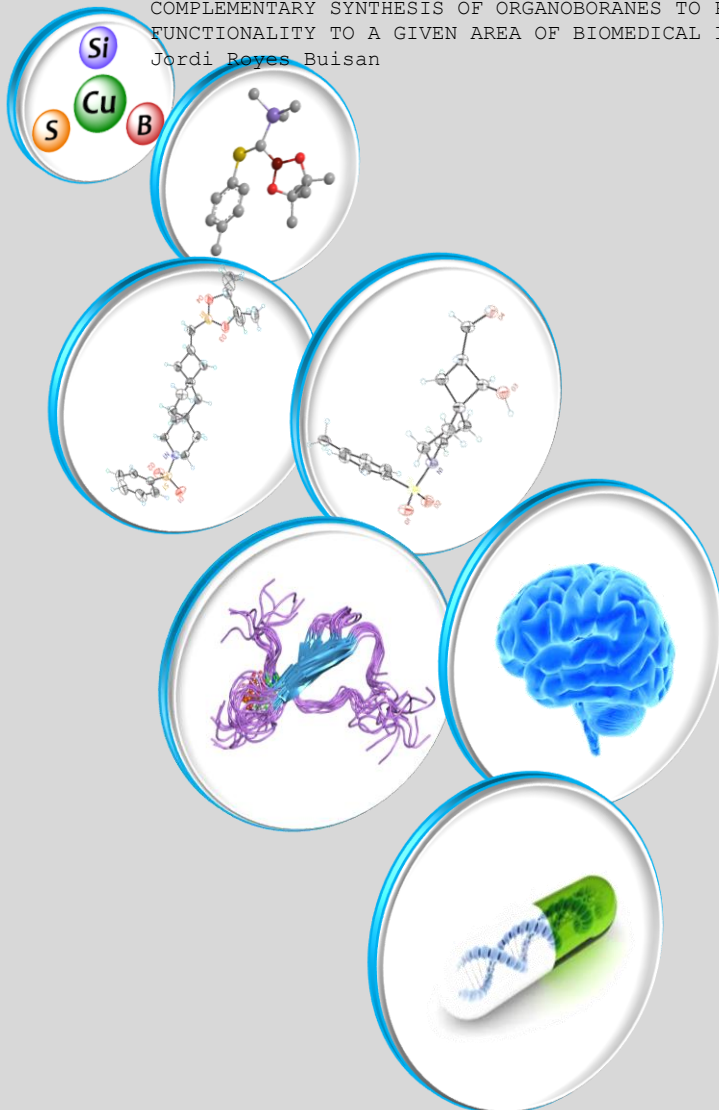
UNIVERSITAT ROVIRA I VIRGILI  
COMPLEMENTARY SYNTHESIS OF ORGANOBORANES TO POPULATE THE CHEMICAL  
FUNCTIONALITY TO A GIVEN AREA OF BIOMEDICAL INTEREST  
Jordi Royes Buisan

UNIVERSITAT ROVIRA I VIRGILI  
COMPLEMENTARY SYNTHESIS OF ORGANOBORANES TO POPULATE THE CHEMICAL  
FUNCTIONALITY TO A GIVEN AREA OF BIOMEDICAL INTEREST  
Jordi Royes Buisan

UNIVERSITAT ROVIRA I VIRGILI

COMPLEMENTARY SYNTHESIS OF ORGANOBORANES TO POPULATE THE CHEMICAL  
FUNCTIONALITY TO A GIVEN AREA OF BIOMEDICAL INTEREST

Jordi Royes Buisan



UNIVERSITAT  
ROVIRA I VIRGILI

